

THE UNIVERSITY OF CALGARY

ADSORPTION OF FOAM-FORMING SURFACTANTS

by

Karin Mannhardt

A THESIS

SUBMITTED TO THE FACULTY OF GRADUATE STUDIES
IN PARTIAL FULFILLMENT OF THE REQUIREMENTS FOR THE
DEGREE OF

Master of Engineering

DEPARTMENT OF

Chemical and Petroleum Engineering

CALGARY, ALBERTA

AUGUST, 1988

© Karin Mannhardt 1988

Permission has been granted to the National Library of Canada to microfilm this thesis and to lend or sell copies of the film.

The author (copyright owner) has reserved other publication rights, and neither the thesis nor extensive extracts from it may be printed or otherwise reproduced without his/her written permission.

L'autorisation a été accordée à la Bibliothèque nationale du Canada de microfilmer cette thèse et de prêter ou de vendre des exemplaires du film.

L'auteur (titulaire du droit d'auteur) se réserve les autres droits de publication; ni la thèse ni de longs extraits de celle-ci ne doivent être imprimés ou autrement reproduits sans son autorisation écrite.

ISBN 0-315-46624-3

THE UNIVERSITY OF CALGARY

FACULTY OF GRADUATE STUDIES

The undersigned certify that they have read, and recommend to the
Faculty of Graduate Studies for acceptance, a thesis entitled,

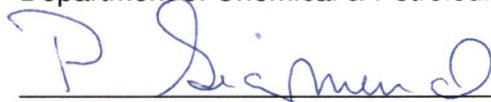
"ADSORPTION OF FOAM-FORMING SURFACTANTS"

submitted by Karin Mannhardt

in partial fulfillment of the requirements for the degree of Master of Engineering.



Dr. R.A. Heidemann, Chairman
Department of Chemical & Petroleum Engineering



Dr. P. Sigmund,
Department of Chemical & Petroleum Engineering



Dr. J. Novosad,
Department of Chemical & Petroleum Engineering



Dr. W.G. Laidlaw,
Department of Chemistry

6 September 1988
Date

ABSTRACT

Surfactants are of interest in several enhanced oil recovery (EOR) processes. They can be used for low tension flooding, mobility control in gas flooding, and blocking and diverting. Adsorption at the solid/liquid interface is a mechanism of surfactant loss and is therefore detrimental to these processes. This thesis deals with several aspects of the adsorption of foam-forming surfactants used in EOR applications.

The starting point for the material presented is the surface excess model for surfactant transport through porous media developed by Huang and Novosad (1986). It is shown that two of the adjustable parameters in the model, the monolayer coverages of surfactant and water, can be determined through independent measurements, thus reducing the number of parameters in the model by two. Experimental data indicate that the selectivity of adsorption, assumed constant in the previous surface excess model, is a decreasing function of concentration. Two functional forms of selectivity, one from thermodynamic principles and the other semi-empirical, are incorporated into the surface excess model and tested with experimental core flood data. It is shown next that surface heterogeneities can affect the adsorption process very strongly. A simple form of surface heterogeneity is incorporated into the model, allowing history matching

of effluent concentrations from core floods run at different injected concentrations with a single adsorption isotherm. By contrast, the previous models required separate isotherms to match different core floods. In the final chapter a model for flow of surfactant mixtures is developed. This model incorporates monomer-micelle equilibrium and the surface excess concept for multicomponent mixtures. The model is shown to represent experimental core flood data well, and it is used to explain the counter-intuitive behavior of a surfactant mixture in a core flood. A model study is carried out to demonstrate some features of the chromatographic movement of surfactant mixtures through porous media and the potential for applying the properties of such mixtures to the formulation of surfactant systems.

ACKNOWLEDGEMENTS

I wish to express my appreciation to Dr. Jerry Novosad of the Petroleum Recovery Institute for the supervision of this work, and for his encouragement, interest, and continual optimism throughout the course of this thesis. Appreciation is extended to Dr. R.A. Heidemann for serving as my thesis supervisor.

Special thanks go to the Petroleum Recovery Institute and past and present members of its staff. PRI gave me the opportunity to complete this degree, provided me with many years of support prior to and during the preparation of this thesis, and supplied the experimental data appearing in the text. Dr. Jim Batycky first introduced me to the field of engineering and provided the impetus for pursuing this degree. Angela Huang is thanked for the use of her model. The majority of the experimental data in this thesis were collected through the careful work of Laurie Hodgins.

I also wish to thank Rosemary French for providing a powerful antidote to countless hours of study, and Werner Brock for his friendship. Finally, thanks to my parents for being a source of inspiration, support, and encouragement always.

TABLE OF CONTENTS

| <u>Chapter</u> | <u>Page</u> |
|---|-------------|
| Title Page | i |
| Approval Page | ii |
| Abstract | iii |
| Acknowledgements | v |
| Table of Contents | vi |
| List of Tables | viii |
| List of Figures | ix |
| Nomenclature | xv |
| 1 Introduction | 1 |
| 2 The Surface Excess Concept in Modelling Adsorption in Flow through Porous Media | 9 |
| 1. The Surface Excess | 9 |
| 2. Modelling Adsorption in Flow through Porous Media | 15 |
| 3. Applications of the Surface Excess Model | 19 |
| 4. Extensions to the Surface Excess Model | 23 |
| 4.1. Independent Evaluation of m_1 and m_2 | 23 |
| 4.2. Dependence of Selectivity on Concentration | 25 |
| 4.3. Heterogeneous Surfaces | 25 |
| 4.4. Adsorption of Surfactant Mixtures | 26 |
| 3 Determination of the Monolayer Coverages of Surfactant and Water | 28 |
| 1. The Specific Surface Area of a Solid | 28 |
| 2. Molecular Area | 32 |
| 3. Determination of the Molecular Area of a Surfactant Molecule from the Gibbs Adsorption Equation | 36 |
| 4. Experimental: Surface Tension Measurement of Foam -Forming Surfactants | 44 |
| 5. Results of Surface Tension Measurements: The Molecular Area of Surfactant Molecules | 47 |
| 6. Chapter Summary | 51 |
| 4 The Dependence of Selectivity on Surfactant Concentration | 52 |
| 1. Experimental: Core Floods | 52 |
| 2. Results: History Matching of Core Floods Using Constant Selectivity | 54 |
| 3. The Functional Form of Selectivity | 64 |
| 4. Results: History Matching of Core Floods Using Variable Selectivity | 73 |

| | | |
|-----|--|-----|
| 5 | The Effect of Surface Heterogeneity on Adsorption | 87 |
| 1. | The Mathematical Treatment of Surface Heterogeneity: A Literature Review | 87 |
| 2. | Surface Heterogeneity with Uniform Distribution | 98 |
| 3. | Two-Component Heterogeneous Solid | 104 |
| 4. | History Matching Core Floods with Heterogeneous Solid .. | 111 |
| 6 | Adsorption of Surfactant Mixtures | 124 |
| 1. | Introduction | 124 |
| 2. | Monomer-Micelle Equilibrium | 127 |
| 3. | Ideal Mixed Micelle Theory | 133 |
| 4. | Literature on the Fundamental Aspects of Surfactant Adsorption | 139 |
| 5. | The Surface Excess Concept for Multicomponent Mixtures | 149 |
| 6. | Modelling Adsorption of Surfactant Mixtures in Flow through Porous Media | 153 |
| 7. | Experimental Procedure | 158 |
| 8. | Results and Discussion | 162 |
| 9. | Model Study | 173 |
| 10. | Chapter Summary | 185 |
| 7 | Summary and Conclusions | 187 |
| | References | 192 |
| | Appendix. Finite Difference Solutions to the Flow Models | A-1 |

LIST OF TABLES

| <u>Table</u> | <u>Page</u> |
|--|-------------|
| 1 Results of the determination of the molecular area of two surfactants at monolayer coverage from surface tension measurement. | 50 |
| 2 Properties of Berea cores used for surfactant adsorption floods. .. | 54 |
| 3 Experimental conditions and matching parameters for constant selectivity model. | 56 |
| 4 Experimental conditions and matching parameters for variable selectivity model with equation (50). | 74 |
| 5 Experimental conditions and matching parameters for variable selectivity model with equation (51). | 82 |
| 6 Experimental conditions and matching parameters obtained from the surface excess model with a two-component heterogeneous solid. ... | 113 |
| 7 Critical micelle concentrations of C_{12} and C_{18} components of Varion CAS. 2% w/w NaCl, 40°C. | 162 |
| 8 Matching parameters for the core flood with C_{12} and C_{18} components of Varion CAS obtained from the surface excess model for ternary mixtures. | 168 |
| 9 System variables used in five hypothetical core floods. | 177 |
| (a) Core and displacement properties (all runs) | |
| (b) Model parameters (all runs) | |
| (c) Variable system parameters | |

LIST OF FIGURES

| <u>Figure</u> | <u>Page</u> |
|---|-------------|
| 1 Typical adsorption isotherms for completely miscible liquids, as calculated from equations (8) and (9) with $S=10$, $m_1=0.0033$ mmole/g, $m_2=0.013$ mmole/g. | 14 |
| 2 Example of a history match obtained with the surface excess model. (Taken from Mannhardt and Novosad, 1987b). | 21 |
| 3 Adsorption isotherm calculated using the model parameters from the match in Figure 2 with equation (8). | 21 |
| 4 Effect of S on the effluent profile. $m_1=0.0055$ mmole/g, $m_2=0.013$ mmole/g, $k_1=1.0$ hr ⁻¹ , $k_2=0.001$ hr ⁻¹ , $\lambda=0.15$ cm. | 24 |
| 5 Effect of m_1 on the effluent profile. $S=500$, $m_2=0.013$ mmole/g, $k_1=1.0$ hr ⁻¹ , $k_2=0.001$ hr ⁻¹ , $\lambda=0.15$ cm. | 24 |
| 6 Distribution of values for the molecular area of water as listed by McClellan and Harnsberger (1967). | 35 |
| 7 Chemical structures of two foam-forming surfactants. | 46 |
| 8 Surface tension of DPES in 2.1% brine. | 48 |
| 9 Surface tension of DPES in 14.7% brine. | 48 |
| 10 Surface tension of betaine in 2.1% brine. | 49 |
| 11 Surface tension of betaine in 14.7% brine. | 49 |
| 12 Core T3 effluent profiles. Constant selectivity model. | 57 |
| 13 Core T11 effluent profiles. Constant selectivity model. | 57 |
| 14 Core T1 effluent profiles. Constant selectivity model. | 58 |
| 15 Core T13 effluent profiles. Constant selectivity model. | 58 |
| 16 Core T6 effluent profiles. Constant selectivity model. | 59 |
| 17 Core T9 effluent profiles. Constant selectivity model. | 59 |
| 18 Core T7 effluent profiles. Constant selectivity model. | 60 |

| | | |
|----|--|----|
| 19 | Core T10 effluent profiles. Constant selectivity model. | 60 |
| 20 | Adsorption isotherms for cores T3 and T11 from constant selectivity model. | 61 |
| 21 | Adsorption isotherms for cores T1 and T13 from constant selectivity model. | 61 |
| 22 | Adsorption isotherms for cores T6 and T9 from constant selectivity model. | 62 |
| 23 | Adsorption isotherms for cores T7 and T10 from constant selectivity model. | 62 |
| 24 | Dependence of selectivity on concentration, calculated from equation (50). | 69 |
| 25 | Dependence of the surface excess on the parameters S_0 and β , calculated from equations (8) and (50). $m_1=0.0027$ or 0.0080 mmole/g, $m_2=0.013$ mmole/g. | 69 |
| 26 | Dependence of selectivity on concentration, calculated from equation (51). | 72 |
| 27 | Dependence of the surface excess on the parameters a and b, calculated from equations (8) and (51). $m_1=0.0027$ mmole/g, $m_2=0.013$ mmole/g. | 72 |
| 28 | Core T3 effluent profiles. Variable selectivity model with equation (50). | 75 |
| 29 | Core T11 effluent profiles. Variable selectivity model with equation (50). | 75 |
| 30 | Core T1 effluent profiles. Variable selectivity model with equation (50). | 76 |
| 31 | Core T13 effluent profiles. Variable selectivity model with equation (50). | 76 |
| 32 | Core T6 effluent profiles. Variable selectivity model with equation (50). | 77 |
| 33 | Core T9 effluent profiles. Variable selectivity model with equation (50). | 77 |
| 34 | Core T7 effluent profiles. Variable selectivity model with equation (50). | 78 |
| 35 | Core T10 effluent profiles. Variable selectivity model with | |

| | |
|--|-----|
| equation (50). | 78 |
| 36 Adsorption isotherms for cores T3 and T11 from constant selectivity model, and variable selectivity model with equation (50). | 79 |
| 37 Adsorption isotherms for cores T1 and T13 from constant selectivity model, and variable selectivity model with equation (50). | 79 |
| 38 Adsorption isotherms for cores T6 and T9 from constant selectivity model, and variable selectivity model with equation (50). | 80 |
| 39 Adsorption isotherms for cores T7 and T10 from constant selectivity model, and variable selectivity model with equation (50). | 80 |
| 40 Core T3 effluent profiles. Variable selectivity model with equation (51). | 83 |
| 41 Core T11 effluent profiles. Variable selectivity model with equation (51). | 83 |
| 42 Adsorption isotherms for cores T3 and T11 from variable selectivity model with equation (51). | 84 |
| 43 Examples of a U-shaped and an S-shaped adsorption isotherm. | 90 |
| 44 The effect of surface heterogeneity (uniform distribution of selectivities) on adsorption. $m_1=0.0033$ mmole/g, $m_1/m_2=0.25$. .. | 102 |
| 45 The effect of surface heterogeneity (uniform distribution of selectivities) on adsorption. $m_1=0.0033$ mmole/g, $m_1/m_2=0.25$. .. | 103 |
| 46 The effect of surface heterogeneity (uniform distribution of selectivities) on adsorption, low concentration range. $m_1=0.0033$ mmole/g, $m_1/m_2=0.25$ | 103 |
| 47 The effect of surface heterogeneity (two-component solid) on adsorption. $m_1=0.0033$ mmole/g, $m_1/m_2=0.25$ | 108 |
| 48 The effect of surface heterogeneity (two-component solid) on adsorption. $m_1=0.0033$ mmole/g, $m_1/m_2=0.25$ | 108 |
| 49 The effect of surface heterogeneity (two-component solid) on adsorption, low concentration range. $m_1=0.0033$ mmole/g, $m_1/m_2=0.25$ | 109 |

| | | |
|----|---|-----|
| 50 | The effect of z_A on the adsorption isotherm of a two-component heterogeneous solid. $m_1=0.0033$ mmole/g, $m_1/m_2=0.25$ | 109 |
| 51 | The effect of S_{OA} on the adsorption isotherm of a two-component heterogeneous solid. $m_1=0.0033$ mmole/g, $m_1/m_2=0.25$ | 110 |
| 52 | The effect of S_{OB} on the adsorption isotherm of a two-component heterogeneous solid. $m_1=0.0033$ mmole/g, $m_1/m_2=0.25$ | 110 |
| 53 | Core T3 effluent profiles. Two-component heterogeneous solid. | 114 |
| 54 | Core T11 effluent profiles. Two-component heterogeneous solid. | 114 |
| 55 | Core T1 effluent profiles. Two-component heterogeneous solid. | 115 |
| 56 | Core T13 effluent profiles. Two-component heterogeneous solid. | 115 |
| 57 | Core T6 effluent profiles. Two-component heterogeneous solid. | 116 |
| 58 | Core T9 effluent profiles. Two-component heterogeneous solid. | 116 |
| 59 | Core T7 effluent profiles. Two-component heterogeneous solid. | 117 |
| 60 | Core T10 effluent profiles. Two-component heterogeneous solid. | 117 |
| 61 | Adsorption isotherms for cores T3 and T11 from heterogeneous model, and homogeneous variable selectivity model with equation (50). | 118 |
| 62 | Adsorption isotherms for cores T1 and T13 from heterogeneous model, and homogeneous variable selectivity model with equation (50). | 118 |
| 63 | Adsorption isotherms for cores T6 and T9 from heterogeneous model, and homogeneous variable selectivity model with equation (50). | 119 |
| 64 | Adsorption isotherms for cores T7 and T10 from heterogeneous | |

| | | |
|----|---|-----|
| | model, and homogeneous variable selectivity model with equation (50). | 119 |
| 65 | Selectivity as a function of concentration, calculated from the best fit parameters (Tables 4 and 6) of the heterogeneous and homogeneous models. | 120 |
| 66 | Monomer concentrations of two surfactant solutions, each containing a single pure surfactant. | 137 |
| 67 | Monomer concentrations of a mixed surfactant system containing two surfactants. | 137 |
| 68 | The fraction of component 1 in the micellar phase in a mixed surfactant system. | 138 |
| 69 | A typical surfactant adsorption isotherm. | 138 |
| 70 | Monomer-micelle equilibrium in a surfactant solution in contact with a solid. | 144 |
| 71 | Structure and composition of Varion CAS, an amphoteric foam-forming surfactant. | 159 |
| 72 | Surface tension of the C_{12} and C_{18} components of Varion CAS. Ratios are on a molar basis. | 163 |
| 73 | Critical micelle concentrations of mixed surfactant solutions containing C_{12} and C_{18} components of Varion CAS. | 163 |
| 74 | Breakthrough curves from a core flood with C_{12} and C_{18} components of Varion CAS. | 165 |
| 75 | History match of a core flood using C_{12} and C_{18} components of Varion CAS. Effluent profiles are for tracer and total surfactant. | 167 |
| 76 | History match of a core flood using C_{12} and C_{18} components of Varion CAS. Effluent profiles are for each component. | 167 |
| 77 | Adsorption isotherms for two components of Varion CAS at $\alpha=0.160$, calculated using cmc's in Table 7 and parameters in Table 8. | 170 |
| 78 | Monomer concentrations of two components of Varion CAS at $\alpha=0.160$ | 170 |
| 79 | Adsorption of surfactant 1 from a mixture. | 178 |
| 80 | Adsorption of surfactant 2 from a mixture. | 178 |

| | | |
|----|---|-----|
| 81 | Overall adsorption from a surfactant mixture. | 179 |
| 82 | Adsorption from a surfactant mixture at $\alpha=0.5$ | 179 |
| 83 | Effluent profiles for run 1. Injected concentration above the cmc. | 182 |
| 84 | Effluent profiles for run 2. Injected concentration below the cmc. | 182 |
| 85 | Effluent profiles for run 3. Injected concentration at the intersection of the component isotherms. | 183 |
| 86 | Effluent profiles for run 4. Surfactant properties were adjusted so as to prevent separation of components. | 183 |
| 87 | Effluent profile for run 5. Injection of surfactant 2 alone. .. | 184 |

NOMENCLATURE

| | |
|-------------------------------|---|
| a | parameter in equation (51) |
| a_i | activity of component i |
| A | specific surface area (cm^2/g) |
| A_m | molecular area ($\text{\AA}^2/\text{molecule}$) |
| b | parameter in equation (51) |
| c | total surfactant concentration (mole/l) |
| c_i | concentration of component i (mole/l) |
| c_i^m | monomer concentration (mole/l) |
| cmc | mixture cmc (mole/l or mole fraction) |
| cmc _{i} | cmc of component i (mole/l or mole fraction) |
| C | parameter in the BET equation, equation (16); constant, equation (37); constant of integration, equation (48); constant, equation (55); concentration in figures with effluent profiles |
| C_0 | injected concentration |
| D | dispersion coefficient (cm^2/hr) |
| E | a measure of the energy of adsorption, equations (52) and (53) |
| f_i | bulk phase activity coefficient of component i |
| f'_i | adsorbed phase activity coefficient of component i |
| k | Boltzmann's constant ($= 1.381 \times 10^{-23}$ Joule/K) |
| k_{im} | kinetic constant of adsorption ($m = 1$) or desorption ($m = 2$) of |

| | |
|-------------|--|
| | component i (hr^{-1}) |
| K_{ij} | defined in equation (94) |
| L | core length (cm) |
| m | parameter in the Gibbs adsorption equation, equation (22) |
| m_i | monolayer coverage of component i per unit mass of adsorbent (mmole/g) |
| n | amount of bulk phase per unit mass of adsorbent (mmole/g) |
| n' | amount of adsorbed phase per unit mass of adsorbent (mmole/g) |
| n_i | amount of component i in the bulk phase per unit mass of adsorbent (mmole/g) |
| n'_i | amount of component i in the adsorbed phase per unit mass of adsorbent (mmole/g) |
| n^o | amount of liquid per unit mass of adsorbent (mmole/g) |
| n_i^e | equilibrium surface excess of component i per unit mass of adsorbent (mmole/g) |
| n_i^o | overall amount of component i per unit mass of adsorbent (mmole/g) |
| $(n_i^e)_l$ | local equilibrium surface excess of component i per unit mass of adsorbent on a local patch of surface (mmole/g) |
| $(n_i^e)_A$ | equilibrium surface excess of component i per unit mass of adsorbent, solid A (mmole/g) |
| $(n_i^e)_B$ | equilibrium surface excess of component i per unit mass of adsorbent, solid B (mmole/g) |
| n_i^{ea} | actual surface excess of component i per unit mass of adsorbent (mmole/g) |

| | |
|----------------|---|
| $(n_i^{ea})_0$ | initial surface excess of component i per unit mass of adsorbent (mmole/g) |
| N | Avogadro's number ($= 6.023 \times 10^{23}$); overall adsorption on a heterogeneous surface, equation (52) |
| N_1 | local adsorption on a patch of surface, equation (52) |
| P | partial pressure, equation (16) |
| P_0 | vapor pressure, equation (16) |
| R | gas constant ($= 8.314 \times 10^4$ dyne cm/mmole K) |
| S | selectivity, binary mixture, defined in equations (7) and (36) |
| S_{ij} | selectivity, multicomponent mixture, defined in equations (101) and (102) |
| S_A | selectivity on solid A (heterogeneous solid) |
| S_B | selectivity on solid B (heterogeneous solid) |
| S_H | upper limit of selectivity (heterogeneous solid) |
| S_L | lower limit of selectivity (heterogeneous solid) |
| S_0 | defined in equation (49) |
| S_{0A} | value of S_0 for solid A (heterogeneous solid) |
| S_{0B} | value of S_0 for solid B (heterogeneous solid) |
| S_{0H} | upper limit of S_0 (heterogeneous solid) |
| S_{0L} | lower limit of S_0 (heterogeneous solid) |
| t | time (hr) |
| t_0 | initial time (hr) |
| t_1 | duration of slug injection (hr) |
| T | absolute temperature ($^{\circ}\text{K}$) |
| v | frontal velocity (cm/hr) |

| | |
|--------------|---|
| V | volume of gas adsorbed, equation (16) |
| V_m | volume of gas adsorbed at monolayer coverage, equation (16) |
| x | salt to surfactant molar ratio, equations (30) and (32), chapter 3; dependent variable (pressure, concentration), equation (52), chapter 5 |
| x_i | bulk phase mole fraction of component i |
| x'_i | adsorbed phase mole fraction of component i |
| x_{id} | mole fraction of component i in the monomer phase |
| x_{i0} | injected mole fraction |
| x_i^o | overall mole fraction of component i |
| x_s | total surfactant mole fraction |
| y | distance along core (cm) |
| z | number of charges on an ionic surfactant |
| z_A | fraction of total surface that is composed of solid A |
| z_B | fraction of total surface that is composed of solid B |
| α | fraction of surfactant 1 in a mixture, surfactant only basis |
| α_m | fraction of surfactant 1 in a mixed micelle, surfactant only basis |
| β | defined in equation (44) |
| Γ_i | Gibbs surface excess of component i per unit interfacial area (mmole/cm ²) |
| Γ_i^a | apparent surface excess of component i per unit interfacial area (mmole/cm ²) |
| Δ | range of values of E, equations (52) and (53); |

| | |
|--------------|--|
| | $\text{cmc}_2 - \text{cmc}_1$, chapter 6 |
| ϵ | elementary charge ($= 1.602 \times 10^{-19}$ Coulomb) |
| λ | dispersion parameter (cm); distribution function in chapter 5 (heterogeneous surface) |
| μ | mean |
| μ_i | chemical potential of species i (dyne cm/mmole), chapter 3; chemical potential of component i in the monomer phase, chapter 6 |
| μ_i^0 | standard chemical potential of component i (dyne cm/mmole) |
| μ_{Mi} | chemical potential of component i in a mixed micelle |
| μ_{MOi} | chemical potential in a pure component i micelle |
| μ_{Oi} | standard chemical potential of non-micellar component i |
| ξ_i | defined in equation (24) |
| ρ | liquid molar density (mmole/cm ³) |
| ρ_r | rock density (g/cm ³) |
| σ | surface tension (dyne/cm); solid/liquid interfacial tension for a mixture (dyne/cm) |
| σ_i^0 | solid/liquid interfacial tension of pure component i (dyne/cm) |
| σ^2 | variance |
| ϕ | porosity (fraction) |
| ψ_0 | potential (Volts) |

CHAPTER 1

INTRODUCTION

The unique properties of surfactants have led to their application in such diverse fields as detergency, mineral processing (flotation), agriculture, emulsion polymerization, printing, pharmaceuticals, corrosion inhibition, and enhanced oil recovery. The desirable characteristics of surfactants that are exploited in all these applications arise from the structure of a surfactant molecule, which consists of a polar (hydrophilic) and a non-polar (hydrophobic) structural group. A consequence of the "amphipathic" nature of the molecule is the formation of aggregates, called micelles, in solution and the tendency of the surfactant molecules to become concentrated at interfaces, either gas/liquid or solid/liquid. This work deals with surfactants used in enhanced oil recovery (EOR), and more specifically with adsorption of foam-forming surfactants at the solid/liquid interface, which in this particular application is a mechanism of surfactant loss and should therefore be minimized.

Several enhanced oil recovery processes make use of surfactants, the best known probably being conventional surfactant flooding. This process relies on a significant lowering of oil/water interfacial tensions by the surfactant, which results in a decrease of the capillary forces that trap the oil in the porous medium. Trapped oil droplets may

thus be released by injection of a surfactant solution into the reservoir. While it is well established that surfactant flooding can recover additional oil, if a sufficient quantity of the surfactant is injected (Gogarty, 1977; Novosad, 1982), careful evaluation of the economics of such a process is required, since the chemicals injected into the reservoir are more expensive than the crude oil to be recovered. It is therefore desirable to inject the lowest quantity of surfactant that still maintains effectiveness in recovering additional oil. Factors determining the economic feasibility of conventional surfactant flooding have been summarized by Gogarty (1977). Uncertainties accompanying the economics of this process include the time required to recover tertiary oil, long-term projection of oil prices, and lack of experience with full-scale application of surfactants in the field.

A second EOR process that makes use of surfactants relies on the foaming capability of a surfactant solution that is co-injected with a gas into the reservoir to form a mobility control foam. In contrast to conventional surfactant flooding, which enhances the microscopic displacement efficiency, this process improves the sweep efficiency of a displacing gas phase. Steam flooding and hydrocarbon gas miscible flooding, the two most frequently applied EOR processes in Canada, both suffer from poor sweep efficiency caused by gravity override and viscous fingering of the low density, low viscosity displacing fluid. There has thus been much interest in recent years in the application of mobility control foams to improve the efficiency of these processes.

Simultaneous injection of gas and surfactant solution will generate a foam in the porous medium, thereby reducing the mobility of the injected gas phase. Preferential flow of the surfactant into the swept zones of the reservoir will divert injected gas to the unswept zones, improving oil recovery from these zones. Promising results have been obtained in several pilot tests with steam foams (Doscher and Kuuskraa, 1982; Dilgren et. al., 1982; Brigham et. al., 1984; Castanier, 1987).

A novel EOR method that uses surfactants to improve sweep efficiency by blocking the more permeable regions of a reservoir has been described recently by Harwell and Scamehorn (1987). This method utilizes precipitation of two different surfactant types when mixed in solution. A dilute solution of surfactant 1 is injected into the reservoir, followed by a brine spacer, and then by surfactant 2. The surfactants are chosen in such a way that the chromatographic velocity of surfactant 1 is lower than that of surfactant 2. Surfactant 2 will therefore overtake surfactant 1 at a distance from the injection well that depends on the velocities of each component and on the size of the brine spacer. Once the two surfactants mix, precipitation of surfactant and blockage of parts of the reservoir will take place.

One of the most important factors affecting the performance of the processes described (or any EOR process that involves the injection of chemicals into a petroleum reservoir) is the rate of propagation of the chemical, which in turn is strongly affected by surfactant losses in the reservoir. Mechanisms of surfactant loss include partitioning into

an immobile fluid phase, precipitation due to changes in ionic strength and/or surfactant composition, chemical degradation of the surfactant, and adsorption at the solid/liquid interface (Novosad, 1982). While complete solubility and long term chemical stability of the surfactant at conditions likely to be encountered in the reservoir should be ensured before injection of the surfactant, entrapment in a residual oil phase, adsorption losses, and changes in surfactant composition by selective adsorption and/or partitioning of some of its components are more difficult to evaluate. Many foam-forming surfactants, particularly those suitable for high salinity and hardness environments (Novosad and Ionescu, 1987), do not partition into an oil phase to any significant extent. For such systems, adsorption at the solid/liquid interface constitutes the most important mechanism of surfactant loss.

In this work the author hopes to elucidate some aspects of surfactant adsorption. Even though the principles involved apply to surfactants in general, the experimental data were collected using foam-forming surfactants. Surfactant partitioning into an oil phase is not considered at this stage, all experiments being performed in oil-free systems.

The importance of developing a good understanding of surfactant loss at the solid/liquid interface has been emphasized repeatedly (Gale and Sandvik, 1973; Bae and Petrick, 1976; Hurd, 1976; Malmberg and Smith, 1977; Lawson and Dilgren, 1978; Novosad, 1982). Adsorption is usually determined by either of two methods: the change in

concentration of a surfactant solution equilibrated with a solid, or the amount of surfactant retained in a core after flooding with a surfactant solution. The first method requires extremely sensitive analytical methods, if small changes in concentration are to be determined accurately (Novosad and Baxter, 1979). Since adsorption levels on reservoir rocks are relatively low compared to materials used in the chemical industry, the usefulness of this method is limited by the sensitivity of the analytical methods used.

The second method allows considerably more accurate determination of adsorption, since the solid/liquid ratio can exceed that in the static test by an order of magnitude. Several authors have used material balance calculations to determine adsorption levels from dynamic tests (Gale and Sandvik, 1973; Bae and Petrick, 1976; Malmberg and Smith, 1977). The information obtained in this way is rather limited in that it yields a single value of adsorption at the injected concentration under consideration, rather than a complete adsorption isotherm. A more detailed evaluation of adsorption is possible by modelling surfactant transport in flow through porous media. Adsorption is often incorporated into the transport equation using the Langmuir rate or equilibrium equations (Trogus et. al., 1977; Satter et. al., 1980; Ziegler and Handy, 1981; Novosad et. al., 1986), or the Langmuir rate equation together with a mass transfer-rate mechanism from the bulk to the surface (Ramirez et. al., 1980). This procedure may be used to obtain the complete adsorption isotherm (the Langmuir isotherm) from a single core flood (Novosad et. al., 1986).

The derivation of the Langmuir equation is straightforward and elegant, but involves severe simplifying assumptions. Its ability to describe many adsorption data, both at the gas/solid and solid/liquid interface, results from the fact that it adequately describes the general shape of many adsorption isotherms. Even though the Langmuir equation is adequate for some systems, a thermodynamically consistent approach to describing adsorption involves the use of surface excess functions (Sircar et. al., 1972). The surface excess has been incorporated into a transport equation for flow through porous media by Huang (1985). The applicability of this model to surfactant adsorption, and its superiority over the Langmuir model have been demonstrated by Huang (1985) and by Mannhardt and Novosad (1987a). Much of the work presented in this thesis is based on the surface excess model, and this model will therefore be reviewed in the next chapter. Refinements and extensions to the model will then be described in the following chapters.

Most of the surfactant adsorption studies appearing in the petroleum literature take a fairly simple approach to the description of adsorption, such as, for example, the Langmuir adsorption isotherm. Data for the specific systems under consideration are measured, but no unifying theory on the underlying principles is presented. There is, however, a very large amount of literature on the behavior of surfactants in solution and on the fundamental aspects of surfactant adsorption. Some of this work will be reviewed briefly in chapter 6.

Reviews on surfactant adsorption have been written by Clunie and Ingram (1983) and Hough and Rendall (1983).

The rock/surfactant systems encountered in petroleum reservoir applications are usually extremely complex. Not only are both the rock and the surfactant multicomponent systems, but the composition of both is often unknown. In contrast, the systems studied in the more fundamental work on surfactant adsorption are usually well-defined, either pure surfactants or well-defined mixtures being used. The solids are usually strongly adsorbing, clean materials such as silica, alumina, and kaolinite, which greatly facilitate measuring adsorption from changes in surfactant concentration. Description of adsorption mechanisms includes factors such as the electrical double layer at the solid surface (Somasundaran et. al., 1964; Somasundaran and Fuerstenau, 1966; Wakamatsu and Fuerstenau, 1968; Dick et. al., 1971; Fuerstenau and Wakamatsu, 1975), monomer-micelle equilibrium in surfactant solutions (Trogus et. al., 1979a, Harwell et. al., 1982, 1985b), lateral interactions between adsorbed surfactant molecules and two-dimensional phase transitions at the interface (Scamehorn et. al., 1982a, 1982b), and detailed electrostatic interactions in the adsorbed layer (Harwell et. al., 1985a). The detailed molecular-level description of the interfacial layer models the distinctive features of surfactant adsorption isotherms adequately in well-defined systems (Scamehorn et. al., 1982a, 1982b; Harwell et. al., 1985a), and allows probing into the mechanisms involved, but would be much more difficult to apply to the complex solids and surfactant mixtures encountered in

enhanced oil recovery. However, the fundamental principles of the behavior of surfactants in solution and at the solid/liquid interface have occasionally been used to explain some of the observations made in core floods (Trogus et. al., 1979b; Harwell et. al., 1982, 1985b).

In chapter 6 of this work some of these principles will be incorporated into the surface excess model in an attempt to model the chromatographic separation of surfactant mixtures in flow through porous media. Such separation of the components of a commercial surfactant mixture by differential adsorption on the solid surface will continuously change the composition of a surfactant flowing through a porous medium, with possibly detrimental effects on enhanced oil recovery. Some of the properties of surfactants may also allow tailoring of surfactant solutions for specific applications. The goal of modelling adsorption of surfactant mixtures, as described in chapter 6, is the detailed evaluation of adsorption of mixtures using relatively straightforward experimental and numerical techniques. The end result should be an easy-to-use and fairly general model that incorporates some of the fundamental work described in the literature. Such a model should be useful both in evaluating and in designing surfactant systems.

CHAPTER 2

THE SURFACE EXCESS CONCEPT IN MODELLING ADSORPTION IN FLOW THROUGH POROUS MEDIA

This chapter will review the surface excess concept and the dispersion equation for flow of an adsorbing chemical through porous media. Both have been used previously by Huang (1985) in modelling surfactant adsorption. Since Huang's model is used as a starting point for much of the material in the following chapters, it will be summarized briefly here.

1. The Surface Excess

The thermodynamic system considered consists of a solid, a bulk liquid, and an adsorbed liquid phase. The adsorbed phase is characterized in terms of the surface excess, which has often been described as the only thermodynamically consistent variable that should be used in describing adsorption (Sircar and Myers, 1971; Sircar et. al., 1972; Everett, 1973; Sircar, 1985a). The surface excess is defined as the difference in solute concentration before and after adsorption at the solid surface, or

$$n_i^e = n^o(x_i^o - x_i) \quad (1)$$

where n_i^e is the surface excess of component i in mmoles per unit mass of adsorbent, n^o is the amount of liquid per unit mass of adsorbent, x_i^o is the overall mole fraction of component i , and x_i is the mole

fraction of component i in the bulk liquid after adsorption. The quantities on the right hand side of this equation are all experimentally measureable, and the surface excess can therefore be determined directly without having to make any assumptions about the structure of the adsorbed phase or about the position of the dividing surface between the bulk and adsorbed phases. In addition to being of immediate practical value, equation (1) can be developed from thermodynamic principles using the Gibbs adsorption equation (Chattoraj and Birdi, 1984).

The material balance equations

$$n^o = n + n' \quad (2)$$

$$n_i^o = n_i + n'_i \quad (3)$$

together with equation (1) can be used to derive an alternate equation for the surface excess:

$$n_i^e = n'(x'_i - x_i) \quad (4)$$

or, equivalently:

$$n'_i = n_i^e + n'x_i \quad (5)$$

In these equations, primed variables refer to the adsorbed phase, unprimed ones to the bulk phase, and the superscript "o" to overall values. n represents amounts of liquid, n_i amounts of component i , and x_i mole fractions of component i , all either in the bulk (unprimed) or adsorbed (primed) phase. Equation (4) clearly demonstrates the relative nature of the surface excess: It is the excess of component i in the

adsorbed phase over the amount that would be present if the concentrations in the bulk and adsorbed phases were equal, i.e. if the solid had no preference for either component in the liquid.

The thermodynamics of excess functions have been described in detail for adsorption from binary liquid mixtures (Sircar and Myers, 1970, 1971; Sircar et. al., 1972; Larionov and Myers, 1971) and for single and multi-component gas adsorption (Sircar, 1985a). Reviews on the subject have been presented by Schay (1969a), Everett (1973), and Chatteraj and Birdi (1984). From these works it is clear that the thermodynamics of adsorption can be described completely using an experimental quantity, the surface excess, eliminating the need for using a derived quantity such as the amount adsorbed. The amount adsorbed is of uncertain theoretical significance, since it requires assumptions about the structure and size of the adsorbed phase.

In much of the adsorption literature it is the surface excess that is determined from concentration differences in batch adsorption tests, but the measured quantity is inaccurately denoted as the amount adsorbed. Equation (5) clearly shows that the amount adsorbed (n'_i) is not equal to the surface excess (n_i^e), the difference being made up by the term $n'x_i$. In dilute solution, however, the bulk phase concentration of component i (x_i) will be small, and surface excess and amount adsorbed will be nearly equal.

The development that follows is for a binary system, with

component 1 taken to be the surfactant and component 2 the solvent.

The quantity of practical interest in surfactant adsorption is usually the amount adsorbed rather than the surface excess. To define the amount adsorbed, a model defining the dividing surface between the bulk and adsorbed phases has to be specified. The frequently used monolayer model of adsorption leads to the definition of the amount adsorbed in the monolayer of a binary system as

$$\frac{1}{n'} = \frac{x'_1}{m_1} + \frac{x'_2}{m_2} \quad (6)$$

where m_1 and m_2 are the amounts of surfactant and water, respectively, required for monolayer coverage of the solid surface. Equation (6) is frequently referred to as a "monolayer assumption", but it has been pointed out by Larionov and Myers (1971) that multilayered adsorption could be modelled equally well using this equation, with m_1 and m_2 then representing the amounts of components 1 and 2 required to fully saturate the adsorptive capacity of the solid. It is important to realize that, even though the surface excess is independent of any definition of the adsorbed phase, the use of equation (6) results in a specific model of adsorption through the introduction of the monolayer assumption.

When the bulk phase concentration of component 1 (x_1) is zero, the adsorbed phase concentration (x'_1) also has to be zero. Similarly, when $x_1=1$, $x'_1=1$ also. Using equation (4), n_1^e is therefore zero at $x_1=0$ and at $x_1=1$, going through a maximum (or minimum) between these

concentrations. Since this can make extrapolation of experimental data unreliable, the selectivity has often been used as a measure of the relative compositions of the bulk and adsorbed phases. The selectivity, sometimes also referred to as the separation factor, is defined as

$$S = \frac{x'_1/x'_2}{x_1/x_2} \quad (7)$$

For positive adsorption of component 1, ($n_1^e > 0$), $S > 1$; for negative adsorption ($n_1^e < 0$), $S < 1$; and for a neutral surface that has no effect on either component in the liquid ($n_1^e = 0$), $S = 1$.

Combining equations (4), (6), and (7) leads to an expression for the surface excess of a monolayer adsorption model:

$$n_1^e = \frac{m_1 x_1 x_2 (S-1)}{S x_1 + (m_1/m_2) x_2} \quad (8)$$

Equations (4) and (6) to (8) can be combined to give the amount of component 1 adsorbed:

$$n'_1 = \frac{m_1 x_1 S}{S x_1 + (m_1/m_2) x_2} \quad (9)$$

For known values of m_1 , m_2 , and S , equations (8) and (9) allow calculation of adsorption isotherms of component 1. Typical examples for two completely miscible components are shown in Figure 1. For a brine/surfactant system, concentrations would be restricted to the low end of the concentration scale by the limited solubility of the surfactant.

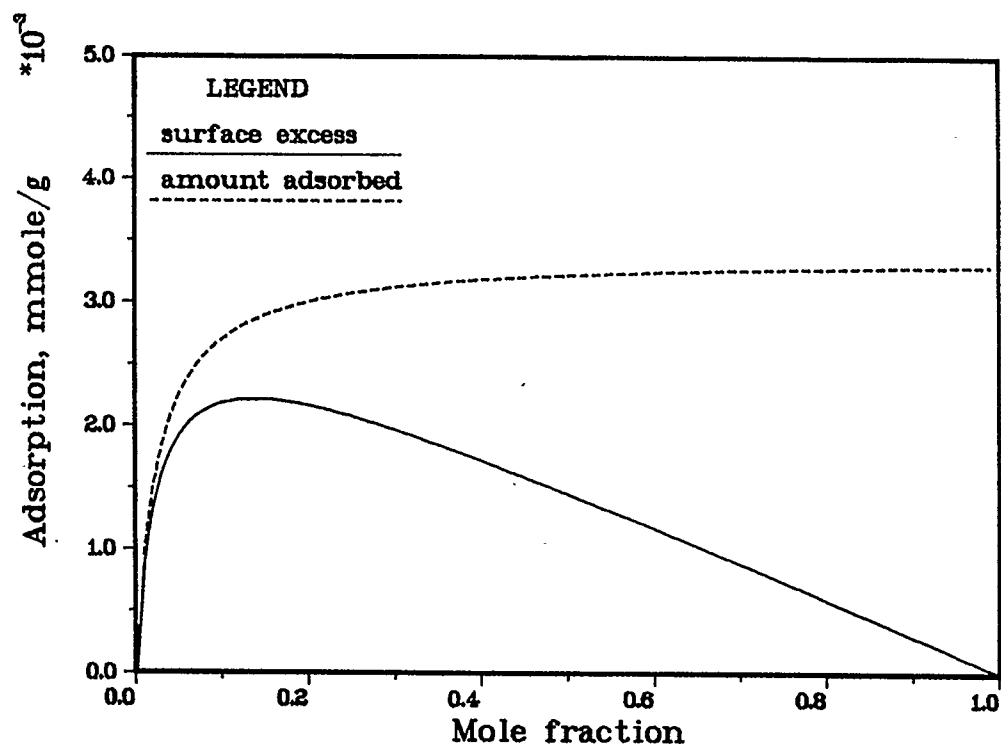


FIGURE 1. Typical adsorption isotherms for completely miscible liquids, as calculated from equations (8) and (9) with $S=10$, $m_1=0.0033$ mmole/g, $m_2=0.013$ mmole/g.

2. Modelling Adsorption in Flow through Porous Media

As has been mentioned in the introduction, adsorption can be determined through batch experiments by measuring the change in concentration of a solution after equilibration with a solid. The surface excess can then be calculated directly from equation (1). Since adsorption levels for the systems studied in this work are very low, batch experiments would yield very small differences between x_1^0 and x_1 , requiring extremely sensitive analytical methods (Novosad and Baxter, 1979). In flow experiments, on the other hand, the solid/liquid ratio can be much higher, allowing more accurate measurement of adsorption from the delayed arrival of a chemical at the core outlet.

Using a mass balance on a differential volume element, the one-dimensional dispersion model for flow through a homogeneous, non-adsorbing porous medium of constant cross-sectional area can be derived as:

$$D \frac{\partial^2 x_1}{\partial y^2} - v \frac{\partial x_1}{\partial y} = \frac{\partial x_1}{\partial t} \quad (10)$$

where y is distance, t is time, D is the dispersion coefficient, and v is frontal velocity. This equation is of the same form as the convective diffusion equation (Bird et. al., 1960), with the diffusion coefficient replaced by a dispersion coefficient. Equation (10) has been used very commonly for flow through porous beds. Various aspects of this equation have been discussed by Coats and Smith (1964) and

Nunge and Gill (1970). Assumptions implicit in equation (10) are constant flow rate, dispersion in the longitudinal direction only, a fluid density and dispersion coefficient that are independent of concentration, and no chemical reaction. If molecular diffusion is assumed to be negligible compared to dispersion, the dispersion coefficient D can be assumed to be proportional to the frontal velocity v (Perkins and Johnston, 1963; Coats and Smith, 1964):

$$D = \lambda v \quad (11)$$

where λ is a dispersion parameter.

Adsorption at the solid/liquid interface can be taken into account by adding an adsorption term to the mass balance equation (equation (10)). Different adsorption terms have been used by different authors, and these include Langmuir rate-controlled and equilibrium adsorption (Gupta, 1972; Trogus et. al., 1977; Ramirez et. al., 1980; Satter et. al., 1980; Ziegler and Handy, 1981; Novosad et. al., 1986), Freundlich equilibrium adsorption (Gupta, 1972), linear equilibrium and linear finite rate adsorption (Lapidus and Amundson, 1952; Gupta and Greenkorn, 1973), and bilinear adsorption (Gupta and Greenkorn, 1973). As has been stated previously, the surface excess is the thermodynamically correct, and therefore most appropriate, variable to describe adsorption. The surface excess has been incorporated into equation (10) to model flow of an adsorbing chemical through a porous medium by Huang (Huang, 1985; Huang and Novosad, 1986):

$$D \frac{\partial^2 x_1}{\partial y^2} - v \frac{\partial x_1}{\partial y} = \frac{\partial x_1}{\partial t} + \frac{1-\phi}{\phi} \frac{\rho_r}{\rho} \frac{\partial n_1^{ea}}{\partial t} \quad (12)$$

where n_1^{ea} is the actual (as opposed to equilibrium) surface excess, ρ_r is the rock density, and ρ is the liquid molar density.

The proper boundary conditions to be used with equations (10) and (12) have been discussed quite extensively in the literature. It has been pointed out by Danckwerts (1953) that the following initial and boundary conditions are appropriate for slug injection of a chemical into a system of finite length:

$$\begin{aligned} x_1(y, 0) &= 0 & 0 \leq y \leq L \\ vx_1(0, t) &= vx_{10} + D \frac{\partial x_1}{\partial y} & 0 < t \leq t_1 \\ vx_1(0, t) &= D \frac{\partial x_1}{\partial y} & t > t_1 \\ \frac{\partial x_1}{\partial y}(L, t) &= 0 & t > 0 \end{aligned} \quad (13)$$

where x_{10} is the mole fraction of surfactant in the injected solution, t_1 is the duration of chemical injection, and L is the core length. These boundary conditions have been confirmed and used by Kramers and Alberda (1953), Aris and Amundson (1957), Brenner (1962), and Satter et. al. (1980). Coats and Smith (1964) have presented a summary and discussion of the various boundary conditions for finite and infinite systems.

The second term on the right hand side of equation (12) can be

expressed in terms of simple first order kinetics:

$$\frac{\partial n_1^{ea}}{\partial t} = k_{1m}(n_1^e - n_1^{ea}) \quad (14)$$

$m = 1$, adsorption
 $m = 2$, desorption

where k_{1m} is the kinetics constant for component 1, n_1^e is the equilibrium surface excess as given by equation (8), and n_1^{ea} is the actual surface excess. When $n_1^e > n_1^{ea}$, adsorption is assumed to take place, and $k_{1m} = k_{11}$. When $n_1^e < n_1^{ea}$, desorption takes place, and $k_{1m} = k_{12}$. The kinetics in equation (14) have been used by Sircar (1985b) for adsorption of gases in adsorption columns, and by Sorbie et. al. (1987) for adsorption of partially hydrolyzed polyacrylamide on sandstone. Huang (1985) and Huang and Novosad (1986) have used equation (14) in the context of surfactant adsorption, and have found it to give satisfactory results.

The complete flow model is then given by equations (8) and (12) to (14). These equations are solved for the concentration at any point in the core at any time step by the finite difference scheme of Barakat and Clark (1966), which uses multi-level finite difference expressions for the partial derivatives in equations (12) and (13). Barakat and Clark have used this finite difference scheme to solve the unsteady heat or diffusion equation of the form

$$\frac{\partial T}{\partial t} = \nabla^2 T$$

Satter et. al. (1980) have used the Barakat and Clark method to solve a dispersion equation of the form of equation (12) with boundary

conditions (13).

There are several advantages to the Barakat and Clark finite difference scheme over the conventional implicit and explicit finite difference methods. It is completely explicit and therefore easier to program and less computationally intensive than the implicit method; yet, unlike the conventional explicit method, it is unconditionally stable without the rigid restrictions on space and time increments. The method has been shown to be accurate and to converge to the solution of the partial differential equation with proper choices of time and space increments (Barakat and Clark, 1966). The accuracy of the numerical scheme when used to solve equations of the form of equation (12) was demonstrated by Satter et. al. (1980). In the absence of adsorption, equation (12) reverts to equation (10), for which analytical solutions have been reported by Brenner (1962) and by Coats and Smith (1964). Results of the numerical solution to equation (12) with zero adsorption have been compared to the analytical solution to equation (10) by Mannhardt and Novosad (1987b), and good agreement was obtained. Details of the numerical solution to the flow model (equations (8) and (12) to (14)) can be found in the Appendix.

3. Applications of the Surface Excess Model

The flow model with surface excess adsorption can be used for detailed evaluation of surfactant adsorption from core floods as follows. A core of porous rock is fully saturated with brine. A slug of

surfactant solution is then injected, followed by brine until the surfactant concentration at the core outlet drops to near-zero. A non-adsorbing tracer is usually injected together with the surfactant to serve as a check on the pore volume, volume of chemical solution injected, and line volumes. In addition, the delay of surfactant breakthrough as compared to tracer breakthrough is a direct measure of adsorption. Effluent samples are collected at the core outlet and analyzed for surfactant and tracer concentrations. When concentrations are plotted against throughput, this results in effluent profiles characteristic of the surfactant, brine, rock, and temperature used in the core flood.

The flow model is then used to match the calculated effluent profiles to the experimental ones by adjusting the six parameters in the model: selectivity, S , monolayer coverage parameters for surfactant and water, m_1 and m_2 , kinetics constants of adsorption and desorption, k_{11} and k_{12} , and the dispersion parameter, λ . The effect of each parameter on the shape of the effluent profile has been described elsewhere (Huang, 1985; Mannhardt and Novosad, 1987b). An example of a history match is shown in Figure 2. Once a match has been obtained, the set of parameters used to obtain the match can be used together with equations (8) and (9) to calculate the complete adsorption isotherm for the system and conditions under consideration. An example is shown in Figure 3, obtained from the effluent profile in Figure 2. A single core flood can thus be used to evaluate the complete surfactant adsorption isotherm.

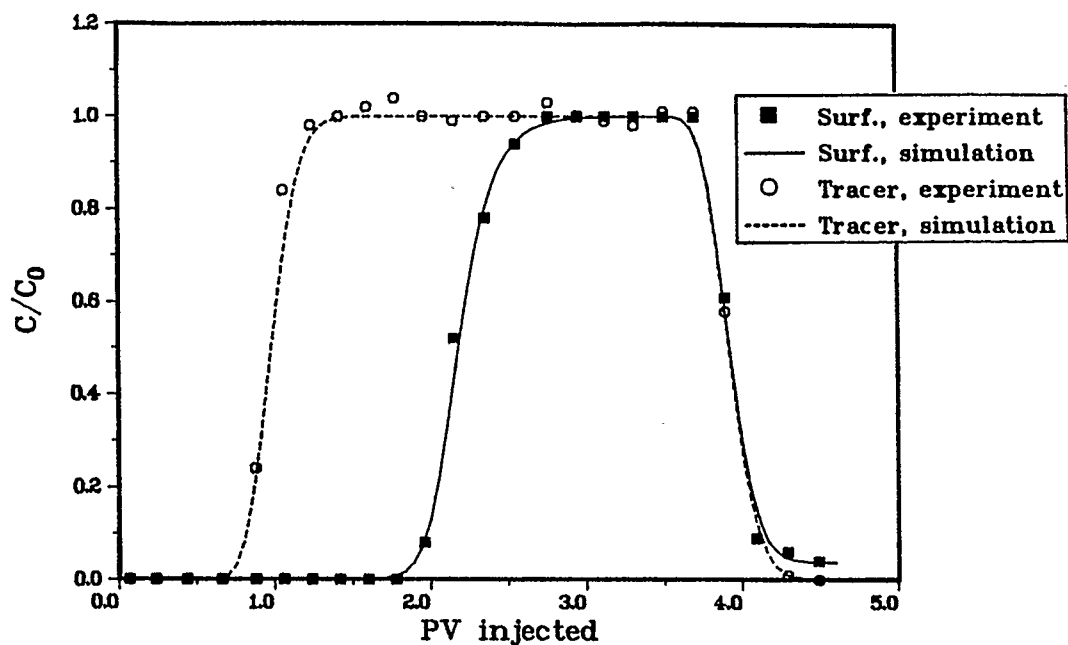


FIGURE 2. Example of a history match obtained with the surface excess model. (Taken from Mannhardt and Novosad, 1987b).

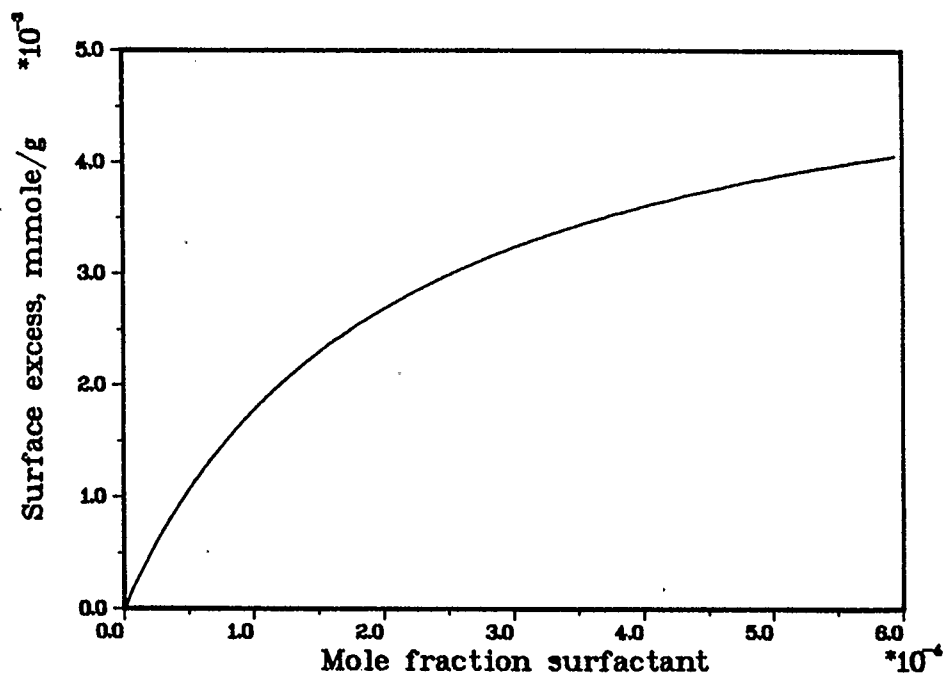


FIGURE 3. Adsorption isotherm calculated using the model parameters from the match in Figure 2 with equation (8). Surface excess and amount adsorbed are practically identical over this concentration range.

This method of analysis has been applied to experimental data from ten core floods by Huang (1985) to evaluate the temperature dependence of adsorption of three foam-forming surfactants that are potential candidates for mobility control in steam flooding. The same model has then been used by Mannhardt and Novosad (1987a, 1987b) to match data from more than thirty core floods with chemically very different surfactants that were being evaluated for their applicability to high salinity and hardness reservoirs (Novosad and Ionescu, 1987). These data yielded information on the dependence of adsorption of these surfactants on temperature and salinity. Even though very differently shaped effluent profiles were obtained for different systems, the model was capable of matching all experimental data satisfactorily.

It should be noted that the adsorption isotherms that can be calculated from equations (8) and (9) once S , m_1 , and m_2 have been obtained from a history match represent the equilibrium situation and do not contain any information on the kinetics of adsorption. This information can, however, be obtained from equation (14). Using the initial condition $n_1^{ea} = (n_1^{ea})_0$ at $t = t_0$, equation (14) can be solved to give the actual surface excess, n_1^{ea} , as a function of time, given the equilibrium surface excess, n_1^e :

$$n_1^{ea} = n_1^e + \left[(n_1^{ea})_0 - n_1^e \right] e^{-k_{1i}(t-t_0)} \quad (15)$$

n_1^e is determined from equation (8) at any concentration of interest using S , m_1 and m_2 from the history match. The actual surface excess

can then be determined as a function of time from equation (15) using k_{1i} , again obtained from the history match. This then allows complete evaluation of equilibrium and time dependent adsorption.

4. Extensions to the Surface Excess Model

In this section some shortcomings of the surface excess model will be outlined. Attempts at overcoming these will then be described in chapters 3 and 4. Also, two extensions to the model will be introduced, details of these appearing in chapters 5 and 6. The surface excess model described in the previous section will therefore serve as a starting point for the material outlined below and presented in more detail in the following chapters.

4.1 Independent Evaluation of m_1 and m_2

Three of the adjustable parameters used in the surface excess model are S , m_1 and m_2 . The effect of S and m_1 on the shape of the effluent profiles is shown in Figures 4 and 5. These curves were generated by simulating injection of 2 pore volumes of a 1% w/w (0.028 M) surfactant solution into a core similar to the cores described in later chapters. The profile for zero adsorption is also shown as a reference point. This curve can be generated by setting $S=1$ (or $m_1=0$, or $k_1=0$). Clearly, both S and m_1 change the effluent profiles in similar ways, which may be indistinguishable when matching somewhat scattered experimental data. Increasing the selectivity of the surface

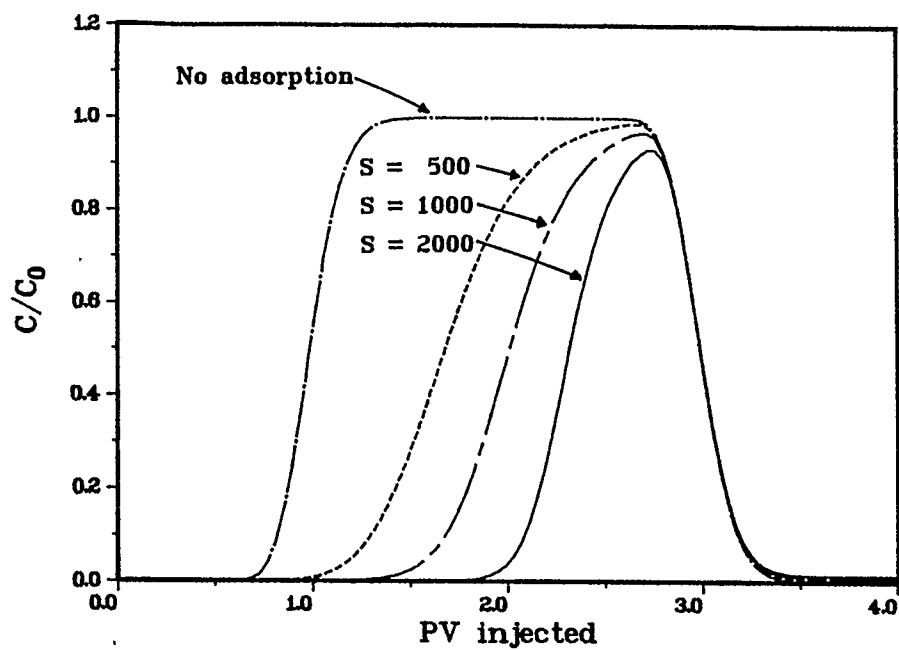


FIGURE 4. Effect of S on the effluent profile. $m_1=0.0055$ mmole/g, $m_2=0.013$ mmole/g, $k_1=1.0$ hr $^{-1}$, $k_2=0.001$ hr $^{-1}$, $\lambda=0.15$ cm.

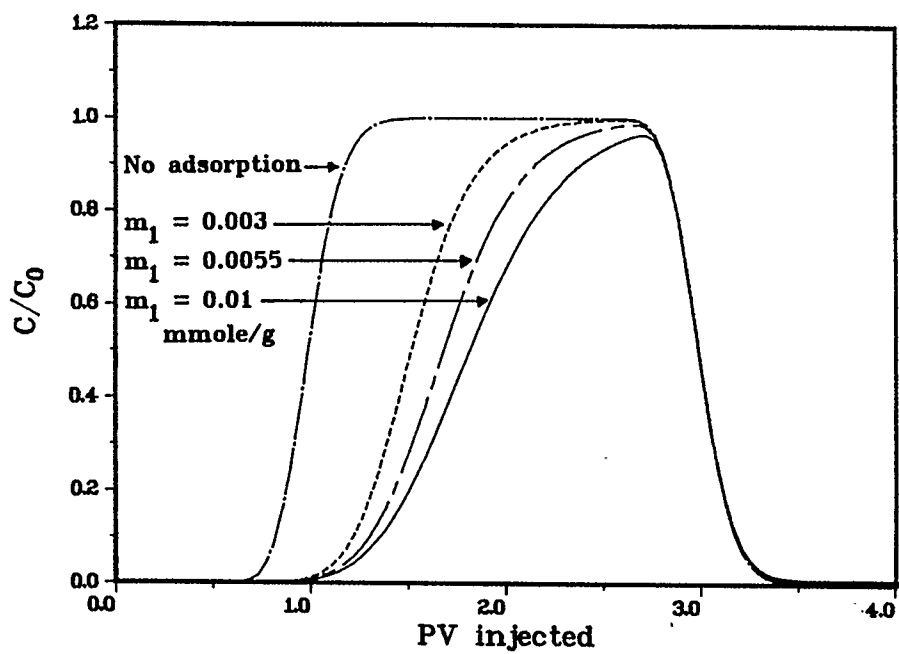


FIGURE 5. Effect of m_1 on the effluent profile. $S=500$, $m_2=0.013$ mmole/g, $k_1=1.0$ hr $^{-1}$, $k_2=0.001$ hr $^{-1}$, $\lambda=0.15$ cm.

for the surfactant (S), or increasing the adsorptive capacity of the rock (m_1) both delay arrival of the surfactant at the core outlet. This means that similar matches of the same set of experimental data can be obtained with different combinations of the parameters S and m_1 . It also means that it is not possible to determine a value of the adsorptive capacity of the rock (m_1) from a history match. For the effluent profile to be determined uniquely by a single set of parameters, an independent method of determining either S or m_1 should therefore be used. A method for estimating values of m_1 and m_2 independently is described in chapter 3. This will then reduce the number of adjustable parameters in the model from six to four.

4.2 Dependence of Selectivity on Concentration

In the model described above, S has been assumed constant. However, S is unlikely to remain constant as concentrations change. Core floods that were run at the same conditions, but at different injected surfactant concentrations showed that a low concentration flood required a higher selectivity than a higher concentration flood to obtain a match with experimental data. This indicates that, for such a system, selectivity should be a decreasing function of concentration. Functional forms of the selectivity will be investigated in chapter 4 and incorporated into the surface excess model.

4.3 Heterogeneous Surfaces

Reservoir rocks invariably consist of different mineral components

and are therefore highly heterogeneous in terms of the adsorptive energy of the solid surface toward the surfactant molecules. Even clean, single-component substances like silica gel, alumina, and activated carbon have been shown to exhibit surface heterogeneity with respect to adsorption of various chemicals. This aspect of adsorption will be discussed in chapter 5, and surface heterogeneities will be incorporated into the flow model, again using the surface excess to model adsorption. Modelling heterogeneous surfaces may eventually lead to the prediction of adsorption from a knowledge of the mineral components of a rock.

4.4 Adsorption of Surfactant Mixtures

Surfactants used in enhanced oil recovery are complex mixtures. The different components in the mixture may have different functions in the recovery of oil. Petroleum sulfonates, for example, are made by sulfonation of petroleum feedstocks that contain a large variety of chemicals in terms of both molecular weight and chemical structure. In such a mixture the lower molecular weight components may help to solubilize the higher molecular weight components, while the interfacial activity required to mobilize oil is provided by the high molecular weight species (Gale and Sandvik, 1973). If the components of such a mixture separate chromatographically by differential adsorption of the components during flow through the porous medium, then the composition of the surfactant solution will change continually, and as a result surfactant performance is likely to change. The same problem

may occur in surfactants that have been blended to optimize performance parameters such as solubility, salt tolerance, interfacial activity, and foaming capability.

A second aspect of the behavior of surfactant mixtures is the possibility of lowering adsorption by mixing of different surfactant types. This aspect of the adsorption of surfactant mixtures is intimately connected to monomer-micelle equilibria in surfactant solutions. Again, when surfactants are mixed to lower adsorption, the problem of chromatographic separation will have to be taken into account.

These topics will be described in chapter 6, and a model for flow of surfactant mixtures through porous media will be developed. This model should allow both the evaluation of adsorption of surfactant mixtures and the design of surfactant systems with low adsorption levels or reduced chromatographic separation of components.

CHAPTER 3

DETERMINATION OF THE MONOLAYER COVERAGES OF SURFACTANT AND WATER

m_1 and m_2 are the moles of surfactant and water, respectively, required for full monolayer coverage of the surface in a unit mass of solid. Independent determination of these quantities reduces the number of parameters in the surface excess model from six to four, and allows determination of a single set of parameters from the effluent profile from a core flood. Estimation of these parameters requires a knowledge of two quantities:

- (i) the specific surface area of the rock, and
- (ii) the surface area that a surfactant or water molecule occupy at the surface.

This chapter will describe methods of estimating these quantities.

1. The Specific Surface Area of a Solid

Knowledge of specific surface areas of solids is of importance in many industrial applications. A wide range of methods for their determination is available, and an immense amount of literature on the subject exists (Young and Crowell, 1962). Despite the variety of methods, the one that appears to be used most commonly and seems to be the standard against which other methods are compared, is still the Brunauer-Emmett-Teller (BET) gas adsorption method, now 50 years old

(Brunauer et. al., 1938, 1967). This method is based on the determination of the volume of a gas adsorbed on a solid close to the condensation temperature of the gas. The most commonly used gas for this purpose is nitrogen, although many other inorganic and organic gases have also been applied (Brunauer et. al., 1938; Young and Crowell, 1962; ; Gregg and Sing, 1967).

The BET method is based on the determination of the volume of gas adsorbed (V) at different partial pressures (P) of the adsorption gas, P_0 being the vapor pressure of the gas. The BET equation is as follows:

$$\frac{P}{V(P_0 - P)} = \frac{1}{V_m C} + \frac{C-1}{V_m C} \frac{P}{P_0} \quad (16)$$

where V_m is the volume adsorbed at monolayer coverage, and C is a parameter related to the energy of adsorption. When the left hand side is plotted against P/P_0 , a straight line usually results over a range of P/P_0 from 0.05 to 0.35. The slope and intercept of this straight line allow determination of V_m and C . From a knowledge of V_m and the molecular area of the gas the specific surface area can be calculated. Different experimental techniques for the BET method have been summarized by Gregg and Sing (1967) and Kantero et. al. (1967), and a few of the more important modifications and expansions of the BET method have been outlined by Young and Crowell (1962) and Brunauer et. al. (1967). The practical value of the BET method lies in its simplicity, but this also gives rise to some of its shortcomings (Young and Crowell, 1962; Brunauer et. al., 1967; Gregg and Sing, 1967). Some of the latter arise from the assumptions of a uniform surface, no

lateral interactions between adsorbed molecules, the constancy of the parameter C , and equivalence of the evaporation-condensation properties in all but the first adsorbed layer. Nevertheless, the BET method is still considered a standard technique for specific surface area determination by gas adsorption.

Various methods employing adsorption from solution are also available, and although these are simpler than gas adsorption methods from an experimental point of view, they are more complex to deal with theoretically. Difficulties associated with these methods have been summarized by Gregg and Sing (1967) and Everett (1973). They derive in part from the uncertainties in the molecular area of the (often rather large and complicated) molecules used and their orientation at the surface. Secondly, the quantity measured experimentally is the change of concentration in solution, or the surface excess, but this is often erroneously equated to the amount adsorbed. In systems of limited solubility, a flat portion in the adsorption isotherm is therefore (inaccurately) interpreted as the saturation adsorption capacity of the solid, while it may just indicate the maximum in the surface excess. This maximum may not be equal to saturation adsorption, as can be seen in Figure 1.

Methods for determining specific surface areas from surface excess adsorption isotherms of completely miscible liquids have been described by Schay (Schay and Nagy, 1966, 1972; Schay, 1969a) and Everett (1964). Most of these methods depend on a portion of the isotherm, or

transformations thereof, being linear or nearly linear, the adsorptive capacity being determined from these sections. Schay's method requires extreme care in the interpretation of the isotherms, and has been criticised quite widely (Everett, 1973; Sircar, 1983, 1985c).

Some other methods for the measurement of specific surface areas include heat of immersion methods (Harkins and Jura, 1944a, 1944b) and mercury porosimetry (Rootare and Prenzlöw, 1967; Baiker and Richarz, 1977). The latter method is used quite extensively in studies of various properties of petroleum reservoir rocks, and may therefore be of some value in determining the surface areas of these materials.

Even though an extensive amount of literature exists on specific surface areas of various catalysts and adsorbents used for separation processes, there is almost none that deals with the surface area of porous reservoir rocks. Some work in this area has been done by Tignor et. al. (1952), Brooks and Purcell (1952), and Donaldson et. al. (1975). In the latter two papers, the specific surface areas of a number of consolidated and unconsolidated rocks and of glass bead packs is determined by the BET method and also by using measurements of permeability together with the Kozeny equation. This equation relates the specific surface area to the permeability, porosity and tortuosity of the rock. Since the permeability is a quantity of general interest in reservoir studies, the Kozeny equation seems to be a logical choice for determining surface areas of reservoir materials. However, it was shown by the above authors that this equation yields reliable results

only with porous materials exhibiting uniform pore sizes (glass beads), and the BET values of surface area were therefore considered more reliable. Values for various sandstones ranged from 0.6 to 6 m²/g, while those for limestones were somewhat lower at 0.06 to 0.5 m²/g.

The surface area of Berea sandstone measured by Donaldson et. al. (1975) ranges from 0.8 to 1.1 m²/g, comparing well with measurements carried out by the Petroleum Recovery Institute (unpublished results). Berea sandstone was the material used for the adsorption studies in this work. Since the literature values for the surface area of this rock were determined by the "standard" BET method, and because of the considerable difficulties associated with adapting any of the other techniques to our systems, an average value of 1 m²/g was assumed for the specific surface area of Berea sandstone in the determination of m_1 and m_2 .

2. Molecular Area

Once the surface area of the rock is known, the other quantities required for calculating m_1 and m_2 are the molecular area of water and that of the surfactant molecule. The considerable uncertainty in determining any molecular area can be appreciated from the articles by Livingston (1949) and McClellan and Harnsberger (1967), who discuss this subject in some detail. McClellan and Harnsberger have tabulated a large number of molecular areas for 85 organic and inorganic molecules. For each molecule, a range of values collected from different sources

is listed. From this listing it is obvious that, even for monatomic gases such as argon, the areas may show a wide distribution of values. The larger the molecule, especially for organic molecules, the wider the spread becomes. Values for nitrogen, the standard used most commonly with the BET method, range from 12.9 to 17.2 Å², 16.2 Å² being used most frequently. For comparison, areas for benzene, which is also used quite commonly in specific surface area determinations, range from 22 to 69 Å². The rather wide range in the molecular area of benzene shows that care has to be taken in assigning a molecular area, particularly for large molecules that may orient themselves in different ways at the surface.

Most of the molecular areas listed by McClellan and Harnsberger have been derived from adsorption studies. This method requires the use of a solid of known specific surface area. However, most methods of determining specific surface areas require a knowledge of the adsorbate's molecular cross-section, and therefore this seems to be a problem with no solution. Moreover, the area that a molecule occupies on one solid may not be the same as on another solid, and, to make matters worse, the solvent may also play an important role in adsorption from solution. The following example illustrates the extent of these difficulties: Allen and Patel (1971) have used microcalorimetry to determine cross-sectional areas of a homologous series of fatty acids, while Maron et. al. (1954) have used a soap titration method for the same fatty acids. Not only do the results differ substantially, but the areas determined by each author show

opposing trends as the homologous series is ascended. For molecules such as fatty acids, the orientation of the molecule at the interface obviously becomes an important factor.

Other methods of determining molecular areas, particularly for gases, include their estimation from the liquid density, from the constant b in the van der Waals equation of state, and from molecular models (Young and Crowell, 1962; Gregg and Sing, 1967; McClellan and Harnsberger, 1967). The method using the liquid density is based on the assumption that a molecule occupies similar volumes in the liquid and adsorbed states. A certain type of packing (for example hexagonal close packing) in the adsorbed layer is also assumed. This method has been elucidated and criticised by Karnaukhov (1985). McClellan and Harnsberger (1967) have shown some correlations of areas derived from different methods.

The molecular area of the simpler of the two molecules of interest in this work, water, has been taken from McClellan and Harnsberger's paper. Figure 6 shows the distribution of values listed by these authors. An average value of 12.5 \AA^2 was used for the determination of m_2 .

Estimates for the molecular area of a surfactant molecule have often been obtained from surface tension measurement and application of the Gibbs adsorption equation. A large number of molecular areas of surfactants determined in this way have been listed by Rosen (1978).

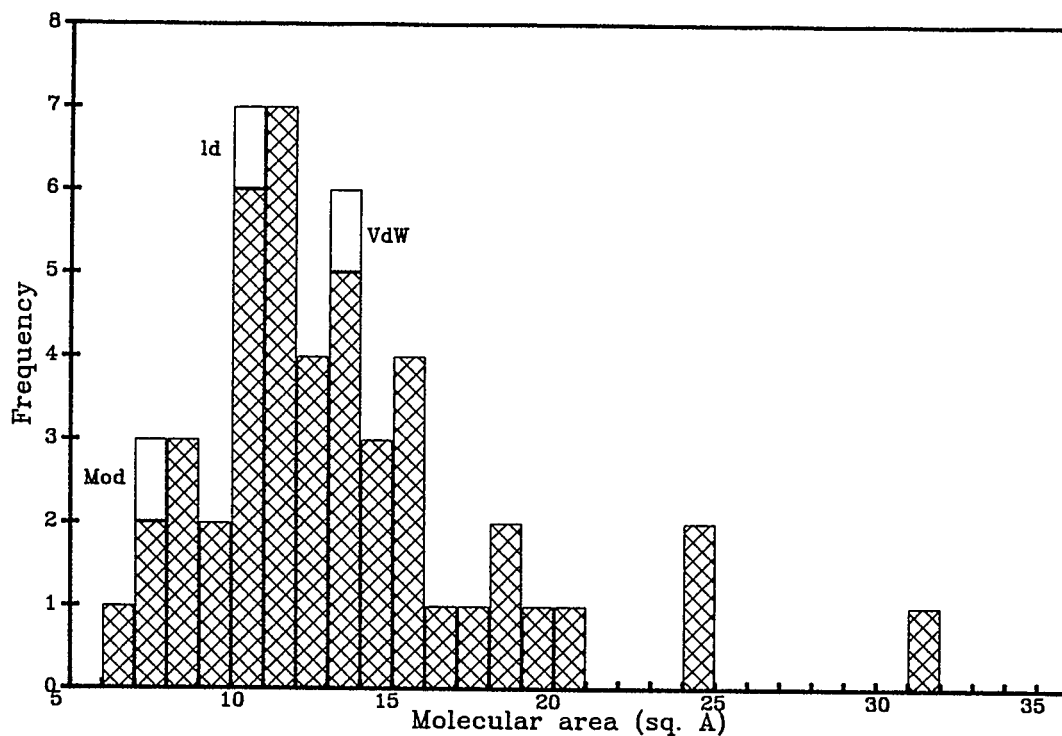


FIGURE 6. Distribution of values for the molecular area of water as listed by McClellan and Harnsberger (1967). The cross-hatched areas were derived from adsorption experiments. The clear areas are from molecular models (Mod), liquid density (ld), and the van der Waals constant b (VdW).

Total number of adsorption values: 46

Average of adsorption values: 12.5 sq. Å (excludes values > 21)

Standard deviation: 3.3 sq. Å

Temperature range of the measurements: 12 to 50 °C

This technique will be described in the next section and applied to two foam-forming surfactants. A different method, based on Maron's soap titration technique (Maron, 1954), has been used by Orr and Breitman (1960).

3. Determination of the Molecular Area of a Surfactant Molecule from the Gibbs Adsorption Equation

One of the effects of dissolving a surfactant in water is the substantial lowering of the surface tension of the aqueous phase, which results from the accumulation of surfactant molecules at the gas/liquid interface. As the surfactant concentration in the bulk solution is increased, the surface tension decreases, until the bulk solution reaches the critical micelle concentration (cmc). At this point a closely packed layer of surfactant molecules exists at the gas/liquid interface. Since no more surfactant will fit into the interfacial layer, the surface tension remains constant on further addition of surfactant to the solution. A sharp break in a plot of surface tension versus surfactant concentration therefore allows determination of the cmc. More importantly in the context of determining m_1 , such a plot also allows determination of the interfacial surfactant concentration, in moles per unit area, and therefore the cross-sectional area of a molecule at the gas/liquid interface. If the assumption is made that the surfactant molecules are arranged similarly in monolayers at the gas/liquid and solid/liquid interfaces, then this method provides a means of determining the area that the surfactant molecule occupies at

the solid/liquid interface.

To state the purpose of this section more clearly then, surface tension data are to be used to determine interfacial surfactant concentrations, and, from these, cross-sectional areas of surfactant molecules in a monolayer.

A number of descriptions of the use of a simplified form of the Gibbs adsorption equation to determine interfacial surfactant concentrations from surface tension data appear in the literature (Cockbain, 1954; Pethica, 1954; Bujake and Goddard, 1965; Weil, 1966):

$$-d\sigma = mRT\Gamma_R d \ln(c_R) \quad (17)$$

In this equation, σ is the surface tension, c_R the bulk surfactant concentration, R the gas constant, T the absolute temperature, Γ_R the surface excess of surfactant per unit surface area, and m is a constant. From this equation it can be seen that the slope of a plot of surface tension against the logarithm of concentration gives the surface excess at any particular concentration. It has often been noted that, for ionic surfactants, m takes the value of 1 in the presence of excess salt, but is equal to 2 in a salt-free surfactant solution. A theoretical basis for this observation is described in a series of papers by Chatteraj (Chatteraj, 1966a, 1966b, 1968a, 1968b, 1969; Chatteraj and Pal, 1972a, 1972b; Chatteraj and Birdi, 1984). A summary of this theory is presented in this section.

The isothermal Gibbs adsorption equation in its most general form is shown in equation (18) below:

$$-d\sigma = \sum_i \Gamma_i d\mu_i \quad (18)$$

where μ_i is the chemical potential and Γ_i the surface excess of component i . Some comments regarding Γ_i are in order at this point, since the surface excess Γ_i used here differs in definition from the surface excess n_i^e described in chapter 2. The surface excess can be defined in different ways; the differences and relationships between these definitions have been very clearly pointed out by Guggenheim and Adam (1933) and by Adamson (1976). Γ_i is the surface excess as originally used by Gibbs. According to Gibbs' definition, a species i in solution has the surface excess Γ_i , if a portion of the liquid containing unit area of surface contains Γ_i moles of species i more than a portion in the interior which contains exactly the same amount of a reference species j . The reference species is often taken as the solvent. Γ_j is therefore taken to be zero in this definition. The quantity Γ_i^a is often referred to as the apparent surface excess. It is used more commonly than Γ_i , since it is more easily visualized and is more symmetrical with respect to the components. A portion of liquid with unit surface area has the surface excess Γ_i^a , if it contains Γ_i^a moles of species i more than a portion in the interior containing exactly the same total number of moles of all species. n_i^e , as used in chapter 2, is equivalent to Γ_i^a , but is expressed on a unit mass of adsorbent basis rather than a unit surface area basis. The Gibbs adsorption equation, which forms the foundation of this section, uses

the Gibbs surface excess Γ_i .

For a solution containing an anionic surfactant RNA_Z and sodium chloride, equation (18) can be written

$$-d\sigma = \Gamma_R d\mu_R + \Gamma_{\text{Na}} d\mu_{\text{Na}} + \Gamma_{\text{Cl}} d\mu_{\text{Cl}} \quad (19)$$

The chemical potential of each solute i can be expressed by

$$\mu_i = \mu_i^{\circ} + RT \ln(f_i c_i) \quad (20)$$

which may be differentiated to give

$$d\mu_i = RT \left[d \ln(f_i) + d \ln(c_i) \right] \quad (21)$$

where f_i , c_i , and μ_i° are the activity coefficient, molar concentration, and standard chemical potential of component i . Substituting equation (21) into equation (19) and rearranging yields

$$-d\sigma = mRT\Gamma_R d \ln(c_R) \quad (22)$$

where

$$m = \xi_R \left[1 + \frac{\Gamma_{\text{Na}}}{\Gamma_R} \frac{\xi_{\text{Na}}}{\xi_R} \frac{d \ln(c_{\text{Na}})}{d \ln(c_R)} + \frac{\Gamma_{\text{Cl}}}{\Gamma_R} \frac{\xi_{\text{Cl}}}{\xi_R} \frac{d \ln(c_{\text{Cl}})}{d \ln(c_R)} \right] \quad (23)$$

and

$$\xi_i = 1 + \frac{d \ln(f_i)}{d \ln(c_i)} \quad (24)$$

If the value of m can be estimated from experimental data, the value of Γ_R can be determined from the slope $d\sigma/d \ln(c_R)$ using equation (22).

Since we will be dealing with constant salt concentration, the term in $d \ln(c_{Cl})$ in equation (23) can be set equal to zero. Electroneutrality of the bulk and surface phases requires that

$$z c_R + c_{Cl} = c_{Na} \quad (25)$$

and

$$z \Gamma_R + \Gamma_{Cl} = \Gamma_{Na} \quad (26)$$

By rearranging equation (26) it can be shown that

$$\frac{\Gamma_{Na}}{\Gamma_R} = \frac{z}{1 - \Gamma_{Cl}/\Gamma_{Na}} \quad (27)$$

while differentiation of equation (25) at constant c_{Cl} gives

$$\frac{d \ln(c_{Na})}{d \ln(c_R)} = \frac{c_R}{c_{Na}} \frac{dc_{Na}}{dc_R} = \frac{z c_R}{z c_R + c_{Cl}} \quad (28)$$

Inspection of equations (23), (24), (27), and (28) then shows that determination of m (at constant c_{Cl}) requires evaluation of ξ_R , ξ_{Na} , and Γ_{Cl}/Γ_{Na} . The former can be obtained from an activity coefficient model, while the latter can be determined using electrical double layer theory.

Chattoraj and Birdi (1984) have used the Debye-Hückel theory to determine the values of ξ_R and ξ_{Na} from equation (24). They found that, at low surfactant and high salt concentrations, ξ_R and ξ_{Na} both approach 1. For the systems studied here, surfactant concentrations are very low (10^{-4} M or less), and relatively high salt concentrations that are representative of reservoir brines are present (2.1 to 15.7% TDS, or, if equivalent NaCl is assumed, 0.36 to 2.7 M). Since the surfactant

is dilute, the assumption that $\xi_R=1$, is probably quite reasonable. Looking at the salt concentration, however, the Debye-Hückel theory should not be applied, since its limit of validity is a salt concentration of 0.1 M at the most (Harned and Owen, 1958; Bockris and Reddy, 1970). Chattoraj and Birdi have, however, summarized experimental evidence that shows that, at surfactant concentrations as low as those used here, the value of m is very close to 1 even at salt concentrations as low as 0.01 M. The higher the salt concentration, the closer m becomes to 1. From the evidence provided by these authors, the assumption that $\xi_{Na}=1$ also would seem very reasonable.

The value of Γ_{Na}/Γ_R (equation (27)) can be estimated by considering the electrical double layer of charged surfactant molecules and their counterions at the interface.

The Helmholtz double layer model considers the adsorbed phase to consist of a negatively charged layer of surfactant molecules, with an equal number of positively charged counterions a distance of the order of a molecular thickness away from the surface. This arrangement resembles the plates of a condenser. The assumption made in this model is $\Gamma_{Cl}=0$, and therefore

$$z\Gamma_R = \Gamma_{Na} \quad (29)$$

Substituting equations (28) and (29) into (23) yields an expression for m :

$$m = \xi_R \left[1 + \frac{\xi_{Na}}{\xi_R} \frac{z^2}{z+x} \right] \quad (30)$$

where $x = c_{Cl}/c_R$, or the salt to surfactant ratio. Setting $\xi_i=1$, m can be seen to approach 1 at high salt concentrations (large x), while $m=1+z$ in the absence of salt, or $m=2$ for a univalent surfactant in the absence of salt.

A more realistic double layer model is provided by the Gouy-Chapman double layer theory. Here the double layer again consists of the (negatively charged) adsorbed surfactant, but the counterions are now distributed non-uniformly in the diffuse part of the double layer. The concentration of positive ions is high near the surface and decreases toward the bulk concentration with distance from the surface. Conversely, the concentration of negatively charged inorganic ions is low near the surface and increases to the bulk phase concentration away from the surface. It has been shown by Bijsterbosch and van den Hul (1967) that in this model the ratio Γ_{Cl}/Γ_{Na} can be expressed by the equation

$$\frac{\Gamma_{Cl}}{\Gamma_{Na}} = - \frac{c_{Cl}}{c_{Na}} e^{\epsilon\psi_0/2kT} \quad (31)$$

where ϵ is the electronic charge, ψ_0 is the potential at the solid surface, and k is Boltzmann's constant. Substituting equations (28) and (31) into (23) results in

$$m = \xi_R \left[1 + \frac{\xi_{Na}}{\xi_R} \frac{z^2}{z + x \left[1 + e^{\epsilon\psi_0/2kT} \right]} \right] \quad (32)$$

Again, with $\xi_i=1$, at high salt concentrations and/or high ψ_0 (ψ_0 being a negative number) m will approach 1, while $m=1+z$ in the absence of salt. In the limit as $\psi_0 \rightarrow -\infty$, m will be the same as in the Helmholtz double layer model.

A third double layer model is the Stern model. This model combines the features of the previous two models in that it assumes that some fraction of the Na^+ counterions remain physically bound to the adsorbed organic anions (as in the Helmholtz model), while the remaining counterions exist in the diffuse part of the double layer. Values of m from this model will always fall in between those from the other two models, since the Stern model reverts to the Helmholtz model or Gouy-Chapman model in the limit when the number of bound counterions approaches a very large value or zero, respectively.

Chattoraj and Pal (1972b) have pointed out that m is only weakly dependent on the value of the surface potential ψ_0 , even for values of x as low as 2. In our systems, x exceeds 2000. From equation (30) or (32) it can be seen that m can therefore be taken as equal to 1 in equation (22). It has also been shown that, if a mixture of salts is present, x can be taken as the ratio of total salt cation to surfactant concentration (Chattoraj and Pal, 1972b). When the surfactant is a mixture of surface active components, the surfactant concentration c_R will simply be the overall concentration of all components (Chattoraj and Pal, 1972b).

For cationic surfactants the treatment of the Gibbs adsorption equation is equivalent to that given above for anionics, and for nonionic surfactants m will obviously be equal to 1, since these do not dissociate. Okumura et. al. (1974) and Nakamura et. al. (1975) have studied amphoteric surfactants in conjunction with the Gibbs adsorption equation. These surfactants contain a positive (eg. quaternary ammonium) and a negative (eg. carboxyl or sulfonate) group within the same molecule. In the context of this thesis this surfactant type is of interest in foam flood applications in high salinity environments. It was found that equation (22) applies to these surfactants with $m=1$ in the absence and presence of salt.

Ample experimental evidence for the applicability of equation (22), either in its "1" or "2" form, exists in the literature. Some earlier work has been mentioned above in conjunction with equation (17). Somewhat more recent measurements have been described by Japanese workers, who have compared values of Γ_R obtained from surface tension measurements and equation (22) with values from direct measurement of Γ_R using radiotracer methods (Tajima et. al., 1970, 1971; Tajima, 1970, 1971; Okumura, 1974; Nakamura, 1975). Excellent agreement between the different methods was obtained.

4. Experimental: Surface Tension Measurement of Foam-Forming Surfactants

Adsorption studies on several foam-forming surfactants have been

carried out by Mannhardt and Novosad (1987a) using the surface excess model described in chapter 2. In that work, the value of m_1 was estimated and kept constant for all surfactant types. In order to be able to use m_1 as an independently measured parameter, the molecular area of two foam-forming surfactants will be established in this section using the Gibbs adsorption equation.

The surfactants were commercial samples of a diphenylethersulfonate/alpha olefin sulfonate blend (DPES) and a betaine (Figure 7). The DPES was supplied by Dow Chemical, Fort Saskatchewan, Alberta, under the trade name Dow XS84321.05. The betaine is an amphoteric surfactant supplied by Albright and Wilson, Whitehaven, UK, under the trade name Empigen BT. Both surfactants have been shown to be suitable for mobility control in high salinity and hardness reservoirs (Novosad and Ionescu, 1987).

The surfactants were dissolved in simulated reservoir brines containing NaCl , CaCl_2 , MgCl_2 , and Na_2SO_4 at weight ratios of 187:35.2:4.78:1. The total solids content of the brines was adjusted to 2.1 and 14.7% by weight, keeping the ratio of components constant. The surface tension of the two surfactants in the two brines was determined as a function of surfactant concentration using the du Nouy ring method. A Fisher Model 20 surface tensiometer was employed in the measurements.

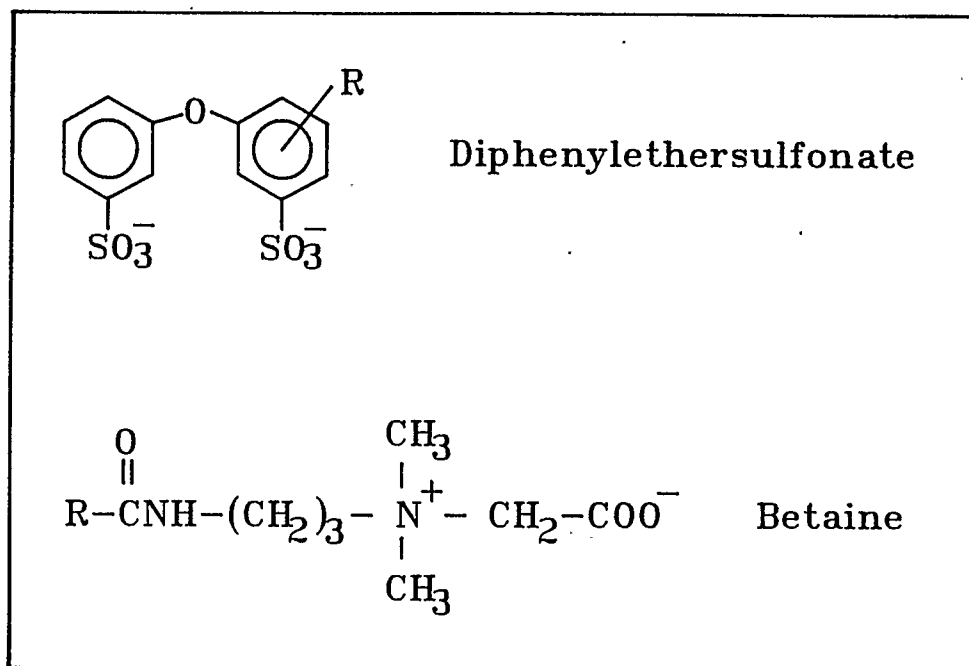


FIGURE 7. Chemical structures of two foam-forming surfactants.

5. Results of Surface Tension Measurements: The Molecular Area of Surfactant Molecules

The surface tensions of the DPES in 2.1 and 14.7% brines are shown as a function of the logarithm of surfactant concentration in Figures 8 and 9. An abrupt change in the surface tension can be seen to occur over a relatively narrow concentration range. The intersection of two nearly linear parts of the curve in this region gives the cmc. For the purpose of measuring the areas covered by molecules at the gas/liquid interface it is assumed that, at the cmc, a closely packed monolayer of surfactant molecules exists. The surface excess Γ_R at monolayer coverage can therefore be calculated from the slope of the curve just below the cmc. The plots of σ versus $\log(c_R)$ are linear over a fairly wide concentration range below the cmc, which greatly simplifies measurement of the slope. This linear concentration range has been observed by many other workers.

Once the slope has been determined, Γ_R (in mmole/cm²) is calculated from equation (22) with $m=1$, or

$$\Gamma_R = - \frac{1}{2.303 RT} \frac{d\sigma}{d \log(c_R)} \quad (33)$$

where $R=8.314 \times 10^4$ dyne cm/mmole K, $T=298$ K, σ is in dyne/cm, and c_R is in g/l (or any other unit of concentration). The molecular area A_m in Å²/molecule is then given by

$$A_m = \frac{10^{19}}{\Gamma_R N} \quad (34)$$

where N is Avogadro's number (6.023×10^{23}). Results of the surface

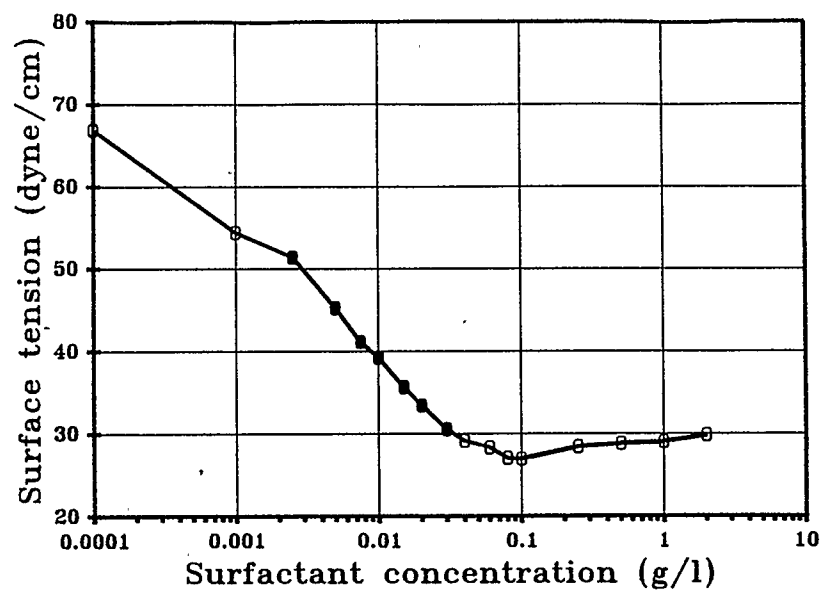


FIGURE 8. Surface tension of DPES in 2.1% brine. The filled points were used for determining $d\sigma/d \log(c_R)$.

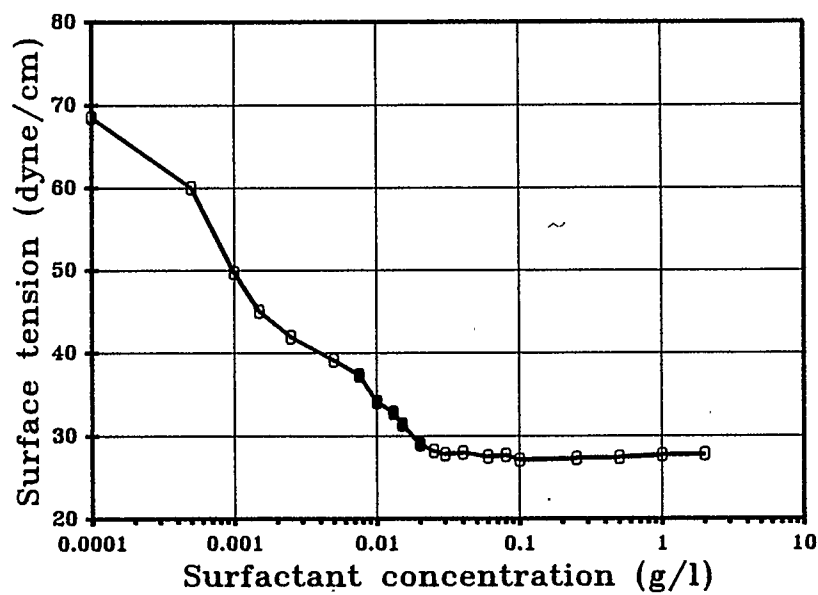


FIGURE 9. Surface tension of DPES in 14.7% brine. The filled points were used for determining $d\sigma/d \log(c_R)$.

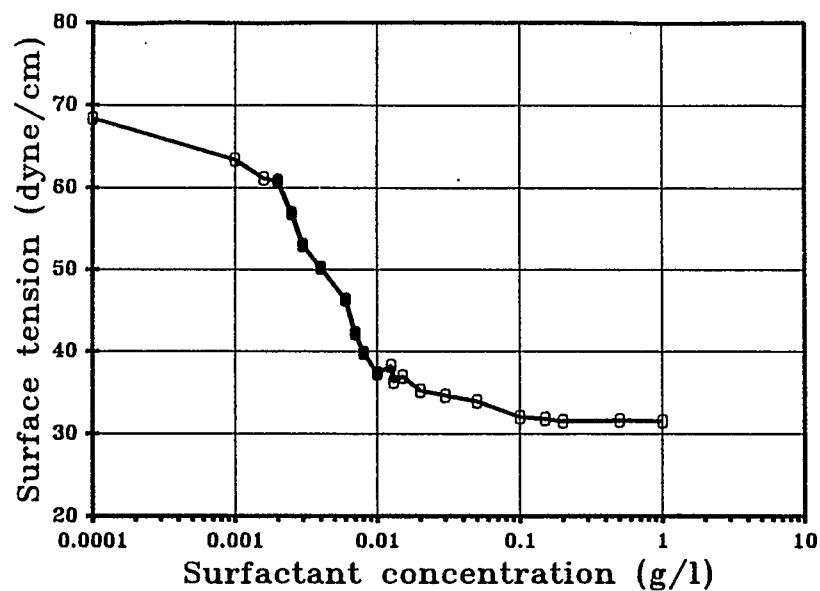


FIGURE 10. Surface tension of betaine in 2.1% brine. The filled points were used for determining $d\sigma/d \log(c_R)$.

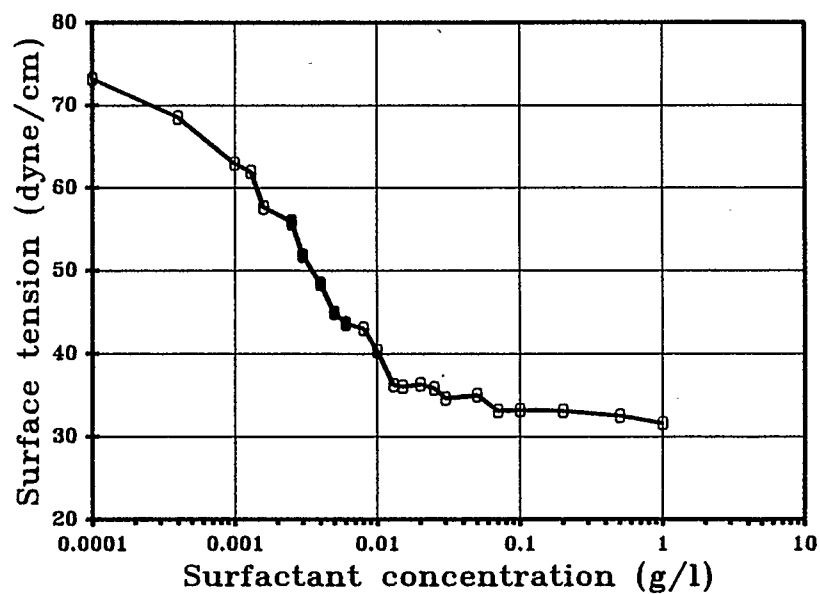


FIGURE 11. Surface tension of betaine in 14.7% brine. The filled points were used for determining $d\sigma/d \log(c_R)$.

tension measurements for the DPES are summarized in Table 1.

Surface tensions for the betaine are shown in Figures 10 and 11. For this surfactant the change to constant surface tension above the cmc seems to occur over a wider concentration range than for the DPES. Molecular areas calculated from the slope just below the cmc are listed in Table 1.

TABLE 1. Results of the determination of the molecular area of two surfactants at monolayer coverage from surface tension measurement.

| | DPES 2.1% brine | DPES 14.7% brine | Betaine 2.1% brine | Betaine 14.7% brine |
|--|-----------------------|-----------------------|-----------------------|------------------------|
| cmc (g/l) | 0.044 | 0.023 | 0.015 | 0.012 |
| Surface excess (mmole/cm ²) | 3.41×10^{-7} | 3.35×10^{-7} | 5.80×10^{-7} | 5.66×10^{-7} |
| Molec. area (sq. Angstrom) | 49 | 50 | 29 | 29 |

The data in Table 1 indicate a molecular area of about 50 \AA^2 for the DPES and 30 \AA^2 for the betaine. Since both brines contain high salt concentrations, no change of Γ_R with salt concentration is observed. Presumably much lower salt concentrations would have to be used to observe the dependence of Γ_R on salinity, as has been described in the literature (Cockbain, 1954; Tajima, 1971; Okumura et. al., 1974). The molecular areas determined here compare well with the values listed for a number of surfactants by Rosen (1978) and by Brandrup and Immergut

(1975), and also with the values cited in the other references appearing in this section.

6. Chapter Summary

The purpose of this chapter was to show how the parameters m_1 and m_2 were estimated from measurements at the gas/liquid interface. This required the determination of the specific surface area of the rock and the molecular area of water and surfactant. Once these quantities are known, m_1 can be calculated from the equation

$$m_1 = \frac{10^{19} A}{A_m N} \quad (35)$$

where m_1 is in mmole/g, A is the rock's specific surface area in cm^2/g , A_m is the molecular area in \AA^2 , and N is Avogadro's number. For the systems considered here, the results can be summarized as follows:

| | |
|--|------------------------------|
| Berea sandstone specific surface area: | $1 \text{ m}^2/\text{g}$ |
| Molecular area of water: | 12.5 \AA^2 |
| Molecular area of surfactant: | 50 \AA^2 (DPES) |
| | 30 \AA^2 (betaine) |

$$m_1 = 0.0033 \text{ mmole/g (DPES)}$$

$$m_1 = 0.0055 \text{ mmole/g (betaine)}$$

$$m_2 = 0.013 \text{ mmole/g (water)}$$

$$m_1/m_2 = 0.25 \text{ (DPES)}$$

$$m_1/m_2 = 0.42 \text{ (betaine)}$$

CHAPTER 4

THE DEPENDENCE OF SELECTIVITY ON SURFACTANT CONCENTRATION

In the surface excess model described in chapter 2, the selectivity has been assumed constant. However, the selectivity is defined as a ratio of concentrations in the adsorbed and bulk phases (equation (7)), and is likely to change as the bulk concentration changes. Experimental measurements of the selectivity appearing in the literature indicate that selectivity decreases with increasing concentration of the more strongly adsorbed component in a binary mixture (Schay, 1969a; Li and Gu, 1979). To test the validity of the assumption of constant selectivity, core floods were run at two different injected concentrations, and the surface excess model was used to match simulated concentration profiles with experimental ones.

1. Experimental: Core Floods

Materials

Berea core: Consolidated sandstone supplied by Cleveland Quarries.

Brine: Synthetic reservoir brine containing NaCl, CaCl_2 , MgCl_2 , and Na_2SO_4 at weight ratios of 187:32.5:4.78:1. The total salt concentration was adjusted to 10.5 and 21.0% by weight.

Surfactant: Dow XS84321.05, a 42% active diphenylethersulfonate/alpha olefin sulfonate blend, supplied by Dow Chemical, Fort Saskatchewan, Alberta. Assumed average molecular weight: 500.

Procedure

The Berea cores were of dimensions 2.5×2.5×15 cm, and had a pore volume of about 20 ml. They were coated with epoxy, and then completely saturated with brine by evacuating them, filling them with CO₂, and then flowing large volumes of brine through them against a backpressure of about 30 psi. The pore volume was determined from the difference in dry and brine saturated weights.

A slug of surfactant solution, at a concentration of either 1 g/l or 10 g/l, was then injected into the core, followed by brine until the surfactant concentration dropped to a negligible level. Tritiated water was injected as a non-adsorbing tracer together with the surfactant. Effluent samples were collected at the core outlet at regular time intervals and analyzed for surfactant and tracer concentrations. Surfactant concentrations were determined by two-phase titration (Reid et. al., 1967), and a scintillation counter was used to analyze for the radioactive tracer. The core floods were run at temperatures from 23 to 75°C, and using brines of 10.5 and 21.0% w/w total dissolved solids (TDS) concentrations.

Core properties for the eight cores used are listed in Table 2.

TABLE 2. Properties of Berea cores used for surfactant adsorption floods.

| Core # | T3 | T11 | T1 | T13 | T6 | T9 | T7 | T10 |
|-------------------------------------|-------|-------|-------|-------|-------|-------|-------|-------|
| Length (cm) | 14.95 | 15.15 | 14.95 | 15.00 | 14.65 | 15.15 | 14.85 | 14.83 |
| Cross-sect. Area (cm ²) | 6.38 | 6.81 | 6.38 | 6.50 | 6.12 | 6.85 | 6.25 | 6.90 |
| Porosity (fraction) | 0.235 | 0.210 | 0.248 | 0.225 | 0.213 | 0.211 | 0.215 | 0.207 |
| Abs. Perm. to Brine (md) | 255 | 234 | 376 | 457 | 176 | 238 | 197 | 196 |
| Rock Density (g/ml) | 2.92 | 2.56 | 2.97 | 2.73 | 2.73 | 2.53 | 2.66 | 2.54 |
| Brine Dens. (mg/ml) | 1052 | 1052 | 1074 | 1074 | 1149 | 1149 | 1134 | 1134 |
| Brine Molar Density (mmole/ml) | 53.9 | 53.9 | 55.1 | 55.1 | 54.2 | 54.2 | 53.4 | 53.4 |

2. Results: History Matching of Core Floods Using Constant Selectivity

The effluent concentrations of surfactant and tracer were normalized with respect to the injected concentrations and plotted against the number of pore volumes injected. The constant selectivity surface excess model was then used to match the experimental data. The best match parameters, together with the experimental conditions, are

listed in Table 3, and the experimental and simulated effluent profiles are shown in Figures 12 to 19.

The history matching was carried out by changing the parameters and observing the effect of each on the shape and position of the concentration profile. The best fit was chosen by visually comparing calculated and experimental data. The values of m_1 and m_1/m_2 used in performing the matching are those determined in the previous chapter. A value of k_1 equal to 1.0 seemed to be adequate for all floods. Rather large changes in this parameter (by a factor of 2 or more) are required to change the effluent profile significantly with respect to the somewhat scattered experimental data. Effluent concentrations are, however, more sensitive to the value of S . Changing S by 10% or more will shift the profile significantly. k_2 affects the shape of the trailing edge of an effluent profile, and increasing λ causes the profile to become more dispersed. The effects of changing the parameters have been described in more detail by Mannhardt and Novosad (1987).

The data in Table 3 show that the core floods were run in pairs, with the members of each pair at the same conditions, but using different injected surfactant concentrations. Figures 12 to 19 show that satisfactory matches were obtained for all floods, but from Table 3 it is obvious that the low concentration floods require considerably higher selectivities than the floods run at higher surfactant concentrations in order to match simulated and experimental data. This

TABLE 3. Experimental conditions and matching parameters for constant selectivity model.

| Core # | T3 | T11 | T1 | T13 | T6 | T9 | T7 | T10 |
|-------------------------------------|--------|--------|--------|--------|--------|--------|--------|--------|
| Surfactant Conc. (g/l) | 1.00 | 9.97 | 1.00 | 9.97 | 1.01 | 10.0 | 1.01 | 10.0 |
| Surfactant Mole Frac. $\times 10^4$ | 0.372 | 3.73 | 0.363 | 3.65 | 0.374 | 3.73 | 0.379 | 3.78 |
| Brine Conc. (% TDS) | 10.5 | 10.5 | 10.5 | 10.5 | 21.0 | 21.0 | 21.0 | 21.0 |
| Temp. (deg. C) | 75 | 75 | 23 | 23 | 50 | 50 | 75 | 75 |
| Slug Vol. (PV) | 1.04 | 0.73 | 1.01 | 0.78 | 2.12 | 0.86 | 2.04 | 1.14 |
| S | 900 | 100 | 1000 | 200 | 940 | 200 | 950 | 160 |
| m_1 (mmole/g) | 0.0033 | 0.0033 | 0.0033 | 0.0033 | 0.0033 | 0.0033 | 0.0033 | 0.0033 |
| m_1/m_2 | 0.25 | 0.25 | 0.25 | 0.25 | 0.25 | 0.25 | 0.25 | 0.25 |
| k_1 (1/hr) | 1.0 | 1.0 | 1.0 | 1.0 | 1.0 | 1.0 | 1.0 | 1.0 |
| k_2 (1/hr) | 0.005 | 0.002 | 0.005 | 0.005 | 0.003 | 0.003 | 0.002 | 0.002 |
| Dispersion Par. (cm) | 0.75 | 0.15 | 0.5 | 0.15 | 0.6 | 0.15 | 0.6 | 0.15 |

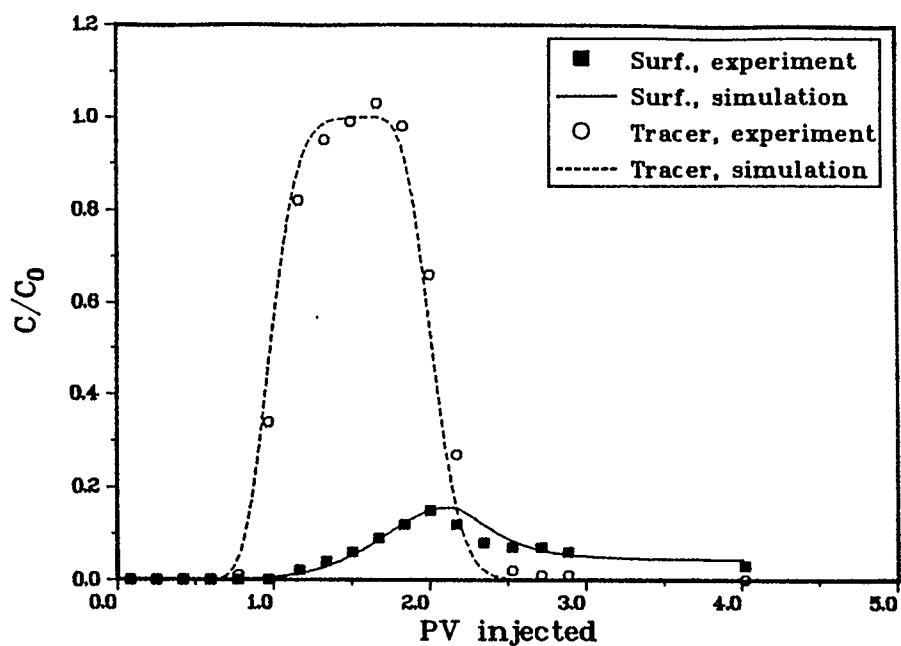


FIGURE 12. Core T3 effluent profiles. Constant selectivity model.

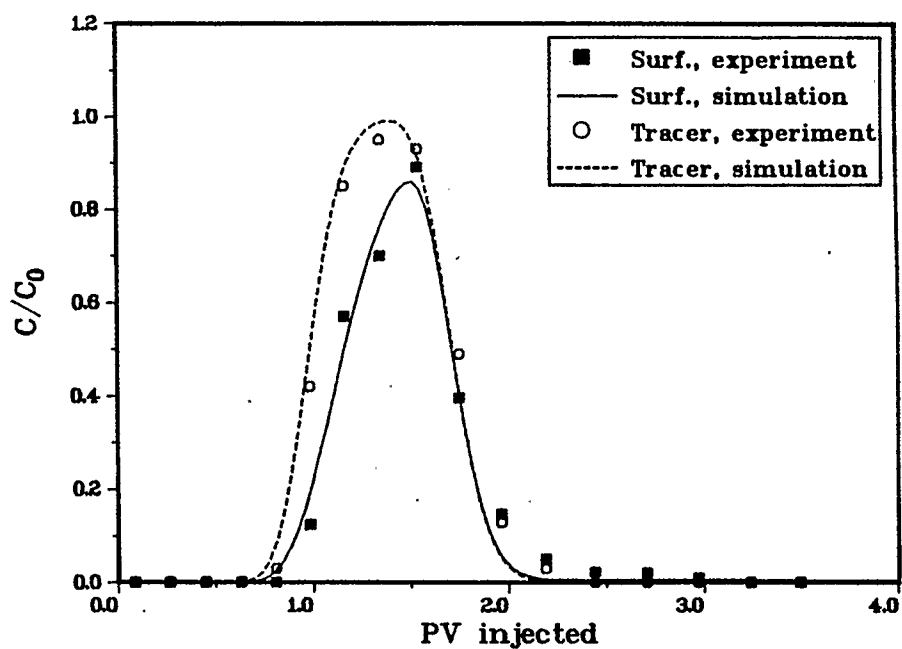


FIGURE 13. Core T11 effluent profiles. Constant selectivity model.

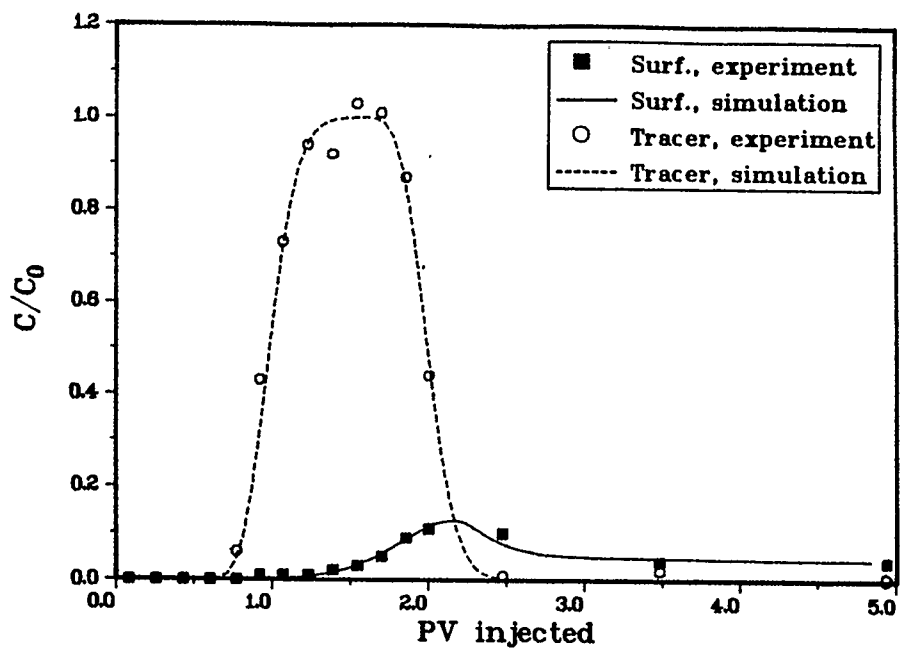


FIGURE 14. Core T1 effluent profiles. Constant selectivity model.

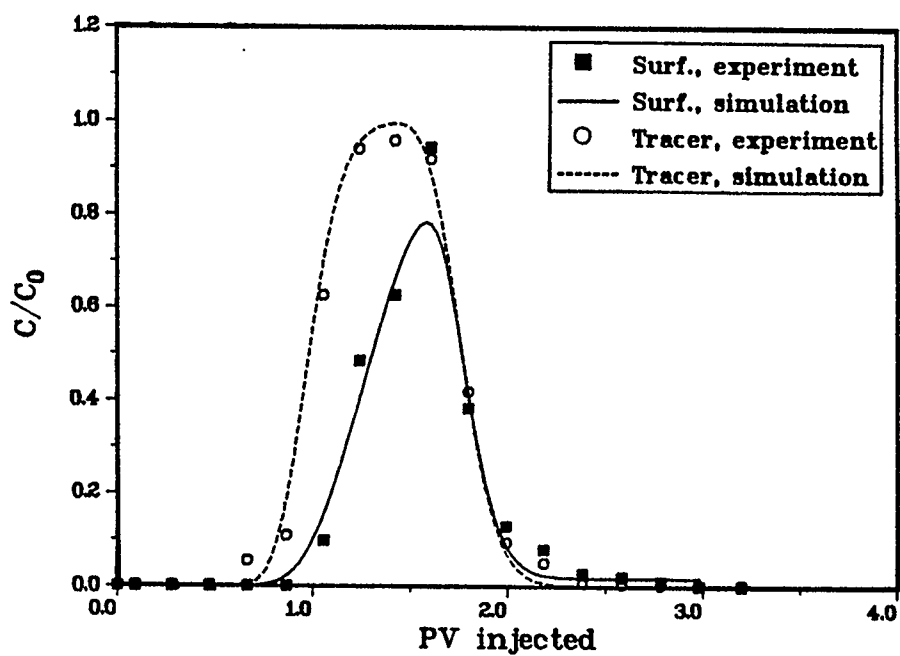


FIGURE 15. Core T13 effluent profiles. Constant selectivity model.

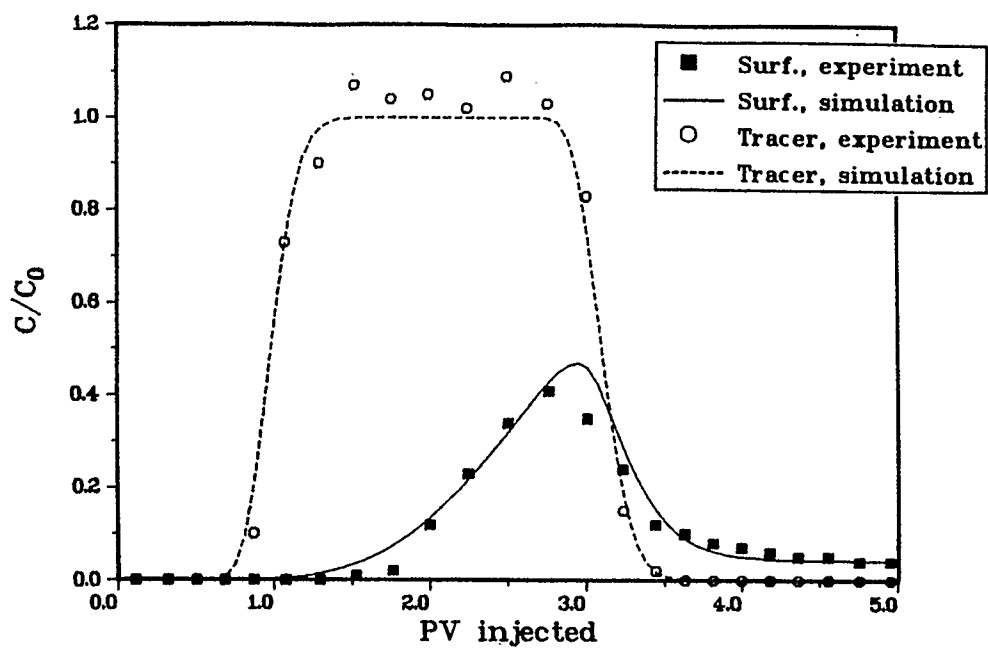


FIGURE 16. Core T6 effluent profiles. Constant selectivity model.

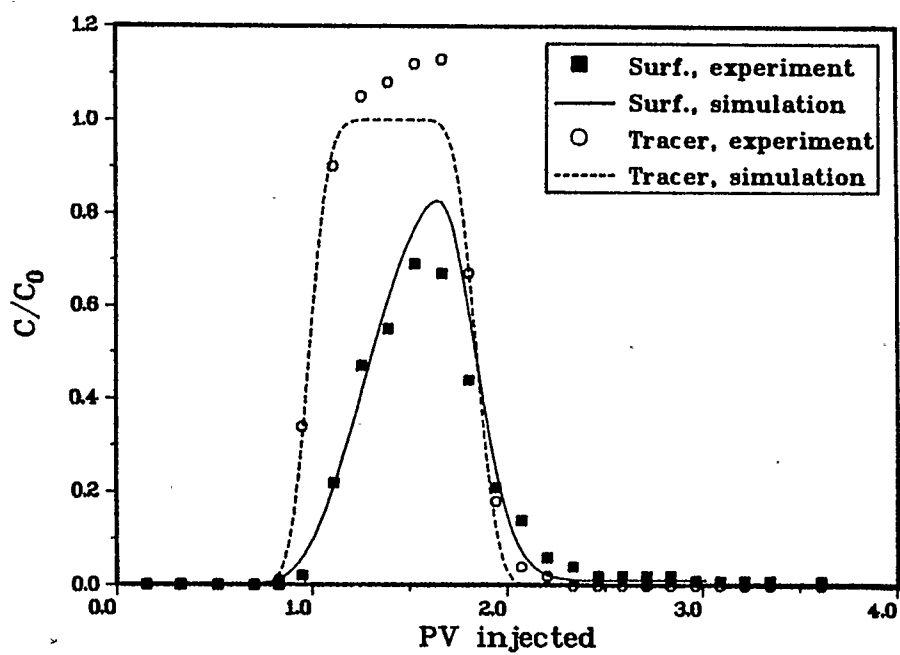


FIGURE 17. Core T9 effluent profiles. Constant selectivity model.

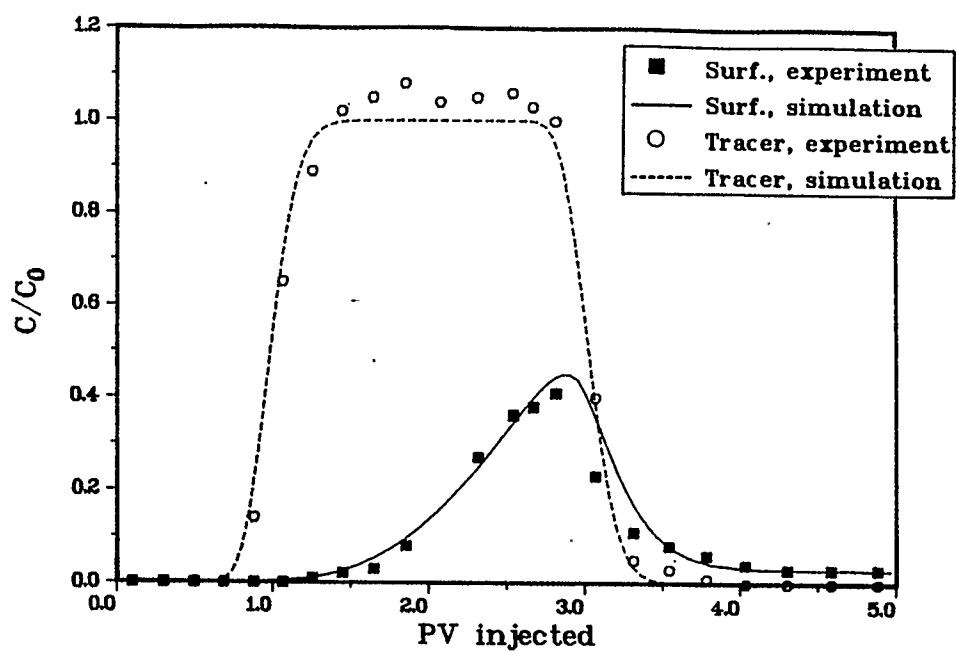


FIGURE 18. Core T7 effluent profiles. Constant selectivity model.

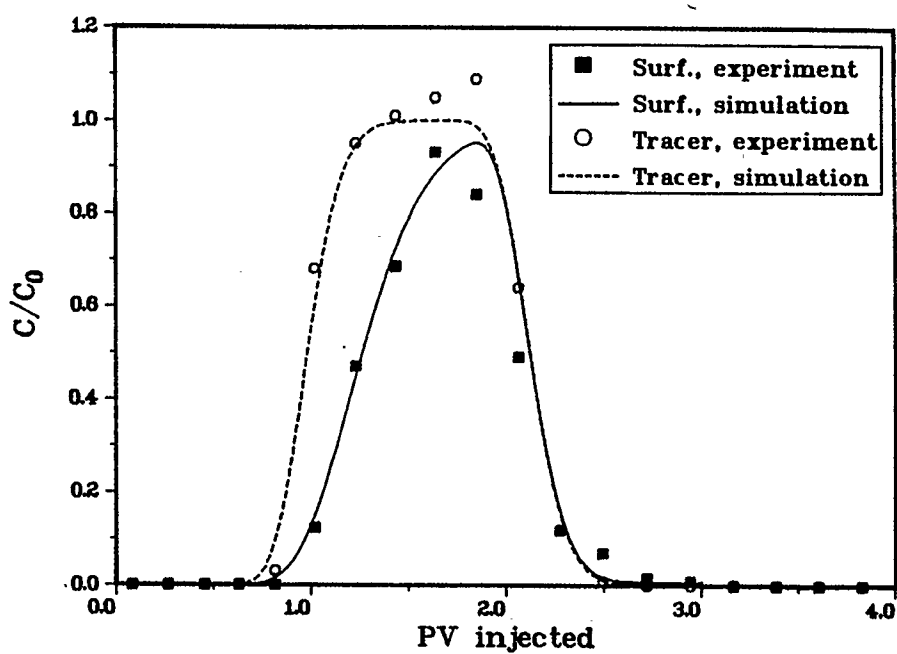


FIGURE 19. Core T10 effluent profiles. Constant selectivity model.

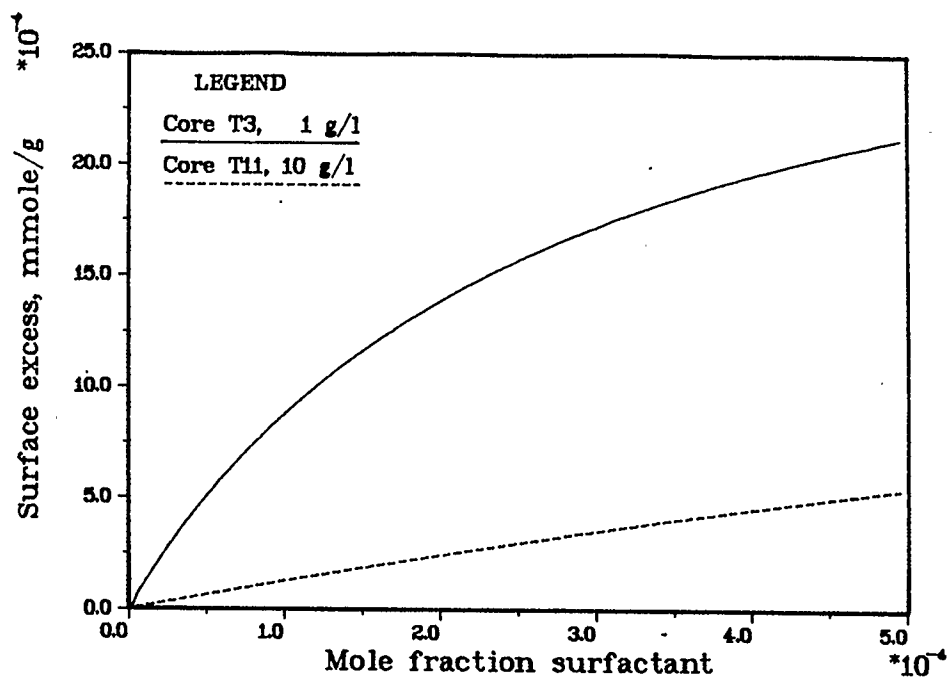


FIGURE 20. Adsorption isotherms for cores T3 and T11 from constant selectivity model.

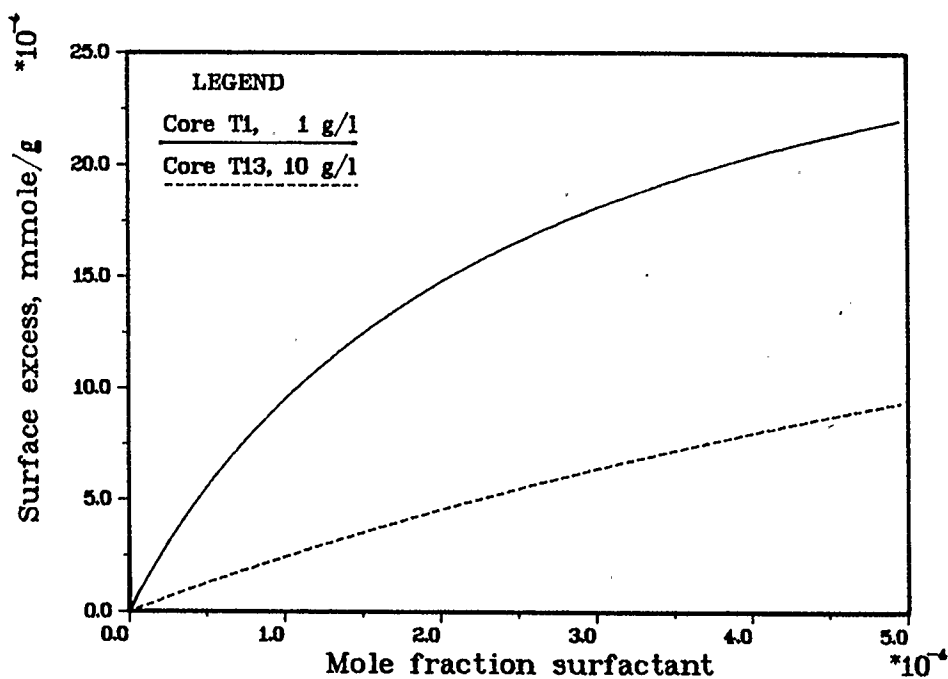


FIGURE 21. Adsorption isotherms for cores T1 and T13 from constant selectivity model.

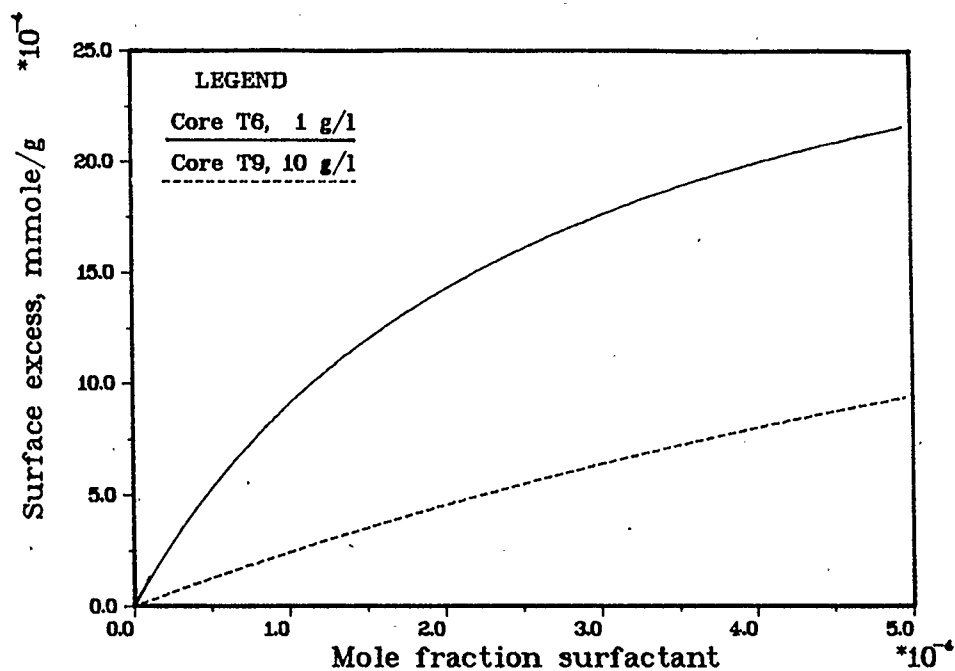


FIGURE 22. Adsorption isotherms for cores T6 and T9 from constant selectivity model.

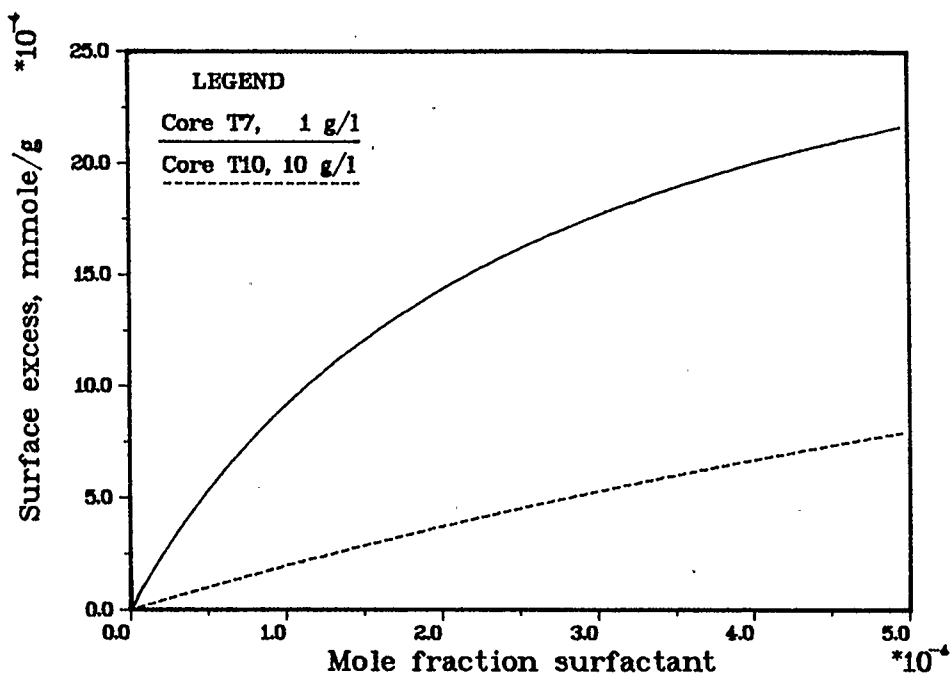


FIGURE 23. Adsorption isotherms for cores T7 and T10 from constant selectivity model.

means that, if adsorption isotherms are calculated using S , m_1 , and m_1/m_2 with equation (8), two different isotherms are obtained at each set of conditions, one using the higher value of S from the low concentration flood, and the other using the lower value of S from the higher concentration flood (Figures 20 to 23). This seems to indicate that an adsorption isotherm generated from history matching parameters is valid only if the injected concentration is close to that used in obtaining the match, or that the isotherm should not be extrapolated beyond the injected concentration. Clearly, it would be much more desirable to generate a single adsorption isotherm from core floods run at any injected concentration at fixed conditions of temperature and salinity.

The data in Table 3 indicate that the assumption of constant S may be too restrictive, and that S should be a decreasing function of concentration. In an attempt to make the model more general by removing the simplifying assumption of constant selectivity, functional forms of the selectivity are investigated and incorporated into the surface excess model.

If the selectivities are taken as a measure of adsorption, the data in Table 3 also show that adsorption of this surfactant increases with decreasing temperature and increasing salinity. This trend has been noted previously by Mannhardt and Novosad (1987a).

3. The Functional Form of Selectivity

Larionov and Myers (1971) have derived a general expression for the selectivity in a binary mixture:

$$S = \frac{f_1 f'_2}{f_2 f'_1} \exp \left[\frac{\sigma A}{RT} \left(\frac{1}{m_1} - \frac{1}{m_2} \right) + \frac{A}{RT} \left(\frac{\sigma_2^0}{m_2} - \frac{\sigma_1^0}{m_1} \right) \right] \quad (36)$$

where σ is the solid/solution interfacial tension, σ_1^0 and σ_2^0 are the solid/pure component interfacial tensions, A is the specific surface area of the adsorbent, and f_i and f'_i are the activity coefficients of component i in the bulk and adsorbed phases, respectively. All other quantities are as previously defined. This equation was derived by equating the fugacities in the bulk and adsorbed phases. The same equation has been developed by Nagy and Schay (1963) and by Schay (1969a).

All quantities on the right hand side of equation (36) are constants, except the ratio of the activity coefficients and the solid/solution interfacial tension σ . Both of these may change with concentration, and thus the selectivity may also depend on concentration. Only if the ratio of the activity coefficients is constant and the molecules of species 1 and 2 are equal in size ($m_1 = m_2$), does S reduce to a constant, since under these conditions

$$S = C \exp \left[\frac{A}{RT} \left(\frac{\sigma_2^0}{m_2} - \frac{\sigma_1^0}{m_1} \right) \right] \quad (37)$$

where C is a constant.

The second criterion, equal-sized molecules, is certainly not

satisfied for a surfactant solution, since the surfactant and water molecules differ widely in their sizes, as was shown in the previous chapter. Neither the interfacial tension at the solid/liquid interface, σ , nor the activity coefficients in the adsorbed phase, f'_i , are amenable to direct experimental measurement. The quantities $(\sigma - \sigma_i^0)$ and f'_1 can, however be determined indirectly by integrating a measured adsorption isotherm, as has frequently been done with miscible liquids (Schay, 1969a; Sircar and Myers, 1970, 1971; Larionov and Myers, 1971; Li and Gu, 1979; Chatteraj and Birdi, 1984). Since the adsorption isotherms for the systems under investigation in this work are not available, the whole purpose of the history matching being to determine these isotherms, this method of determining $(\sigma - \sigma_i^0)$ and f'_1 cannot be applied here.

An expression for S as a function of x_1 can be derived from equation (36) following Sircar's (1984b) treatment. In much of Sircar's work, the adsorbed phase has been considered ideal, since the activity coefficients in the adsorbed phase are extremely difficult to deal with (Sircar and Myers, 1970; Sircar, 1983, 1984a, 1984b). For example, it has been pointed out by Sircar (1983) that the effects of adsorbed phase non-idealities and surface heterogeneities on the adsorption isotherm are impossible to separate from each other, neither being accessible to direct experimental measurement. Moreover, ideal or non-ideal behavior in the bulk phase cannot be correlated with ideal or non-ideal behavior in the adsorbed phase (Nagy and Schay, 1963; Schay, 1969a, 1969b; Li and Gu, 1979). The adsorbed phase activity

coefficients are therefore assumed constant in this work, and, since surfactant concentrations and concentration ranges are small, bulk phase activity coefficients are also taken to be constant.

If the Gibbs surface excess of a reference species, taken to be species 2 (water), is set equal to zero according to Gibbs' definition of the surface excess, the Gibbs adsorption equation for a surfactant (species 1) in water (species 2) can be written (equation (18))

$$-d\sigma = \Gamma_1 d\mu_1 \quad (38)$$

(The surfactant solution is considered to be a pseudobinary mixture of a single surfactant in brine.) The relationship between the Gibbs surface excess, Γ_1 , and the apparent surface excess, Γ_1^a , both on a mole per unit area basis, is given by

$$\Gamma_1 = \Gamma_1^a / x_2 \quad (39)$$

(Guggenheim and Adam, 1933; Schay, 1969a; Chatteraj and Birdi, 1984). Multiplying by the specific surface area, A , allows conversion from Γ_1^a to the surface excess n_1^e , on a mole per unit mass of solid basis:

$$A\Gamma_1 = n_1^e / x_2 \quad (40)$$

The chemical potential of species 1 can be expressed as

$$\mu_1 = \mu_1^o + RT \ln(a_1) \quad (41)$$

where a_1 is the activity of the surfactant and μ_1^o is the chemical potential of pure component 1. Substituting equations (40) and (41) into (38) gives

$$\begin{aligned}
 -A d\sigma &= \frac{RTn_1^e}{x_2} d \ln(a_1) \\
 &= \frac{RTn_1^e}{a_1 x_2} d(a_1)
 \end{aligned} \tag{42}$$

Taking logarithms of equation (36) and differentiating with respect to a_1 , taking into account that the activity coefficients are considered constant, gives

$$\frac{d\sigma}{da_1} = \frac{RT}{A} \frac{m_1}{1-\beta} \frac{d \ln(S)}{da_1} \tag{43}$$

where

$$\beta = m_1/m_2 \tag{44}$$

Solving equation (42) for n_1^e and substituting for $d\sigma/da_1$ from equation (43),

$$n_1^e = - \frac{m_1 a_1 x_2}{1-\beta} \frac{d \ln(S)}{da_1} \tag{45}$$

Equating equations (45) and (8) then gives, after some rearrangement and again taking f_1 to be constant,

$$\frac{dS}{dx_1} = - \frac{S(S-1)(1-\beta)}{(S-\beta)x_1 + \beta} \tag{46}$$

When the inverse of equation (46) is taken, the following first order linear differential equation is obtained:

$$\frac{dx_1}{dS} + \frac{(S-\beta)x_1}{S(S-1)(1-\beta)} = - \frac{\beta}{S(S-1)(1-\beta)} \tag{47}$$

Equation (47) can easily be solved to give

$$x_1 = \frac{1}{S-1} \left[CS^{-\beta/(1-\beta)} - 1 \right] \tag{48}$$

where C is a constant of integration. Using the condition that $\sigma \rightarrow \sigma_2^0$ and $S \rightarrow S_0$ when $x_1 \rightarrow 0$, where

$$S_0 = \lim_{x_1 \rightarrow 0} (S) = \frac{f_1 f'_2}{f_2 f'_1} \exp \left[\frac{A}{RT} \frac{\sigma_2^0 - \sigma_1^0}{m_1} \right] \quad (49)$$

the constant C can be evaluated and substituted into equation (48) to give, after some rearrangement, the following equation:

$$S = S_0 (Sx_1 + x_2)^{(\beta-1)/\beta} \quad (50)$$

Equation (50) then is the required dependence of selectivity on surfactant concentration, S_0 and β being the selectivity in the limit of zero surfactant concentration and the ratio of surfactant to water monolayer coverages, respectively. $A\sigma_1^0$ and $A\sigma_2^0$ are free energies of adsorption of the pure components, and these are negative quantities. Since the surfactant is adsorbed preferentially over water, σ_1^0 is larger than σ_2^0 in absolute value, and S_0 will therefore likely be greater than 1 (if σ_1^0 is large and/or the ratio of the activity coefficients is close to 1). Also, β will be less than 1, since the surfactant molecule occupies a larger area than the water molecule and therefore $m_1 < m_2$. For a surfactant in solution it is then likely that $S_0 > 1$ and $\beta < 1$, and under these conditions S will be a decreasing function of concentration. Some functional forms of S (with $S_0 > 1$ and $\beta < 1$) and the effect of S_0 and β on the shape of this function are shown in Figure 24. Note that equation (50) cannot be solved for S explicitly. Newton's method has been used to calculate the curves in Figure 24. The effect of S_0 and β on the adsorption isotherm is shown in Figure 25. These isotherms were calculated by combining equations

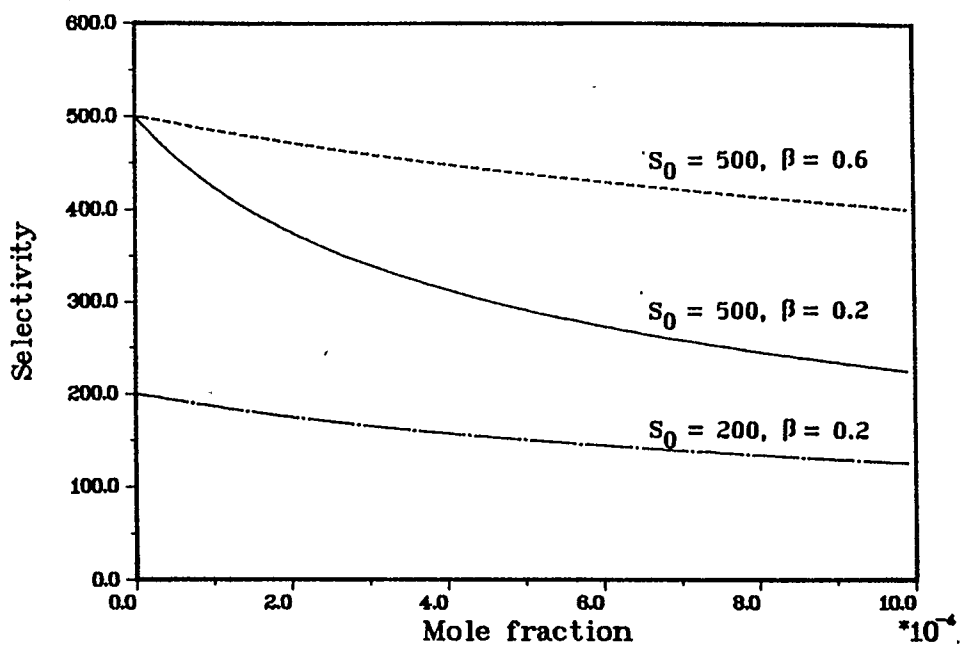


FIGURE 24. Dependence of selectivity on concentration, calculated from equation (50).

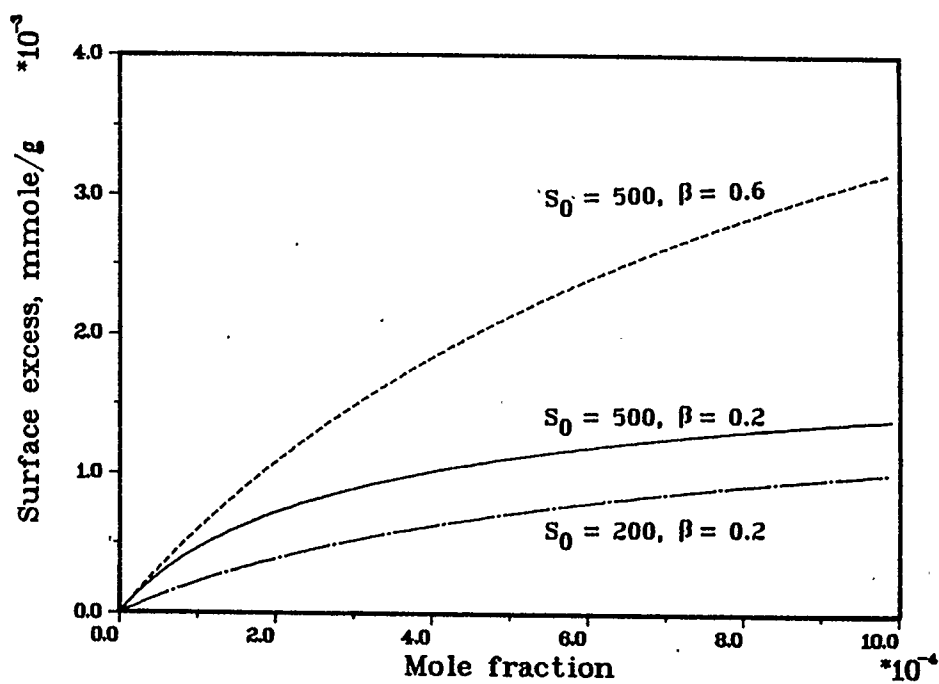


FIGURE 25. Dependence of the surface excess on the parameters S_0 and β , calculated from equations (8) and (50). $m_1=0.0027$ or 0.0080 mmole/g, $m_2=0.013$ mmole/g.

(8) and (50).

Many theories of adsorption assume that there is an "adsorbed phase", since this allows application of well-known thermodynamic relations to adsorption studies without the need of a detailed knowledge of the intermolecular forces in the adsorbed layer. It has frequently been realized, however, that the "adsorbed phase" is of microscopic dimensions and under the influence of forces emanating from the solid (Schay, 1969b, Larionov and Myers, 1971; Everett, 1973). The treatment of adsorption equilibrium by thermodynamic methods that were developed for equilibria between autonomous phases may therefore be questionable. On these grounds Schay (1969b) has used kinetical-statistical considerations to derive a functional relation between selectivity and concentration in a binary system. Schay's relation is based on dynamic and energetic considerations of the adsorption-desorption equilibrium, and is of the following form:

$$\ln(S) = ax_1 + b \quad (51)$$

where a and b are constants. Schay has tested equation (51) against several binary liquid mixtures. Only 4 of the 14 systems tested follow the linear relationship between $\ln(S)$ and x_1 , and the theory is therefore very tentative, in its author's own words. The equation is included here, because its origin is based on completely different principles than equation (50). It has been incorporated into the surface excess model to test its effect on surfactant effluent profiles, but, because of its semi-empirical nature, only limited testing has been performed.

The function in equation (51) is either monotonically increasing or monotonically decreasing, depending on the values of a and b . The value of S at $x_1=0$ is determined by b , while a determines the slope of the curve. It should be noted that S can cross the line $S=1$ at some concentration. This means that the surface excess can switch from preferential adsorption of one component to preferential adsorption of the other component. The point at which $S=1$, and therefore $n_1^e=0$, is known as an adsorption azeotrope. With equation (50), on the other hand, the selectivity will never cross 1, except when $S_0=1$, in which case $S=1$ at all concentrations. With equation (50), S will always be either greater than 1 or less than 1 over the whole concentration range, depending on the values of S_0 and β .

The effect of a and b on selectivity, as calculated from equation (51), is shown in Figure 26, with the corresponding adsorption isotherms in Figure 27. Only cases for decreasing selectivities are shown, since these are of more interest in the present application.

Equations (50) and (51) can easily be incorporated into the flow model as follows. For each concentration in each grid block in the core the selectivity is calculated using either of these two equations. The equilibrium surface excess is then calculated using equation (8) together with the calculated selectivity. It should be noted that, using equation (50), no parameters are added to the model, the parameter S simply being replaced by the parameter S_0 , while β is

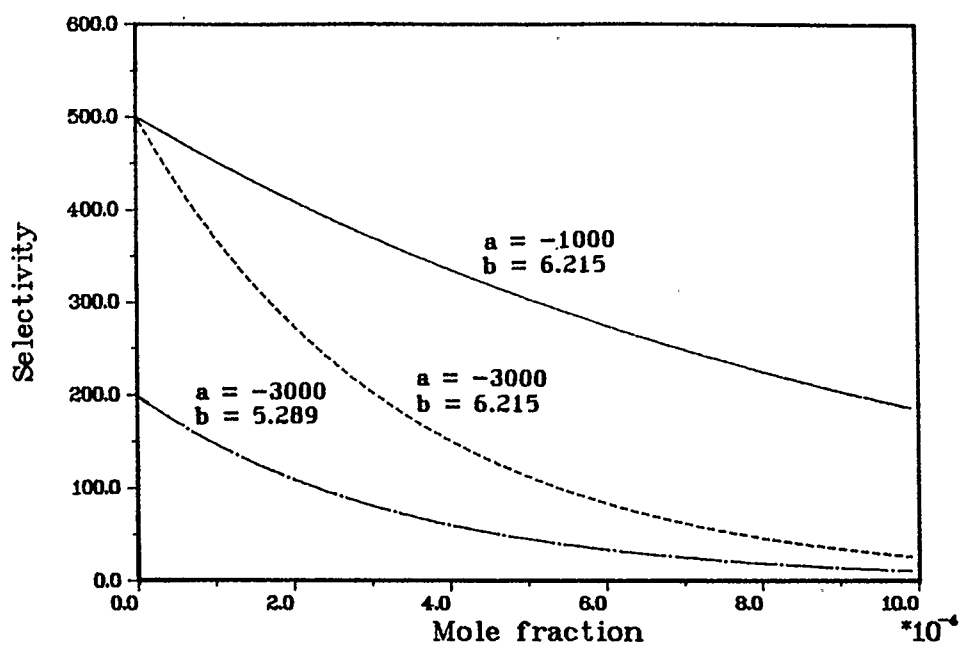


FIGURE 26. Dependence of selectivity on concentration, calculated from equation (51).

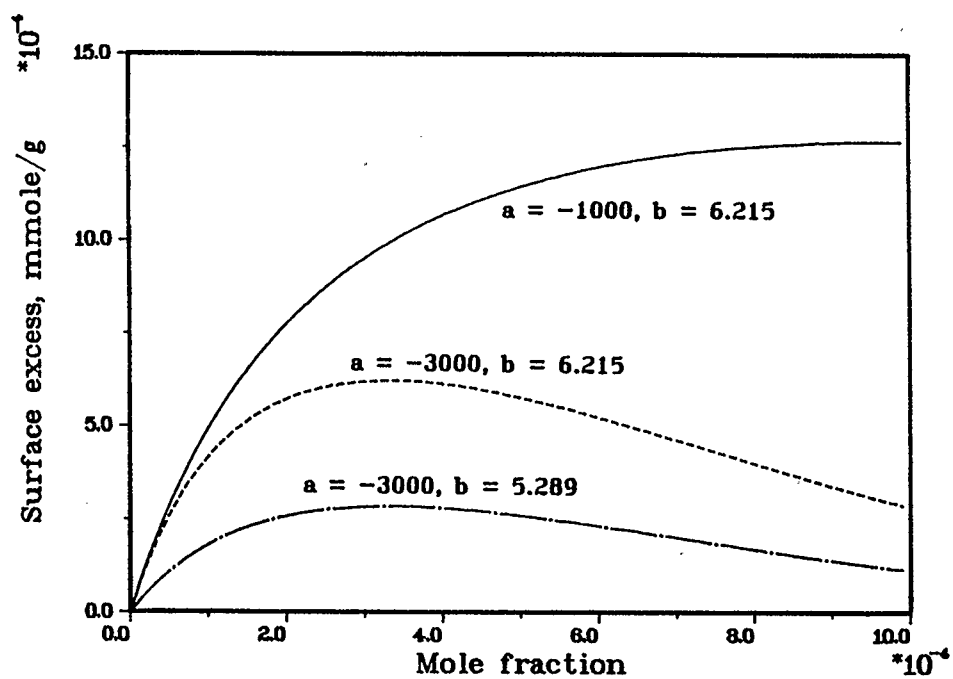


FIGURE 27. Dependence of the surface excess on the parameters a and b , calculated from equations (8) and (51). $m_1=0.0027$ mmole/g, $m_2=0.013$ mmole/g.

determined independently as described in chapter 3. With equation (51), however, the parameter S is replaced by the parameters a and b , thus increasing the number of parameters by one.

Details of the numerical solution to the flow model can be found in the Appendix.

4. Results: History Matching of Core Floods Using Variable Selectivity

The same core floods that were described in conjunction with the constant selectivity model in sections 1 and 2 of this chapter were re-matched using the variable selectivity model with equation (50). The best match parameters obtained with this model are listed in Table 4, and the effluent profiles are shown in Figures 28 to 35. The history matches in these figures are quite similar to those in Figures 12 to 19. From Table 4 it is obvious that two different values of S_0 are still required to match the high and low concentration floods. In fact, the values of S_0 in Table 4 are equal to or only slightly higher than the values of S in Table 3.

The reason for the inability of the variable selectivity model to match high and low concentration floods with a single value of S_0 becomes clear when the adsorption isotherms are calculated, as shown in Figures 36 to 39 for both the constant and variable selectivity models. Clearly, calculating the selectivity from equation (50) does not change

TABLE 4. Experimental conditions and matching parameters for variable selectivity model with equation (50).

| Core # | T3 | T11 | T1 | T13 | T6 | T9 | T7 | T10 |
|-------------------------------------|--------|--------|--------|--------|--------|--------|--------|--------|
| Surfactant Conc. (g/l) | 1.00 | 9.97 | 1.00 | 9.97 | 1.01 | 10.0 | 1.01 | 10.0 |
| Surfactant Mole Frac. $\times 10^4$ | 0.372 | 3.73 | 0.363 | 3.65 | 0.374 | 3.73 | 0.379 | 3.78 |
| Brine Conc. (% TDS) | 10.5 | 10.5 | 10.5 | 10.5 | 21.0 | 21.0 | 21.0 | 21.0 |
| Temp. (deg. C) | 75 | 75 | 23 | 23 | 50 | 50 | 75 | 75 |
| Slug Vol. (PV) | 1.04 | 0.73 | 1.01 | 0.78 | 2.12 | 0.86 | 2.04 | 1.14 |
| S_0 | 900 | 100 | 1070 | 200 | 980 | 220 | 1020 | 180 |
| m_1 (mmole/g) | 0.0033 | 0.0033 | 0.0033 | 0.0033 | 0.0033 | 0.0033 | 0.0033 | 0.0033 |
| m_1/m_2 | 0.25 | 0.25 | 0.25 | 0.25 | 0.25 | 0.25 | 0.25 | 0.25 |
| k_1 (1/hr) | 1.0 | 1.0 | 1.0 | 1.0 | 1.0 | 1.0 | 1.0 | 1.0 |
| k_2 (1/hr) | 0.005 | 0.002 | 0.005 | 0.005 | 0.003 | 0.003 | 0.002 | 0.002 |
| Dispersion Par. (cm) | 0.75 | 0.15 | 0.5 | 0.15 | 0.6 | 0.15 | 0.6 | 0.15 |

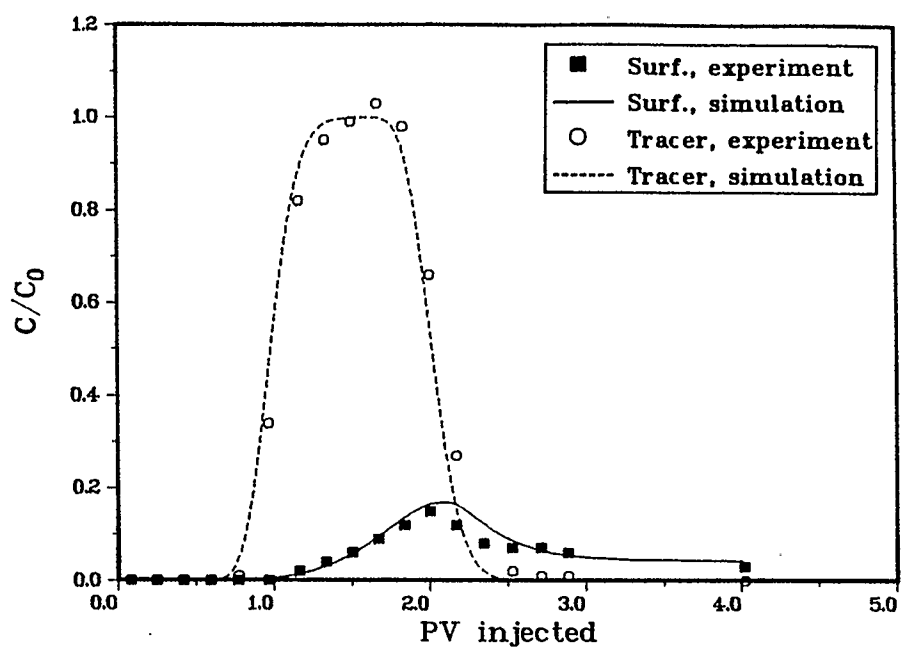


FIGURE 28. Core T3 effluent profiles. Variable selectivity model with equation (50).

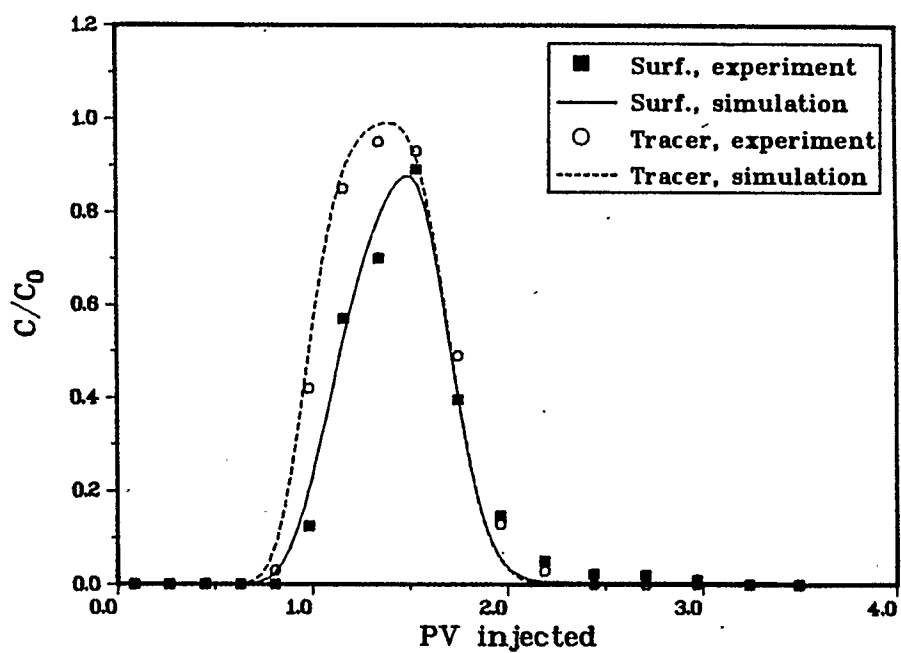


FIGURE 29. Core T11 effluent profiles. Variable selectivity model with equation (50).

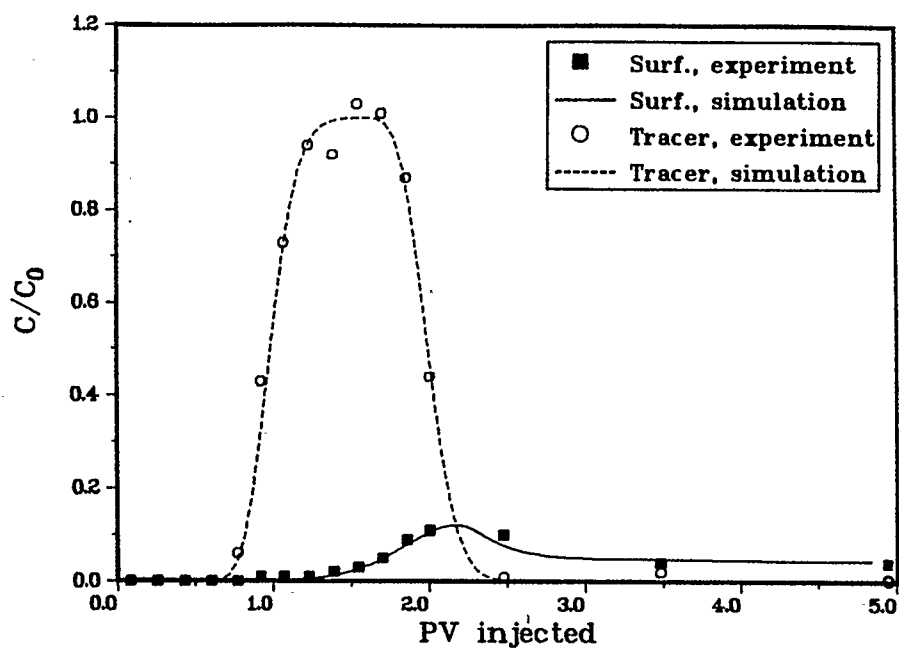


FIGURE 30. Core T1 effluent profiles. Variable selectivity model with equation (50).

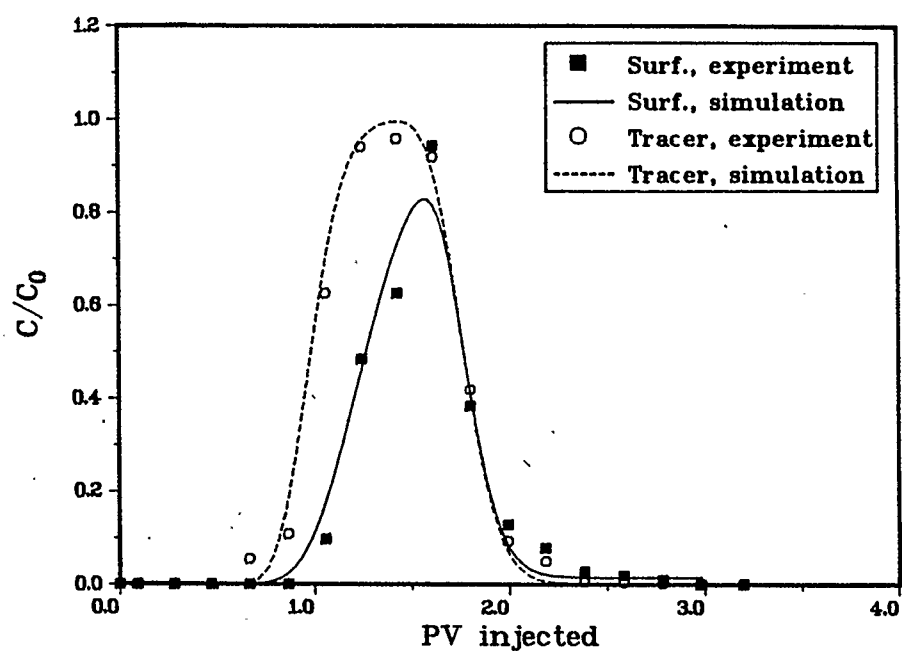


FIGURE 31. Core T13 effluent profiles. Variable selectivity model with equation (50).

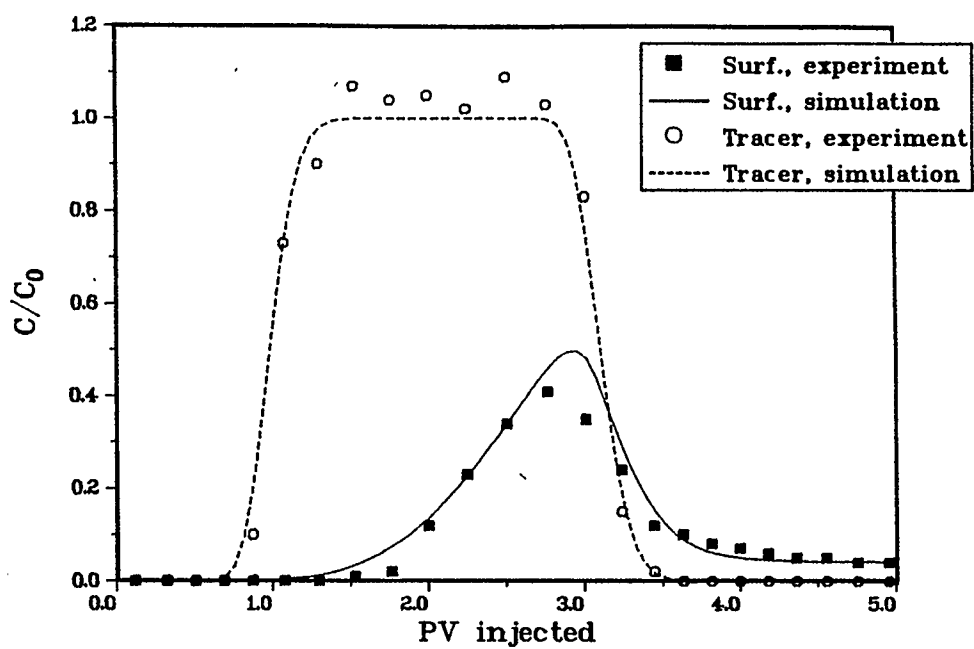


FIGURE 32. Core T6 effluent profiles. Variable selectivity model with equation (50).

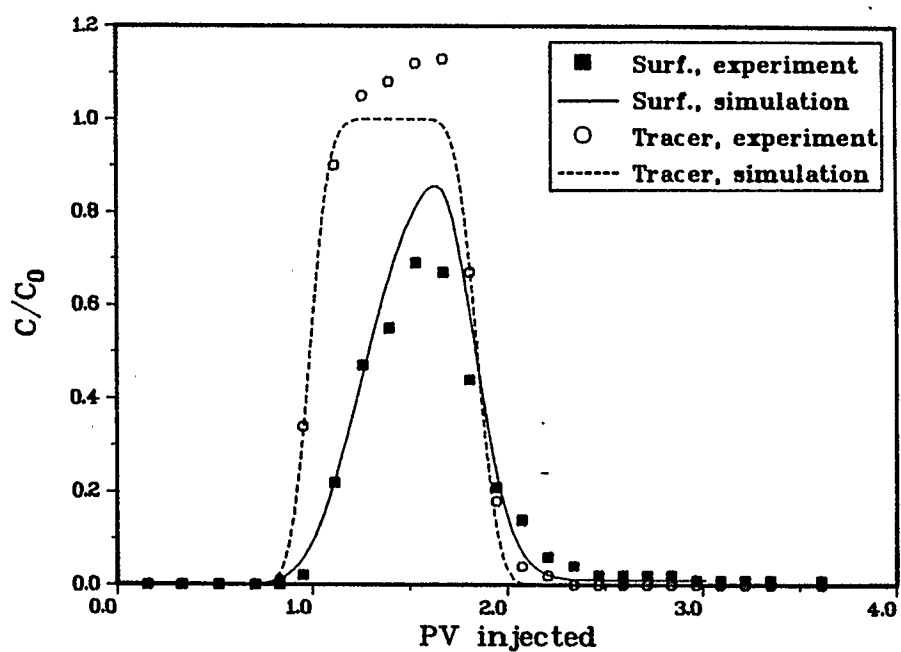


FIGURE 33. Core T9 effluent profiles. Variable selectivity model with equation (50).

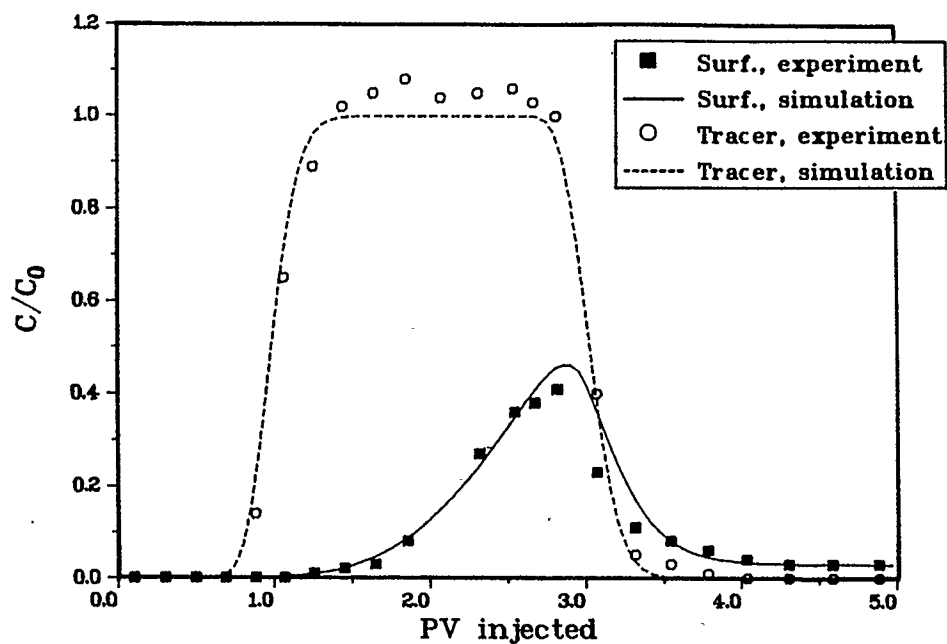


FIGURE 34. Core T7 effluent profiles. Variable selectivity model with equation (50).

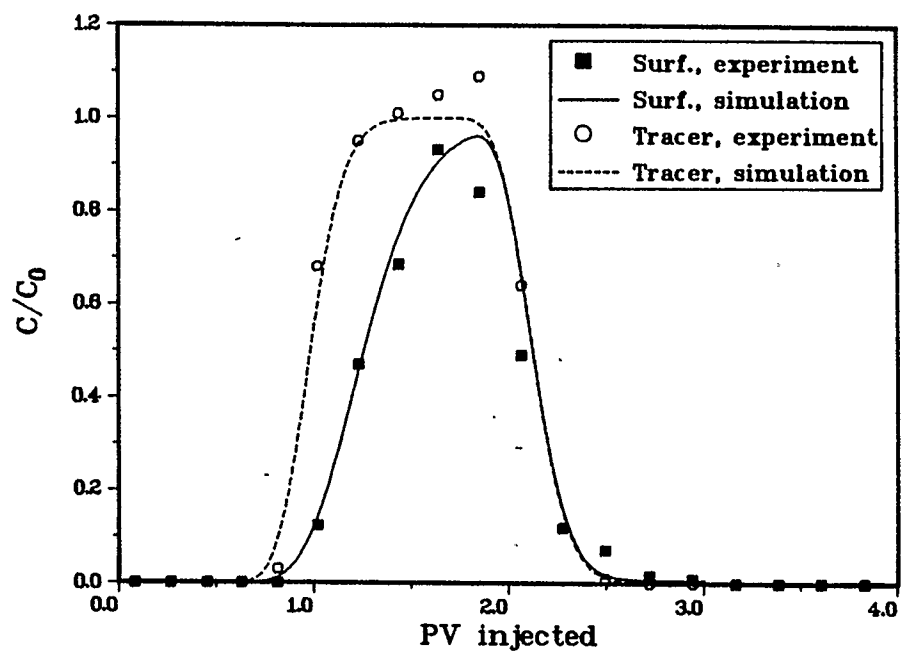


FIGURE 35. Core T10 effluent profiles. Variable selectivity model with equation (50).

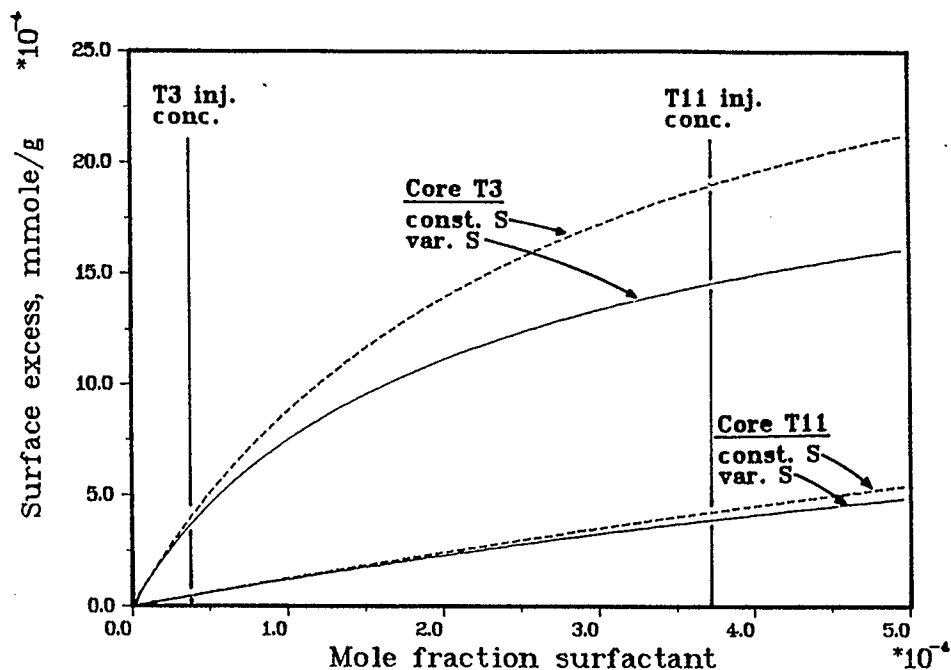


FIGURE 36. Adsorption isotherms for cores T3 and T11 from constant selectivity model, and variable selectivity model with equation (50).

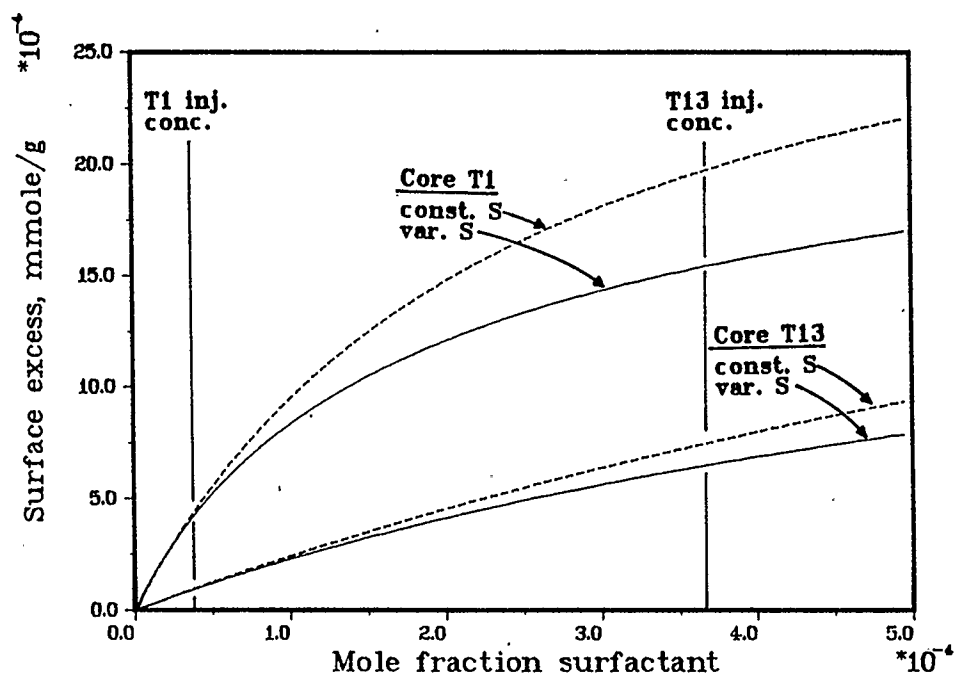


FIGURE 37. Adsorption isotherms for cores T1 and T13 from constant selectivity model, and variable selectivity model with equation (50).

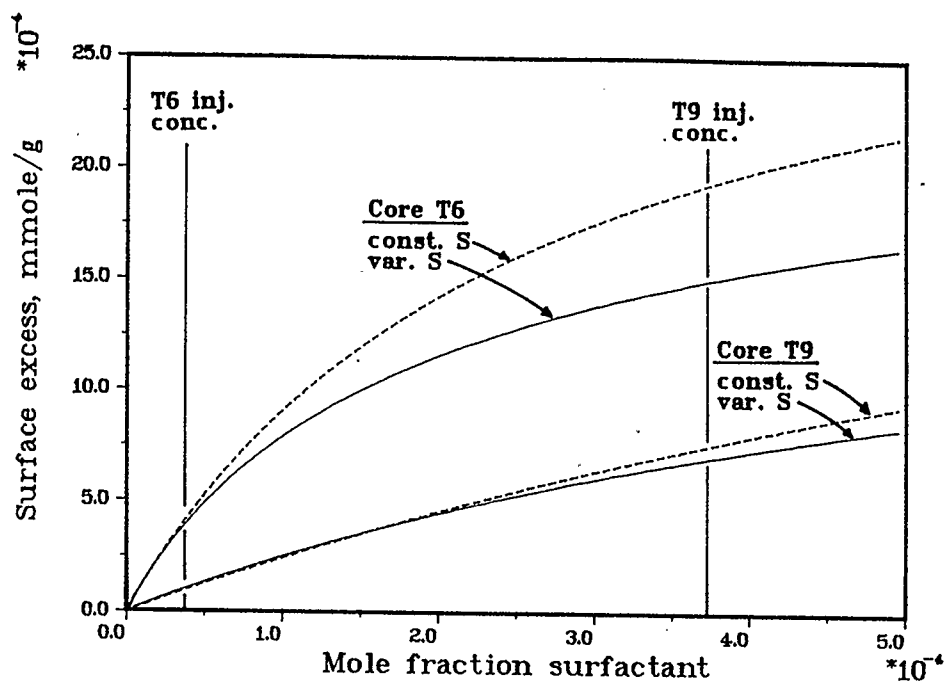


FIGURE 38. Adsorption isotherms for cores T6 and T9 from constant selectivity model, and variable selectivity model with equation (50).

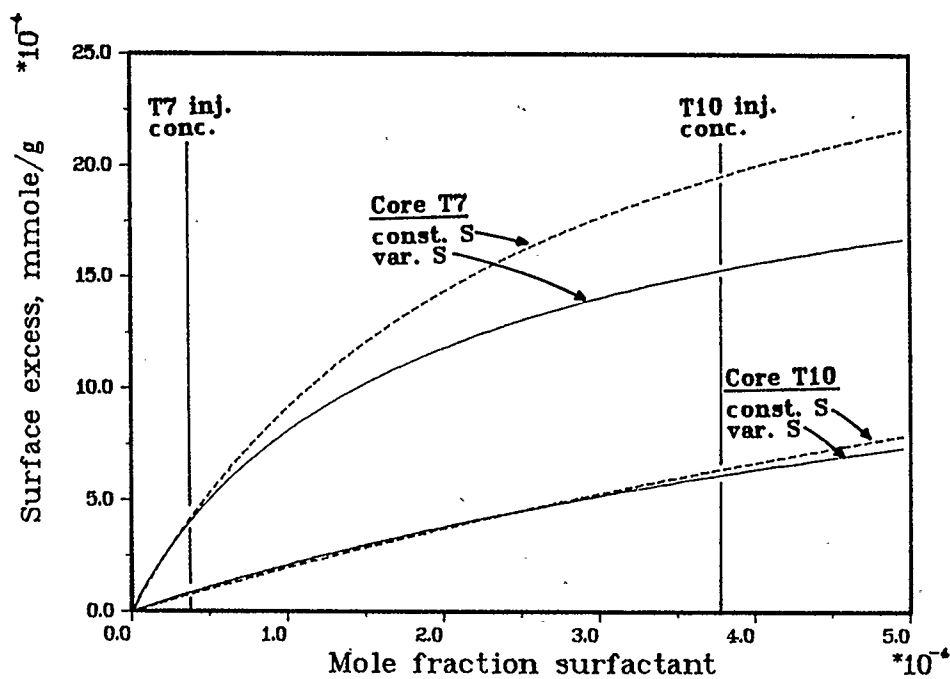


FIGURE 39. Adsorption isotherms for cores T7 and T10 from constant selectivity model, and variable selectivity model with equation (50).

the magnitude or shape of the isotherms greatly, and two different isotherms are still generated from the high and low concentration floods at the same conditions.

To obtain an estimate on what values of S_0 and β would be required to match both floods, the values of S and the injected surfactant mole fractions from Table 3 for cores T3 and T11 were substituted into equation (50). This gives two equations in the two unknowns S_0 and β , which, upon solution, should give the functional form of selectivity that passes through the points (x_1, S) for each of the two floods. The value of S_0 obtained in this way is 10^{12} , while the value of β converts to a molecular area of 8100 \AA^2 for the surfactant molecule. Both of these values are unrealistically high.

The surface excess model with equation (51) was also used with the experimental data of cores T3 and T11. History matches are shown in Figures 40 and 41, and matching parameters in Table 5. While the simulated effluent profiles do not match the experimental ones quite as well as was the case with equation (50), both the high and the low concentration floods can be matched with the same values of the parameters a and b . The reason for this may be the introduction of an additional adjustable parameter into the model.

The adsorption isotherm obtained from the parameters in Table 5 and equations (51) and (8) is shown in Figure 42. Both the surface excess and the amount adsorbed go through a maximum. The surface excess

TABLE 5. Experimental conditions and matching parameters for variable selectivity model with equation (51).

| Core # | T3 | T11 |
|--|--------|--------|
| Surfactant Conc. (g/l) | 1.00 | 9.97 |
| Surfactant Mole Frac. $\times 10^4$ | 0.372 | 3.73 |
| Brine Conc. (% TDS) | 10.5 | 10.5 |
| Temp. (deg. C) | 75 | 75 |
| Slug Vol. (PV) | 1.04 | 0.73 |
| a | -7500 | -7500 |
| b | 6.85 | 6.85 |
| m_1 (mmole/g) | 0.0033 | 0.0033 |
| m_1/m_2 | 0.25 | 0.25 |
| k_1 (1/hr) | 1.0 | 1.0 |
| k_2 (1/hr) | 0.005 | 0.002 |
| Dispersion Par. (cm) | 1.2 | 0.3 |

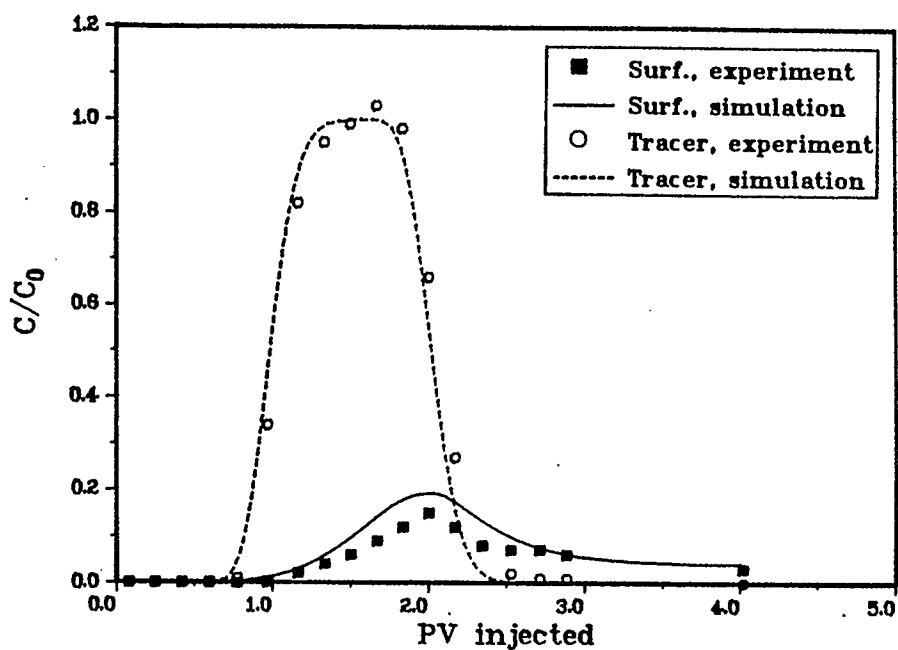


FIGURE 40. Core T3 effluent profiles. Variable selectivity model with equation (51).

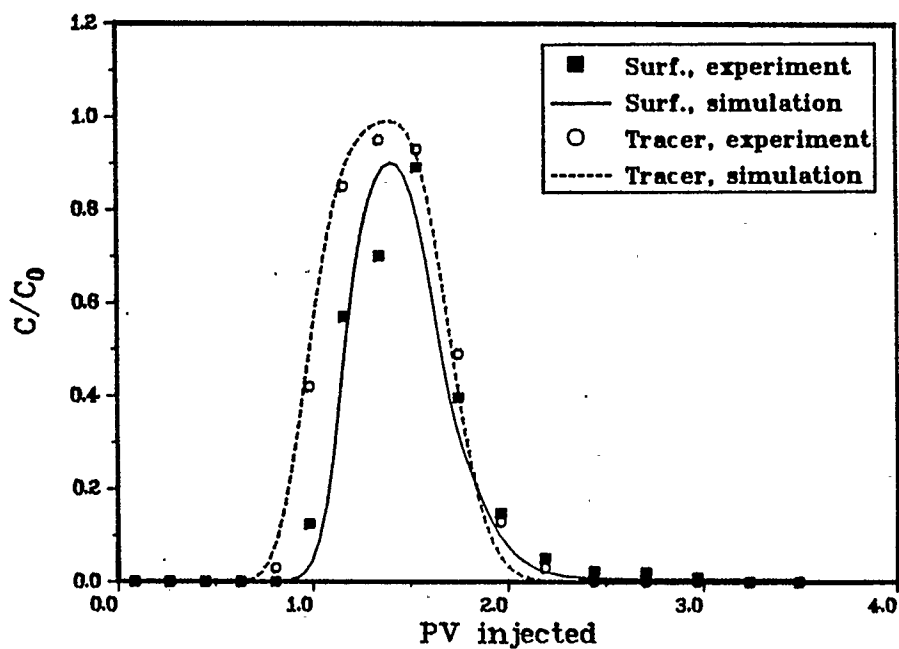


FIGURE 41. Core T11 effluent profiles. Variable selectivity model with equation (51).

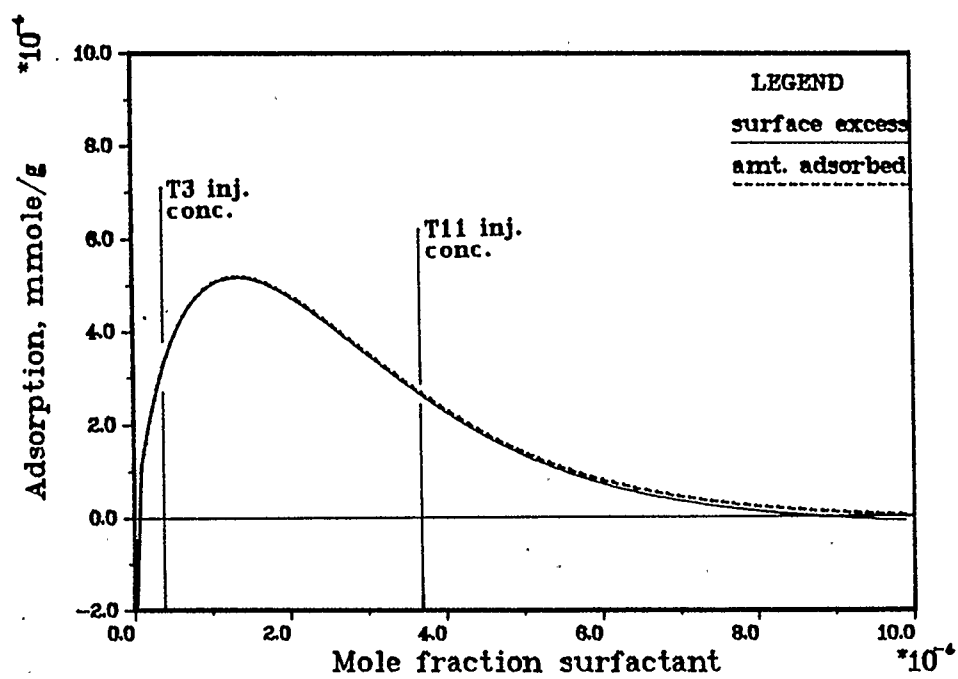


FIGURE 42. Adsorption isotherms for cores T3 and T11 from variable selectivity model with equation (51).

becomes negative at a mole fraction of about 9×10^{-4} (0.048 M or 2.4% w/w), and the amount adsorbed approaches zero. A point of zero surface excess is called an adsorption azeotrope. At this point the composition of the bulk and adsorbed phases is equal, and there is a reversal from preferential adsorption of one component to preferential adsorption of the other. While adsorption azeotropes have been observed for many miscible liquids, it seems unlikely that water would adsorb preferentially over the surfactant at surfactant concentrations as low as 2.5% w/w. Equation (51) therefore generates an isotherm that may become physically unrealistic at surfactant mole fractions within the range used in EOR applications.

In summary, then, equation (50) can be derived from the thermodynamics of adsorption, with certain simplifying assumptions. While this equation, when incorporated into the surface excess model, can match high and low concentration floods separately, it cannot match both floods with the same set of parameters. This means that two different adsorption isotherms are still generated at one set of conditions. Using the semi-empirical equation (51) in the flow model does allow history matching of both floods with the same set of parameters, but unrealistic adsorption isotherms are generated. The isotherm calculated using this equation does yield some useful information, however: It indicates that, in order to match both high and low concentration floods, an isotherm that rises steeply at very low concentrations and then becomes almost level is required.

Expressing the selectivity as a function of concentration makes the surface excess model more sound theoretically. Figures 36 to 39 indicate that equation 50 shifts the adsorption isotherms in the right direction, but that this effect is not strong enough to match both floods with one isotherm. This would suggest that equation (50) is too simple a function, or that there are other factors that the model does not yet take into account. It may also indicate that the effluent profile obtained at a given injection concentration is not very sensitive to the shape of the adsorption isotherm at concentrations much lower than the injected concentration.

In an attempt to improve this imperfection in the model, another simplifying assumption is removed from the model in the next chapter.

CHAPTER 5

THE EFFECT OF SURFACE HETEROGENEITY ON ADSORPTION

In this chapter an additional aspect of adsorption at the solid/liquid interface is introduced into the surface excess model: the effect of surface heterogeneities. In this context surface heterogeneity refers to the adsorbent-adsorbate interaction energy, which can vary at different adsorption sites on the solid surface. It is well known that surface heterogeneities can have a very strong effect on adsorption isotherms of gases and liquids (Young and Crowell, 1962; Adamson, 1976; Jaroniec et. al., 1981). In fact, it has been stated by Harwell et. al. (1985a) that "a satisfactory theory for surfactant adsorption must necessarily incorporate ... surface heterogeneities". The solids of interest in this work, naturally occurring rocks, are certainly highly heterogeneous with respect to their mineral components. A rock surface is therefore likely to exhibit a range of free energies of adsorption towards a solution in contact with it.

1. The Mathematical Treatment of Surface Heterogeneity:

A Literature Review

One of the earliest attempts at dealing with heterogeneous surfaces is attributed to the work of Langmuir in 1918 (Young and

Crowell, 1962). Although the importance of surface heterogeneity to adsorption of gases and liquids at the solid surface has long been recognized, the problems associated with the measurement and quantitative mathematical description of surface heterogeneities are far from being solved (Everett, 1965; Rudzinski and Jaroniec, 1974). From a review by Jaroniec et. al. (1981) it is evident that a great deal of effort has been devoted to adsorption on heterogeneous surfaces, and also that this is a problem of great complexity. While the literature dealing with gas adsorption on such surfaces is extensive, less has been written on adsorption of binary liquid mixtures on heterogeneous surfaces, and much less still on adsorption of multi-component liquids.

Heterogeneities on a solid surface arise from its complex crystallographic and geometric structure, and from its chemical composition. The variety of crystal faces and/or functional groups exposed to the adsorbate, imperfections or defects in the crystal structure, and tightly bound impurities may render the surface heterogeneous in an energetic sense. A multi-component solid, such as a petroleum reservoir rock, will obviously be highly heterogeneous in terms of its adsorption potential towards different components in solution. Another source of heterogeneity, encountered in microporous solids, is associated with their complex pore structure, which consists of micropores with a range of dimensions and shapes. In real adsorption systems, heterogeneous solids are much more common than homogeneous ones, a fact that is often overlooked in the description of adsorption

at the solid surface.

Surface heterogeneities cannot easily be measured directly, but they can be inferred from their effect on an adsorption isotherm. Direct experimental evidence of the effect of the degree of surface heterogeneity on adsorption is rather scant. Narang and Ramakrishna (1970a, 1970b) have shown that samples of chromium(III)oxide that were obtained by decomposition of ammonium dichromate at different temperatures exhibit different adsorption behavior towards benzene/cyclohexane mixtures. The effect of modifying the heterogeneity of carbon black samples by different heat treatments on adsorption isotherms of methanol/benzene and n-butanol/benzene mixtures has been demonstrated by Coltharp and Hackerman (1973a, 1973b). Increasing the heterogeneity of the surface has a rather drastic effect on the methanol/benzene isotherms, changing them from U-shaped to S-shaped (Figure 43). A U-shaped isotherm exhibits preferential adsorption of the same component throughout the concentration range, whereas an S-shaped isotherm changes from preferential adsorption of one component to the other at the adsorption azeotrope. The same effect, a change from U-shaped to S-shaped isotherms with increasing surface heterogeneity, has been shown in model studies by Dabrowski et. al. (1979) and Sircar (1983, 1984a, 1984b). Theoretical and experimental studies are thus consistent in this respect.

Halsey and Taylor (1947) were the first to attempt a rigorous treatment of adsorption on heterogeneous surfaces by introducing their

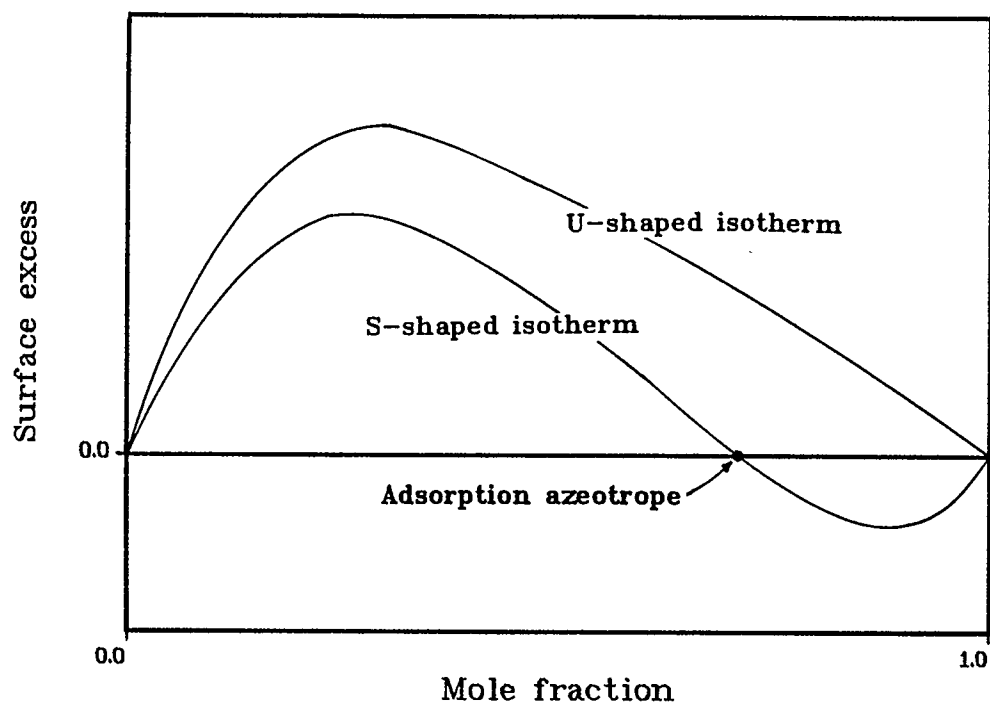


FIGURE 43. Examples of a U-shaped and an S-shaped adsorption isotherm.

now famous "integral equation". Even though this equation is more than 40 years old, it still forms the basis for a quantitative description of surface heterogeneities. The integral equation assumes the surface to consist of sites with a range of values of some energy parameter E . The probability of there being an adsorption energy between E and $E+dE$ is described by a distribution function $\lambda(E)$. The overall adsorption isotherm can then be obtained by integration of the contributions of each site as follows:

$$N(x) = \int_{\Delta} N_1(x, E) \lambda(E) dE \quad (52)$$

$N(x)$ is the overall adsorption, which is a function of pressure in gas adsorption or concentration in adsorption of liquids. The dependent variable (pressure or concentration) is denoted by x . $N_1(x, E)$ is the local adsorption isotherm on a site of adsorption energy E , $\lambda(E)dE$ is the fraction of total sites having energies between E and $E+dE$, and Δ is the range of possible values of E . Normalization requires that

$$\int_{\Delta} \lambda(E) dE = 1 \quad (53)$$

The application of probability to the description of surface heterogeneity is a convenient mathematical tool, but is not meant to suggest that site energies are random variables. The statistical approach is thus a macroscopic, approximate way of applying solution thermodynamics to surface phenomena. Another approach would involve the molecular description of the surface, but because of the difficulties associated with this approach it has not been used.

Equation (52) has been applied to both gas and liquid adsorption. In the case of gases, N and N_1 are usually taken to be the overall and local surface coverages, respectively, and E is the adsorbent-adsorbate interaction energy. For liquids, N and N_1 have been taken as surface excess, amount adsorbed, or mole fraction in the adsorbed phase, again overall or local, by different authors, and E may be the difference in adsorption energies of the components of a liquid, an equilibrium constant of the bulk phase/adsorbed phase exchange reaction, or the selectivity. The choice of variables is usually made in such a way as to facilitate the solution of equation (52).

Equation (52) contains three functions, $N(x)$, $N_1(x,E)$ and $\lambda(E)$. Only one of these, the overall adsorption isotherm $N(x)$, can be measured experimentally. Two approaches have therefore been taken in describing heterogeneous surfaces. In the first one, a simple functional form, such as the Langmuir equation, is assumed for the local isotherm $N_1(x,E)$, and $\lambda(E)$ is determined from experimental $N(x)$ data by inversion of the integral in equation (52). The second approach assumes functional forms for $N_1(x,E)$ and $\lambda(E)$ such that equation (52) can be integrated to give the function $N(x)$. This function can then be matched to experimental data through a number of adjustable parameters.

The much quoted work of Sips (1948, 1950) is one of the earliest attempts at inverting equation (52) to determine $\lambda(E)$. The Langmuir equation is assumed to represent the local adsorption isotherm, and a

generalized Freundlich equation describes the overall isotherm. Stieltjes transform techniques are used to determine $\lambda(E)$, which in this case turns out to be exponential in form. Many of the analytical solutions to the integral equation make use of Stieltjes transforms (Misra, 1970; Rudzinski et. al., 1973; Waksmundzki et. al., 1975; Oscik et. al., 1976, 1977; Sircar, 1983, 1984c). This technique allows both the inversion of the integral equation to determine $\lambda(E)$ when the functional forms of $N_1(x,E)$ and $N(x)$ are assumed, and direct integration of equation (52) when the functional forms of $N_1(x,E)$ and $\lambda(E)$ are assumed. Most authors have taken the first approach, while Sircar, in a series of papers on gas and liquid adsorption, has chosen the direct integration route, using Stieltjes transform or Laplace transform techniques, or straightforward integration (Sircar, 1983, 1984a, 1984b, 1984c, 1984d). Sircar's work yields equations directly applicable to modelling of adsorptive separation processes of gaseous and liquid systems. An important point to be taken from Sircar's papers is that different local isotherms (Langmuir and Jovanovic), or different distribution functions (gamma and uniform) may yield overall isotherms that are equally acceptable in representing experimental data. A similar conclusion was reached in a theoretical study by Misra (1970, 1973), also by using the Langmuir and Jovanovic local isotherms. From this it may be concluded that the integral equation does not provide an absolute measure of surface heterogeneities, but should rather be used as a tool for comparative purposes. Independent experimental methods would have to be found for the determination of absolute heterogeneities.

If the functions in equation (52) are chosen so as to allow analytical solution, the kinds of functional dependencies are severely limited, and the system is forced into a mold dictated by the solution procedure. In order to avoid this restriction, a number of numerical solution techniques have been described. The best known of these is probably Adamson and Ling's (1961) method of successive approximation, in which the overall adsorption isotherm is in the form of experimental points, and the distribution function is calculated graphically using an iterative approach. No restriction is placed on the local isotherm; it can be the Langmuir equation (Adamson and Ling, 1961), the BET equation for multilayer adsorption (Dormant and Adamson, 1972), or any other form. It has been pointed out, however, that this method may suffer from convergence problems (Van Dongen, 1973; Adamson, 1976). Other numerical methods have been described by Van Dongen (1973), Rudzinski and Jaroniec (1974), House (1978), and House and Jaycock (1978). All these methods involve the determination of $\lambda(E)$ using numerical techniques for minimizing deviations between calculated and experimental data. A method based on orthonormal functions has been described by Jaroniec and Rudzinski (1975).

A large variety of local isotherms has been used in equation (52). In many cases, using a well known equation for the local isotherm and some distribution function results in another well known equation for the overall isotherm. Thus a local Langmuir isotherm and an exponential distribution result in an overall Freundlich isotherm (Kindl et. al.,

1973; Adamson, 1976). Similarly, using the Langmuir isotherm with other distribution functions gives overall generalized Freundlich (Sips, 1950), Temkin (Kindl et. al., 1973), or Dubinin-Radushkevich isotherms (Oscik et. al., 1976). In this way the energy distribution functions for many pairs of local and overall adsorption isotherms have been found. By far the most commonly used local isotherm in gas adsorption is the Langmuir equation (Sips, 1948, 1950; Adamson and Ling, 1961, Misra, 1970; D'Arcy and Watt, 1970; Kindl et. al., 1973; Jaroniec and Rudzinski 1975; Sircar, 1984c). Other local isotherms used with the integral equation include the Jovanovic isotherm (Misra, 1973; Rudzinski and Jaroniec, 1974; Sircar, 1984d), the condensation approximation (a step function) or modifications thereof (Hobson, 1965a, 1965b; Cerofelini, 1971; Dabrowski et. al., 1979), the BET or modified BET equation (Dormant and Adamson, 1972; Oscik et. al., 1977), and an extended Hill-de-Boer equation (Van Dongen, 1973). D'Arcy and Watt (1970) have split the overall isotherm into three contributing terms representing strong adsorbent-adsorbate interactions, weak adsorbent-adsorbate interactions, and multilayer adsorption. In the case of liquid mixtures, the surface excess is usually used with equation (52) (Rudzinski et. al., 1973; Waksmundzki et. al., 1975; Oscik et. al., 1976, 1977; Dabrowski et. al., 1979; Sircar, 1983, 1984a, 1984b). Sircar has substituted equation (8) for the local adsorption isotherm into equation (52), and this approach will be taken later in this chapter.

The distribution functions that have been used with or determined

from equation (52) are just as diverse as the local isotherm equations. They include various exponential forms (Sips, 1948; Misra, 1970, 1973; Waksmundzki et. al., 1975), exponential polynomials (Van Dongen, 1973), the Maxwell-Boltzmann distribution (Kindl et. al., 1973), the gamma distribution (Sircar, 1983, 1984c, 1984d), the uniform distribution (Sircar, 1984a, 1984b), and Gaussian-like distributions (Rudzinski and Partyka, 1981; Rudzinski et. al., 1982). Myers (1986) has used the concept of specificity of adsorption of binary liquid mixtures, in which the solid consists of sites allowing adsorption of either one of the components only, and sites allowing competitive adsorption of both components. In microporous solids, the shape of the adsorption isotherm is affected by structural heterogeneities of the micropores. For these materials, the distribution of a structural parameter, such as the pore radius, is used in an equation similar to (52). Adsorption on microporous solids has been addressed by Jaroniec (1986, 1987), Sircar (1986), and McEnaney et. al. (1987).

Two important conclusions can be drawn from the literature on surface heterogeneity. The first concerns the form of the distribution function $\lambda(E)$. It has been noted by several authors that the form of $\lambda(E)$ depends on the choice of the local isotherm, and that different distributions lead to equally good representations of experimental data (Adamson, 1976; Sircar, 1983, 1984a). Treating the surface as homogeneous, on the other hand, gives a less satisfactory fit between theory and experiment, indicating that the surface should be treated as heterogeneous even though the overall adsorption isotherm may not be

very sensitive to the functional form of $\lambda(E)$. Rudzinski and Jaroniec (1974), Jaroniec and Rudzinski (1975), and Adamson (1976) have compared distribution functions obtained by different solution methods of equation (52) using the same experimental data. Even though these distributions often show the same trends in their mean and spread, they are generally far from being equal, throwing some doubt on the physical significance of the distribution function. Until surface heterogeneities can be measured independently, the criterion for an acceptable distribution function will remain the degree of success in fitting the integral equation to experimental adsorption isotherms.

The second important point is that adsorbed phase non-idealities and surface heterogeneities cannot be separated from each other (Everett, 1965; Gregg and Sing, 1967; Sircar, 1983; Myers, 1986). The combined effect of both can only be determined indirectly from a measured adsorption isotherm. A change in shape in an adsorption isotherm may thus be attributed to either of these two contributing factors, or both. S-shaped isotherms have frequently been explained by considering non-idealities in the bulk and adsorbed phases (Sircar and Myers, 1970; Li and Gu, 1979). However, it has been shown in model studies by Sircar (1983, 1984a, 1984b) and Dabrowski et. al. (1979) that a change from U-shaped to S-shaped isotherms can equally well be caused by surface heterogeneities, an observation confirmed by the experimental work of Coltharp and Hackerman (1973a, 1973b). In fact, studies by Dabrowski et. al. (1979) and O'Brien and Myers (1986) indicate that the effect of surface heterogeneities completely

dominates the effect of adsorbed phase non-idealities and may thus be the more important of the two factors.

2. Surface Heterogeneity with Uniform Distribution

Most treatments of liquid adsorption on heterogeneous solids make the simplifying assumption of equal-sized molecules (Rudzinski et. al., 1973; Waksmundzki et. al., 1975; Oscik et. al., 1976, 1977; Dabrowski et. al., 1979; O'Brien and Myers, 1986). Sircar (1983, 1984a, 1984b) has addressed the cases of both equal-sized and unequal-sized molecules, using the surface excess (equation (8)) as the local adsorption isotherm and integrating equation (52) with an assumed form of the distribution function. The energy parameter is taken to be the selectivity. For equal-sized molecules ($\beta=m_1/m_2=1$) Sircar uses the gamma distribution or the uniform distribution. For unequal-sized molecules, the integral equation cannot be solved analytically with the gamma distribution, and the uniform distribution is used. Since Sircar's approach is directly applicable to the description of adsorption used in this work, it will be tested for our systems in this section.

Using the surface excess, equation (52) becomes

$$n_1^e = \int_{S_{OL}}^{S_{OH}} (n_1^e)_1 \lambda(S_0) dS_0 \quad (54)$$

where $(n_1^e)_1$ is the local surface excess of a patch of surface, n_1^e is

the overall surface excess, S_0 is the selectivity in the limit of zero concentration (equation (49)), and S_{OL} and S_{OH} are lower and upper limits of S_0 , respectively. The local surface excess is given by equation (8), repeated below,

$$(n_1^e)_1 = \frac{m_1 x_1 x_2 (S-1)}{Sx_1 + \beta x_2} \quad (8)$$

and $\lambda(S_0)$ is taken to be the uniform distribution,

$$\lambda(S_0) = C \quad (55)$$

where C is a constant. The normalization requirement

$$\int_{S_{OL}}^{S_{OH}} \lambda(S_0) dS_0 = 1 \quad (56)$$

upon integration, leads to

$$\lambda(S_0) = \frac{1}{S_{OH} - S_{OL}} \quad (57)$$

Equation (50), repeated below,

$$S = S_0 (Sx_1 + x_2)^{(\beta-1)/\beta} \quad (50)$$

can be differentiated to give

$$dS_0 = \frac{Sx_1 + \beta x_2}{\beta (Sx_1 + x_2)^{(\beta-1)/\beta + 1}} dS \quad (58)$$

Equations (8), (57) and (58) are substituted into (54) to give

$$n_1^e = \frac{m_1 x_1 x_2}{\beta (S_{OH} - S_{OL})} \int_{S_L}^{S_H} \frac{S - 1}{(Sx_1 + x_2)^{(\beta-1)/\beta + 1}} dS \quad (59)$$

Since the independent variable has been changed from S_0 to S , the

limits of integration are changed from S_{OL} and S_{OH} to S_L and S_H , where

$$S_L = S_{OL}(S_L x_1 + x_2)^{(\beta-1)/\beta} \quad (60)$$

$$S_H = S_{OH}(S_H x_1 + x_2)^{(\beta-1)/\beta} \quad (61)$$

Integration of equation (59) leads to

$$n_1^e = \frac{m_1}{S_{OH} - S_{OL}} \frac{x_2}{x_1} \left\{ \left[\left(\frac{S_H}{S_{OH}} \right)^{1/(\beta-1)} - \left(\frac{S_L}{S_{OL}} \right)^{1/(\beta-1)} \right] + \frac{1}{\beta-1} \left[\frac{S_{OH}}{S_H} - \frac{S_{OL}}{S_L} \right] \right\} \quad (62)$$

Equation (62) is the adsorption isotherm for a heterogeneous surface with uniform distribution of S_0 . It contains the parameters S_{OL} and S_{OH} , m_1 and β being determined independently as described in chapter 3, and S_L and S_H being given by equations (60) and (61) at any concentration.

The mean, μ , and the variance, σ^2 , of the uniform distribution are given by

$$\mu = \frac{S_{OH} + S_{OL}}{2} \quad (63)$$

$$\sigma^2 = \frac{(S_{OH} - S_{OL})^2}{12} \quad (64)$$

The mean value of S_0 is a measure of the overall affinity between the solid and the surfactant, while the variance gives the spread in S_0 . A large variance therefore means a high degree of heterogeneity, while a variance of zero represents a homogeneous surface.

The effect of heterogeneity on adsorption with the uniform distribution was determined by calculating adsorption isotherms from equation (62). The values of m_1 and β were kept constant at 0.0033 mmole/g and 0.25, respectively, as determined in chapter 3. Figure 44 shows three isotherms with the same value of μ (1.2), but increasing degrees of heterogeneity, as indicated by the values of σ^2 . The homogeneous case ($\sigma^2=0$) results in a U-shaped isotherm, as expected. Increasing the heterogeneity changes the shape of the isotherm significantly and forces it towards an S-shape. These isotherms were generated at the rather low value of $\mu=1.2$. From Table 4 in the previous chapter it is evident that the selectivities of the surfactant/rock system under investigation in this work are in the range of 100 to 1000. The effect of heterogeneity on the adsorption isotherm at an average selectivity of $\mu=100$ is shown in Figure 45. Clearly, increasing the heterogeneity has a much smaller effect at high values of μ , even with values of σ^2 as high as 3270. Note that, at any value of μ , the maximum variance is determined by the restriction $S_{OL} \geq 0$. The maximum variance for $\mu=100$ is therefore $\sigma^2=3330$ at $S_{OL}=0$.

The full concentration range from $x_1=0$ to $x_1=1$ has been plotted in Figure 45. Two of the isotherms have been re-plotted in Figure 46 using an expanded scale more representative of the systems of this work. Isotherms at $\mu=1000$, both homogeneous ($\sigma^2=0$) and highly heterogeneous ($\sigma^2=3.33 \times 10^5$) have also been included in the figure to cover the range of selectivities used in matching the core floods of the previous chapter. From the figure it is quite obvious that even a high degree of

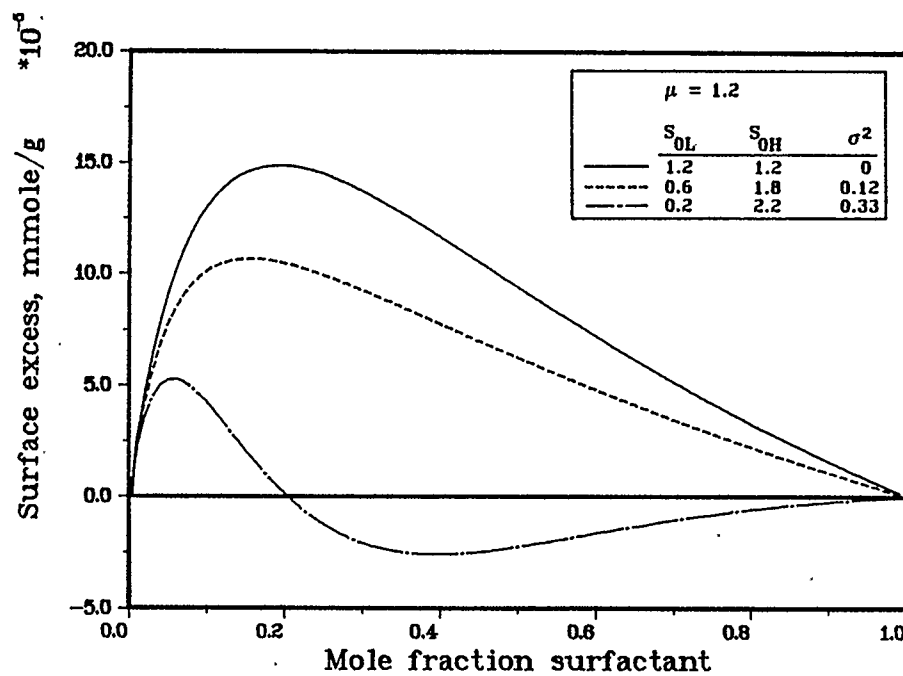


FIGURE 44. The effect of surface heterogeneity (uniform distribution of selectivities) on adsorption. $m_1=0.0033$ mmole/g, $m_1/m_2=0.25$.

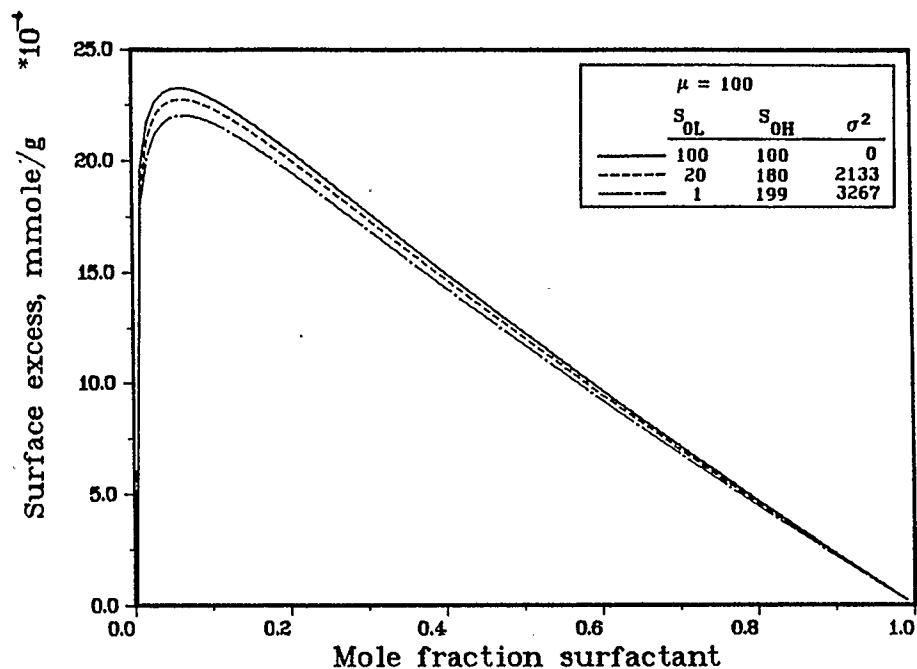


FIGURE 45. The effect of surface heterogeneity (uniform distribution of selectivities) on adsorption. $m_1=0.0033$ mmole/g, $m_1/m_2=0.25$.

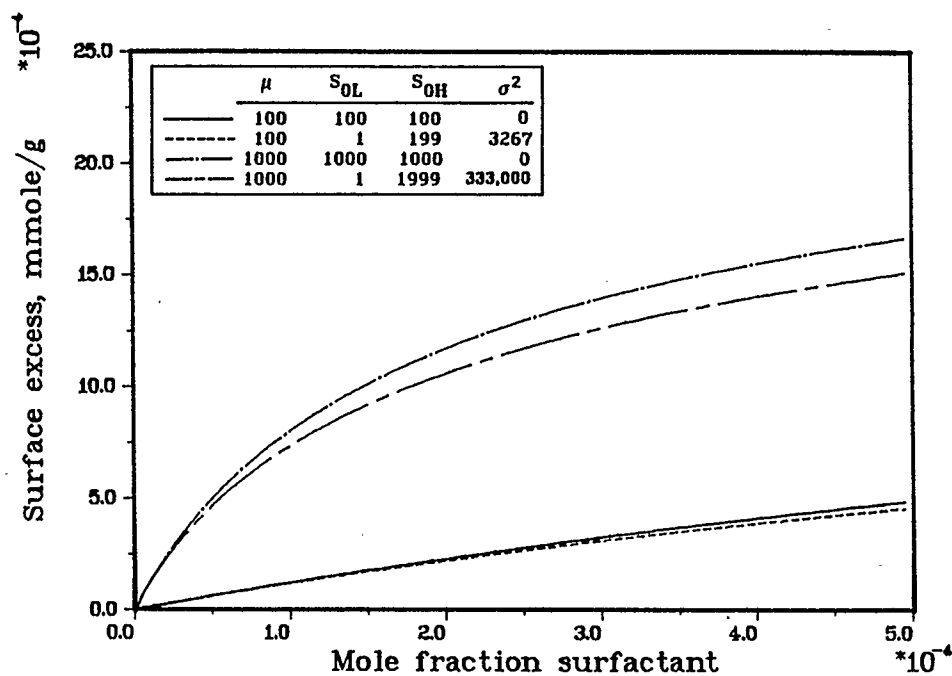


FIGURE 46. The effect of surface heterogeneity (uniform distribution of selectivities) on adsorption, low concentration range. $m_1=0.0033$ mmole/g, $m_1/m_2=0.25$.

heterogeneity does not change the isotherm to any great extent, either in magnitude or in shape. In fact, isotherms very nearly the same as the heterogeneous ones in Figure 46 can be generated using the homogeneous model with slightly lower selectivities than those indicated for the homogeneous isotherms in the figure ($S_0=800$ and $S_0=95$ instead of $S_0=1000$ and $S_0=100$).

Since the uniform distribution function does not affect the adsorption isotherms very strongly at the selectivities and concentrations of interest, this function would not be adequate in matching high and low concentration core floods with a single isotherm. Referring to Figures 36 to 39, if an isotherm is to represent both high and low concentration floods, it should represent the isotherm for the low concentration flood in the low concentration range, and that of the higher concentration flood at the higher concentrations representative of this flood. As has been noted at the end of the previous chapter, this would require an isotherm that rises steeply at very low concentrations and then approaches a slope of zero. Clearly the uniform distribution does not fulfill this requirement, since it results in isotherms of the same shape as those previously obtained in Figures 36 to 39.

3. Two-Component Heterogeneous Solid

With the uniform distribution, the probabilities of finding any value of S_0 between the limits S_{0L} and S_{0H} are equal. An approach that

may be considered the other extreme is taken in this section. The distribution of selectivities is described by two delta functions, implying that the solid consists of two components (A and B), each with its own value of S_0 (S_{0A} and S_{0B}), and each contributing a fraction z_A or z_B (with $z_A + z_B = 1$) to the total surface area of the solid. In this treatment the integral equation (52) is, in effect, converted from a continuous distribution to a discrete distribution, in this case to a sum of two terms. The overall surface excess is then given by

$$n_1^e = z_A (n_1^e)_A + z_B (n_1^e)_B \quad (65)$$

or, substituting equation (8) for $(n_1^e)_A$ and $(n_1^e)_B$,

$$n_1^e = z_A \frac{m_1 x_1 x_2 (S_A - 1)}{S_A x_1 + \beta x_2} + z_B \frac{m_1 x_1 x_2 (S_B - 1)}{S_B x_1 + \beta x_2} \quad (66)$$

where S_A and S_B are the selectivities of each solid component. These selectivities are taken as concentration dependent, and are given by equation (50) as

$$S_A = S_{0A} (S_A x_1 + x_2)^{(\beta-1)/\beta} \quad (67)$$

$$S_B = S_{0B} (S_B x_1 + x_2)^{(\beta-1)/\beta} \quad (68)$$

where S_{0A} and S_{0B} are the values of S_0 for solids A and B, respectively. The parameters of equation (66) are thus z_A , S_{0A} , and S_{0B} .

To calculate the amount of surfactant adsorbed (n_1'), equation (9) was used in chapters 2 and 4. This equation cannot be used here, since

there is no single value of selectivity. The amount of component 1 adsorbed can, however, be calculated as follows without using the selectivity. The total amount adsorbed of both components is given by equation (6) as

$$n' = \frac{m_1 m_2}{m_2 x'_1 + m_1 x'_2} \quad (69)$$

Substituting this equation into equation (4) and solving for x'_1 gives

$$x'_1 = \frac{\beta n_1^e + m_1 x_1}{m_1 - n_1^e (1 - \beta)} \quad (70)$$

with

$$x'_2 = 1 - x'_1 \quad (71)$$

Equations (70) and (71) allow calculation of x'_1 and x'_2 from the surface excess, which can be obtained from equation (66). The adsorbed phase mole fractions are substituted into equation (69) to obtain n' , and n'_1 is then given by

$$n'_1 = n_1^e + n' x_1 \quad (72)$$

Equations (70) and (71), together with the bulk phase mole fractions, also allow the determination of an "effective" selectivity from the defining equation of selectivity (equation (7)). Substituting this effective selectivity into equation (9) results in the same value of n'_1 as equation (72).

The average selectivity of the two-component solid is given by

$$\mu = z_A^{S_{OA}} + z_B^{S_{OB}} \quad (73)$$

and the variance by

$$\sigma^2 = z_A z_B (S_{OA} - S_{OB})^2 \quad (74)$$

As before, the variance is a measure of the degree of heterogeneity, which, according to equation (74), is determined by the difference of selectivities and the relative surface area that each solid contributes. The maximum contribution from the relative surface areas to surface heterogeneity occurs at $z_A = z_B = 0.5$. Therefore, the greater the difference between S_{OA} and S_{OB} , and the closer to 0.5 the values of z_A and z_B , the more heterogeneous the surface becomes. For z_A or z_B equal to 1, or for $S_{OA} = S_{OB}$, the isotherm equation (66) reverts to the homogeneous case.

To determine the effect of heterogeneity on adsorption, isotherms were calculated using equation (66) in a manner analogous to that used with the uniform distribution. Figure 47 shows four isotherms of increasing degree of heterogeneity, but with a low average selectivity μ . As with the uniform distribution, increasing the heterogeneity of the surface results in a change from a U-shaped to an S-shaped isotherm. Figure 48 shows the effect of heterogeneity at a higher value of μ . In these figures the heterogeneity is changed first by increasing $(S_{OA} - S_{OB})$ and then by increasing z_A . Inversion to an S-shape does not take place at $\mu = 100$, but, unlike with the uniform distribution, heterogeneity can affect the isotherm significantly even at high μ . Figure 49 shows the same isotherms over a lower concentration range.

The effect of the parameters z_A , S_{OA} and S_{OB} on the adsorption isotherm is shown in Figures 50 to 52. As expected, increasing any of

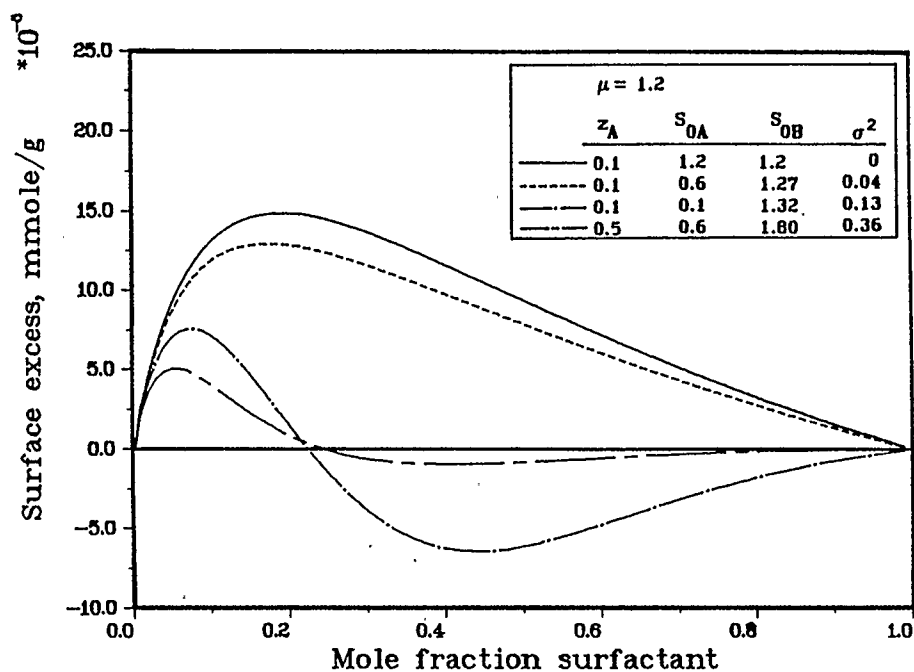


FIGURE 47. The effect of surface heterogeneity (two-component solid) on adsorption. $m_1=0.0033$ mmole/g, $m_1/m_2=0.25$.

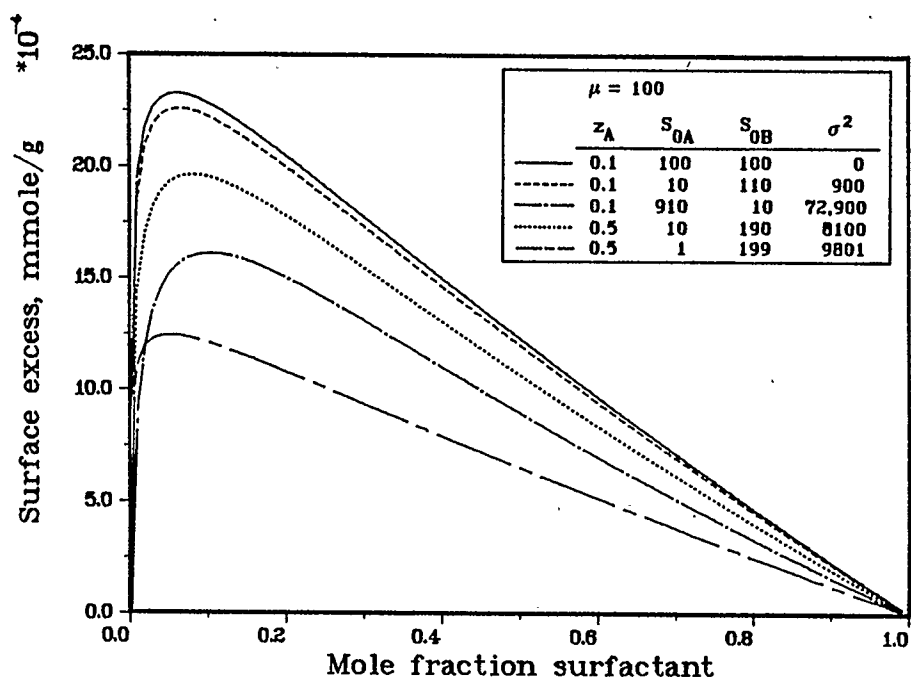


FIGURE 48. The effect of surface heterogeneity (two-component solid) on adsorption. $m_1=0.0033$ mmole/g, $m_1/m_2=0.25$.

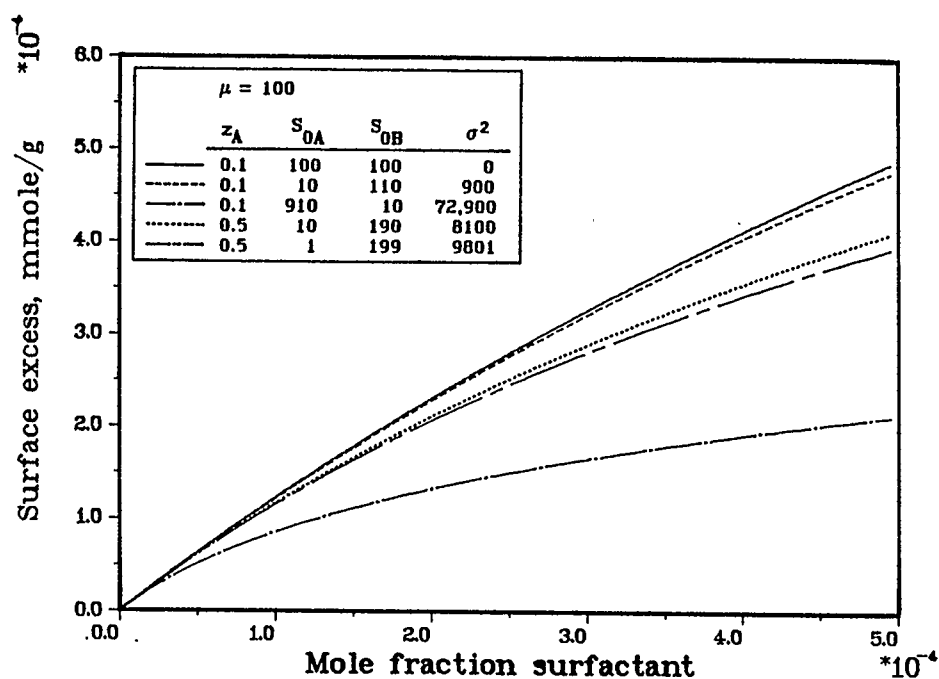


FIGURE 49. The effect of surface heterogeneity (two-component solid) on adsorption, low concentration range. $m_1=0.0033$ mmole/g, $m_1/m_2=0.25$.

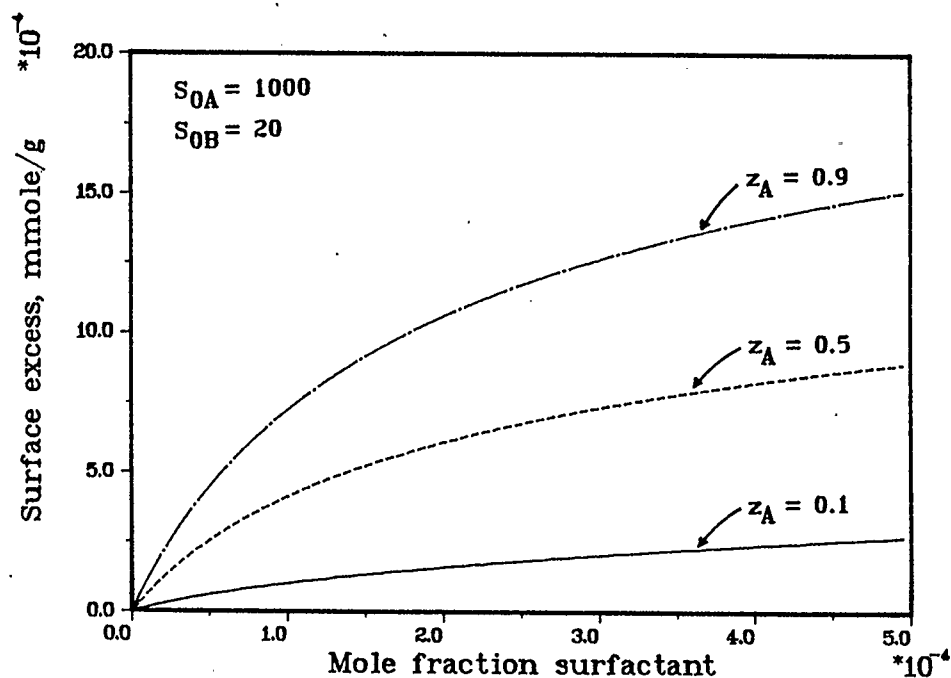


FIGURE 50. The effect of z_A on the adsorption isotherm of a two-component heterogeneous solid. $m_1=0.0033$ mmole/g, $m_1/m_2=0.25$.

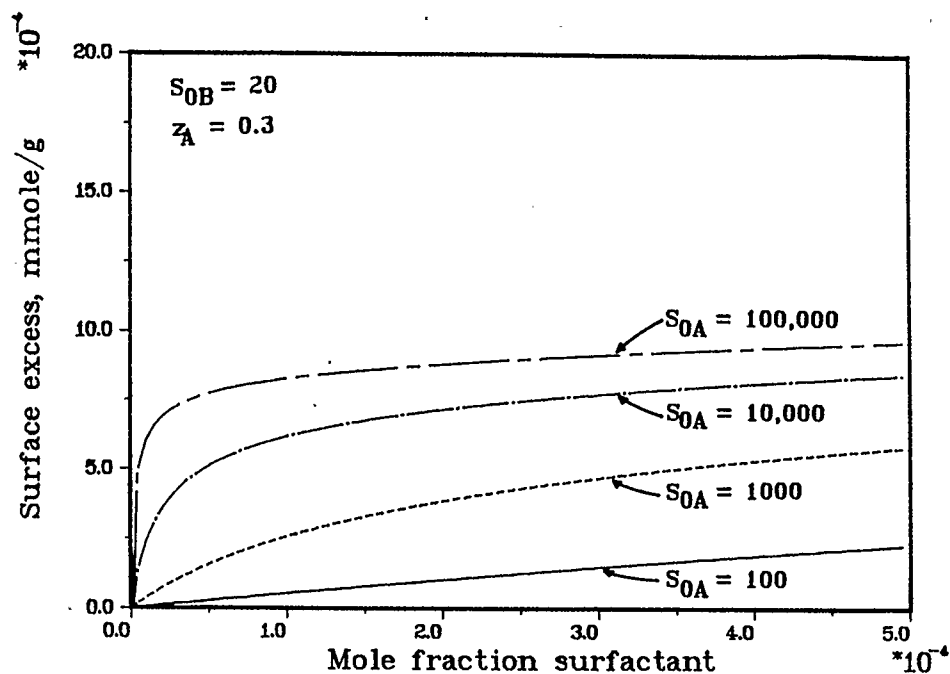


FIGURE 51. The effect of S_{0A} on the adsorption isotherm of a two-component heterogeneous solid. $m_1 = 0.0033$ mmole/g, $m_1/m_2 = 0.25$.

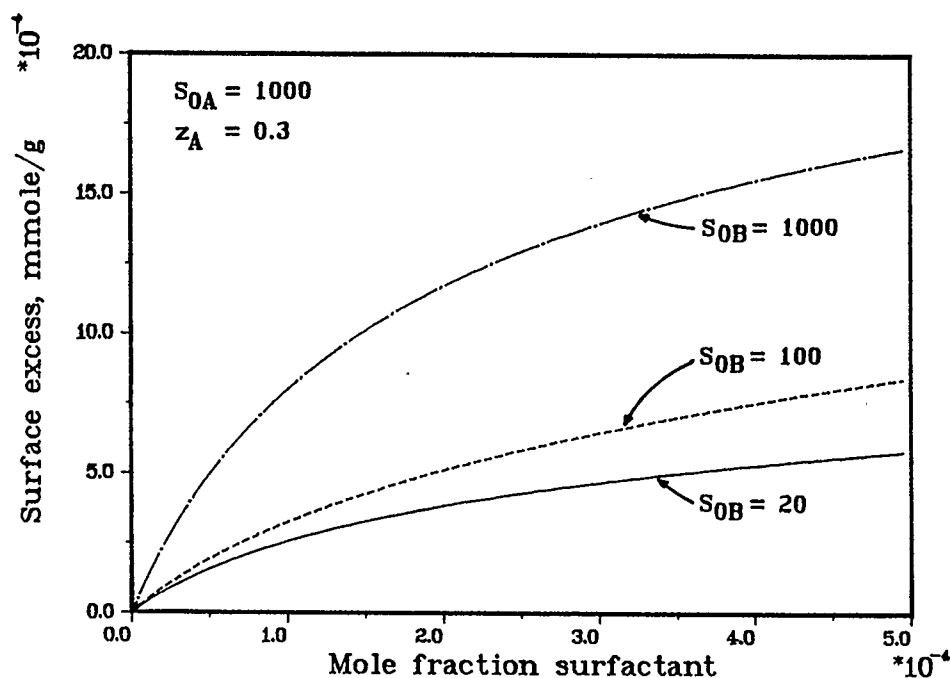


FIGURE 52. The effect of S_{0B} on the adsorption isotherm of a two-component heterogeneous solid. $m_1 = 0.0033$ mmole/g, $m_1/m_2 = 0.25$.

these parameters increases adsorption, since increasing z_A increases the amount of surface with the higher selectivity, and increasing S_{OA} or S_{OB} increases the average selectivity of the solid. An interesting effect that will be important in matching core effluent profiles is observed in Figure 51. Increasing S_{OA} causes the isotherm to rise more steeply near $x_1=0$ and then to become almost constant. This shape is desirable for matching high and low concentration core floods with a single set of parameters, as has been noted at the end of chapter 4.

4. History Matching Core Floods with Heterogeneous Solid

Surface heterogeneities can be incorporated into the flow model, described in chapter 2, quite simply by using equation 66 instead of equation 8 to calculate the equilibrium surface excess. Note that the selectivities of each solid component, S_A and S_B , are taken to be concentration dependent (equations (67) and (68)), as was discussed in the previous chapter. Details of the solution to the flow model appear in the Appendix.

The two-component heterogeneous solid was used to match simulated and experimental surfactant effluent profiles for the same core floods that were described previously. The results, shown in Figures 53 to 60 and Table 6, indicate that satisfactory matches were obtained for all floods. The ability to match the experimental data is not unique to this model, but now for the first time low and high concentration floods can be matched with the same set of parameters. The parameters

in Table 6 were then used, together with equation (66), to calculate one adsorption isotherm for each pair of core floods. These are shown in Figures 61 to 64. For comparison, the adsorption isotherms obtained by modelling a homogeneous surface with equation (50) are also shown. The important point here is that the heterogeneous model generates a single adsorption isotherm for each pair of core floods, while separate isotherms are generated for the members of a pair by the homogeneous model. The heterogeneous model is thus superior in that it generates a single isotherm at each set of conditions. Even though it may be argued that the increased flexibility of the heterogeneous model is due to a larger number of parameters, this is compensated by the fact that it matches two core floods with the same set of parameters.

The effective selectivity for cores T3 and T11 was calculated as described in section 3 above and is shown in Figure 65, together with selectivities calculated for the same cores using the homogeneous model with equation (50). Again, a single curve is obtained with the heterogeneous model, while two different curves are required by the homogeneous model. The figure illustrates the required functional form of the selectivity. Equation (50) by itself, although a decreasing function of concentration, does not generate the required shape of the selectivity, while introducing surface heterogeneity in the form of a two-component solid does.

The data in Table 6 indicate that z_A is constant for all floods. This is quite reasonable, since the solid was Berea sandstone in all

TABLE 6. Experimental conditions and matching parameters obtained from the surface excess model with a two-component heterogeneous solid.

| Core # | T3 | T11 | T1 | T13 | T6 | T9 | T7 | T10 |
|-------------------------------------|--------|--------|--------|--------|--------|--------|--------|--------|
| Surfactant Conc. (g/l) | 1.00 | 9.97 | 1.00 | 9.97 | 1.01 | 10.0 | 1.01 | 10.0 |
| Surfactant Mole Frac. $\times 10^4$ | 0.372 | 3.73 | 0.363 | 3.65 | 0.374 | 3.73 | 0.379 | 3.78 |
| Brine Conc. (% TDS) | 10.5 | 10.5 | 10.5 | 10.5 | 21.0 | 21.0 | 21.0 | 21.0 |
| Temp. (deg. C) | 75 | 75 | 23 | 23 | 50 | 50 | 75 | 75 |
| Slug Vol. (PV) | 1.04 | 0.73 | 1.01 | 0.78 | 2.12 | 0.86 | 2.04 | 1.14 |
| z_A | 0.17 | 0.17 | 0.17 | 0.17 | 0.16 | 0.16 | 0.17 | 0.17 |
| S_{0A} | 10,000 | 10,000 | 12,000 | 12,000 | 20,000 | 20,000 | 20,000 | 20,000 |
| S_{0B} | 10 | 10 | 75 | 75 | 100 | 100 | 70 | 70 |
| m_1 (mmole/g) | 0.0033 | 0.0033 | 0.0033 | 0.0033 | 0.0033 | 0.0033 | 0.0033 | 0.0033 |
| m_1/m_2 | 0.25 | 0.25 | 0.25 | 0.25 | 0.25 | 0.25 | 0.25 | 0.25 |
| k_1 (1/hr) | 1.0 | 1.0 | 1.0 | 1.0 | 1.0 | 1.0 | 1.0 | 1.0 |
| k_2 (1/hr) | 0.005 | 0.002 | 0.005 | 0.005 | 0.003 | 0.003 | 0.002 | 0.002 |
| Dispersion Par. (cm) | 1.0 | 0.15 | 1.0 | 0.15 | 1.5 | 0.4 | 2.0 | 0.5 |

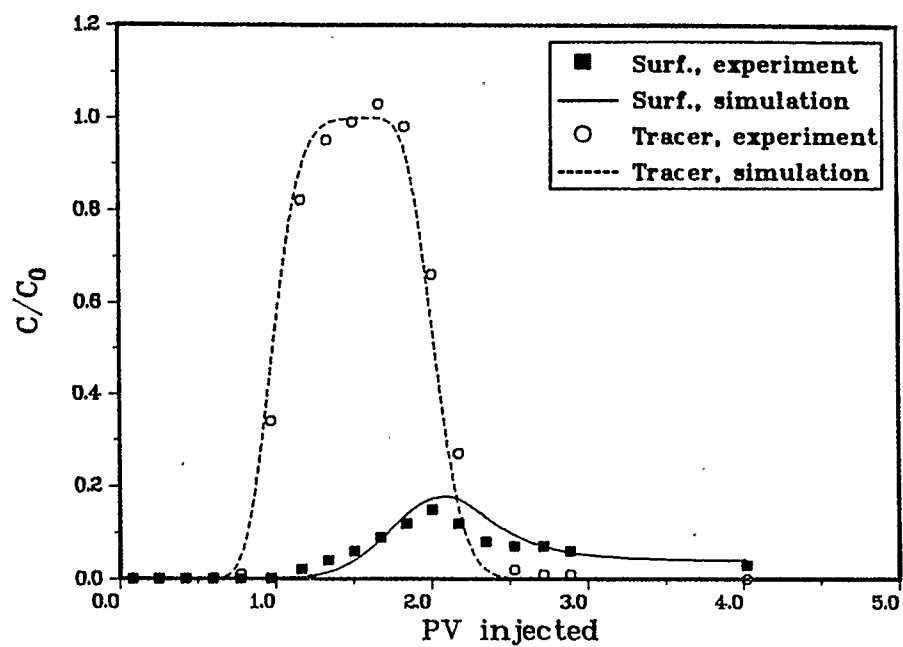


FIGURE 53. Core T3 effluent profiles. Two-component heterogeneous solid.

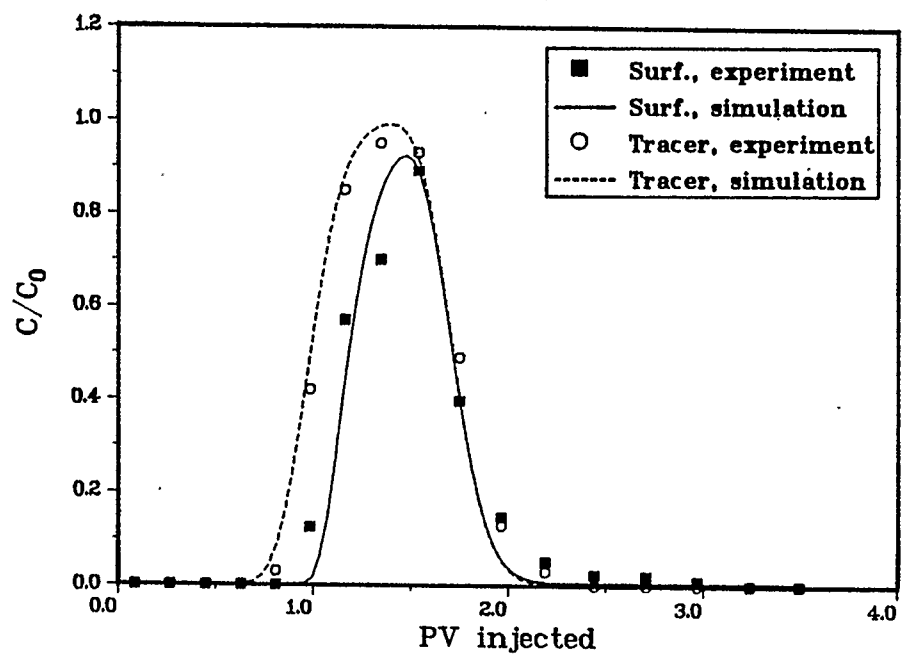


FIGURE 54. Core T11 effluent profiles. Two-component heterogeneous solid.

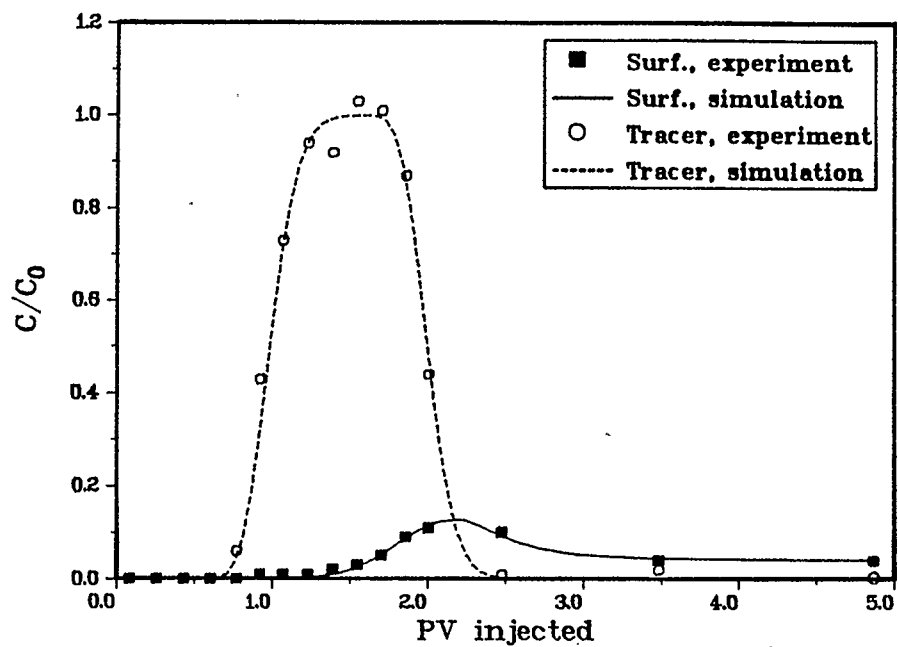


FIGURE 55. Core T1 effluent profiles. Two-component heterogeneous solid.

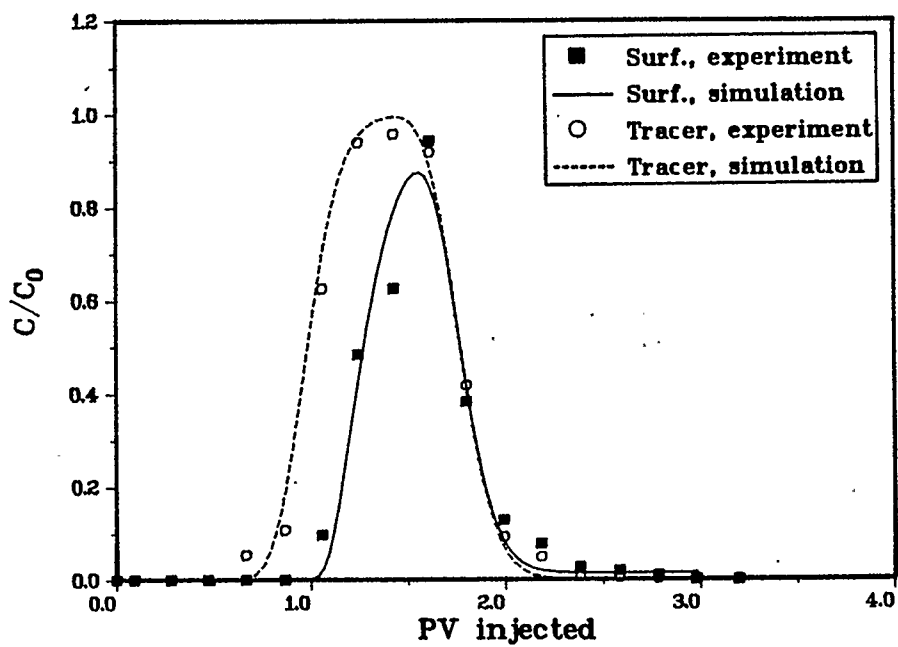


FIGURE 56. Core T13 effluent profiles. Two-component heterogeneous solid.

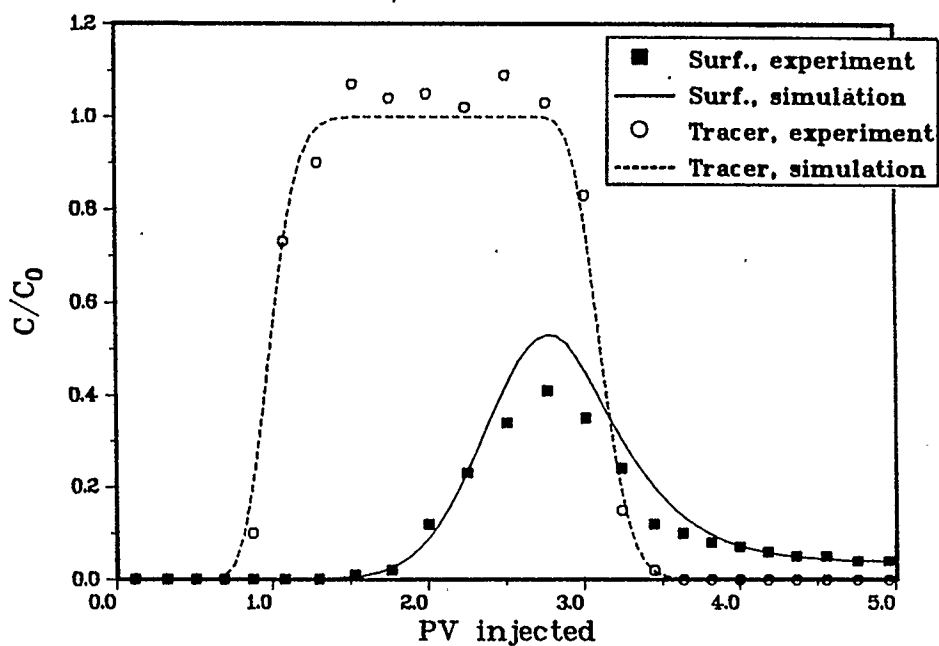


FIGURE 57. Core T6 effluent profiles. Two-component heterogeneous solid.

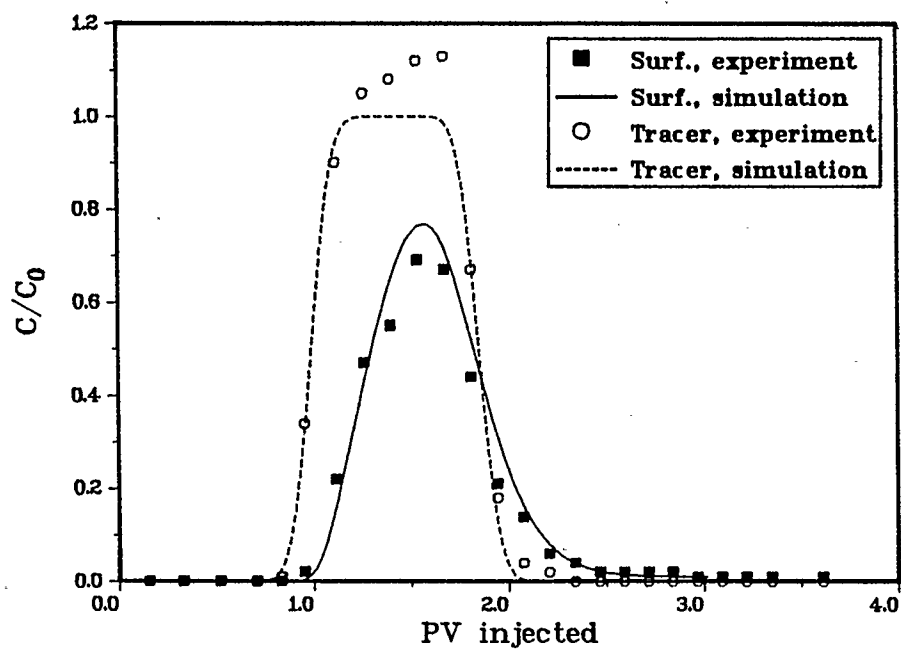


FIGURE 58. Core T9 effluent profiles. Two-component heterogeneous solid.

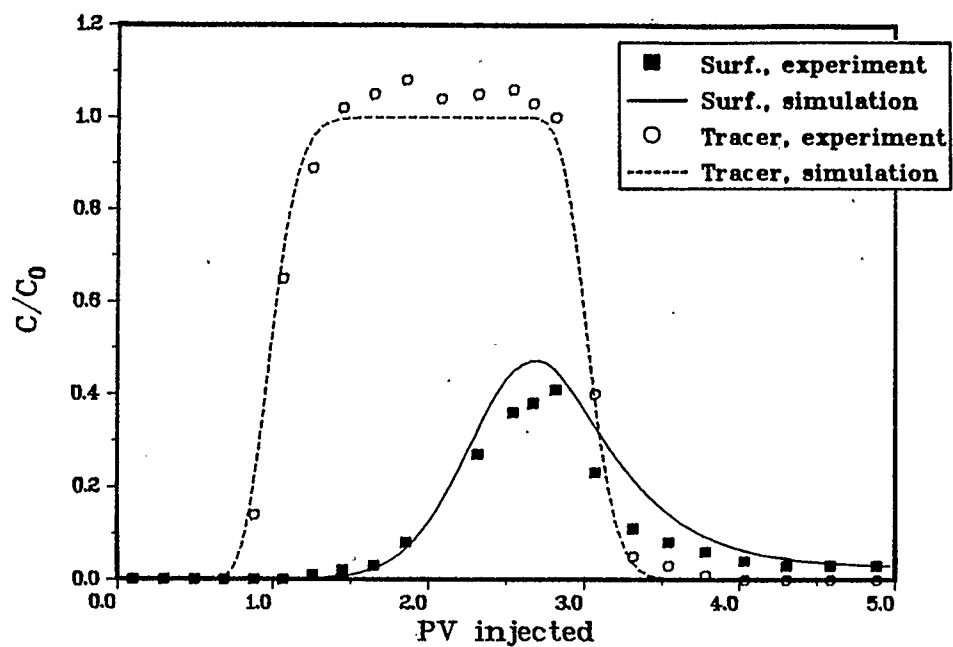


FIGURE 59. Core T7 effluent profiles. Two-component heterogeneous solid.

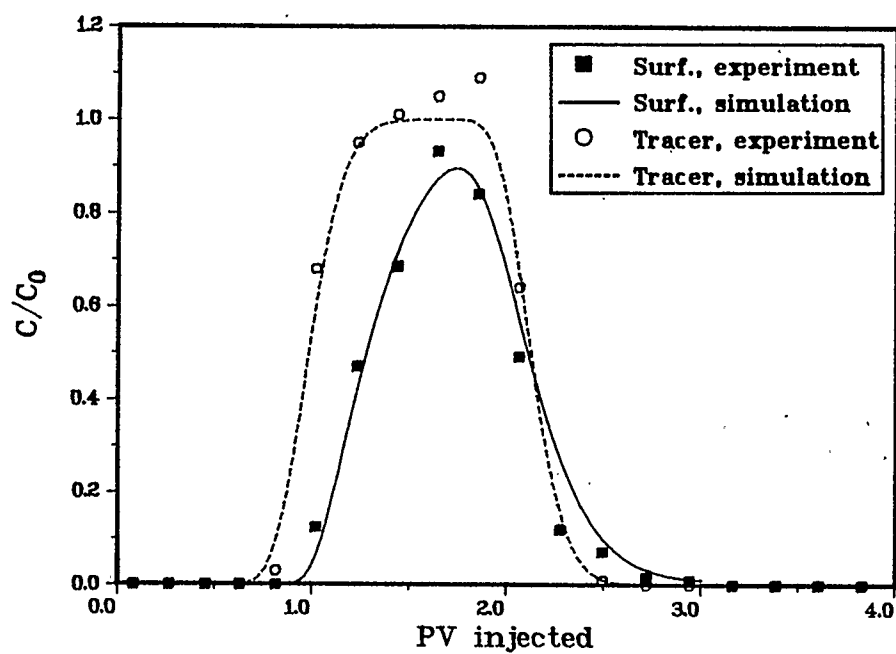


FIGURE 60. Core T10 effluent profiles. Two-component heterogeneous solid.

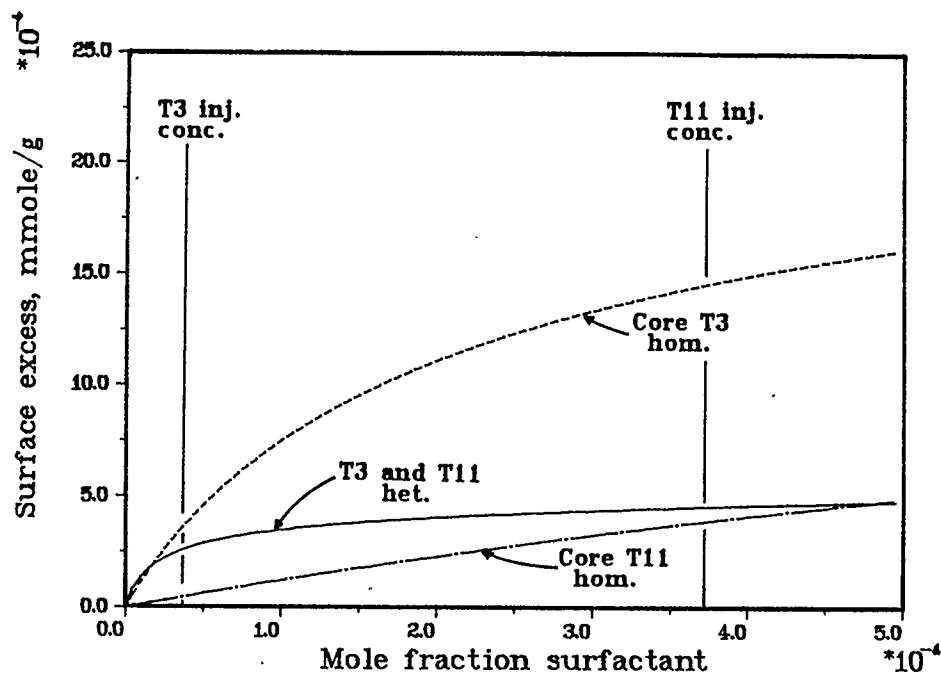


FIGURE 61. Adsorption isotherms for cores T3 and T11 from heterogeneous model, and homogeneous variable selectivity model with equation (50).

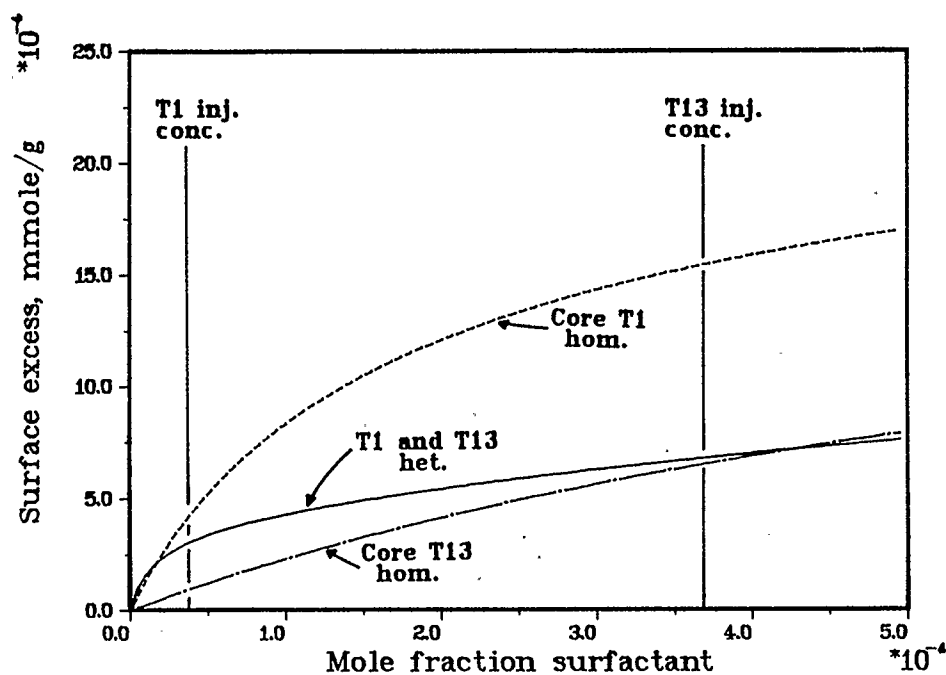


FIGURE 62. Adsorption isotherms for cores T1 and T13 from heterogeneous model, and homogeneous variable selectivity model with equation (50).

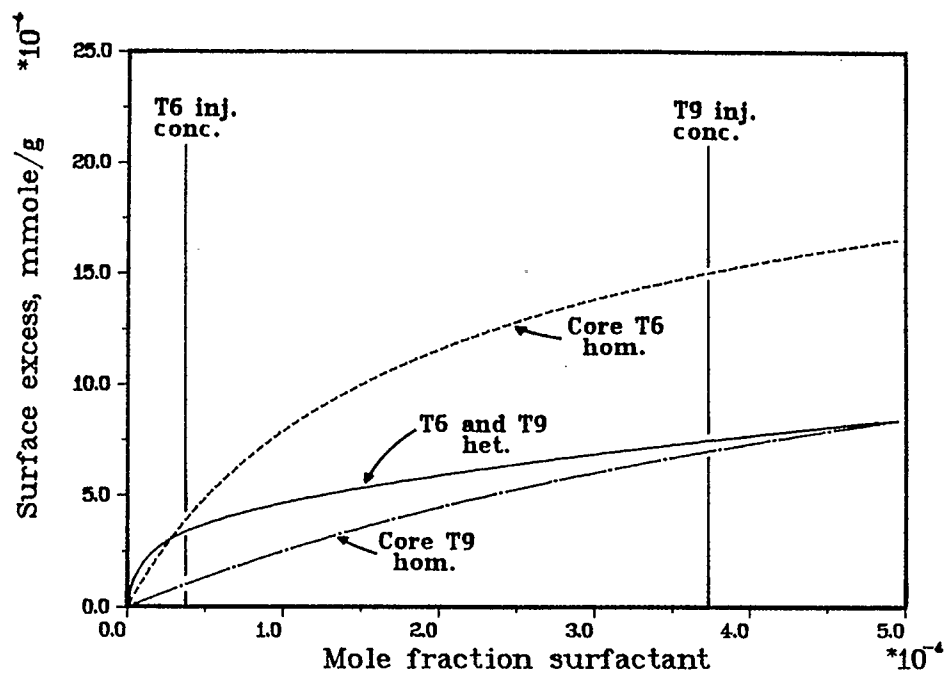


FIGURE 63. Adsorption isotherms for cores T6 and T9 from heterogeneous model, and homogeneous variable selectivity model with equation (50).

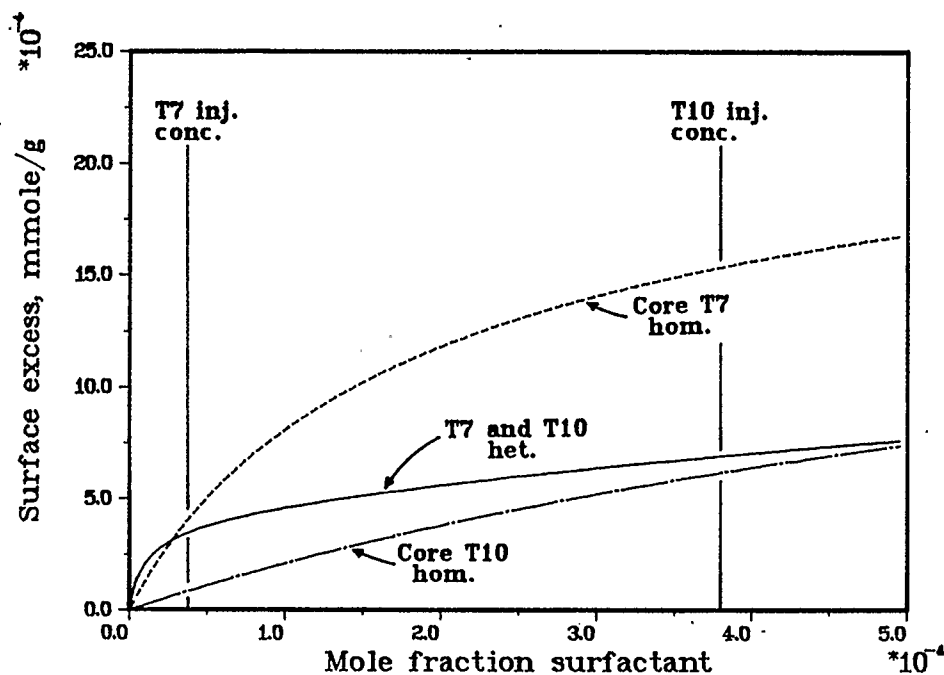


FIGURE 64. Adsorption isotherms for cores T7 and T10 from heterogeneous model, and homogeneous variable selectivity model with equation (50).

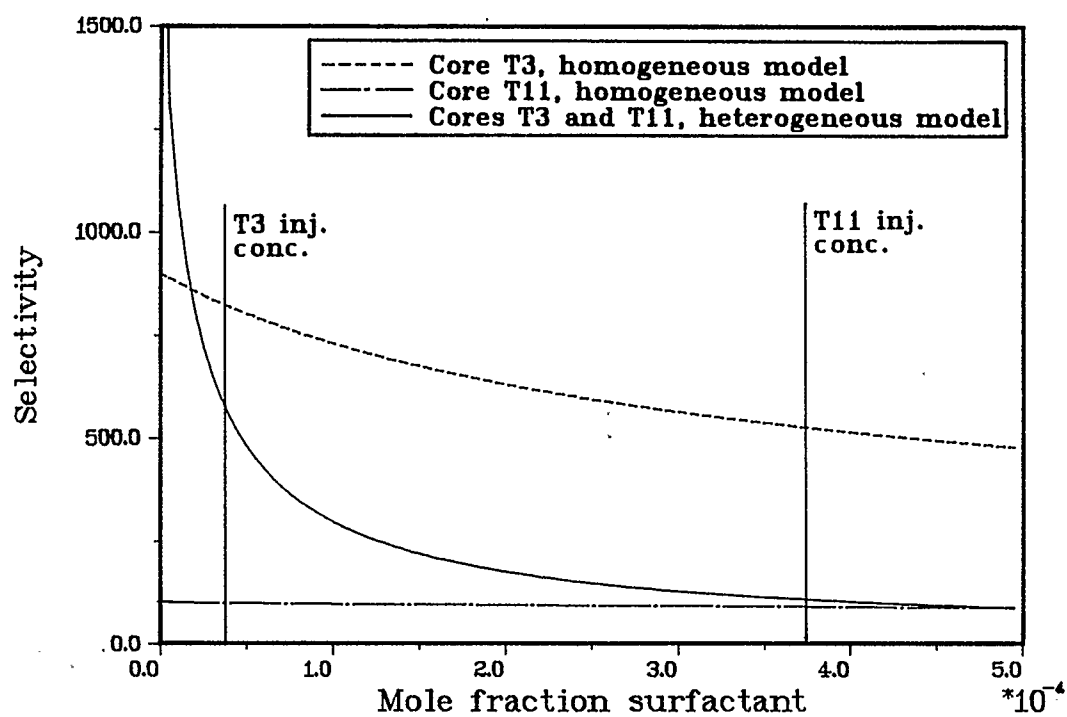


FIGURE 65. Selectivity as a function of concentration, calculated from the best fit parameters (Tables 4 and 6) of the heterogeneous and homogeneous models.

cases. Temperature seems to affect S_{OB} more strongly than S_{OA} , S_{OB} increasing with decreasing temperature, while increasing the brine salinity increases S_{OA} and S_{OB} .

It has been noted in much of the literature on adsorption on heterogeneous surfaces that the adsorption isotherm is quite insensitive to the choice of distribution function, or, stated differently, that different distribution functions may represent the same experimental isotherm equally well. Apparently this is not true for the two distributions and the surfactant/rock system used in this work. The two-component solid allows matching of core floods run at different concentrations, while the uniform distribution does not. The two-component solid is capable of generating a certain shape of isotherm, but the uniform distribution is not.

In conclusion it may be said that the adsorption isotherms generated using the two-component solid are likely to be more realistic and more useful for interpolation of adsorption data, simply because they represent two core floods rather than just one, and therefore greatly reduce the risk of extrapolating to concentrations other than the injected concentration. From Figures 61 to 64 and Table 4 it is obvious that history matches obtained with the model utilizing a homogeneous surface yield higher selectivities in floods with lower surfactant concentrations. The extrapolation of data beyond surfactant concentrations used in the flood should therefore be done with extreme caution. The figures also indicate that the effluent profile of the

higher concentration flood is not sensitive to the shape of the adsorption isotherm at concentrations much lower than the injected concentration. By contrast, the isotherms obtained with the heterogeneous model are representative of the whole concentration range from the low to the high injected concentration.

While there is no direct experimental evidence for the correctness of the two-component surface, its success in matching the experimental effluent profiles suggests that it has some physical significance. This view is supported by the fact that any rock sample is likely to be highly heterogeneous because it consists of an array of different minerals, and because different crystal faces of the same mineral may exhibit different adsorbent-adsorbate interactions. Support to the heterogeneous model is also given by the statement made by other authors that heterogeneous surfaces are probably much more common than homogeneous ones, and that heterogeneities play a dominant role in the adsorption process.

In order to attach more meaning to the parameters of the model, independent measurement of the mineral components of the rock and their adsorption behavior would be required. Once such measurements are available and the model is shown to correlate with them, adsorption on a rock may be predicted on the basis of a knowledge of its components. The two-component heterogeneous model can easily be extended to multicomponent surfaces. However, this will increase the number of parameters by two for each component added. Some independent

measurement of the parameters is therefore necessary for these to retain any physical meaning, rather than just being adjustable parameters.

CHAPTER 6

ADSORPTION OF SURFACTANT MIXTURES

1. Introduction

Surfactants used in practical applications are almost always complex multicomponent mixtures of surface active compounds. The reason for this can be two-fold: Many surfactants are synthesized from starting materials that are mixtures, since this is more economical and more feasible from a technical point of view than working with isomerically pure materials. Secondly, different surfactants may be mixed to design surfactant systems that are optimized in terms of performance parameters such as solubility, salt tolerance, interfacial tension, foaming capacity, adsorption on solids, detergency, or solubilization. In many applications, surfactant mixtures exhibit synergistic properties superior to those of each individual component, and it may therefore not even be desirable to work with pure surfactants.

Surfactants used in enhanced oil recovery are mixtures for the same reasons just stated for surfactants in general. Even though these mixtures may be more effective in recovering oil than pure components, a problem that is a direct consequence of blending surfactants is the chromatographic separation of the components during flow through the porous medium by differential adsorption on the solid or differential partitioning into an oil phase. Such separation of the components

changes the composition of the mixture continuously, thereby changing its properties and most likely its ability to recover oil. It is therefore important to understand the chromatographic movement of a surfactant mixture through the reservoir and its implications on oil recovery.

Petroleum sulfonates are commonly used in surfactant flooding. These surfactants are manufactured by sulfonation of refinery streams and therefore contain a huge variety of compounds. Gale and Sandvik (1973) have shown that a range of equivalent weights of the components of petroleum sulfonates is desirable in that the high equivalent weight fraction provides the interfacial activity required for oil recovery, the low equivalent weight fraction enhances the solubility of the mixture, and the intermediate equivalent weights act as sacrificial adsorbates. These authors have also shown that the high equivalent weight components adsorb preferentially at the solid/liquid interface, and that this strongly affects oil recovery. The work of Bae and Petrick (1976) also indicates chromatographic separation of petroleum sulfonates, while Lawson and Dilgren (1978) have found no such effect.

Much work has recently been carried out on tailoring surfactant systems by mixing different surfactant types. Mixtures of carboxymethylated ethoxylates and dialkyl benzene sulfonates have been shown to be effective in high salinity brines, and to be invariant in terms of phase behavior to changes in temperature and salinity (Balzer, 1987). The mixture can be customized for a particular reservoir by

changing the proportion or structure of the components. In mixtures of alkylphenyl ethoxy alcohols and alkylphenyl ethoxy sulfonates, the nonionic component enhances the solubility of the anionic component, while the anionic component prevents phase separation of the nonionic one (Austad et. al., 1987). Westerkamp and Menz (1987) have shown that mixtures of alkylphenyl ethoxylates or propoxylates and commercial sulfonates can be adapted to a wide variety of reservoir conditions. Mixtures of ethoxylates and alkyl sulfonates have been studied by Pusch et. al. (1987). All these authors realize the importance of developing a good understanding of the differential adsorption of such mixtures and its effect on surfactant performance.

Research into all aspects of the behavior of surfactant mixtures has increased rapidly over the last ten years. It has led to a better understanding of many interesting phenomena in mixed surfactant systems and to new applications of such mixtures. An overview of some aspects of the behavior of surfactant mixtures has been presented by Scamehorn (1986a, 1986b). This chapter will review some of the literature on the fundamental aspects of the adsorption of surfactants and surfactant mixtures, with the goal of applying these principles to modelling of the chromatographic movement of the components of a foam-forming surfactant. Monomer-micelle equilibria play an important role in surfactant adsorption and will therefore be described in the next section. The surface excess will again be used to model adsorption, requiring extension of the surface excess model from binary to multicomponent mixtures. A model for transport of a ternary surfactant

mixture through porous media will be developed. Experimental data collected from a core flood using two purified components of a commercial foam-forming surfactant will be presented and modelled using the surface excess model for ternary mixtures.

2. Monomer-Micelle Equilibrium

A unique property of surfactants that arises from the amphipathic nature of a surfactant molecule is the tendency to form aggregates, either in solution (micelles), or at the gas/liquid interface (monolayers), or at the solid/liquid interface (admicelles or hemimicelles). Below a certain concentration, known as the critical micelle concentration (cmc), surfactant molecules exist as single, dispersed molecules in solution. When the surfactant concentration is increased to the cmc, the molecules begin to form micelles, whereby the hydrophobic portion of the molecule is removed from the aqueous environment and is in contact with other hydrophobic groups inside the micelle. The interior of a micelle is believed to have a structure resembling that of liquid paraffin (Shinoda, 1963). The hydrophilic portion of the molecule is exposed to the aqueous phase on the outside of the micelle. At any concentration above the cmc, surfactant molecules in the micelles are in equilibrium with those existing as monomers.

A good understanding of monomer-micelle equilibrium is essential to any process involving surfactants, since the process may depend

either on micelle properties or on monomer concentration and composition. For example, solubilization of compounds into micelles depends on micelle composition, while adsorption at the solid/liquid interface and surface or interfacial tension lowering depend on the monomer concentration. In this work, interest is focused on adsorption at the solid/liquid interface.

It is generally believed that surfactant monomers adsorb at the solid surface, but micelles do not. The monomer concentration determines the chemical potential of individual species in solution, and it is this chemical potential that provides the driving force for adsorption. A mathematical description of monomer-micelle equilibrium is therefore essential to an adsorption model that takes into account the dependence of adsorption on monomer concentration.

From the above discussion it should be obvious that the cmc is an important parameter in surfactant systems, since this is the concentration at which monomer-micelle equilibrium first sets in. In general, the more hydrophobic a surfactant molecule, the lower is its cmc, i.e. the molecules tend to aggregate at lower concentrations. Equivalently, higher salt concentrations make the aqueous solution more polar and lower the cmc of a surfactant. The factors influencing the cmc have been reviewed extensively by Shinoda (1963). These include the hydrocarbon chain length in the hydrophobic part of the surfactant molecule, the number and type of hydrophobic groups, the number, type and position of polar groups, and the concentration and type of added

electrolyte or other additives. Many physical properties of surfactant solutions change abruptly at the cmc, allowing the cmc to be determined fairly easily by measuring such a property as a function of concentration. Some of the more commonly used methods of determining the cmc employ the measurement of electrical conductance, surface tension, dye solubilization, or light scattering (Shinoda, 1963; Rosen, 1978).

The behavior of surfactant solutions is commonly described using the pseudophase-separation model (Shinoda, 1963; Scamehorn, 1986a, 1986b), which considers the micelles to be a separate thermodynamic phase in equilibrium with the monomer phase. This is analogous to vapor-liquid equilibrium, where a dilute phase is in equilibrium with a condensed phase. The cmc in monomer-micelle equilibrium is then similar to the dew point in vapor-liquid equilibrium. Even though some of the assumptions made in the pseudophase-separation model have not been verified experimentally (Scamehorn, 1986b), it has proven to be a valuable tool in the description of many phenomena observed in surfactant solutions.

In a surfactant solution below the cmc, the monomer concentration is equal to the overall surfactant concentration, since no micelles have yet been formed. When the concentration of a solution containing a single pure surfactant is raised above the cmc, the monomer concentration remains constant at the value of the cmc, since any surfactant added will now be incorporated into the micellar phase. In a

single surfactant system, determining the monomer concentration is therefore simply a matter of measuring the cmc. The same is not true in a mixed surfactant system. Consider, for example, a binary surfactant mixture in water. Such a mixture will have its cmc at some overall concentration at which mixed micelles containing both surfactant components will form. However, one component may be more hydrophobic than the other and will therefore be incorporated into the micelles more readily. The proportion of this component will then be higher in the micellar phase than in the overall solution. The monomer phase, on the other hand, will become enriched in the other component, and, unlike in a single surfactant system, the monomer concentration will continue to change above the cmc. The composition of both the monomer and the micellar phases will also change with increasing concentration, and it is the concentration and composition of the monomer phase that determines how much of each component will be adsorbed. A model that describes monomer-micelle equilibrium in mixed surfactant systems must be capable of predicting the cmc of the mixture, the monomer concentration, and the composition of monomer and micellar phases.

Several such models have been put forward, ranging from very simple to very complex. The earliest, and also the simplest, of these is the ideal mixed micelle model, several versions of which have been described by Lange (1953), Lange and Beck (1973), Shinoda (1954), Mysels and Otter (1961), and Clint (1975). Nishikido et. al. (1975) have extended the binary mixture models of these authors to multicomponent mixtures. Different versions of the ideal mixed micelle

model appear in the literature, and some confusion as to which version applies to a specific system (nonionic versus ionic surfactant, water versus salt solution) has been resolved by Funasaki (1978). The basic assumption of the ideal mixed micelle model is, obviously, ideal mixing of surfactants in the micellar phase. This implies that interactions between unlike components in the micelle are very similar to interactions between like components, or that activity coefficients in the micellar phase are unity. This model predicts that the cmc of any mixture will fall between the cmc's of the pure components. It applies to surfactants that are members of a homologous series, i.e. have the same polar group, but hydrocarbon chains of different lengths.

Dissimilar surfactants generally do not follow ideal mixed micelle theory, as indicated by the fact that their mixture cmc may be lower than the cmc of either pure component. This behavior is observed in mixtures of unlike ionic surfactants or ionic and nonionic surfactants. Hydrocarbon surfactants usually exhibit negative deviations from ideality, meaning that the mixture cmc falls below that predicted by the ideal theory. This indicates that micelles are formed more easily in the mixture than with the pure components, or that mixing of surfactants makes the formation of micelles energetically more favorable. Interestingly, mixtures of hydrocarbon and fluorocarbon surfactants often exhibit positive deviations from ideality, indicating weaker interactions between the hydrocarbon and fluorocarbon chains in the micelle. Cmc's of nonideal mixed micelles can be predicted accurately using regular solution theory to model activity coefficients

in the micellar phase. Rubingh (1978) has described the regular solution model for binary surfactant mixtures, and Holland and Rubingh (1983) have extended this model to multicomponent mixtures.

A criterion for the applicability of the models just described has usually been agreement between theoretical and experimental cmc's, since the cmc is an easily measured quantity. A much more severe test would be agreement between measured and calculated monomer concentrations. Direct experimental measurement of monomer concentrations is, however, orders of magnitude more difficult than measuring cmc's. Although attempts at measuring monomer concentration by various techniques have been made, no generally applicable method is known as yet (Scamehorn, 1986a), and, as has been pointed out by Scamehorn (1986b), there is a great need for such a method. Osborne-Lee et. al. (1983) have described an ultrafiltration method that shows considerable promise.

Osborne-Lee et. al. (1985) have used their ultrafiltration method to show that the regular solution theory of mixed micellization predicts cmc's accurately, but, for many systems, is less accurate in predicting monomer concentrations. This deviation from the regular solution model is caused by significant contributions of the excess entropy of mixing to the excess free energy of mixing. The excess entropy of mixing is, by definition, neglected in regular solution theory. Osborne-Lee et. al. (1985) and Osborne-Lee and Schechter (1986) have developed a model of mixed micelle formation that takes into

account the excess entropy of mixing and predicts monomer concentrations quite accurately. Kamrath and Franses (1986) have used the mass action model to describe nonideal mixed micelles. This model is applicable to micelles of low aggregation number, where treatment of small micelles as a separate phase may not be realistic.

The most interesting aspect of mixed surfactant systems in the context of this work is probably the depression of the cmc below the cmc's of the pure components. A lower cmc is equivalent to a lower monomer concentration, which in turn may lead to lower adsorption.

3. Ideal Mixed Micelle Theory

Later in this chapter, the ideal mixed micelle theory will be applied to the members of a homologous series of surfactants, and will be incorporated into the surface excess model to describe the chromatographic transport of mixtures of such surfactants through porous media. The equations pertinent to the theory will therefore be summarized in this section. The derivation follows the treatment by Clint (1975). Even though Clint has applied his equations to nonionic surfactants, Lange and Beck (1973) and Funasaki (1978) have shown that the same equations apply to ionic surfactants in salt solutions.

Consider a mixture of two surfactants of total concentration c . The mole fraction of surfactant 1, on a surfactant only basis, is α , that of surfactant 2 thus being $1-\alpha$. Below the cmc of the mixture,

$$c_1^m = \alpha c \quad (75)$$

$$c_2^m = (1-\alpha)c \quad (76)$$

where c_1^m and c_2^m are the monomer concentrations of surfactants 1 and 2, respectively. Above the cmc, the concentration of surfactant 1 in the micelles is $\alpha c - c_1^m$, and its mole fraction, on a surfactant only basis, is

$$\alpha_m = \frac{\alpha c - c_1^m}{c - c_1^m - c_2^m} \quad (77)$$

The chemical potential of component 1 in the ideal mixed micelles is

$$\mu_{M1} = \mu_{M01} + RT \ln(\alpha_m) \quad (78)$$

where μ_{M01} is the chemical potential in a pure component 1 micelle. The monomer phase is dilute, and is considered to be an ideal solution. The chemical potential of component 1 in the monomer phase is then

$$\mu_1 = \mu_{01} + RT \ln(c_1^m) \quad (79)$$

where μ_{01} is the standard chemical potential of non-micellar component 1. At the cmc of pure component 1,

$$\mu_{M01} = \mu_{01} + RT \ln(\text{cmc}_1) \quad (80)$$

where cmc_1 is the cmc of pure component 1. At equilibrium, $\mu_{M1} = \mu_1$, and therefore, from equations (78), (79), and (80),

$$c_1^m = \alpha_m \text{cmc}_1 \quad (81)$$

Similarly for component 2,

$$c_2^m = (1-\alpha_m) \text{cmc}_2 \quad (82)$$

Eliminating α_m from equations (81) and (82) gives

$$c_2^m = \left[1 - \frac{c_1^m}{cmc_1} \right] cmc_2 \quad (83)$$

and substituting equation (77) into (81) leads to

$$c_1^m = \left[\frac{\alpha c - c_1^m}{c - c_1^m - c_2^m} \right] cmc_1 \quad (84)$$

Eliminating c_2^m from equations (83) and (84) gives a quadratic equation in c_1^m :

$$(c_1^m)^2 \left[\frac{cmc_2}{cmc_1} - 1 \right] + c_1^m \left[c - cmc_2 + cmc_1 \right] - \alpha c cmc_1 = 0 \quad (85)$$

which can be solved for c_1^m :

$$c_1^m = \frac{-(c-\Delta) \pm [(c-\Delta)^2 + 4\Delta\alpha c]^{1/2}}{2 \left[\frac{cmc_2}{cmc_1} - 1 \right]} \quad (86)$$

with

$$\Delta = cmc_2 - cmc_1 \quad (87)$$

At the mixture cmc , combination of equations (75) and (81), and (76) and (82) gives the two equations

$$\alpha c = \alpha_m cmc_1 \quad (88)$$

$$(1-\alpha)c = (1-\alpha_m) cmc_2 \quad (89)$$

which, on elimination of α_m , result in an expression for the cmc of the mixture:

$$\frac{1}{cmc} = \frac{\alpha}{cmc_1} + \frac{1-\alpha}{cmc_2} \quad (90)$$

To calculate the cmc and the monomer concentrations in the mixture, one needs to know the pure component cmc's, the total surfactant concentration, and the value of α . The cmc is then calculated from equation (90). Below the cmc, the monomer concentrations are given by equations (75) and (76). Above the cmc, the monomer concentration of surfactant 1 can be calculated using the positive root of equation (86). The surfactant 2 monomer concentration is then obtained from equation (83), and the relative amounts of each component in the micelles from equation (77).

To illustrate the use of these equations, monomer concentrations have been calculated for two surfactants with $\text{cmc}_1 = 10^{-5}\text{M}$ and $\text{cmc}_2 = 5 \times 10^{-4}\text{M}$. Monomer concentrations for each single surfactant system are shown in Figure 66. As expected, they increase linearly with surfactant concentration below the cmc, but remain constant at the value of the cmc at overall concentrations higher than the cmc. When the two surfactants are mixed, with $\alpha = 0.1$, the monomer concentrations in Figure 67 result. Below the mixture cmc ($8.5 \times 10^{-5}\text{M}$), the monomer concentrations again increase in proportion to the overall surfactant concentration. Above the cmc, however, surfactant 1, which has the lower cmc, is preferentially incorporated into micelles, and its concentration in the monomer phase therefore decreases. Surfactant 2, on the other hand, becomes enriched in the monomer phase, and its monomer concentration increases above the cmc. Figure 68 shows the change in α_m , the fraction of component 1 in the micellar phase, with total surfactant concentration. Initially α_m is much higher than the

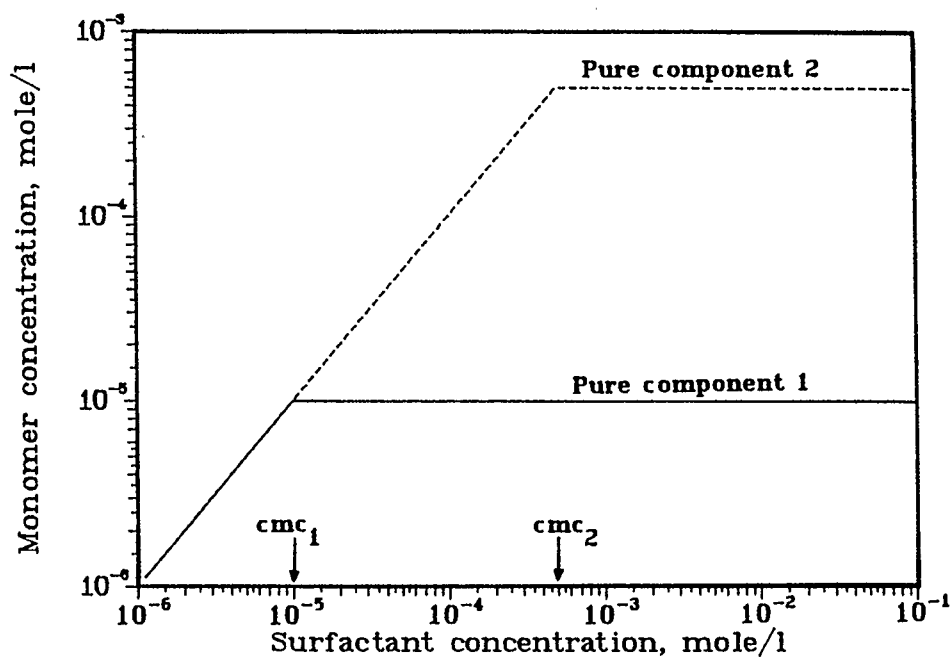


FIGURE 66. Monomer concentrations of two surfactant solutions, each containing a single pure surfactant.

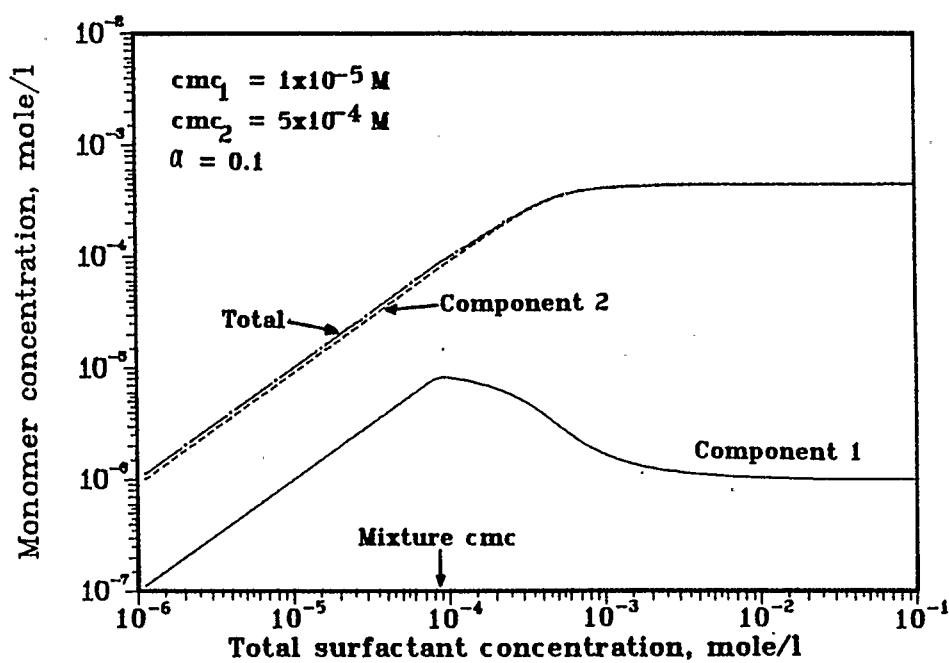


FIGURE 67. Monomer concentrations of a mixed surfactant system containing two surfactants.

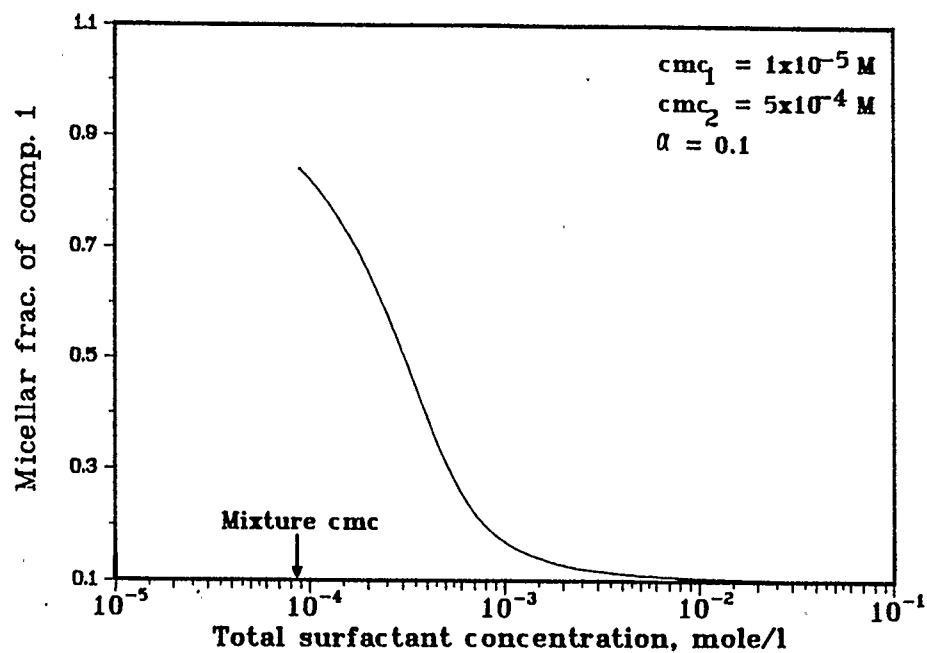


FIGURE 68. The fraction of component 1 in the micellar phase in a mixed surfactant system.

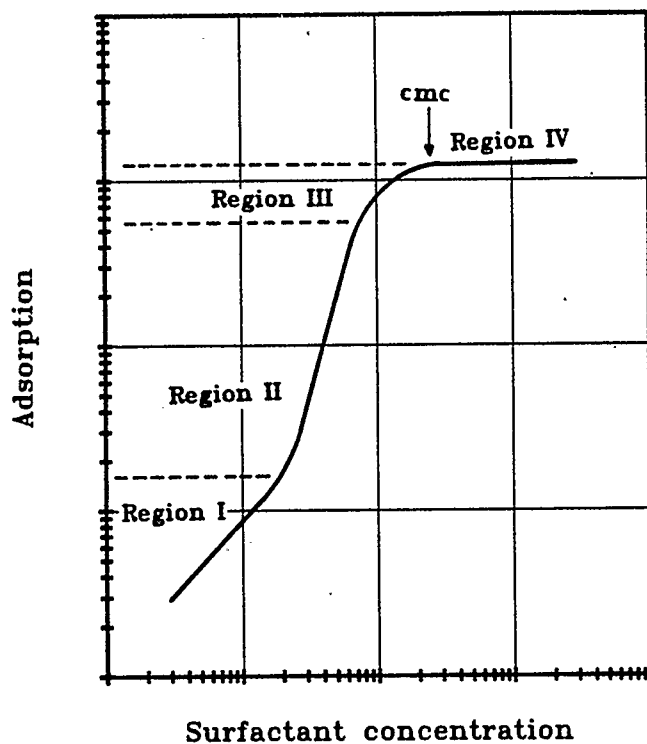


FIGURE 69. A typical surfactant adsorption isotherm.

overall fraction of surfactant 1 in the mixture ($\alpha=0.1$), demonstrating enrichment of this surfactant in the micelles. At high surfactant concentrations, the value of α_m approaches the overall value of 0.1, since most of the total surfactant is now in the micelles, the monomer phase being comparatively dilute.

4. Literature on the Fundamental Aspects of Surfactant Adsorption

In parallel to the surfactant adsorption studies appearing in the petroleum literature, a large amount of more fundamental work on the mechanisms of surfactant adsorption has been carried out over the last 30 years. The latter usually employs relatively clean, single-component solids, such as alumina, quartz, or kaolinite, and single pure surfactants or well-defined mixtures of pure surfactants. Since most of the solids used are highly adsorptive because of their large specific surface area and a surface charge opposite to the charge of the surfactant ion, adsorption can conveniently be measured through concentration changes in batch experiments.

A common theme that runs through much of the literature on surfactant adsorption from the early to the very recent studies is the shape of surfactant adsorption isotherms on polar solids such as oxides. Much of the earlier work on this subject has come from Fuerstenau and his coworkers. A schematic of an adsorption isotherm of an ionic surfactant on a solid of opposite charge is shown in Figure 69. This isotherm can be divided into four regions. In region I (the

Henry's Law region), the slope of the log-log plot is usually close to unity. At these low adsorption densities, individual ions are scattered across the surface, and adsorption is believed to take place mainly by counterion binding or ion exchange at the surface. At a certain well-defined concentration, called the hemi-micelle or critical admicelle concentration (c_{ac}), the slope of the isotherm increases sharply. The increased rate of adsorption in region II is caused by the surfactant forming aggregates (hemi-micelles or admicelles) at the surface through van der Waals interactions between the surfactant hydrocarbon chains. The attractive forces between surfactant molecules are much the same as those in micelle formation in solution, but the c_{ac} is usually one or two orders of magnitude lower than the cmc. At this stage the surfactant molecules in the adsorbed layer are believed to be packed vertically with the polar groups at the solid surface. Through the strong attractive forces between surfactant molecules, adsorption continues beyond neutralization of the surface charge, causing a reversal of the sign of this charge. In region III the rate of adsorption decreases because the surfactant molecules now have to approach the surface against electrostatic repulsion. Region IV is characterized by plateau adsorption, which usually commences at a concentration equal to the cmc. The beginning of plateau adsorption at the cmc provides strong experimental evidence for the theory that adsorption takes place from the monomer phase only. The fact that both monomer concentration and adsorption reach a constant value at the cmc seems to suggest a direct correlation between the two. It should be realized, however, that the adsorption sites on the solid may be filled

before the cmc is reached, in which case plateau adsorption is determined by the adsorptive capacity of the solid rather than by the monomer concentration.

Overwhelming evidence for the mechanism of surfactant adsorption described above has been obtained from electrokinetic studies (Fuerstenau, 1956; Somasundaran et. al., 1964; Somasundaran and Fuerstenau, 1966; Wakamatsu and Fuerstenau, 1968), heat of immersion measurements (Roy and Fuerstenau, 1968), and from some rather interesting experiments using fluorescence probes to elucidate the structure of the adsorbed layer (Chandar et. al., 1987). Much effort has been dedicated to the determination of factors that influence adsorption levels and the transition points between the adsorption regions illustrated in Figure 69. These factors include surfactant type (Rosen and Nakamura, 1977; Scamehorn, 1982b; Somasundaran and Gryte, 1985), the hydrocarbon chain length of the surfactant molecule (Fuerstenau, 1956; Somasundaran et. al., 1964; Wakamatsu and Fuerstenau, 1968), the structure of the hydrocarbon chain (Dick et. al., 1971), salt type and concentration (Fuerstenau, 1956; Somasundaran and Hanna, 1979; Somasundaran and Gryte, 1985; Somasundaran, 1987), mineralogy of the adsorbent (Somasundaran and Gryte, 1985), and solution pH (Fuerstenau, 1956; Somasundaran and Fuerstenau, 1966; Fuerstenau and Wakamatsu, 1975). The surface of an oxide usually carries a charge that is very strongly dependent on the pH of the solution in contact with it. In general, a surfactant adsorbs strongly, if the pH is such that the solid surface and the surfactant molecule

are oppositely charged. Adsorption does, however, also take place with surfactants on solids of equal charge, or with nonionic surfactants on charged solids. All the experimental data collected using homologous series of surfactants indicate that adsorption increases with increasing size of the hydrophobe, or that the higher molecular weight species adsorb more strongly. This point will be of some importance in the experimental work to be described in a later section.

There has been much discussion on the number of layers of surfactant molecules adsorbed at the solid/liquid interface (Hough and Rendall, 1983; Clunie and Ingram, 1983). Surface coverage determinations are usually carried out by estimating the solid's specific surface area and the size of the surfactant molecule. Some of the experimental data reported indicate that adsorption approximates a monolayer, others indicate bilayer or even multilayer adsorption (Somasundaran and Fuerstenau, 1966; Roy and Fuerstenau, 1968; Wakamatsu and Fuerstenau, 1968; Zimmels et. al., 1975; Rosen and Nakamura, 1977; Scamehorn et. al., 1982a, 1982b; Brode, 1988). Harwell et. al. (1985a) have stated that a bilayer forms on the high energy patches of surface, while low energy patches are covered with sparsely adsorbed single molecules that may form a bilayer at progressively higher solution concentrations. This then re-introduces the concept of heterogeneous surfaces. It has been stated by both Scamehorn et. al. (1982a) and Harwell et. al. (1985a) that it is essential to include surface heterogeneities into any model of adsorption, if it is to represent experimental data accurately. Evidence for bilayer coverage has been

obtained from wettability and contact angle measurements (O'Connor and Sanders, 1956; Brode, 1988). The first layer of surfactant molecules is thought to adsorb with the polar group at the solid surface and the hydrophobe extended into the solution, rendering the surface hydrophobic. At higher surfactant concentrations, a second layer adsorbs by association of its hydrocarbon chains with those in the first layer. The polar groups of the second layer are thus exposed to the bulk solution, with a resultant change of the wettability of the surface to hydrophilic. From data in all the literature cited above, it is probably fair to say that a structure somewhere between a monolayer and a bilayer exists at the solid surface.

Surfactant adsorption isotherms of single surfactants and mixtures have been modelled by Trogus et. al. (1979a), Scamehorn et. al. (1982a, 1982b, 1982c) and Harwell et. al. (1985a). All these models include monomer-micelle equilibrium in the description of adsorption, usually in the form of ideal mixed micelle theory. Many of the unique features of surfactant adsorption, particularly in surfactant mixtures, are controlled by monomer-micelle equilibrium, the reason being the competition of both the micellar and the adsorbed phases for molecules from the monomer phase. Figure 70 illustrates the equilibrium between the three phases. An important point to note from this figure is the exchange of molecules between the monomer and micellar phases, and between the monomer and adsorbed phases. Since micelles are believed not to adsorb, there is no direct exchange between the micellar and adsorbed phases.

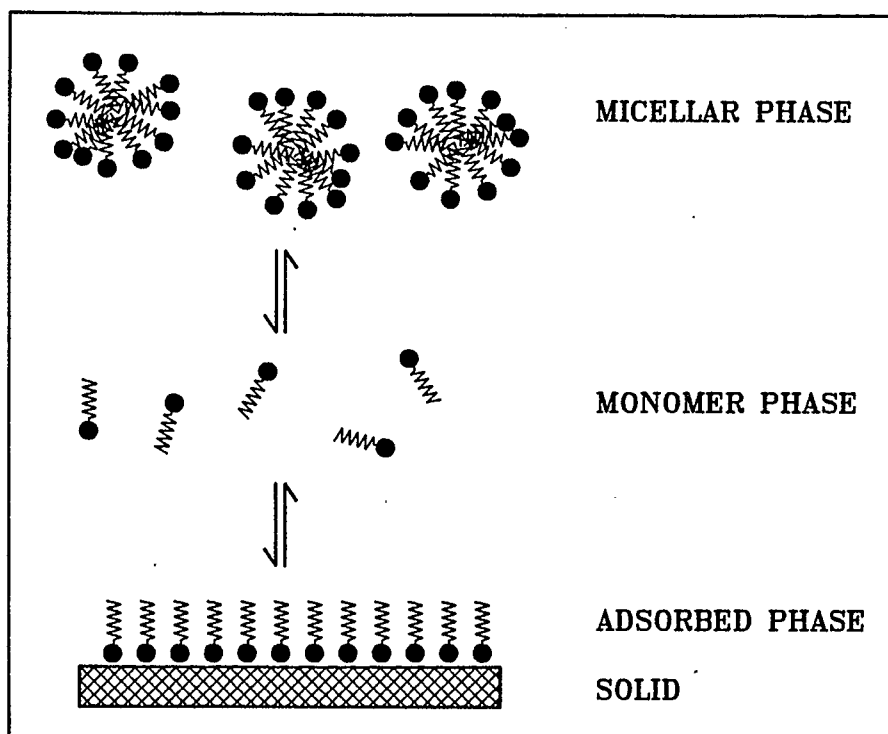


FIGURE 70. Monomer-micelle equilibrium in a surfactant solution in contact with a solid. Note that there is no direct exchange between the micellar and adsorbed phases.

In a surfactant mixture all three phases will be mixed, that is they will contain all surfactant components, but the composition of the phases will be different from each other and from the overall composition of the solution. Consider, for example, a mixture containing two surfactants. If the component that adsorbs more strongly is also the one that micellizes preferentially, then the micellar phase may incorporate this component to a greater extent than the other component and may thus protect it from being adsorbed. Conversely, the adsorption of a less strongly adsorbing component may increase by mixing it with a more strongly adsorbing component, since the latter may incorporate the former into mixed admicelles at concentrations lower than those at which the former would form admicelles by itself. Above the cmc of a surfactant mixture, the monomer phase continually changes its concentration and composition with increasing overall concentration. An overall increase in monomer concentration tends to increase adsorption. On the other hand, a decrease in monomer concentration of the higher molecular weight component, which is also the more strongly adsorbing component, by preferential micellization tends to decrease adsorption. There is therefore a delicate balance of effects in a surfactant mixture, with adsorption being determined by the concentration and composition of the phases in equilibrium.

Model studies by Trogus et. al. (1979a) have shown that adsorption isotherms of a surfactant mixture may exhibit maxima and minima before reaching plateau adsorption, and that a mixture of surfactants may

exhibit lower plateau adsorption than either pure component. Experimental data on the adsorption of surfactant mixtures have been presented by Scamehorn et. al. (1982b, 1982c) and Somasundaran (1987). Scamehorn et. al. (1983) have used a reduced adsorption isotherm to predict adsorption of mixtures from pure component adsorption, and Scamehorn et. al. (1983) and Roberts et. al. (1986) have attempted to describe admicelle formation by analogy with micelle formation using ideal solution theory.

The discussion above has dealt with work carried out by measuring adsorption in the static mode. The concepts described have been used by Trogus et. al. (1979b) and Harwell et. al. (1982, 1985b) to model flow of surfactant mixtures through porous media. Harwell et. al. (1985b) have presented experimental data from core floods to confirm the applicability of their model. Both authors use ideal mixed micelle theory in conjunction with a model of adsorption at the solid/liquid interface.

Some of the more interesting observations made by these authors are as follows. In a low concentration ($< \text{cmc}$) flood, the less strongly adsorbing component of a binary surfactant mixture is produced at the core outlet first, as expected. However, if the injected concentration is above the cmc, and if the component with the higher tendency to adsorb also has the lower cmc, then this component may be shielded from adsorption in the micellar phase. Contrary to expectation, the more strongly adsorbing component may then be produced first. Presumably

there is an intermediate concentration at which the components do not separate at all during flow through the porous medium. It should be noted that reversal of the elution order may not take place, if the affinity between the more strongly adsorbing component and the surface is high enough to dominate its lower monomer concentration, or if the component with the higher tendency to adsorb is also the one with the higher cmc.

Trogus et. al. (1979b) have found in their model studies that a surfactant mixture can be formulated in such a way as to minimize adsorption. Similarly, fractionation during flow through the porous medium can be minimized or even eliminated by taking advantage of the phenomena described above (Harwell et. al., 1982, 1985b). Balzer (1987) has measured adsorption of mixtures of caboxymethylated ethoxylates and dialkyl benzene sulfonates on quartz, and has found adsorption of the mixture to be significantly lower than that of either pure component. It has also been observed that fractionation of components is severe at low injected concentrations, but can be reduced greatly by using higher injection concentrations. An interesting prediction from the model studies is the elution of surfactant from a core at concentrations higher than the injected concentration. That this is, indeed, possible has been confirmed experimentally by Bae and Petrick (1976), Ziegler and Handy (1981), Trogus et. al. (1979b), and Harwell et. al. (1985b).

The unexpected overshoot in concentration can again be explained using monomer-micelle equilibrium. For example, the monomer concentration of one component in a binary surfactant mixture may decrease with

increasing overall concentration, as shown in Figure 67. This may cause this component to desorb, resulting in an increase in its bulk concentration, possibly to a value exceeding the injected concentration.

From the above discussion it is obvious that the pseudophase-separation model is a powerful tool that is capable of explaining many unexpected phenomena in mixed surfactant systems. In the following section, the surface excess concept will be extended to multicomponent mixtures. Together with the ideal mixed micelle theory of section 3, it will then be incorporated into a flow model for transport of surfactant mixtures through porous media. The resulting model will be thermodynamically more sound than the Trogus model, since it uses the surface excess concept rather than the idealized description of adsorption (Henry's Law) used by Trogus et. al. (1979b). Trogus uses his model with hypothetical systems to show the kind of behavior that may be seen in surfactant mixtures. No experimental data are presented. Also, the model presented here will be considerably simpler than the rather complex model of Harwell et. al. (1985b). Harwell combines a complicated description of adsorption based on electrostatic interactions between molecules in the adsorbed layer with a theory for the movement of concentration waves through the porous medium. The surface excess concept that is used in this work provides a straightforward, yet perfectly general, description of adsorption. Different degrees of complexity can be incorporated into the surface excess model by considering functional forms of the selectivity or

surface heterogeneities.

5. The Surface Excess Concept for Multicomponent Mixtures

The surface excess concept has been discussed in chapter 2, where it was applied to the description of adsorption of a binary mixture (surfactant in water). Minka and Myers (1973) have developed the corresponding equations for multicomponent mixtures.

As has been shown in chapter 2, the surface excess of component i in a mixture can be expressed as

$$n_i^e = n'(x'_i - x_i) \quad (91)$$

The amount adsorbed in a monolayer in equilibrium with a multicomponent liquid is given by

$$\frac{1}{n'} = \sum_j \frac{x'_j}{m_j} \quad (92)$$

This equation is equivalent to equation (6), and the same remarks made in connection with that equation apply. By equating fugacities in the bulk and adsorbed phases, Minka and Myers (1973) have derived the following equation, relating mole fractions in both phases:

$$f_i x_i = f'_i x'_i \exp \left[- \frac{A}{RT} \frac{\sigma - \sigma_i^o}{m_i} \right] \quad (93)$$

where the variables are as defined previously. Minka and Myers (1973) define K_{ij} as

$$K_{ij} = \frac{f'_i f_j}{f'_j f_i} \exp \left[\frac{\sigma A}{RT} \left(\frac{1}{m_j} - \frac{1}{m_i} \right) + \frac{A}{RT} \left(\frac{\sigma_i^O}{m_i} - \frac{\sigma_j^O}{m_j} \right) \right] \quad (94)$$

Inserting n' from equation (92) and x'_i from equation (93) into (91), multiplying by

$$\left[\frac{f'_i}{f_i} \exp \left(- \frac{A}{RT} \frac{\sigma - \sigma_i^O}{m_i} \right) \right] / \left[\frac{f'_i}{f_i} \exp \left(- \frac{A}{RT} \frac{\sigma - \sigma_i^O}{m_i} \right) \right] = 1 \quad (95)$$

and taking into account the expression for K_{ij} (equation (94)) leads to

$$n_i^e = \frac{x_i \left[1 - \frac{f'_i}{f_i} \exp \left(- \frac{A}{RT} \frac{\sigma - \sigma_i^O}{m_i} \right) \right]}{\sum_j K_{ij} x_j / m_j} \quad (96)$$

The second term in the numerator can be multiplied by

$$\sum_j x'_j = 1 = \sum_j \frac{f'_j x_j}{f'_j} \exp \left[\frac{A}{RT} \frac{\sigma - \sigma_j^O}{m_j} \right] \quad (97)$$

Using the definition of K_{ij} from equation (94) then gives

$$n_i^e = \frac{x_i - \sum_j x_i x_j K_{ij}}{\sum_j K_{ij} x_j / m_j} \quad (98)$$

Multiplying the first term in the numerator by

$$\sum_j x_j = 1 \quad (99)$$

finally leads to the following expression for the surface excess in a multicomponent mixture:

$$n_i^e = \frac{\sum_j x_i x_j (1 - K_{ij})}{\sum_j x_j K_{ij} / m_j} \quad (100)$$

The selectivity S_{ij} is defined as

$$S_{ij} = \frac{x'_i/x'_j}{x_i/x_j} \quad (101)$$

and is given by equation (36) as

$$S_{ij} = \frac{f_i f'_j}{f_j f'_i} \exp \left[\frac{\sigma A}{RT} \left(\frac{1}{m_i} - \frac{1}{m_j} \right) + \frac{A}{RT} \left(\frac{\sigma_j^0}{m_j} - \frac{\sigma_i^0}{m_i} \right) \right] \quad (102)$$

From equations (94) and (102),

$$S_{ij} = 1/K_{ij} \quad (103)$$

The following properties of the quantity S_{ij} can easily be verified from equation (101) or (102):

$$\begin{aligned} S_{ij} &= 1 \quad (i = j) \\ S_{ij} &= 1/S_{ji} \\ S_{ij} &= S_{ip} S_{pj} \end{aligned} \quad (104)$$

As has been discussed before, S_{ij} is, in general, a function of concentration, since the activity coefficients and the solid/liquid interfacial tension σ depend on concentration.

In a ternary mixture containing two surfactants (components 1 and 2) in brine (component 3) equation (100), together with relations (103) and (104), becomes, after rearrangement

$$n_1^e = \frac{x_1 x_2 S_{13} (S_{12}^{-1}) + x_1 x_3 S_{12} (S_{13}^{-1})}{S_{12} S_{13} x_1 / m_1 + S_{13} x_2 / m_2 + S_{12} x_3 / m_3} \quad (105)$$

$$n_2^e = \frac{x_1 x_2 S_{23} (1 - S_{12}) + x_2 x_3 (S_{23}^{-1})}{S_{12} S_{23} x_1 / m_1 + S_{23} x_2 / m_2 + x_3 / m_3} \quad (106)$$

The surface excess of component 3 can be calculated from the relation

$$n_1^e + n_2^e + n_3^e = 0 \quad (107)$$

Note that only two selectivities need to be specified for the ternary system, for example S_{13} and S_{23} . The third selectivity in equations (105) and (106), S_{12} , is dependent on these two selectivities through the relations (104). In the model to be described in the following section, S_{13} and S_{23} are used as input, since these are a measure of the affinity of each surfactant for the surface, as compared to the affinity of the solvent for the surface.

Equation (93) can be written for component j and solved for x'_j . Using equations (95), (97), and (94) in the same manner as above leads to an expression for the mole fractions in the adsorbed phase:

$$x'_j = \frac{x_j K_{ij}}{\sum_j x_j K_{ij}} \quad (108)$$

Using selectivities instead of K_{ij} , and taking into account relations (104), the mole fractions in the adsorbed phase in a ternary mixture can be written as follows:

$$\begin{aligned} x'_1 &= \frac{S_{13}x_1}{S_{13}x_1 + S_{23}x_2 + x_3} \\ x'_2 &= \frac{S_{23}x_2}{S_{13}x_1 + S_{23}x_2 + x_3} \\ x'_3 &= \frac{x_3}{S_{13}x_1 + S_{23}x_2 + x_3} \end{aligned} \quad (109)$$

At any bulk phase concentration, these equations allow calculation of the adsorbed phase mole fractions, which can then be substituted into equation (92) to determine n' for given monolayer coverages m_j . The amount adsorbed of each component is then given by a rearranged form of

equation (91):

$$n'_i = n_i^e + n'x_i \quad (110)$$

where n_i^e is determined from equations (105), (106) or (107).

The equations presented above allow the determination of the surface excess and the amount adsorbed for a multicomponent mixture. Minka and Myers (1973) have applied these equations to miscible liquids to predict adsorption from a ternary mixture using only binary mixture data.

It has been stated previously that S_{ij} depends on concentration. A concentration dependence of selectivity in a binary mixture has been derived in chapter 4. For a ternary mixture, a similar derivation becomes much more difficult; in fact, it may not be possible to explicitly derive equations equivalent to equation (50). As a first approximation, the selectivities S_{ij} have been taken as constants in the model to follow.

6. Modelling Adsorption of Surfactant Mixtures in Flow through Porous Media

A model for transport of multicomponent mixtures through porous media follows directly from the model for binary mixtures presented in chapter 2. Although the model described in this chapter is restricted to ternary mixtures (two surfactants in brine), extension to more components is straightforward. The same assumptions that have been

discussed in connection with the binary model in chapter 2 apply here. The major difference between the two models, other than the expansion from binary to ternary mixtures, is the incorporation of monomer-micelle equilibrium into the new model. This is done by calculating adsorption levels on the basis of monomer concentrations rather than total surfactant concentrations. While the model discussed in chapter 2 describes flow of any adsorbing chemical through porous media, the model presented here applies specifically to surfactants because of the incorporation of monomer-micelle equilibrium.

Mass balance equations for each surfactant can be written as follows:

$$D \frac{\partial^2 x_1}{\partial y^2} - v \frac{\partial x_1}{\partial y} = \frac{\partial x_1}{\partial t} + \frac{1-\phi}{\phi} \frac{\rho_r}{\rho} \frac{\partial n_1^{ea}}{\partial t} \quad (111)$$

$$D \frac{\partial^2 x_2}{\partial y^2} - v \frac{\partial x_2}{\partial y} = \frac{\partial x_2}{\partial t} + \frac{1-\phi}{\phi} \frac{\rho_r}{\rho} \frac{\partial n_2^{ea}}{\partial t} \quad (112)$$

where x_1 and x_2 are the mole fractions of surfactants 1 and 2, brine being component 3, and n_1^{ea} and n_2^{ea} are the actual surface excess of surfactants 1 and 2. All other variables have been previously defined. Boundary and initial conditions are

$$\begin{aligned} x_1(y, 0) &= 0 & 0 \leq y \leq L \\ vx_1(0, t) &= vx_{10} + D \frac{\partial x_1}{\partial y} & 0 < t \leq t_1 \\ vx_1(0, t) &= D \frac{\partial x_1}{\partial y} & t > t_1 \end{aligned} \quad (113)$$

$$\frac{\partial x_1}{\partial y}(L, t) = 0 \quad t > 0$$

for component 1, and

$$\begin{aligned} x_2(y, 0) &= 0 & 0 \leq y \leq L \\ vx_2(0, t) &= vx_{20} + D \frac{\partial x_2}{\partial y} & 0 < t \leq t_1 \\ vx_2(0, t) &= D \frac{\partial x_2}{\partial y} & t > t_1 \\ \frac{\partial x_2}{\partial y}(L, t) &= 0 & t > 0 \end{aligned} \quad (114)$$

for component 2. x_{10} and x_{20} denote injected surfactant mole fractions.

First order kinetics are again used in the adsorption term:

$$\frac{\partial n_1^{ea}}{\partial t} = k_{1m}(n_1^e - n_1^{ea}) \quad (115)$$

$$\frac{\partial n_2^{ea}}{\partial t} = k_{2m}(n_2^e - n_2^{ea}) \quad (116)$$

$m = 1$, adsorption

$m = 2$, desorption

As before, adsorption takes place if $n_i^e > n_i^{ea}$, and desorption if $n_i^e < n_i^{ea}$. Equations (115) and (116) imply that the rate of adsorption of each component depends only on that same component's surface excess, or that the rate of adsorption of one component is not affected by another component already adsorbed at the surface. These kinetic equations are a first approximation and may have to be refined.

Equations (115) and (116) require a knowledge of the equilibrium surface excesses n_i^e . Since these surface excesses are to be based on

monomer rather than overall concentrations, monomer concentrations need to be determined first using the appropriate equations from section 3. These are repeated below, with molar concentrations replaced by mole fractions for consistency in units.

From the overall mole fractions of each component, the value of α is calculated:

$$\alpha = x_1/x_s \quad (117)$$

where x_s is the overall surfactant mole fraction. The cmc of the mixture is then determined from the pure component cmc's:

$$\frac{1}{\text{cmc}} = \frac{\alpha}{\text{cmc}_1} + \frac{1-\alpha}{\text{cmc}_2} \quad (118)$$

where the cmc's are expressed on a mole fraction basis. If $x_s < \text{cmc}$, then

$$\begin{aligned} x_{1d} &= \alpha x_s \\ x_{2d} &= (1-\alpha)x_s \\ x_{3d} &= 1 - x_{1d} - x_{2d} \end{aligned} \quad (119)$$

where x_{id} are mole fractions in the monomer (dispersed) phase. If $x_s \geq \text{cmc}$, then

$$x_{1d} = \frac{-(x_s - \Delta) + \left[(x_s - \Delta)^2 + 4\alpha\Delta x_s \right]^{1/2}}{2 \left[\frac{\text{cmc}_2}{\text{cmc}_1} - 1 \right]} \quad (120)$$

$$x_{2d} = \left[1 - \frac{x_{1d}}{\text{cmc}_1} \right] \text{cmc}_2 \quad (121)$$

$$x_{3d} = 1 - x_{1d} - x_{2d} \quad (122)$$

If each component is adsorbed on the rock to a different extent, the

value of α changes continually as the surfactant mixture flows through the porous medium. α and the mixture cmc therefore have to be recalculated at each point in the core at each time step.

Once the monomer concentrations are known, the equilibrium surface excesses n_i^e can be determined from equations (105) and (106), with overall mole fractions replaced by monomer mole fractions:

$$n_1^e = \frac{x_{1d}x_{2d}S_{13}(S_{12}^{-1}) + x_{1d}x_{3d}S_{12}(S_{13}^{-1})}{S_{12}S_{13}x_{1d}/m_1 + S_{13}x_{2d}/m_2 + S_{12}x_{3d}/m_3} \quad (123)$$

$$n_2^e = \frac{x_{1d}x_{2d}S_{23}(1-S_{12}) + x_{2d}x_{3d}(S_{23}^{-1})}{S_{12}S_{23}x_{1d}/m_1 + S_{23}x_{2d}/m_2 + x_{3d}/m_3} \quad (124)$$

where S_{13} and S_{23} are input parameters and $S_{12} = S_{13}/S_{23}$. This completes the description of the surface excess model for ternary mixtures.

The equations above are solved by the Barakat and Clark finite difference scheme, which has been discussed in chapter 2. Details of the solution procedure can be found in the Appendix. The transport equations for the two components are coupled through the mole fractions and the selectivities in equations (123) and (124). The selectivities essentially express the competitive nature of the adsorption of the three components in solution. S_{13} and S_{23} represent the affinity of the surface for each surfactant as compared to water, while S_{12} is a measure of the relative attraction between each surfactant and the surface.

The model contains a set of four parameters for each component: selectivities S_{13} and S_{23} , monolayer coverages m_1 and m_2 , kinetic constants of adsorption k_{11} and k_{21} , and kinetic constants of desorption k_{12} and k_{22} . Additional parameters are the monolayer coverage of water m_3 and the dispersion parameter λ , defined in equation (11). The monolayer coverages can again be estimated from determinations of the specific surface area of the solid and the molecular area of the molecules involved. λ has been taken equal for both surfactants; this restriction can, however, easily be removed, if necessary.

7. Experimental Procedure

The surfactant employed in the experimental part of the study of surfactant mixtures was a commercial surfactant with the trade name Varion CAS supplied by the Sherex Chemical Company, Dublin, Ohio. This surfactant has been found to be a good foamer for gas mobility control in high salinity and hardness reservoirs (Novosad and Ionescu, 1987). It is a sulfobetaine with the structure shown in Figure 71. The commercial mixture contains four major components differing in the length of their hydrophobes as shown in the figure.

Quantitative analysis of Varion CAS was performed using a Waters high performance liquid chromatography (HPLC) system with a differential refractive index detector. The column was a Novapak alkylphenyl reverse phase column (3.9 mm \times 15 cm). Separation of

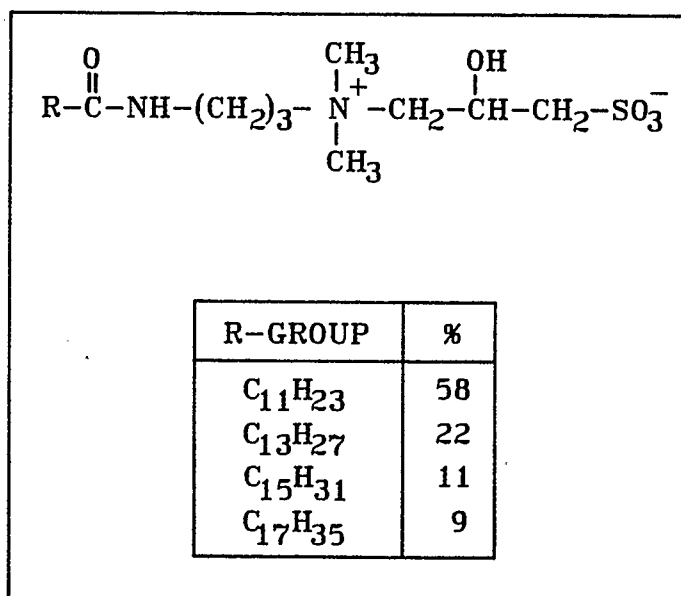


FIGURE 71. Structure and composition of Varion CAS, an amphoteric foam-forming surfactant.

components was achieved using isocratic elution with an isopropanol/water mixture (volume ratio 36:64).

Quantities of the order of several grams of each of the components of Varion CAS were obtained by separating the commercial mixture into its components using a Waters preparative chromatography system with a Waters PrepPak 500 C_{18} reverse phase column (5.7 cm \times 30 cm) and a differential refractometer. The mobile phase was a mixture of isopropanol and water, with ratios depending on the component to be isolated. Several passes through the column were required before the pure components were recovered. The purity of the surface active components was assessed by reinjection into the analytical HPLC, and was estimated to be at least 98%. The C_{12} component contained about 19% w/w NaCl, since the NaCl that is present in the commercial mixture was not retained by the chromatography column, and was therefore concentrated in the first eluted fraction (C_{12}). The amount of NaCl in the C_{12} fraction was determined by titration with silver nitrate (Greenberg et. al., 1980). The NaCl did not interfere with subsequent measurements, since these were carried out in NaCl brine.

Further experimental work was carried out with the purified C_{12} and C_{18} components of Varion CAS, and with mixtures of these. The cmc's of the pure components and of mixtures containing C_{12} : C_{18} at molar ratios of 88:12 and 45:55 were determined by measuring surface tension as a function of concentration. The cmc is given by the concentration at which the plot of surface tension versus logarithm of concentration

abruptly changes its slope to a value of approximately zero. Surface tensions were measured by the du Nouy ring method using a Fisher Model 20 surface tensiometer. All measurements were carried out in 2% w/w NaCl brine at 40°C. The slightly elevated temperature was required to provide sufficient solubility of the C₁₈ component.

A core flood was performed using the same general procedure that has been outlined in chapter 4. A Berea sandstone core (2.56 cm × 2.56 cm × 15.0 cm, pore volume 20.5 ml, absolute permeability to air 670 md) was saturated with 2% w/w NaCl brine at 40°C. A surfactant slug containing a mixture of the C₁₂ and C₁₈ components of Varion CAS in 2% NaCl was injected at a constant flow rate of 2.1 ml/hr at 40°C. Total surfactant concentration was $9.60 \times 10^{-3} \text{ M}$ (4.18 g/l) with C₁₂:C₁₈ at a molar ratio of 84:16. The maximum concentration of C₁₈ that could be used was limited by its rather low solubility. A radioactive non-adsorbing tracer (tritiated water) was injected with the surfactant to serve as a check on the pore volume, line volumes, and volume of solution injected. The volume of surfactant solution injected was 61.6 ml. This was followed by brine until the surfactant and tracer concentration dropped to a low level. Effluent samples were collected at the core outlet at regular time intervals. These were analyzed for C₁₂ and C₁₈ concentrations using the analytical HPLC, and for the tracer with a scintillation counter.

8. Results and Discussion

The results of the surface tension measurements of the pure components and mixtures are shown in Figure 72. Problems with the du Nouy ring method resulted in rather low accuracy in the surface tensions, particularly for the C_{18} . The errors in the values shown in Figure 72 are estimated to be about 10%.

Table 7. Critical micelle concentrations of C_{12} and C_{18} components of Varion CAS. 2% w/w NaCl, 40°C.

| Mole % C_{12} | Critical micelle concentration | | |
|-----------------|--------------------------------|----------------------|--------|
| | (mole/l) | (mole frac.) | (g/l) |
| 100.0 | 5.6×10^{-4} | 1.0×10^{-5} | 0.24 |
| 87.9 | 9.3×10^{-5} | 1.7×10^{-6} | 0.040 |
| 44.8 | 1.9×10^{-5} | 3.4×10^{-7} | 0.0089 |
| 0.0 | 1.7×10^{-5} | 3.2×10^{-7} | 0.0086 |

Cmc's for the pure components and mixtures were determined from Figure 72 and are listed in Table 7. Using the pure component cmc's and equation (90), the theoretical cmc's for mixtures of these components were calculated. Measured and calculated cmc's are compared in Figure 73. Agreement is good, with the measured cmc's falling slightly below the theoretical ones. Part of the reason for this is most likely the accuracy of the measurement. It is also possible that the C_{12} and C_{18} components are sufficiently different to cause slight deviations from

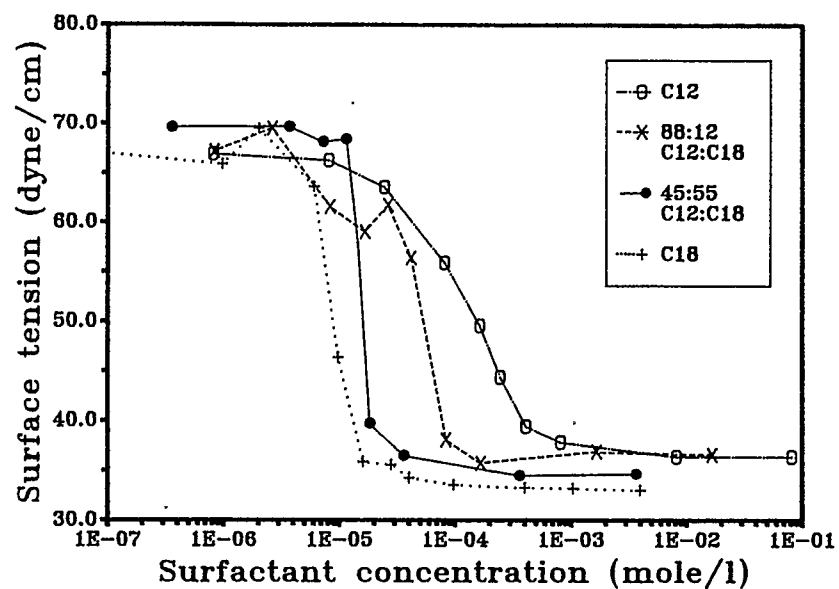


FIGURE 72. Surface tension of the C_{12} and C_{18} components of Varion CAS. Ratios are on a molar basis.

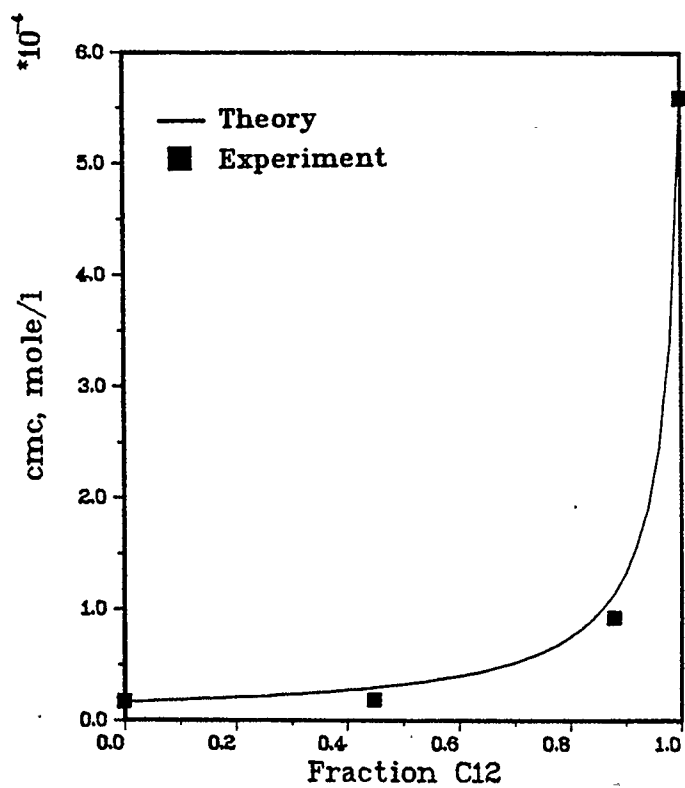


FIGURE 73. Critical micelle concentrations of mixed surfactant solutions containing C_{12} and C_{18} components of Varion CAS.

ideal mixing in the micelles. It may be said, however, that ideal mixed micelle theory is a good approximation for these two surfactants.

Normalized effluent concentrations from the core flood are shown in Figure 74 for the non-adsorbing tracer and for each surfactant. Effluent concentrations have been normalized with respect to each component's or the overall injected concentration. Three interesting observations can be made from Figure 74. Firstly, the higher molecular weight component is produced from the core first, indicating that it is being adsorbed less. This seems to contradict the observation made in many batch adsorption studies in the literature which indicate that adsorption increases as a homologous series of surfactants is ascended. The same trend has been observed in batch tests with the components of Varion CAS: The higher molecular weight components adsorb more strongly (Petroleum Recovery Institute, unpublished data). The rather unexpected results of the core flood can be explained on the basis of monomer-micelle equilibrium, as will be discussed below.

A second interesting observation can be made with regard to the trailing edges of the curves in Figure 74. The C_{12} component is being eluted from the core at a normalized concentration of about 0.1 long after surfactant injection has stopped. The C_{18} concentration, however, drops to zero fairly rapidly after starting chase brine injection. Apparently the C_{12} component is slowly desorbing from the rock, while the C_{18} is bound tightly enough that no measurable desorption takes place. Another factor contributing to the C_{18} remaining adsorbed on the

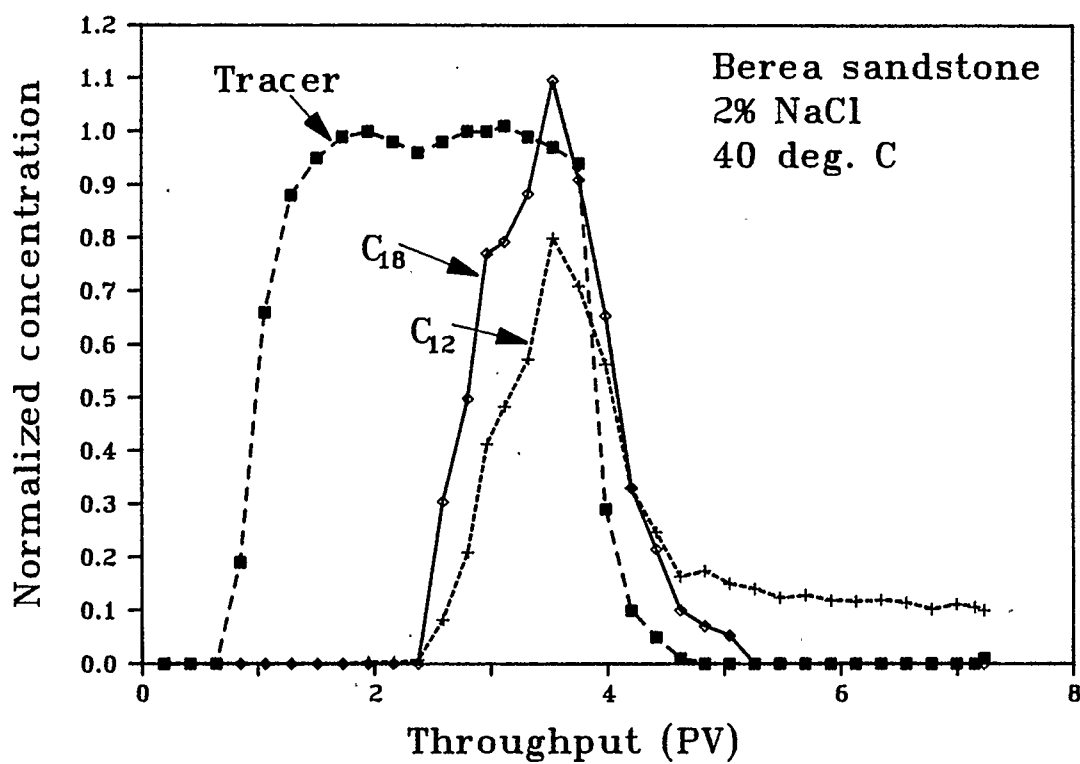


FIGURE 74. Breakthrough curves from a core flood with C_{12} and C_{18} components of Varion CAS.

rock may be its low solubility, which may prevent it from going into the bulk phase more readily. The trailing edges of the effluent profiles then indicate that the affinity of the surface for the C_{18} is higher than for the C_{12} . Nevertheless, C_{18} is retained less, as indicated by its earlier breakthrough at the core outlet.

The third point to be noted from Figure 74 is that the peak of the C_{18} curve occurs at a normalized concentration greater than 1. As has been previously noted, similar observations have been made by other workers. While there is only one data point at a concentration greater than 1 in Figure 74, it is quite possible that this effect is real. Again, the explanation lies in the monomer-micelle equilibrium, as will be discussed below.

The surface excess model for ternary mixtures was used to match the data in Figure 74. The results are shown in Figures 75 and 76, and the parameters used to obtain the match are listed in Table 8. C_{18} has been taken as component 1, C_{12} as component 2, and brine as component 3. The figures show an excellent match for the tracer, and good agreement between experimental and simulated surfactant concentrations. The trailing edge of C_{12} is poorly represented by the model. This part of the curve seems to be indifferent to further increases in the kinetic constant of desorption. This is caused by incorporation of monomer-micelle equilibrium into the adsorption model, since, in the absence of monomer-micelle equilibrium, increasing the desorption rate constant has a strong effect on the trailing edge. Apparently the

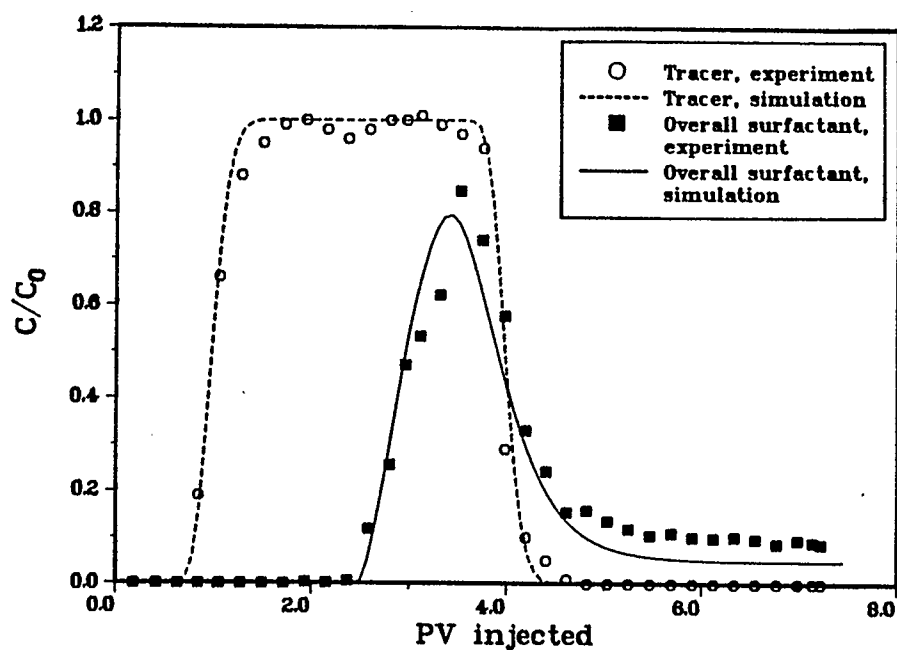


FIGURE 75. History match of a core flood using C_{12} and C_{18} components of Varion CAS. Effluent profiles are for tracer and total surfactant.

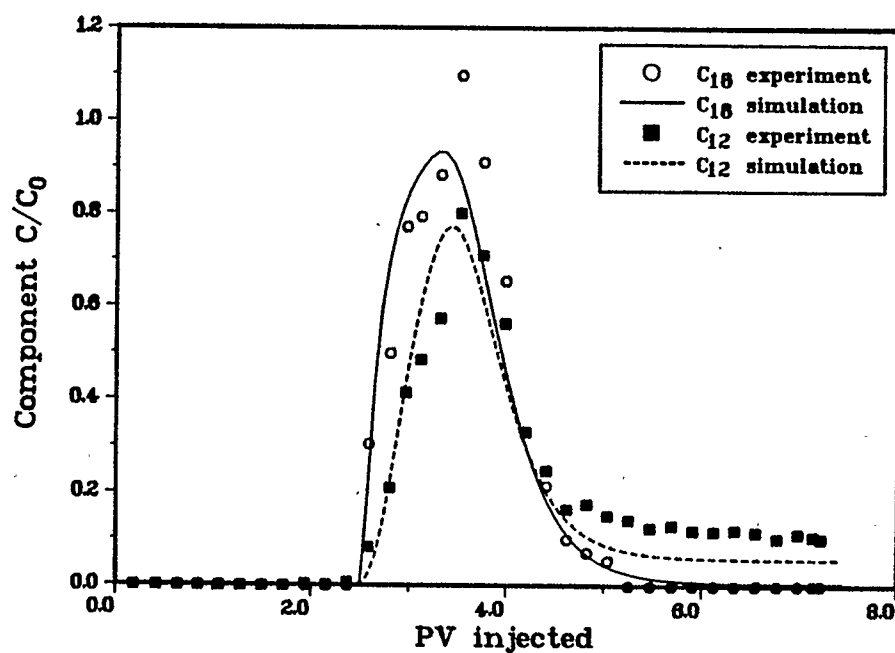


FIGURE 76. History match of a core flood using C_{12} and C_{18} components of Varion CAS. Effluent profiles are for each component.

Table 8. Matching parameters for the core flood with C_{12} and C_{18} components of Varion CAS obtained from the surface excess model for ternary mixtures. Component 1: C_{18} , component 2: C_{12} , component 3: brine. Monolayer coverages are based on an average molecular area of $30 \text{ \AA}^2/\text{molecule}$, obtained from surface tension measurements. The monolayer coverage of water is as described in chapter 3.

| | |
|-----------------|--------------------------|
| S_{13} | 120,000 |
| S_{23} | 24,000 |
| m_1 | 0.0055 mmole/g |
| m_2 | 0.0055 mmole/g |
| m_3 | 0.013 mmole/g |
| k_{11} | 1.0 hr^{-1} |
| k_{21} | 1.0 hr^{-1} |
| k_{12} | 0.0005 hr^{-1} |
| k_{22} | 0.05 hr^{-1} |
| Dispersion par. | 2.0 cm |

desorption of the C_{12} in this region is controlled by the equilibrium surface excess ($(n_2^e - n_2^{ea})$ in equation (116)) rather than the kinetics constant (k_{22} in the same equation). At this stage in the flood the bulk solution contains only desorbed C_{12} at a concentration that is still above the cmc. Since the C_{12} monomer concentration is therefore constant, the exchange of C_{12} molecules with the surface is near equilibrium, and the rate of desorption is slow even when the rate constant of desorption is large. The peak effluent concentration of C_{18}

is also not modelled accurately. This region of the C_{18} profile could be improved somewhat by increasing the kinetics of desorption of C_{18} . This would, however, result in a poorer fit of the trailing edge at the same time. The matching parameters in Table 8 were therefore chosen to give a good fit for the maximum number of experimental points.

The simulated effluent profiles reproduce the observed order of elution of the components. Even though the selectivity of C_{18} is much higher than that of C_{12} (Table 8), C_{18} is produced at the core outlet first. The selectivities indicate that the affinity of the surface for C_{18} is higher than for C_{12} , a conclusion that was reached before from observation of the experimental points at the trailing end of the concentration profiles. To explain the earlier elution of the C_{18} that takes place in spite of its higher selectivity, it is necessary to look at the adsorption isotherms.

Adsorption isotherms can be calculated using the parameters in Table 8 together with equations (123) and (124). Calculation of the monomer concentrations from equations (119) or (120) to (122) for substitution into equations (123) and (124) is also necessary. The resulting adsorption isotherms are shown in Figure 77. Note that these isotherms were plotted for the constant value of $\alpha=0.160$, which is the fraction of C_{18} in the injected solution. In the flow situation, α would not be constant, since the relative concentrations of the components change by differential adsorption during flow through the core. Adsorption isotherms for any value of α can, however, easily be

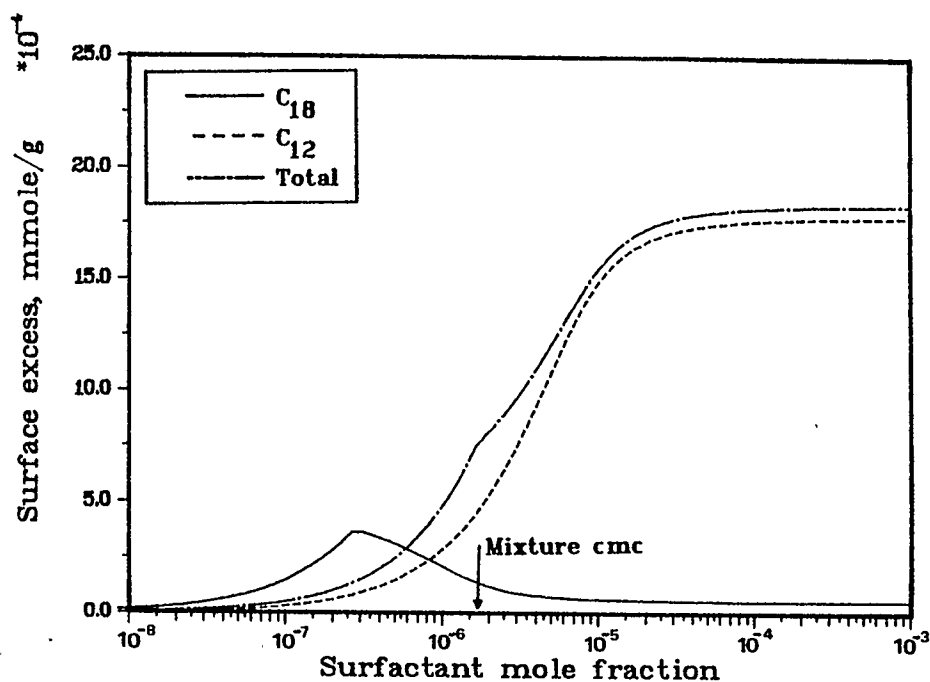


FIGURE 77. Adsorption isotherms for two components of Varion CAS at $\alpha=0.160$, calculated using cmc's in Table 7 and parameters in Table 8. The surface excess of each surfactant has been plotted against its own mole fraction.

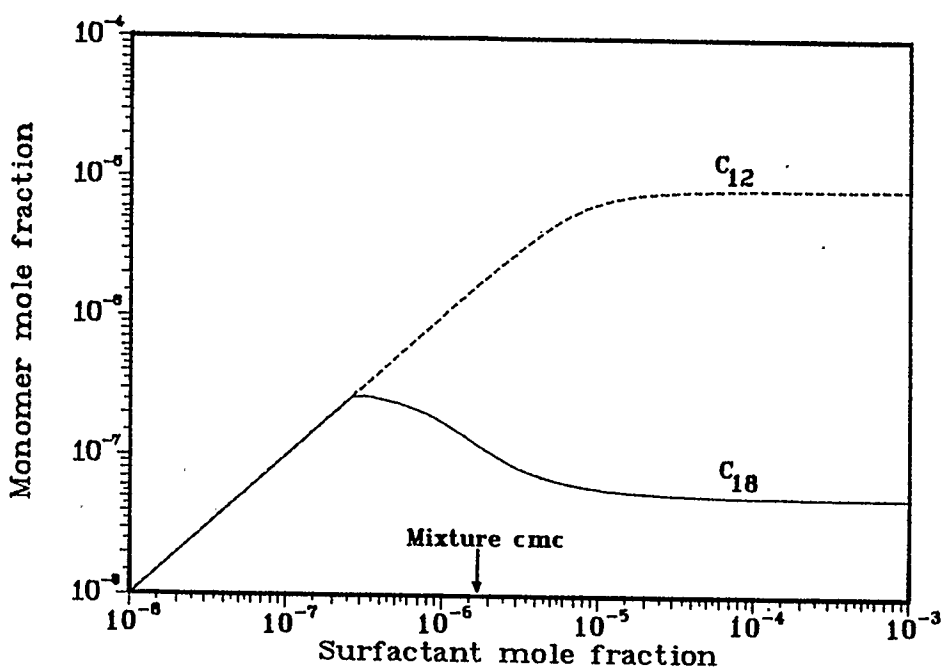


FIGURE 78. Monomer concentrations of two components of Varion CAS at $\alpha=0.160$. The monomer concentration of each surfactant has been plotted against its own mole fraction.

calculated to give a family of curves with α as a parameter. An example will be given in the following section.

Below the cmc of the mixture, as indicated in Figure 77, C_{18} adsorbs more strongly because of its higher selectivity. Above the cmc, however, C_{18} prefers the micellar phase, as indicated by its lower cmc (Table 7). Its monomer concentration therefore decreases with increasing concentration (Figure 78), and its adsorption consequently also decreases (Figure 77). The cmc of C_{12} is more than an order of magnitude higher than that of C_{18} , and it therefore has a much higher concentration in the monomer phase, causing its higher adsorption level above the cmc. There are thus two competing mechanisms in the adsorption of this surfactant mixture: the affinity between the surfactant and the solid (selectivity) and the monomer concentrations. Below the cmc the selectivity dominates, while the monomer concentration takes over at concentrations above the cmc. Since the injected concentration in this particular core flood was well above the cmc, the effect of monomer concentration dominates. C_{18} is therefore adsorbed less and is produced from the core first.

The adsorption isotherms in Figure 77 can also serve to explain effluent concentrations exceeding the injected concentration of the component with the lower cmc. Since the surface excess of this component decreases with increasing concentration, it may begin to desorb even when the overall surfactant concentration is still increasing at that particular point in the core. The bulk concentration

of C_{18} may therefore increase sufficiently for it to reach levels higher than its injected concentration. This effect will be stronger for higher values of the rate constant of desorption, while it may not be noticeable for very low rates of desorption. Raising the value of k_{12} from 0.0005 to 0.01 hr^{-1} will cause the peak effluent concentration of the C_{18} to exceed 1.

The discussion presented in this chapter immediately raises the question how the neglect of monomer-micelle equilibrium in the models presented in the previous chapters affects the adsorption isotherms generated from history matching with these models. The data presented in the previous chapters were obtained with commercial surfactant mixtures. Modelling monomer-micelle equilibria of such mixtures is not straightforward, because they may contain not only components that are members of a homologous series of surfactants, but also several different surfactant types. Mixing in the micelles is therefore unlikely to be ideal. While non-ideal mixed micelle theories are available, the application of these requires a fairly detailed knowledge of the composition of the surfactant mixture and the properties of the individual components. Oftentimes the composition of commercial mixtures is, however, unknown. While these problems may be difficult to solve, they will have to be addressed in order to make the binary mixture models presented in previous chapters more generally applicable.

The flow model for surfactant mixtures can be used for binaries by

setting one of the injected concentrations to zero. This will result in a model equivalent to the constant selectivity model presented before, with the difference that monomer-micelle equilibrium is taken into account. The model can therefore be used as an approximation with the pseudobinary mixtures described in the previous chapters. However, the surfactant solution will then be treated as a true binary, and not as the pseudobinary that it actually represents. This means that the monomer-micelle equilibrium will assume a single component in solution, and will therefore not be capable of modelling the changes in monomer concentrations that occur in surfactant mixtures above the cmc. Nevertheless, the adsorption isotherms obtained may be a closer representation of the real situation than those obtained by completely ignoring monomer-micelle equilibrium. This is another point that needs further investigation. Preliminary results with cores T1 and T13 of the previous chapters have shown promising results. Matching these floods with the model of this chapter, using the same parameters for the high and low concentration floods, results in better matches than with the previous constant selectivity model, but not as good a match as with the heterogeneous model. Since the surfactant used in these floods is a mixture of different surfactant types, ideal mixed micelle theory can at best be expected to be a crude approximation to its behavior.

9. Model Study

A model study was carried out to test the features and capabilities of the surface excess model for ternary mixtures.

The effect of the model parameters on the effluent profiles has been tested first. The model contains four parameters for each surface active component: S_{i3} , m_i , k_{i1} and k_{i2} ($i=1,2$), in addition to m_3 and λ . As has been discussed in chapter 3, the values of m_i can be measured independently, and can therefore be removed from the list of adjustable parameters. The effect of m_i on the effluent profiles was still tested in order to determine to what extent inaccuracies in the measurement of m_i affect calculated effluent profiles. The results of the parametric study can be summarized as follows.

In general, adjustments in selectivity, monolayer coverage or kinetics of one component also affect the other component. This is to be expected, since adsorption of one component is not independent from the other component (equations (123) and (124)). The effect on the component in question is, however, substantially larger. For example, changing S_{13} will affect component 1 much more strongly than component 2.

In the following discussion, component 1 represents the component with the lower cmc and the higher selectivity. Increasing S_{13} delays breakthrough of component 1, but has the opposite effect on component 2. Increasing S_{23} delays component 2 strongly and component 1 slightly. Similar trends are observed when the kinetic constants of adsorption, k_{i1} are increased. The kinetics of adsorption also affect the shape of the leading edge of the concentration profile, faster kinetics

producing sharper peaks.

The kinetics of desorption seem to affect predominantly the component under consideration. For component 2, the value of k_{22} changes the trailing edge of the effluent profile, while, with component 1, the peak concentration is also affected by adjustments in k_{12} . The maximum effluent concentration of the latter component, which is the component with the lower cmc, may exceed its injected concentration at high rates of desorption. This is caused by the preferential incorporation of this component into micelles with a resulting decrease in its monomer concentration and therefore its equilibrium adsorption level. The effluent concentration of the component with the larger cmc will never exceed the injected concentration, even at high rates of desorption, since its monomer concentration increases monotonically with increasing concentration.

The effect of the monolayer coverages, m_i , can easily be predicted from equations (123) and (124). Increasing any value of m_i will increase adsorption, the effect being, however, relatively small even when m_i is changed by a factor of 2. Finally, the effect of the dispersion parameter λ is straightforward: An increase in dispersion leads to a larger spread in effluent concentrations.

In order to study some of the phenomena that may be observed when surfactant mixtures flow through porous media, the surface excess model was used to model flow of a surfactant mixture through a hypothetical

core. The properties and model parameters of the hypothetical system are listed in Table 9 for five simulated core floods to be described below. Component 1 is again taken to be the component with the lower cmc and the higher selectivity. It should be noted that this is a reasonable combination, since a lower cmc implies a higher molecular weight (a larger hydrophobe), which in turn usually means a higher affinity for the solid/liquid interface.

Adsorption isotherms for the hypothetical surfactants have been plotted in Figures 79 to 81 for each component and for the total surfactant, with α as a parameter. α is the fraction of total surfactant that constitutes component 1. Figures 79 and 80 show that adsorption levels of each component are reduced by addition of a second component. The overall adsorption (Figure 81) falls between those of the pure components. Below the cmc, adding component 1 (increasing α) increases overall adsorption, since addition of the component with the higher selectivity increases the average selectivity of the mixture. Above the cmc, adding component 1 reduces overall adsorption, since component 1 now adsorbs less than 2 because of its lower monomer concentration.

Adsorption isotherms for $\alpha=0.5$ have been re-plotted in Figure 82. Note that the isotherms for components 1 and 2 intersect. When a hypothetical core flood is run using $\alpha=0.5$ with injected concentrations well above the cmc (Table 9, run 1), the effluent concentrations in Figure 83 are produced, with component 1 eluting ahead of component 2.

Table 9. System variables used in five hypothetical core floods.

(a) Core and displacement properties (all runs):

| | |
|----------------|-------------|
| Length | 15.0 cm |
| Cross-section | 6.25 cm |
| Porosity | 0.2 |
| Rock density | 2.7 g/ml |
| Liquid density | 1000 mg/ml |
| | 55 mmole/ml |
| Flow rate | 2.0 ml/hr |

(b) Model parameters (all runs):

| | | | |
|-----------------|---------------|----------|-------------------------|
| m_1 | 0.004 mmole/g | k_{11} | 1.0 hr^{-1} |
| m_2 | 0.004 mmole/g | k_{21} | 1.0 hr^{-1} |
| m_3 | 0.013 mmole/g | k_{12} | 0.001 hr^{-1} |
| Dispersion par. | 0.15 cm | k_{22} | 0.001 hr^{-1} |

(c) Variable system parameters

| | RUN 1 | RUN 2 | RUN 3 | RUN 4 | RUN 5 |
|-------------------|----------------------|----------------------|----------------------|----------------------|----------------------|
| x_{10} | 3.5×10^{-4} | 0.8×10^{-5} | 2.0×10^{-5} | 3.5×10^{-4} | 0.0 |
| x_{20} | 3.5×10^{-4} | 0.8×10^{-5} | 2.0×10^{-5} | 3.5×10^{-4} | 3.5×10^{-4} |
| cmc_1 | 1.0×10^{-5} | 1.0×10^{-5} | 1.0×10^{-5} | 1.0×10^{-5} | 1.0×10^{-5} |
| cmc_2 | 5.0×10^{-5} | 5.0×10^{-5} | 5.0×10^{-5} | 1.5×10^{-5} | 5.0×10^{-5} |
| S_{13} | 10,000 | 10,000 | 10,000 | 10,000 | 10,000 |
| S_{23} | 5,000 | 5,000 | 5,000 | 6,500 | 5,000 |
| Slug vol. (PV) | 1.0 | 15.0 | 10.0 | 1.0 | 1.0 |

(x_{i0} and cmc_i in terms of mole fractions)

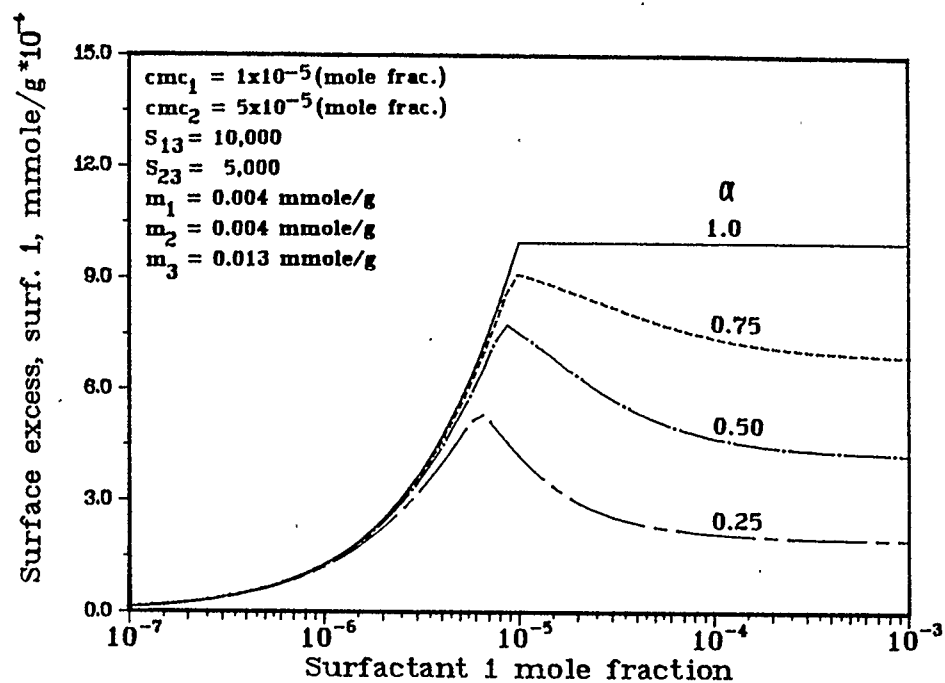


FIGURE 79. Adsorption of surfactant 1 from a mixture.

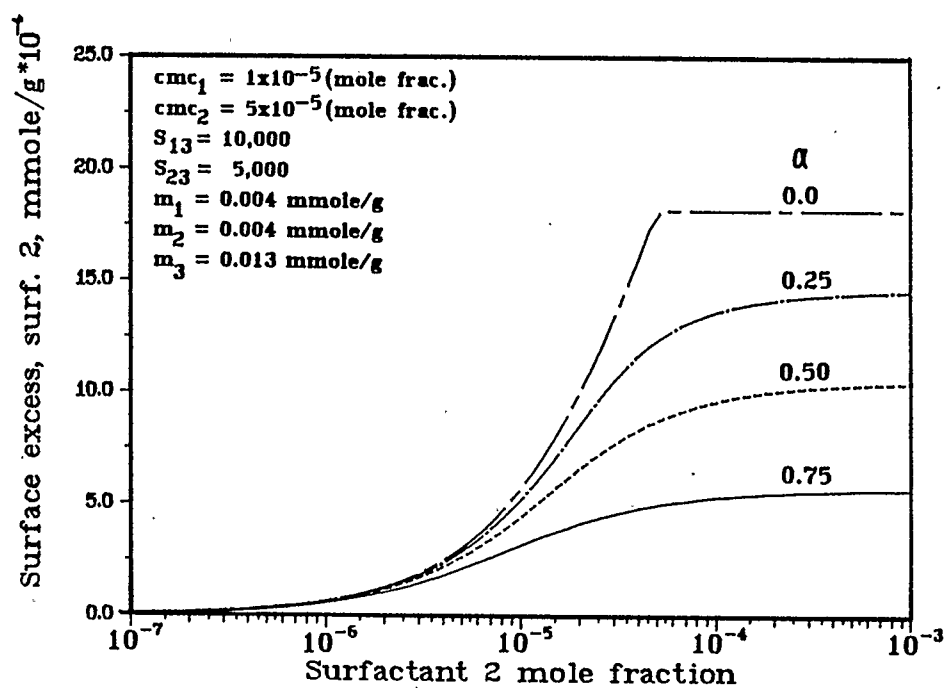


FIGURE 80. Adsorption of surfactant 2 from a mixture.

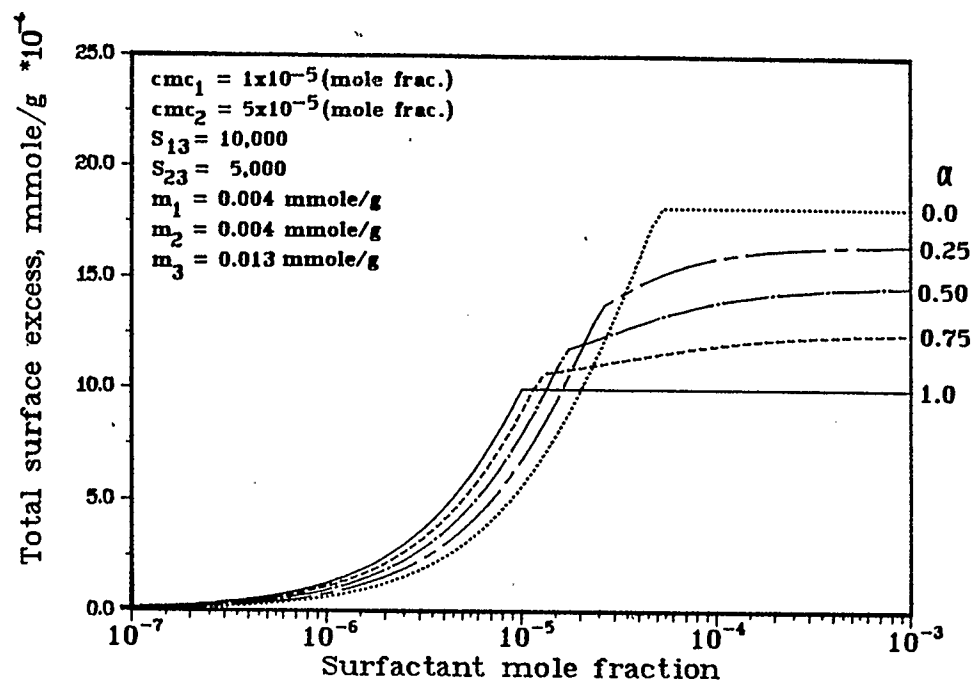


FIGURE 81. Overall adsorption from a surfactant mixture.

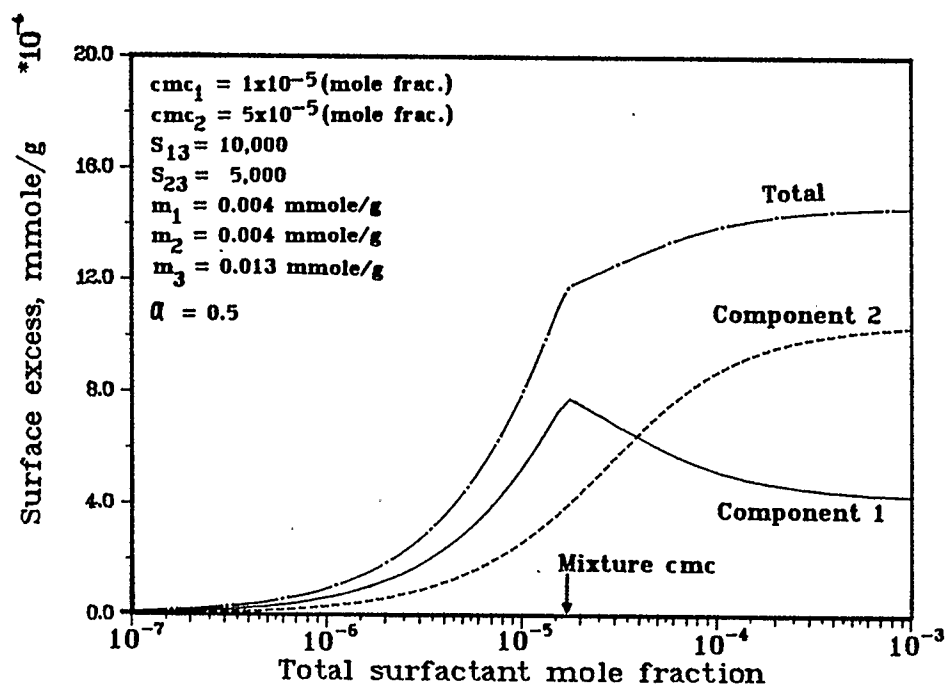


FIGURE 82. Adsorption from a surfactant mixture at $\alpha=0.5$.

As has been discussed before, the earlier breakthrough of the higher selectivity component is caused by its preferential micellization and resulting lower monomer concentration. Component 1 thus adsorbs less at this injected concentration in spite of its higher selectivity. When the injected concentration is slightly below the cmc (Table 9, run 2), the order of elution is reversed (Figure 84), since at such low concentrations no micelles are present and the higher selectivity of component 1 controls its adsorption. Note that separation of components is much more severe at such low concentrations, an observation that has led other workers to conclude that injection of small high-concentration slugs is preferable over large low-concentration slugs (Trogus et. al., 1979b; Harwell et. al., 1982). If the injected concentration is at the intersection of the adsorption isotherms in Figure 82 (Table 9, run 3), separation of components can be eliminated completely, as shown in Figure 85.

It should be noted that the adsorption isotherms of the two components may not intersect. For example, if the selectivity S_{23} is lowered from 5000 to 500 in the system described above, the difference in the selectivities of the components becomes large enough for component 1 to adsorb more strongly at all concentrations. Component 1 will now elute from a core last at any injected concentration. Also, one may not be able to predict the order of elution by looking at the adsorption isotherms that were calculated at the constant value of α of the injected solution. In the flow situation α changes continually, and this may obscure the elution order that might be expected from the

adsorption isotherms. The only way of predicting the elution is then by simulating the flow situation.

It is desirable in most EOR applications to prevent chromatographic separation of components. The concentration at the intersection of the isotherms may be too low for practical applications, since the surfactant may not propagate at such low concentrations. Note from Figure 85 that approximately 7 pore volumes of surfactant solution are injected before any surfactant is produced from the core outlet. There are, however, other ways of preventing separation of components. For example, component 2 may be chosen as a higher molecular weight surfactant than in the previous runs. This means that its cmc will be lowered and that its selectivity will most likely be higher. These two variables may be adjusted such that no separation of components is observed (Table 9, run 4, Figure 86). If cmc's of a number of surfactants of interest and selectivities with respect to any particular solid are available, surfactants may be mixed in such a way that differential adsorption is minimized. It can also be shown with the surface excess model that adjusting the ratio of the components may reduce separation of components.

The effect that addition of a second surfactant has on adsorption of the first is shown in Figures 87 and 83. In the flood in Figure 87, surfactant 2 is injected by itself at a mole fraction of 3.5×10^{-4} (Table 9, run 5). Almost no surfactant is produced from the core. Adding an equal concentration of surfactant 1 to the injected solution

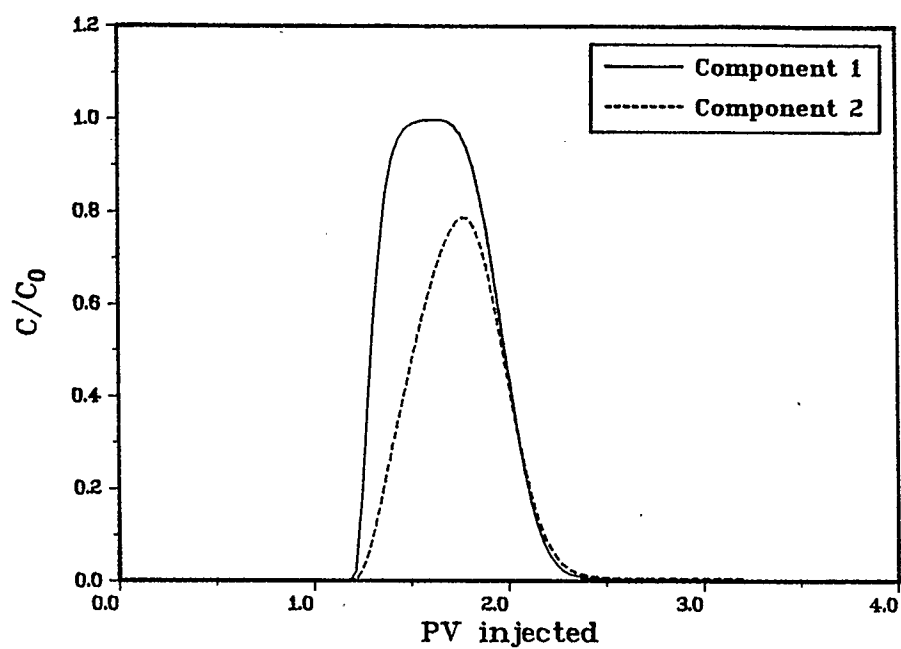


FIGURE 83. Effluent profiles for run 1. Injected concentration above the cmc.

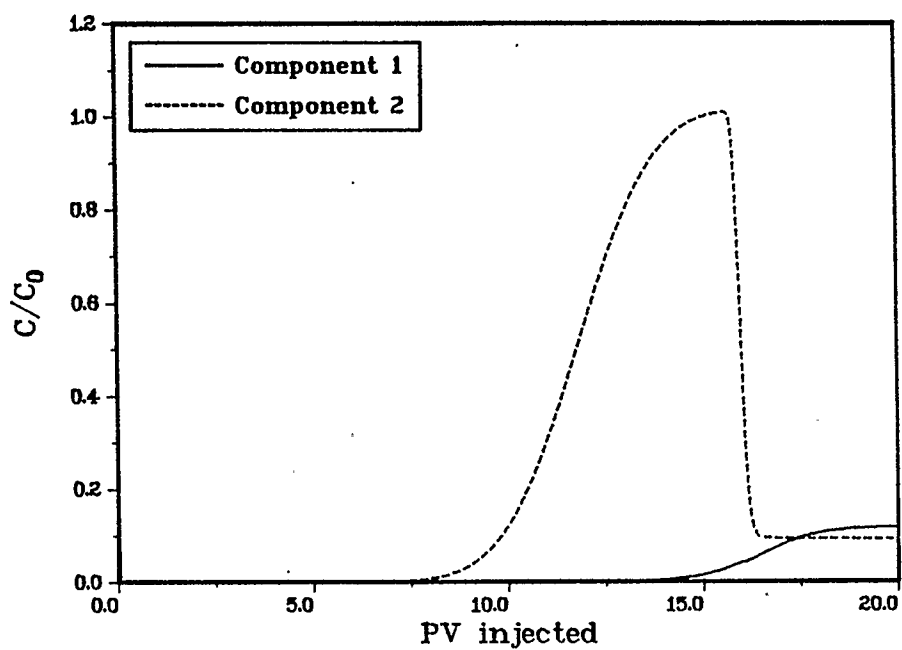


FIGURE 84. Effluent profiles for run 2. Injected concentration below the cmc.

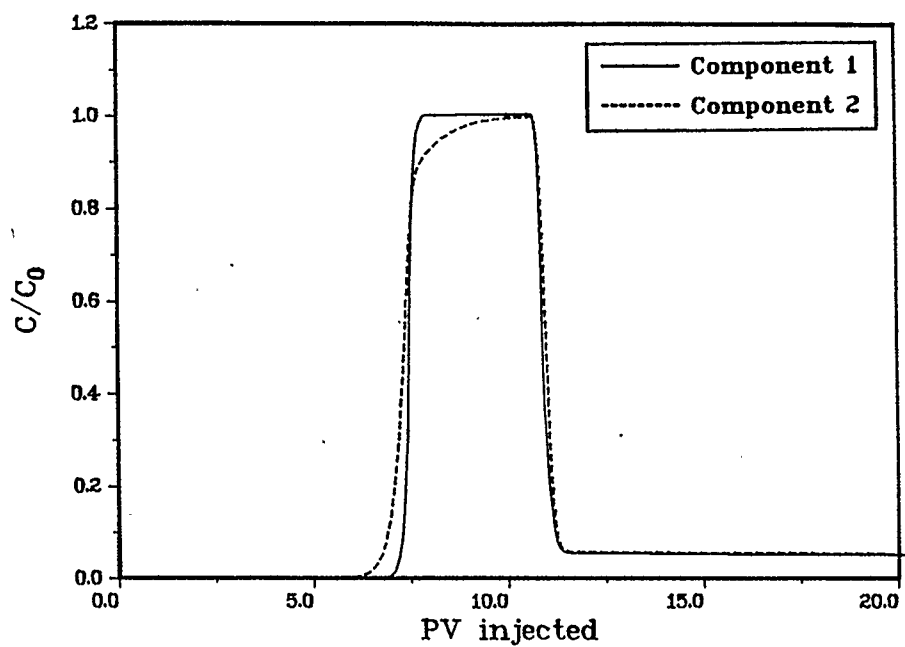


FIGURE 85. Effluent profiles for run 3. Injected concentration at the intersection of the component isotherms.

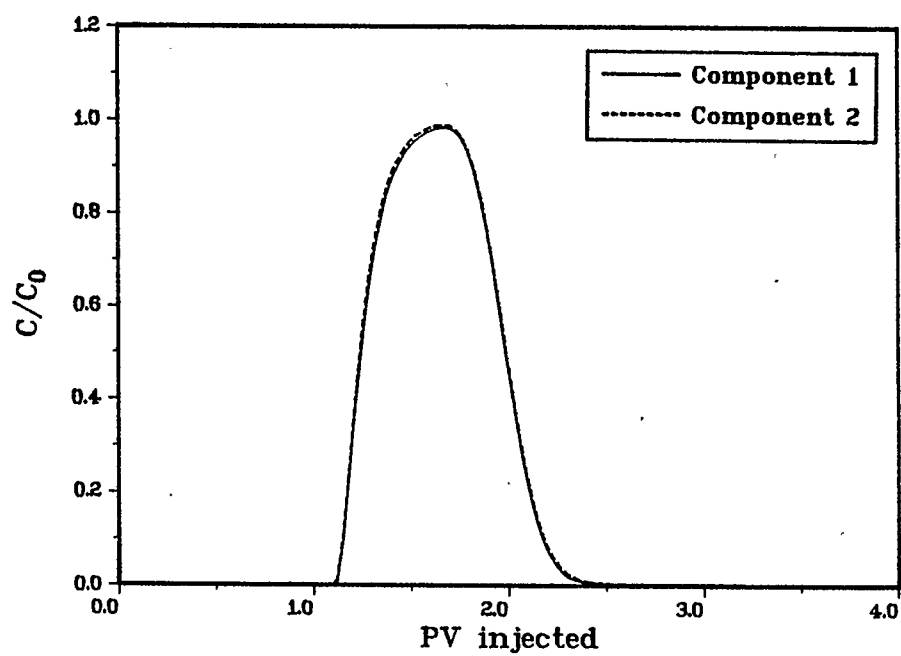


FIGURE 86. Effluent profiles for run 4. Surfactant properties were adjusted so as to prevent separation of components.

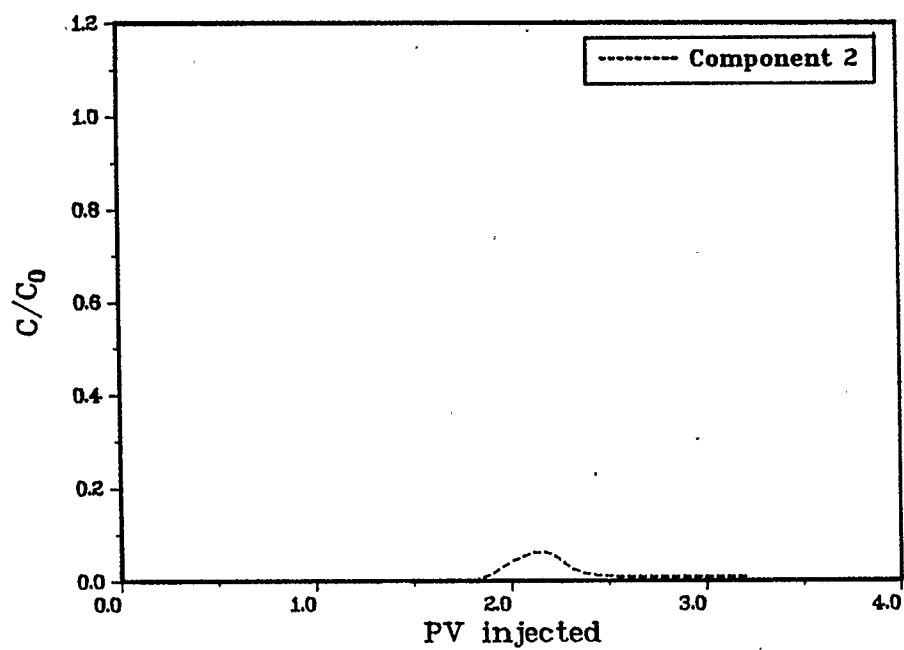


FIGURE 87. Effluent profile for run 5. Injection of surfactant 2 alone.

results in the effluent concentrations shown in Figure 83 (Table 9, run 1). Substantially less component 2 is now adsorbed, resulting in production of significant amounts of this surfactant from the core. This example demonstrates the possibility of adding sacrificial adsorbates to a surfactant solution in order to protect the more valuable component from being adsorbed.

The examples in this chapter have shown that the flow model for surfactant mixtures allows the prediction and explanation of the behavior of surfactant mixtures in flow through porous media. It may also aid in formulating surfactant systems that exhibit desirable properties.

10. Chapter Summary

This chapter has reviewed some of the fundamental aspects of adsorption of surfactants and surfactant mixtures and their implications on surfactant applications in EOR. The importance of monomer-micelle equilibrium to adsorption of surfactant mixtures has been discussed, and the surface excess concept has been extended to multicomponent mixtures.

A model has been developed that incorporates monomer-micelle equilibrium (in the form of ideal mixed micelle theory) and the surface excess concept for ternary mixtures into a transport equation for flow through porous media. The model is shown to describe adsorption of the

components of a commercial foam-forming surfactant satisfactorily. A model study with a hypothetical system has demonstrated some features of the behavior of surfactant mixtures in flow through porous media.

CHAPTER 7

SUMMARY AND CONCLUSIONS

This thesis has dealt with four major topics, all related to adsorption at the solid/liquid interface, and more specifically adsorption of surfactants used in EOR applications. All four areas use as a starting point the adsorption model for flow of surfactants through porous media developed by Huang and Novosad (1986), and this model is therefore reviewed in chapter 2.

Chapter 3 deals with a method that allows independent estimation of two of the model's parameters: the monolayer coverages of surfactant and water on a solid. By measuring these parameters independently, the number of adjustable parameters is reduced by two, and the set of parameters that provides a match with experimental effluent concentrations from core floods becomes unique.

In chapter 4 it is shown that different adsorption isotherms may be obtained from history matching two core floods performed in the same system at different injected surfactant concentrations. It is pointed out that this may be caused by the assumption of constant selectivity. Therefore two dependencies of selectivity on surfactant concentration are introduced into the model, one being developed from the thermodynamics of adsorption of unequal-sized molecules, and the other semi-empirical. The first approach renders the model more sound

theoretically, but the resulting decrease in selectivity at higher concentrations does not modify the adsorption isotherms sufficiently. Therefore there are other factors that the adsorption model does not yet take into account.

One such factor may be surface heterogeneities, discussed in chapter 5. It is shown that a very simple distribution function for the selectivity, equivalent to a two-component solid, is capable of matching core floods performed at different surfactant concentrations with one adsorption isotherm. Since Berea sandstone, the solid used in the experimental work, contains two major components (quartz and kaolinite), the two-component solid seems to be a reasonable assumption.

Finally, chapter 6 deals with the adsorption of surfactant mixtures. It is shown that monomer-micelle equilibrium is an important phenomenon that may dominate the adsorption process at concentrations above the cmc, and may explain the counter-intuitive behavior of some surfactant mixtures. A model for flow of surfactant mixtures through porous media is developed. This model makes use of ideal mixed micelle theory and the surface excess concept for multicomponent mixtures. Its validity is demonstrated by history matching effluent concentrations of a core flood performed with the C_{12} and C_{18} components of an amphoteric foam-forming surfactant. A model study is carried out to show the unique behavior that may be observed with surfactant mixtures in flow through porous media. It is shown how the properties of surfactant

mixtures can be used to advantage in formulating surfactant systems with desirable adsorption properties.

Some suggestions for further work on the topics touched in this thesis are as follows. Future work in the area of surfactant adsorption on highly heterogeneous solids, such as petroleum reservoir rocks, should involve the measurement of adsorption on rock samples of known mineralogical composition. It may then be possible to assign selectivities to specific combinations of surfactant and solid, which may lead to the possibility of predicting adsorption on a rock from a knowledge of its composition. The effect of surface heterogeneities may be even more important in surfactant mixtures than in single surfactant solutions, since different patches of surface may attract different components of a mixture to different extents.

First order kinetics have been used in all the flow models. These may have to be refined, particularly in the model for surfactant mixtures. Also, attractive interactions between surfactant molecules in the adsorbed phase are known to exist. Taking into account such interactions through activity coefficients in the adsorbed phase may lead to a better description of the adsorption process.

The flow model for surfactant mixtures developed in this work describes a relatively simple system: A mixture of two surface active components that follow ideal mixing in the micelles. In order to model flow of more complex surfactant mixtures the model will have to be

expanded to multicomponent mixtures that do not follow ideal mixed micelle theory. Simplifying assumptions regarding these mixtures will most likely have to be made, since their exact composition is often unknown. Monomer-micelle equilibrium should, in the future, be included even in the model that treats the surfactant solution as a pseudobinary mixture.

Our understanding of the behavior of surfactant mixtures and their application in tailor-made surfactant systems is far from complete. The design of surfactant mixtures will have to take into account more than one effect of the mixing process. For example, the goal of mixing surfactants may be to minimize adsorption or reduce chromatographic separation in EOR applications. At the same time, care has to be taken that other desirable properties of the surfactant solution, such as foaming capability, interfacial tension lowering, or phase behavior, are not adversely affected. As far as adsorption is concerned, a mixture that is likely to show reduced adsorption is one that exhibits large negative deviations from ideality in the mixed micelles. Such behavior leads to incorporation of surfactant molecules into micelles at concentrations lower than the pure component cmc's, resulting in a lowered monomer concentration. On the other hand, preferred micellization in the bulk may also indicate preferred hemimicellization at the surface. Experiment will have to determine which is the stronger effect.

Surfactant mixtures are thus interesting both from a theoretical

and from a practical point of view. Great potential exists in the application of custom tailored surfactant mixtures in many areas of industry, but much experimentation is still required to more fully understand these mixtures. The model presented in this work will provide a starting point for further investigations in the area of surfactant mixtures for EOR applications.

REFERENCES

- Adamson, A.W., and Ling, I., Effect of Radiation on the Surfaces of Solids. I. Analysis of Adsorption Isotherms to Obtain Site Energy Distributions, Adv. in Chem. Series 33, 51 (1961).
- Adamson, A.W., "Physical Chemistry of Surfaces", 3rd edition, John Wiley & Sons (1976).
- Allen, T., and Patel, R.M., The Adsorption of Long-Chain Fatty Acids on Finely Divided Solids Using a Flow Microcalorimeter, J. Coll. Int. Sci. 35, 647 (1971).
- Aris, R., and Amundson, N.R., Some Remarks on Longitudinal Mixing or Diffusion in Fixed Beds, AIChE J. 3, 280 (1957).
- Austad, T., Hansen, T.A., and Staurland, G., Adsorption of Ethoxylated Surfactants on Reservoir Minerals - An Experimental Study, paper presented at the 4th European Symposium on Enhanced Oil Recovery, Hamburg, West Germany, Oct. 27-29, 1987.
- Bae, J.H., and Petrick, C.B., Adsorption of Petroleum Sulfonates in Berea Cores, SPE paper #5819, presented at the Improved Oil Recovery Symposium of the Soc. of Pet. Eng. of AIME, Tulsa, Okla., March 22-24, 1976.
- Baiker, A., and Richarz, W., Vergleich von Meßmethoden zur Bestimmung der Porenradienverteilung und spezifischen Oberfläche poröser Katalysatoren, Chemie-Ingenieur-Technik 49, 399 (1977).
- Balzer, D., Phase Behaviour, Core Flooding and Retention Studies of Caboxymethylated Ethoxylates Blended with Sulfonates, paper presented at the 4th European Symposium on Enhanced Oil Recovery, Hamburg, West Germany, Oct. 27-29, 1987.
- Barakat, H.Z., and Clark, J.A., On the Solution of the Diffusion Equations by Numerical Methods, ASME Trans., J. Heat Transfer 88, 421 (1966).
- Bijsterbosch, B.H., and van den Hul, H.J., Comments on the Paper, "Gibbs Equation for the Adsorption of Organic Ions in Presence and Absence of Neutral Salts", by D.K. Chattoraj, J.Phys. Chem. 71, 1169 (1967).
- Bird, R.B., Stewart, W.E., and Lightfoot, E.N., "Transport Phenomena", John Wiley & Sons (1960).

Bockris, J.O'M., and Reddy, A.K.N., "Modern Electrochemistry", Plenum Press (1970).

Brandrup, J., and Immergut, E.H., "Polymer Handbook", 2nd edition, John Wiley & Sons (1975).

Brenner, H., The Diffusion Model of Longitudinal Mixing in Beds of Finite Length. Numerical Values, Chem. Eng. Sci. 17, 229 (1962).

Brigham, W.E., Marcou, J.A., Sanyal, S.K., Malito, O.P., and Castanier, L.M., A Field Experiment of Improved Steam Drive with In-Situ Foaming, SPE paper #12784, presented at the California Regional Meeting, Long Beach, Ca., April 11-13, 1984.

Brode, P.F. III, Adsorption of Ultra-Long-Chain Zwitterionic Surfactants on a Polar Solid, Langmuir 4, 176 (1988).

Brooks, C.S., and Purcell, W.R., Surface Area Measurements on Sedimentary Rocks, Petroleum Trans. AIME 195, 289 (1952).

Brunauer, S., Emmett, P.H., and Teller, E., Adsorption of Gases in Multimolecular Layers, J. Am. Chem. Soc. 60, 309 (1938).

Brunauer, S., Copeland, L.E., and Kantro, D.L., The Langmuir and BET Theories, in "The Solid-Gas Interface", vol. 1, p. 77, ed. by E.A. Flood, Marcel Dekker (1967).

Bujake, J.E., and Goddard, E.D., Surface Composition of Sodium Lauryl Sulphonate and Sulphate Solutions by Foaming and Surface Tension, Trans. Faraday Soc. 61, 190 (1965).

Castanier, L.M., Steam with Additives: Field Projects of the Eighties, paper presented at the 4th European Symposium on EOR, Hamburg, West Germany, Oct. 27-29, 1987.

Cerofelini, C.F., Adsorption and Surface Heterogeneity, Surface Sci. 24, 391 (1971).

Chandar, P., Somasundaran, P., and Turro, N.J., Fluorescence Probe Studies on the Structure of the Adsorbed Layer of Dodecyl Sulfate at the Alumina-Water Interface, J. Coll. Int. Sci. 117, 31 (1987).

Chattoraj, D.K., Gibbs Equation for the Adsorption of Organic Ions in Presence and Absence of Neutral Salt, J. Phys. Chem. 70, 2687 (1966a).

Chattoraj, D.K., Gibbs Equation for Polyelectrolyte Adsorption, J. Phys. Chem. 70, 3743 (1966b).

Chattoraj, D.K., Application of Debye-Hückel Limiting Law to Gibbs Equation for Electrolyte Adsorption, J. Coll. Int. Sci. 26, 379 (1968a).

Chattoraj, D.K., Gibbs Equation for the Mixed Adsorption of Organic

Acid and its Salt, Indian J. Chem 6, 309 (1968b).

Chattoraj, D.K., Models of Electrical Double Layer and Gibbs Equation for Adsorption of Electrolytes, J. Coll. Int. Sci. 29, 399 (1969).

Chattoraj, D.K., and Pal, R.P., Gibbs Adsorption Equation for Multicomponent Solution: Part I - Variation of Concentrations of Non-Electrolyte and Neutral Salts, Indian J. Chem. 10, 410 (1972a).

Chattoraj, D.K., and Pal, R.P., Gibbs Adsorption Equation for Multicomponent Solution: Part II - Variation of Concentration of Organic Ions, Indian J. Chem. 10, 417 (1972b).

Chattoraj, D.K., and Birdi, K.S., "Adsorption and the Gibbs Surface Excess", Plenum Press (1984).

Clint, J.H., Micellization of Mixed Nonionic Surface Active Agents, J. Chem. Soc., Faraday Trans. I 71, 1327 (1975).

Clunie, J.S., and Ingram, B.T., Adsorption of Nonionic Surfactants, in "Adsorption from Solution at the Solid/Liquid Interface", p. 105, ed. by G.D. Parfitt and C.H. Rochester, Academic Press (1983).

Coats, K.H., and Smith, B.D., Dead-End Pore Volume and Dispersion in Porous Media, Soc. Pet. Eng. J. 4, 73 (1964).

Cockbain, E.G., The Adsorption of Sodium Dodecyl Sulphate at the Oil-Water Interface and Application of the Gibbs Equation, Trans. Faraday Soc. 50, 874 (1954).

Coltharp, M.T., and Hackerman, N., Heterogeneity in Solution Adsorption: Edge Carbon and Oxide Coverages, I. Methanol-Benzene, J. Coll. Int. Sci. 43, 176 (1973a).

Coltharp, M.T., and Hackerman, N., Heterogeneity in Solution Adsorption: Edge Carbon and Oxide Coverages, II. n-Butanol-Benzene, J. Coll. Int. Sci. 43, 185 (1973b).

Dabrowski, A., Oscik, J., Rudzinski, W., and Jaroniec, M., Effects of Surface Heterogeneity in Adsorption from Binary Liquid Mixtures, II. Adsorption from Nonideal Bulk Solutions, J. Coll. Int. Sci. 69, 287 (1979).

Danckwerts, P.V., Continuous Flow Systems. Distribution of Residence Times, Chem. Eng. Sci. 2, 1 (1953).

D'Arcy, R.L., and Watt, I.C., Analysis of Sorption Isotherms of Non-Homogeneous Sorbents, Trans. Faraday Soc. 66, 1236 (1970).

Dick, S.G., Fuerstenau, D.W., and Healy, T.W., Adsorption of Alkylbenzene Sulfonate (A.B.S.) Surfactants at the Alumina-Water Interface, J. Coll. Int. Sci. 37, 595 (1971).

Dilgren, R.E., Deemer, A.R., and Owens, K.B., The Laboratory and Field Testing of Steam/Noncondensable Gas Foams for Mobility Control in Heavy Oil Recovery, SPE paper #10774, presented at the California Regional Meeting of the Soc. of Pet. Eng., San Francisco, Ca., March 24-26, 1982.

Donaldson, E.C., Kendall, R.F., Baker, B.A., and Manning, F.S., Surface Area Measurement of Geologic Materials, Soc. Pet. Eng. J. 15, 111 (1975).

Dormant, L.M., and Adamson, A.W., Application of the BET Equation to Heterogeneous Surfaces, J. Coll. Int. Sci. 38, 285 (1972).

Doscher, T.M., and Kuuskraa, V.A., Reviving Heavy Oil Reservoirs with Foam and Steam, Oil and Gas J. 80, 99 (1982).

Everett, D.H., Thermodynamics of Adsorption from Solution, Part 1 - Perfect Systems, Trans. Faraday Soc. 60, 1803 (1964).

Everett, D.H., Thermodynamics of Adsorption from Solution, Part 2 - Imperfect Systems, Trans. Faraday Soc. 61, 2478 (1965).

Everett, D.H., Adsorption at the Solid/Liquid Interface: Non-Aqueous Systems, in "Colloid Science. Specialist Periodical Reports", vol. 1, p. 49, ed. by D.H. Everett, The Chemical Society, London (1973)

Fuerstenau, D.W., Streaming Potential Studies on Quartz in Solutions of Aminium Acetates in Relation to the Formation of Hemimicelles at the Quartz-Solution Interface, J. Phys. Chem. 60, 981 (1956).

Fuerstenau, D.W., and Wakamatsu, T., Effect of pH on the Adsorption of Sodium Dodecanesulphonate at the Alumina/Water Interface, Faraday Discuss. Chem. Soc. 59, 157 (1975).

Funasaki, N., The Thermodynamics of Micellization of Surfactants in the Presence and Absence of Salt, J. Coll. Int. Sci. 67, 384 (1978).

Gale, W.W., and Sandvik, E.I., Tertiary Surfactant Flooding: Petroleum Sulfonate Composition-Efficacy Studies, Soc. Pet. Eng. J. 13, 191 (1973).

Gogarty, W.B., Oil Recovery with Surfactants: History and a Current Appraisal, in "Improved Oil Recovery by Surfactant and Polymer Flooding", p. 27, ed. by D.O. Shah and R.S. Schechter, Academic Press (1977).

Greenberg, A.E., Connors, J.J., Jenkins, D., and Franson, M.A.H., "Standard Methods for the Examination of Water and Wastewater", 15th edition, American Public Health Association (1980).

Gregg, S.J., and Sing, K.S.W., "Adsorption, Surface Area and Porosity", Academic Press (1967).

Guggenheim, E.A., and Adam, N.K., The Thermodynamics of Adsorption at the Surface of Solutions, Proc. Roy. Soc. (London), Ser. A 139, 218 (1933).

Gupta, S.P., Dispersion and Adsorption in Porous Media, Ph.D. thesis, Purdue University, 1972.

Gupta, S.P., and Greenkorn, R.A., Dispersion during Flow in Porous Media with Bilinear Adsorption, Water Resources Research 9, 1357 (1973).

Halsey, G., and Taylor, H.S., The Adsorption of Hydrogen on Tungsten Powder, J. Chem. Phys. 15, 624 (1947).

Harkins, W.D., and Jura, G., Surfaces of Solids XII. An Absolute Method for the Determination of the Area of a Finely Divided Crystalline Solid, J. Amer. Chem. Soc. 66, 1362 (1944a).

Harkins, W.D., and Jura, G., Surfaces of Solids XIII. A Vapor Adsorption Method for the Determination of the Area of a Solid without the Assumption of a Molecular Area, and the Areas Occupied by Nitrogen and Other Molecules on the Surface of a Solid, J. Amer. Chem. Soc. 66, 1366 (1944b).

Harned, H.S., and Owen, B.B., "The Physical Chemistry of Electrolytic Solutions", 3rd edition, Reinhold Publishing Corp. (1958).

Harwell, J.H., Helfferich, F.G., and Schechter, R.S., Effect of Micelle Formation on Chromatographic Movement of Surfactant Mixtures, AIChE J. 28, 448 (1982).

Harwell, J.H., Hoskins, J.C., Schechter, R.S., and Wade, W.H., Pseudophase Separation Model for Surfactant Adsorption: Isomerically Pure Surfactants, Langmuir 1, 251 (1985a).

Harwell, J.H., Schechter, R.S., and Wade, W.H., Surfactant Chromatographic Movement: An Experimental Study, AIChE J. 31, 415 (1985b).

Harwell, J.H., and Scamehorn, J.F., Enhanced Oil Recovery by Surfactant-Enhanced Volumetric Sweep Efficiency, U.S. Dept. of Energy, DOE/BC/10845-5 (DE87001241) (1987).

Hobson, J.P., A New Method for Finding Heterogeneous Energy Distributions from Physical Adsorption Isotherms, Can. J. Phys. 43, 1934 (1965a).

Hobson, J.P., Analysis of Physical Adsorption Isotherms on Heterogeneous Surfaces at Very Low Pressures, Can. J. Phys. 43, 1941 (1965b).

Holland, P.M., and Rubingh, D.N., Nonideal Multicomponent Mixed Micelle Model, J. Phys. Chem. 87, 1984 (1983).

Hough, D.B., and Rendall, H.M., Adsorption of Ionic Surfactants, in "Adsorption from Solution at the Solid/Liquid Interface", p. 247, ed. by G.D. Parfitt and C.H. Rochester, Academic Press (1983).

House, W.A., Surface Heterogeneity Effects in Adsorption from Solution, Chem. Phys. Lett. 60, 169 (1978).

House, W.A., and Jaycock, M.J., A Numerical Algorithm for the Determination of the Adsorptive Energy Distribution Function from Isotherm Data, Coll. Poly. Sci. 256, 52 (1978).

Huang, Y.-H., The Surface Excess Concept in Modelling Adsorption in Porous Media, M.Eng. thesis, The University of Calgary, 1985.

Huang, A.Y., and Novosad, J.J., Modelling of Adsorption of Foam-Forming Surfactants in Porous Media, in "Fundamentals of Adsorption", p. 265, ed. by A.I. Liapis, Engineering Foundation (1986).

Hurd, B.G., Adsorption and Transport of Chemical Species in Laboratory Surfactant Waterflooding Experiments, SPE paper #5818, presented at the Improved Oil Recovery Symposium of the Soc. of Pet. Eng. of AIME, Tulsa, Okla., March 22-24, 1976.

Jaroniec, M., and Rudzinski, W., General Method for Evaluating the Energy Distribution Function from the Observed Adsorption Isotherm, Coll. Poly. Sci. 253, 683 (1975).

Jaroniec, M., Patrykiewicz, A., and Borowko, M., Statistical Thermodynamics of Monolayer Adsorption from Gas and Liquid Mixtures on Homogeneous and Heterogeneous Solid Surfaces, in "Progress in Surface and Membrane Science", vol. 14, p. 1, ed. by D.A. Cadenhead and J.F. Danielli, Academic Press (1981).

Jaroniec, M., Heterogeneity Effects in Solute Adsorption from Dilute Solutions on Microporous Solids, in "Fundamentals of Adsorption", p. 277, ed. by A.I. Liapis, Engineering Foundation (1986).

Jaroniec, M., A New Concept for the Theoretical Description of Solute Adsorption from Dilute Solutions on Solids, Langmuir 3, 673 (1987).

Kamrath, R.F., and Franses, E.I., New Mathematical Models of Mixed Micellization, in "Phenomena in Mixed Surfactant Systems", ACS Symposium Series 311, p. 44, ed. by J.F. Scamehorn, American Chemical Society (1986).

Kantro, D.L., Brunauer, S., and Copeland, L.E., BET Surface Areas - Methods and Interpretations, in "The Solid-Gas Interface", p. 413, ed. by E.A. Flood, Marcel Dekker (1967).

Karnaukhov, A.P., Improvement of Methods for Surface Area Determinations, J. Coll. Int. Sci. 103, 311 (1985).

- Kindl, B., Pachovski, R.A., Spencer, B.A., and Wojciechowski, B.W., General Model for the Adsorption of Gases on Solids, J. Chem. Soc., Faraday Trans I 69, 1162 (1973).
- Kramers, H., and Alberda, G., Frequency Response Analysis of Continuous Flow Systems, Chem. Eng. Sci. 2, 173 (1953).
- Lange, H., Über die Mizellenbildung in Mischglösungen homologer Paraffinkettensalze, Kolloid-Z. 131, 96 (1953).
- Lange, H., and Beck, K.-H., Zur Mizellbildung in Mischlösungen homologer und nichthomologer Tenside, Kolloid-Z. u. Z. Polymere 251, 424 (1973).
- Lapidus, L., and Amundson, N.R., Mathematics of Adsorption in Beds. VI. The Effect of Longitudinal Diffusion in Ion Exchange and Chromatographic Columns, J. Phys. Chem. 56, 984 (1952).
- Larionov, O.G., and Myers, A.L., Thermodynamics of Adsorption from Nonideal Solutions of Nonelectrolytes, Chem. Eng. Sci. 26, 1025 (1971).
- Lawson, J.B., and Dilgren, R.E., Adsorption of Sodium Alkyl Aryl Sulfonates on Sandstone, Soc. Pet. Eng. J. 18, 75 (1978).
- Li, P., and Gu, T., Thermodynamics of Adsorption from Perfect Binary Liquid Mixtures on Silica Gel, Scientia Sinica 22, 1384 (1979).
- Livingston, H.K., The Cross-Sectional Areas of Molecules Adsorbed on Solid Surfaces, J. Coll. Sci. 4, 447 (1949).
- Malmberg, E.W., and Smith, L., The Adsorption Losses of Surfactants in Tertiary Recovery Systems, in "Improved Oil Recovery by Surfactant and Polymer Flooding", p. 275, ed. by D.O. Shah and R.S. Schechter, Academic Press (1977).
- Mannhardt, K., and Novosad, J.J., Modelling Adsorption of Foam-Forming Surfactants, paper presented at the 4th European Symposium on Enhanced Oil Recovery, Hamburg, West Germany, Oct. 27-29, 1987a.
- Mannhardt, K., and Novosad, J.J., Modelling Adsorption of Foam-Forming Surfactants Using the Surface Excess Model, Petroleum Recovery Institute Report 1987-10, Calgary, Canada (1987b).
- Maron, S.H., Elder, M.E., and Ulevitch, I.N., Determination of Surface Area and Particle Size of Synthetic Latex by Adsorption. I. Latices Containing Fatty Acid Soaps, J. Coll. Sci. 9, 89 (1954).
- McClellan, A.L., and Harnsberger, H.F., Cross-Sectional Areas of Molecules Adsorbed on Solid Surfaces, J. Coll. Int. Sci. 23, 577 (1967).
- McEnaney, B., Mays, T.J., and Causton, P.D., Heterogeneous Adsorption on Microporous Carbons, Langmuir 3, 695 (1987).

Minka, C., and Myers, A.L., Adsorption from Ternary Liquid Mixtures on Solids, *AIChE J.* 19, 453 (1973).

Misra, D.N., New Adsorption Isotherm for Heterogeneous Surfaces, *J. Chem. Phys.* 52, 5499 (1970).

Misra, D.N., Jovanovich Adsorption Isotherm for Heterogeneous Surfaces, *J. Coll. Int. Sci.* 43, 85 (1973).

Myers, A.L., Molecular Thermodynamics of Adsorption of Gas and Liquid Mixtures, in "Fundamentals of Adsorption", p. 3, ed. by A.I. Liapis, Engineering Foundation (1986).

Mysels, K.J., and Otter, R.J., Thermodynamic Aspects of Mixed Micelles - Application to an Empirically Established Equilibrium, *J. Coll. Sci.* 16, 474 (1961).

Nagy, L.G., and Schay, G., Adsorption of Binary Liquid Mixtures on Solid Surfaces. Thermodynamical Discussion of the Adsorption Equilibrium, I, *Acta Chim. Acad. Sci. Hung.* 39, 365 (1963).

Nakamura, A., Tajima, K., and Sasaki, T., The Effect of the pH on the Adsorption of an Ampholytic Surfactant, N-Dodecyl- β -Alanine, at the Aqueous Surface, *Bull. Chem. Soc. Japan* 48, 214 (1975).

Narang, K.C., and Ramakrishna, V., Surface Properties of Chromium Oxide Obtained from Ammonium Dichromate, *Indian J. Chem.* 8, 919 (1970a).

Narang, K.C., and Ramakrishna, V., Adsorption on Cr_2O_3 Samples from Binary Liquid Mixtures of Cyclohexane and Benzene at 30 °C, *Indian J. Chem.* 8, 923 (1970b).

Nishikido, N., Moroi, Y., and Matuura, R., The Micelle Formation of Mixtures of Polyoxyethylene Type Nonionic Surfactants in Aqueous Solutions, *Bull. Chem. Soc. Japan* 48, 1387 (1975).

Novosad, J., and Baxter, L.A., Adsorption of Pure Surfactant and Petroleum Sulfonate at the Solid-Liquid Interface, Petroleum Recovery Institute Research Report RR-42, Calgary, Canada (1979).

Novosad, J., Surfactant Retention in Berea Sandstone - Effects of Phase Behavior and Temperature, *Soc. Pet. Eng. J.* 22, 962 (1982).

Novosad, J., Maini, B.B., and Huang, A., Retention of Foam-Forming Surfactants at Elevated Temperatures, *J. Can. Pet. Tech.* 25, 42 (1986).

Novosad, J.J., and Ionescu, E.F., Foam Forming Surfactants for Beaverhill Lake Carbonates and Gilwood Sands Reservoirs, paper #87-38-80, presented at the 38th Annual Technical Meeting of the Petroleum Society of CIM, Calgary, Alberta, June 7-10, 1987.

Nunge, R.J., and Gill, W.N., Mechanisms Affecting Dispersion and Miscible Displacement, in "Flow through Porous Media", p. 179, ACS Publications (1970).

O'Brien, J.A., and Myers, A.L., Activity Coefficients for Adsorption of Laterally Interacting Molecules on a Random Heterogeneous Solid Surface, in "Fundamentals of Adsorption", p. 451, ed. by A.I. Liapis, Engineering Foundation (1986).

O'Connor, D.J., and Sanders, J.V., Hydrophobic Monolayers on Platinum, Mica, and Silica, J. Coll. Sci. 11, 158 (1956).

Okumura, T., Nakamura, A., Tajima, T., and Sasaki, T., Radiotracer Studies of the Adsorption of an Ampholytic Surfactant, N-Dodecyl- β -Alanine at the Aqueous Surface, Bull. Chem. Soc. Japan 47, 2986 (1974).

Orr, R.J., and Breitman, L., Molecular Areas of Soaps at the Surface of Latex Particles, Can. J. Chem. 38, 668 (1960).

Osborne-Lee, I.W., Schechter, R.S., and Wade, W.H., Monomer-Micelle Equilibrium of Aqueous Surfactant Solutions by the Use of Ultrafiltration, J. Coll. Int. Sci. 94, 179 (1983).

Osborne-Lee, I.W., Schechter, R.S., Wade, W.H., and Barakat, Y., A New Theory and New Results for Mixed Nonionic-Anionic Micelles, J. Coll. Int. Sci. 108, 60 (1985).

Osborne-Lee, I.W., and Schechter, R.S., Nonideal Mixed Micelles. Thermodynamic Models and Experimental Comparisons, in "Phenomena in Mixed Surfactant Systems", ACS Symposium Series 311, p. 30, ed. by J.F. Scamehorn, American Chemical Society (1986).

Oscik, J., Dabrowski, A., Jaroniec, M., and Rudzinski, W., Effects of Surface Heterogeneity in Adsorption from Binary Liquid Mixtures. I. Adsorption from Ideal Solutions, J. Coll. Int. Sci. 56, 403 (1976).

Oscik, J., Dabrowski, A., and Rudzinski, W., On the Formation of Multilayers in Adsorption from Binary Liquid Mixtures, Coll. Poly. Sci. 255, 50 (1977).

Perkins, T.K., and Johnston, O.C., A Review of Diffusion and Dispersion in Porous Media, Soc. Pet. Eng. J. 3, 70 (1963).

Pethica, B.A., The Adsorption of Surface Active Electrolytes at the Air/Water Interface, Trans. Faraday Soc. 50, 413 (1954).

Pusch, G., Rosenthal, G., and Albertsen, M., Evaluation of the Surfactant Flood Process by Investigating the Surfactant Partitioning in the Porous Medium and in the Effluent, paper presented at the 4th European Symposium on Enhanced Oil Recovery, Hamburg, West Germany, Oct. 27-29, 1987.

- Ramirez, W.F., Schuler, P.J., and Friedman, F., Convection, Dispersion and Adsorption of Surfactants in Porous Media, Soc. Pet. Eng. J. 20, 430 (1980).
- Reid, V.W., Longman, G.F., and Heinerth, E., Determination of Anionic-Active Detergents by Two-Phase Titration, Tenside 4, 292 (1967).
- Roberts, B.L., Scamehorn, J.F., and Harwell, J.H., Adsorption of a Mixture of Anionic Surfactants on Alumina, in "Phenomena in Mixed Surfactant Systems", ACS Symposium Series 311, p. 200, ed. by J.F. Scamehorn, American Chemical Society (1986).
- Rootare, H.M., and Prenzlow, C.F., Surface Areas from Mercury Porosimeter Measurements, J. Phys. Chem. 71, 2733 (1967).
- Rosen, M.J., and Nakamura, Y., The Relationship of Structure to Properties in Surfactants. 6. The Adsorption of α,ω -Bis (Sodium p-Sulphophenoxy) Alkanes on Alumina, J. Phys. Chem. 81, 873 (1977).
- Rosen, M.J., "Surfactants and Interfacial Phenomena", John Wiley & Sons (1978).
- Roy, P., and Fuerstenau, D.W., The Heat of Immersion of Alumina into Aqueous Sodium Dodecyl Sulfonate Solutions, J. Coll. Int. Sci. 26, 102 (1968).
- Rubingh, D.N., Mixed Micelle Solutions, in "Solution Chemistry of Surfactants", vol. 1, p. 337, ed. by K.L. Mittal, Plenum Press (1978).
- Rudzinski, W., Oscik, J., and Dabrowski, A., Adsorption from Solutions on Patchwise Heterogeneous Solids, Chem. Phys. Lett. 20, 444 (1973).
- Rudzinski, W., and Jaroniec, M., Adsorption on Heterogeneous Surfaces. A New Method for Evaluating the Energy Distribution Function, Surface Sci. 42, 552 (1974).
- Rudzinski, W., and Partyka, S., Adsorption from Solution on Solid Surfaces. Effects of Surface Heterogeneity on Adsorption Isotherms and Heats of Immersion, J. Chem. Soc., Faraday Trans. I 77, 2577 (1981).
- Rudzinski, W., Narkiewicz-Michalek, J., and Partyka, S., Adsorption from Solution onto Solid Surfaces. Effects of Topography of Heterogeneous Surfaces on Adsorption Isotherms and Heats of Adsorption, J. Chem. Soc., Faraday Trans. I 78, 2361 (1982).
- Satter, A., Shum, Y.M., Adams, W.T., and Davis, L.A., Chemical Transport in Porous Media with Dispersion and Rate-Controlled Adsorption, Soc. Pet. Eng. J. 20, 129 (1980).
- Scamehorn, J.F., Schechter, R.S., and Wade, W.H., Adsorption of Surfactants on Mineral Oxide Surfaces from Aqueous Solutions. I. Isomerically Pure Anionic Surfactants, J. Coll. Int. Sci. 85, 463

(1982a).

Scamehorn, J.F., Schechter, R.S., and Wade, W.H., Adsorption of Surfactants on Mineral Oxide Surfaces from Aqueous Solutions. II. Binary Mixtures of Anionic Surfactants, J. Coll. Int. Sci. 85, 479 (1982b).

Scamehorn, J.F., Schechter, R.S., and Wade, W.H., Adsorption of Surfactants on Mineral Oxide Surfaces from Aqueous Solutions. III. Binary Mixtures of Anionic and Nonionic Surfactants, J. Coll. Int. Sci. 85, 494 (1982c).

Scamehorn, J.F., Schechter, R.S., and Wade, W.H., A Reduced Adsorption Isotherm for Surfactant Mixtures, J. Am. Oil Chem. Soc. 60, 1345 (1983).

Scamehorn, J.F., An Overview of Phenomena Involving Surfactant Mixtures, in "Phenomena in Mixed Surfactant Systems", ACS Symposium Series 311, p. 1, ed. by J.F. Scamehorn, American Chemical Society (1986a).

Scamehorn, J.F., Behavior and Applications of Surfactant Mixtures, in "Phenomena in Mixed Surfactant Systems", ACS Symposium Series 311, p. 324, ed. by J.F. Scamehorn, American Chemical Society (1986b).

Schay, G., and Nagy, L.G., Specific Surface Area Determination by Liquid Adsorption, Acta Chim. Acad. Sci. Hung. 50, 207 (1966).

Schay, G., Adsorption of Solutions of Nonelectrolytes, in "Surface and Colloid Science", vol. 2, p. 155, ed. by E. Matijevic, Wiley Interscience (1969a).

Schay, G., Tentative Kinetic Interpretation of Adsorption Isotherms of Binary Mixtures of Non-Electrolytes, Acta Chim. Acad. Sci. Hung. 60, 237 (1969b).

Schay, G., and Nagy, L.G., Critical Discussion of the Use of Adsorption Measurements from the Liquid Phase for Surface Area Estimation, J. Coll. Int. Sci. 38, 302 (1972).

Shinoda, K., The Critical Micelle Concentration of Soap Mixtures (Two-Component Mixture), J. Phys. Chem. 58, 541 (1954).

Shinoda, K., The Formation of Micelles, in "Colloidal Surfactants", by K. Shinoda, T. Nakagawa, B.-I. Tamamushi, and T. Isemura, chapter 1, Academic Press (1963).

Sips, R., On the Structure of a Catalyst Surface, J. Chem. Phys. 16, 490 (1948).

Sips, R., On the Structure of a Catalyst Surface. II, J. Chem. Phys. 18, 1024 (1950).

Sircar, S., and Myers, A.L., Statistical Thermodynamics of Adsorption from Liquid Mixtures on Solids. I. Ideal Adsorbed Phase, J. Phys. Chem 74, 2828 (1970).

Sircar, S., and Myers, A.L., A Thermodynamic Consistency Test for Adsorption from Binary Liquid Mixtures on Solids, AIChE J. 17, 186 (1971).

Sircar, S., Novosad, J., and Myers, A.L., Adsorption from Liquid Mixtures on Solids: Thermodynamics of Excess Properties and their Temperature Coefficients, I & EC Fund. 11, 249 (1972).

Sircar, S., Adsorption of Binary Liquid Mixtures on Heterogeneous Adsorbents, J. Chem. Soc., Faraday Trans. I 79, 2085 (1983).

Sircar, S., Adsorption of Binary Liquid Mixtures on Heterogeneous Adsorbents with Uniform Energy Distribution, Surface Sci. 148, 478 (1984a).

Sircar, S., Adsorption from Binary Liquid Mixtures of Unequal Adsorbate Sizes on Heterogeneous Adsorbents, Surface Sci. 148, 489 (1984b).

Sircar, S., New Adsorption Isotherm for Energetically Heterogeneous Adsorbents, J. Coll. Int. Sci. 98, 306 (1984c).

Sircar, S., Effect of Local Isotherm on Adsorbent Heterogeneity, J. Coll. Int. Sci. 101, 452 (1984d).

Sircar, S., Excess Properties and Thermodynamics of Multicomponent Gas Adsorption, J. Chem. Soc., Faraday Trans. I 81, 1527 (1985a).

Sircar, S., Excess Properties and Column Dynamics of Multicomponent Gas Adsorption, J. Chem. Soc., Faraday Trans. I 81, 1541 (1985b).

Sircar, S., Adsorbent Surface Area Determination by Measurement of Adsorption from Liquid Mixtures, 17th Biennial Conf. on Carbon (1985c).

Sircar, S., Adsorption and Condensation of Vapors on Heterogeneous Porous Adsorbents, in "Fundamentals of Adsorption", p. 515, ed. by A.I. Liapis, Engineering Foundation (1986).

Somasundaran, P., Healy, T.W., and Fuerstenau, D.W., Surfactant Adsorption at the Solid-Liquid Interface - Dependence of Mechanism on Chain Length, J. Phys. Chem. 68, 3562 (1964).

Somasundaran, P., and Fuerstenau, D.W., Mechanisms of Alkyl Sulfonate Adsorption at the Alumina-Water Interface, J. Phys. Chem. 70, 90 (1966).

Somasundaran, P., and Hanna, H.S., Adsorption of Sulfonates on Reservoir Rocks, Soc. Pet. Eng. J. 19, 221 (1979).

Somasundaran, P., and Gryte, C.C., Adsorption from Flooding Solutions

in Porous Media. A Study of Interactions of Surfactants and Polymers with Reservoir Minerals, U.S. Dept. of Energy DOE/BC/10082-27 (DE85000130) (1985).

Somasundaran, P., Adsorption from Flooding Solutions in Porous Media. A Study of Interactions of Surfactants and Polymers with Reservoir Minerals, U.S. Dept. of Energy DOE/BC/10848-5 (DE87001233) (1987).

Sorbie, K.S., Johnson, P.A.V., Hubbard, S., and Temple, J., Non-Equilibrium Effects in the Adsorption of Polyacrylamide onto Sandstone: Experimental and Modelling Studies, paper presented at the 4th European Symposium on Enhanced Oil Recovery, Hamburg, West Germany, Oct. 27-29, 1987.

Tajima, K., Muramatsu, M., and Sasaki, T., Radiotracer Studies on Adsorption of Surface Active Substance at Aqueous Surface. I. Accurate Measurement of Adsorption of Tritiated Sodium Dodecylsulfate, Bull. Chem. Soc. Japan 43, 1991 (1970).

Tajima, K., Radiotracer Studies on Adsorption of Surface Active Substance at Aqueous Surface. II. The Effect of Excess Salt on the Adsorption of Sodium Dodecylsulfate, Bull. Chem. Soc. Japan 43, 3063 (1970).

Tajima, K., Radiotracer Studies on Adsorption of Surface Active Substance at Aqueous Surface. III. The Effects of Salt on the Adsorption of Sodium Dodecylsulfate, Bull. Chem. Soc. Japan 44, 1767 (1971).

Tajima, K., Iwahashi, M., and Sasaki, T., Radiotracer Studies on Adsorption of Surface Active Substance at Aqueous Surface. IV. Direct Measurement of Adsorption of Tritiated Nonionic Surfactant, Bull. Chem. Soc. Japan 44, 3251 (1971).

Tignor, E.M., Noonan, J.F., and Lockwood, W.N., Pore Studies of Petroleum-Reservoir Sandstones, Producers Monthly, May 1952, p. 16.

Trogus, F.J., Sophany, T., Schechter, R.S., and Wade, W.H., Static and Dynamic Adsorption of Anionic and Nonionic Surfactants, Soc. Pet. Eng. J. 17, 337 (1977).

Trogus, F.J., Schechter, R.S., and Wade, W.H., A New Interpretation of Adsorption Maxima and Minima, J. Coll. Int. Sci. 70, 293 (1979a).

Trogus, F.J., Schechter, R.S., Pope, G.A., and Wade, W.H., Adsorption of Mixed Surfactant Systems, J. Pet. Tech. 31, 769 (1979b).

Van Dongen, R.H., Evaluation of the Adsorption Potential Distribution Function from Observed Adsorption Isotherms, Surf. Sci. 39, 341 (1973).

Wakamatsu, T., and Fuerstenau, D.W., The Effect of Hydrocarbon Chain Length on the Adsorption of Sulfonates at the Solid/Water Interface, Adv. in Chem. Series 79, 161 (1968).

Waksmundzki, A., Dawidowicz, A., Sokolowski, S., and Jaroniec, M., Studies on Energetic Heterogeneity of Adsorbents by Means of Liquid Chromatography, *Chromatographia* 8, 234 (1975).

Weil, I., Surface Concentration and the Gibbs Adsorption Law. The Effect of the Alkali Metal Cations on Surface Behavior, *J. Phys. Chem.* 70, 133 (1966).

Westerkamp, A., and Menz, D., Surfactant System for Chemical Flooding a Highly Saline North German Reservoir, paper presented at the 4th European Symposium on Enhanced Oil Recovery, Hamburg, West Germany, Oct. 27-29, 1987.

Young, D.M., and Crowell, A.D., "Physical Adsorption of Gases", Butterworths (1962).

Ziegler, V.M., and Handy, L.L., Effect of Temperature on Surfactant Adsorption in Porous Media, *Soc. Pet. Eng. J.* 21, 218 (1981).

Zimmels, Y., Lin, I.J., and Friend, J.P., The Relation between Step-Wise Bulk Association and Interfacial Phenomena for Some Aqueous Surfactant Solutions, *Coll. Poly. Sci.* 253, 404 (1975).

APPENDIX

FINITE DIFFERENCE SOLUTIONS TO THE FLOW MODELS

1. General Solution

The finite difference solutions that are general to all the flow models presented in this thesis will be developed in this section. The features specific to each particular model will then be outlined in the remaining sections.

The Barakat and Clark finite difference scheme employs both forward and backward formulas using the following difference expressions:

Forward sweep:

$$\frac{\partial^2 x_i}{\partial y^2} = \frac{(x_i)_{j+1}^n - (x_i)_j^n - (x_i)_j^{n+1} + (x_i)_{j-1}^{n+1}}{(\Delta y)^2} \quad (A-1)$$

$$\frac{\partial x_i}{\partial y} = \frac{(x_i)_j^{n+1} - (x_i)_{j-1}^{n+1} + (x_i)_{j+1}^n - (x_i)_j^n}{2(\Delta y)} \quad (A-2)$$

$$\frac{\partial x_i}{\partial t} = \frac{(x_i)_j^{n+1} - (x_i)_j^n}{\Delta t} \quad (A-3)$$

Backward sweep:

$$\frac{\partial^2 x_i}{\partial y^2} = \frac{(x_i)_{j+1}^{n+1} - (x_i)_j^{n+1} - (x_i)_j^n + (x_i)_{j-1}^n}{(\Delta y)^2} \quad (A-4)$$

$$\frac{\partial x_i}{\partial y} = \frac{(x_i)_j^n - (x_i)_{j-1}^n + (x_i)_{j+1}^{n+1} - (x_i)_j^{n+1}}{2(\Delta y)} \quad (A-5)$$

$$\frac{\partial x_i}{\partial t} = \frac{(x_i)_j^{n+1} - (x_i)_j^n}{\Delta t} \quad (A-6)$$

In these expressions, x_i is the mole fraction of surfactant i , subscripts (j) indicate grid blocks, and superscripts (n) represent time levels. Δy and Δt are space and time increments, respectively. The average value of x_i from forward and backward formulas is taken as the concentration in a particular grid block at any particular time level.

Using the expressions

$$v = \frac{q}{A\phi}$$

and

$$D = \lambda v = \lambda \frac{q}{A\phi}$$

the transport equation (equation (12) or (111) and (112)) can be written as:

$$\frac{\lambda q \rho}{A\phi} \frac{\partial^2 x_i}{\partial y^2} - \frac{q \rho}{A\phi} \frac{\partial x_i}{\partial y} = \rho \frac{\partial x_i}{\partial t} + \frac{1-\phi}{\phi} \rho_r \frac{\partial n_i^{ea}}{\partial t} \quad (A-7)$$

The forward difference expression for equation (A-7) is obtained by substituting equations (A-1) to (A-3) and equation (14), (115), or (116) into (A-7):

$$\begin{aligned}
& \frac{\lambda q \rho}{A \phi} \frac{(x_i)_{j+1}^n - (x_i)_j^n - (x_i)_j^{n+1} + (x_i)_{j-1}^n}{(\Delta y)^2} \\
& - \frac{q \rho}{A \phi} \frac{(x_i)_j^{n+1} - (x_i)_{j-1}^{n+1} + (x_i)_{j+1}^n - (x_i)_j^n}{2(\Delta y)} = \rho \frac{(x_i)_j^{n+1} - (x_i)_j^n}{\Delta t} \\
& + \frac{1-\phi}{\phi} \rho_r k_{im} \left[(n_i^e)_j^n - (n_i^{ea})_j^n \right] ; \quad j = 2, J-1 \quad (A-8)
\end{aligned}$$

where k_{im} is the kinetic constant of adsorption ($m=1$) or desorption ($m=2$) of surfactant i . Adsorption takes place when $n_i^e \geq n_i^{ea}$, and desorption when $n_i^e < n_i^{ea}$. Grid blocks are numbered from $j=1$ to $j=J$. If we let

$$C_1 = \frac{\rho}{\Delta t}$$

$$C_2 = \frac{\lambda q \rho}{A \phi (\Delta y)^2}$$

$$C_3 = \frac{q \rho}{2 A \phi (\Delta y)}$$

then, on rearrangement of equation (A-8), an explicit expression for $(x_i)_j^{n+1}$ in terms of known concentrations is obtained:

$$\begin{aligned}
(x_i)_j^{n+1} = & \left\{ (C_2 + C_3) (x_i)_{j-1}^{n+1} + (C_1 - C_2 + C_3) (x_i)_j^n + (C_2 - C_3) (x_i)_{j+1}^n \right. \\
& \left. - \frac{1-\phi}{\phi} \rho_r k_{im} \left[(n_i^e)_j^n - (n_i^{ea})_j^n \right] \right\} / (C_1 + C_2 + C_3) ; \quad j = 2, J-1 \quad (A-9)
\end{aligned}$$

The initial condition sets concentrations in all grid blocks to zero initially. The boundary conditions can be discretized as follows:

$y = 0, 0 < t \leq t_1:$

$$(x_i)_1^{n+1} = x_{i0} + \lambda \frac{-3(x_i)_1^{n+1} + 4(x_i)_2^n - (x_i)_3^n}{2(\Delta y)}$$

or, on rearrangement,

$$(x_i)_1^{n+1} = \left[x_{i0} + \frac{\lambda}{2(\Delta y)} \left[4(x_i)_2^n - (x_i)_3^n \right] \right] / \left[1 + \frac{3\lambda}{2(\Delta y)} \right] \quad (A-10)$$

$y = 0, t > t_1:$

$$(x_i)_1^{n+1} = \lambda \frac{-3(x_i)_1^{n+1} + 4(x_i)_2^n - (x_i)_3^n}{2(\Delta y)}$$

or, on rearrangement,

$$(x_i)_1^{n+1} = \left[\frac{\lambda}{2(\Delta y)} \left[4(x_i)_2^n - (x_i)_3^n \right] \right] / \left[1 + \frac{3\lambda}{2(\Delta y)} \right] \quad (A-11)$$

$y = L, t > 0:$

$$\frac{(x_i)_{J-2}^{n+1} - 4(x_i)_{J-1}^{n+1} + 3(x_i)_J^{n+1}}{2(\Delta y)} = 0$$

Once again, on rearrangement,

$$(x_i)_J^{n+1} = \frac{1}{3} \left[4(x_i)_{J-1}^{n+1} - (x_i)_{J-2}^{n+1} \right] \quad (A-12)$$

Backward difference expressions can be obtained in a similar way by substituting equations (A-4) to (A-6) and equation (14), (115), or (116) into (A-7):

$$(x_i)_j^{n+1} = \left\{ (C_2 - C_3) (x_i)_{j+1}^{n+1} + (C_1 - C_2 - C_3) (x_i)_j^n + (C_2 + C_3) (x_i)_{j-1}^n \right. \\ \left. - \frac{1-\phi}{\phi} \rho_r k_{im} \left[(n_i)_j^n - (n_i)_{j-1}^n \right] \right\} / (C_1 + C_2 - C_3) ; \quad j = J-1, 2 \quad (A-13)$$

$y = 0, 0 < t \leq t_1:$

$$(x_i)_1^{n+1} = \left[x_{i0} + \frac{\lambda}{2(\Delta y)} \left[4(x_i)_2^{n+1} - (x_i)_3^{n+1} \right] \right] / \left[1 + \frac{3\lambda}{2(\Delta y)} \right] \quad (A-14)$$

$y = 0, t > t_1:$

$$(x_i)_1^{n+1} = \left[\frac{\lambda}{2(\Delta y)} \left[4(x_i)_2^{n+1} - (x_i)_3^{n+1} \right] \right] / \left[1 + \frac{3\lambda}{2(\Delta y)} \right] \quad (A-15)$$

$y = L, t > 0:$

$$(x_i)_J^{n+1} = \frac{1}{3} \left[4(x_i)_{J-1}^n - (x_i)_{J-2}^n \right] \quad (A-16)$$

Note that the term including the surface excess in equations (A-9) and (A-13) is modelled explicitly. Once x_i has been calculated from these equations, the new equilibrium surface excess $(n_i^e)_j^{n+1}$ can be calculated from equation (8), (66), or (123) and (124), depending on which model is being used. The actual surface excess at the new time level is then calculated from the difference expression corresponding to the rate of adsorption equation (equation (14) or (115) and (116)):

$$\frac{(n_i^{ea})_j^{n+1} - (n_i^{ea})_j^n}{\Delta t} = k_{im} \left[(n_i^e)_j^{n+1} - (n_i^{ea})_j^{n+1} \right]; \quad j = 2, J-1$$

or

$$(n_i^{ea})_j^{n+1} = \left[\frac{1}{\Delta t} (n_i^{ea})_j^n + k_{im} (n_i^e)_j^{n+1} \right] / \left[\frac{1}{\Delta t} + k_{im} \right]; \quad (A-17)$$

$$j = 2, J-1$$

The value of k_{im} is taken as the kinetic constant of adsorption when the actual surface excess is less than or equal to the equilibrium surface excess, otherwise k_{im} is the kinetic constant of desorption.

Equations (A-9) to (A-17), together with the appropriate equations for the equilibrium surface excess, provide the complete solution to the flow model.

2. Flow Model with Constant Selectivity

This model is applied to a single surfactant in solution in chapters 2 and 4. x_i , n_i^e and n_i^{ea} in the equations of the previous section can therefore be replaced by x_1 , n_1^e and n_1^{ea} , respectively. k_{11} becomes k_{11} (adsorption) or k_{12} (desorption), and the equilibrium surface excess is given by equation (8). Equations (A-9) to (A-17), together with (8), provide the complete solution to this flow model.

3. Flow Model with Non-Constant Selectivity

The same comments made for the constant selectivity model in the previous section apply. The only difference is in the usage of equation (8). Instead of using a constant value of selectivity, the selectivity is calculated from equation (50) or (51) using the surfactant mole fraction calculated for that grid block. Solution of equation (50) for S is by Newton's method.

4. Flow Model with Heterogeneous Solid

Again, the only difference between this model and the model of section 2 lies in the calculation of the equilibrium surface excess, which is now determined from equation (66). The selectivities, S_A and S_B , are functions of concentration, and are calculated from equations (67) and (68) using Newton's method.

5. Flow Model for Surfactant Mixtures

This model describes transport of two surfactants rather than just one. There will therefore be two sets of equations (A-9) to (A-17), one with $i=1$, and one with $i=2$. The two sets are coupled through the expressions for the equilibrium surface excesses n_1^e and n_2^e (equations (123) and (124)). In order to use these equations the monomer mole fractions first have to be calculated using equations (119) or (120) to (122). The calculation procedure for this model can be summarized as follows.

The surfactant mole fraction of each component is calculated in any grid block at any time level using equations (A-9) and (A-13). Note that the concentration in the grid block is taken to be the average from forward and backward difference schemes in all models. Once the surfactant mole fractions are known, α is determined in that particular grid block from equation (117), and the cmc of the solution in that grid block is obtained from equation (118). Monomer mole fractions can then be found from equations (119) or (120) to (122), which are

substituted into (123) and (124) to determine the equilibrium surface excesses, n_1^e and n_2^e . The actual surface excesses, n_1^{ea} and n_2^{ea} , can now be calculated from equation (A-17). These calculations are carried out for each grid block, and then proceed to the following time level.

6. Fortran Programs

Fortran programs have been written for all the flow models described in this thesis. The following programs are available from the author on request:

FLOWMOD1: Constant selectivity flow model.

FLOWMOD2: Variable selectivity flow model. The selectivity is given by equation (50).

FLOWMOD3: Variable selectivity flow model. The selectivity is given by equation (51).

FLOWMOD4: Variable selectivity flow model for a two-component heterogeneous solid. The selectivity is given by equations (67) and (68).

SELECTIVITY: Program that calculates selectivity or, in the case of heterogeneous solids, effective selectivity, as a function of concentration using

- (a) equation (50),
- (b) equation (51),
- (c) a heterogeneous surface with uniform distribution of S_0 ,
- (d) a two-component heterogeneous surface.

ISOTHERM: Program that calculates adsorption isotherms for the following cases:

- (a) constant selectivity,
- (b) variable selectivity with equation (50),
- (c) variable selectivity with equation (51),
- (d) a heterogeneous surface with uniform distribution of S_0 and variable selectivities given by equations (60) and (61),
- (e) a two-component heterogeneous surface with variable selectivities given by equations (67) and (68).

The above models are for pseudobinary mixtures. They do not incorporate monomer-micelle equilibrium.

FLOWTMIX: Flow model for ternary mixtures. Includes monomer-micelle equilibrium.

ISOTMIX: Program that calculates adsorption isotherms for a ternary mixture. Includes monomer-micelle equilibrium.